INTERNATIONAL DOCTORAL
SCHOOL OF THE USC

Joan
Miguel Ávila

PhD Thesis

Transition Metal-Catalyzed Annulations in Biological Media

Santiago de Compostela, 2022

Doctoral Programme in Chemical Science and Technology

TESE DE DOUTORAMENTO

Transition Metal-Catalyzed Annulations in Biological Media

Joan Miguel Ávila

ESCOLA DE DOUTORAMENTO INTERNACIONAL

PROGRAMA DE DOUTORAMENTO EN CIENCIA E TECNOLOXÍA QUÍMICA

SANTIAGO DE COMPOSTELA

2022

USC
UNIVERSIDADE
DE SANTIAGO
DE COMPOSTELA

D./Dña. **Joan Miguel Ávila**

Título da tese: **Transition Metal-Catalyzed Annulations in Biological Media**

Presento mi tesis, siguiendo el procedimiento adecuado al Reglamento y declaro que:

1) La tesis abarca los resultados de la elaboración de mi trabajo.
2) De ser el caso, en la tesis se hace referencia a las colaboraciones que tuvo este trabajo.
3) Confirmo que la tesis no incurre en ningún tipo de plagio de otros autores ni de trabajos presentados por mí para la obtención de otros títulos.
4) La tesis es la versión definitiva presentada para su defensa y coincide la versión impresa con la presentada en formato electrónico.

Y me comprometo a presentar el Compromiso Documental de Supervisión en el caso que el original no esté depositado en la Escuela.

En **Santiago de Compostela**, **22 de abril de 2022**.

Asdo. Joan Miguel Ávila

USC
UNIVERSIDADE DE SANTIAGO DE COMPOSTELA

USC
UNIVERSIDADE
DE SANTIAGO
DE COMPOSTELA

AUTORIZACIÓN DEL DIRECTOR / TUTOR DE LA TESIS

Transition Metal-Catalyzed Annulations in Biological Media

D. José Luis Mascareñas Cid

Dª. María Tomás Gamasa

INFORMAN:

Que la presente tesis, se corresponde con el trabajo realizado por D. Joan Miguel Ávila, bajo mi dirección/tutorización, y autorizo su presentación, considerando que reúne los requisitos exigidos en el Reglamento de Estudios de Doctorado de la USC, y que como director de esta no incurre en las causas de abstención establecidas en la Ley 40/2015.

De acuerdo con lo indicado en el Reglamento de Estudios de Doctorado, declara también que la presente tesis doctoral es idónea para ser defendida en base a la modalidad de Monográfica con reproducción de publicaciones, en los que la participación del doctorando fue decisiva para su elaboración y las publicaciones se ajustan al Plan de Investigación.

En Santiago de Compostela, 22 de abril de 2022

USC
UNIVERSIDADE DE SANTIAGO DE COMPOSTELA

Asdo. José Luis Mascareñas Cid

Asdo. María Tomás Gamasa

USC
UNIVERSIDADE
DE SANTIAGO
DE COMPOSTELA

“A moderately good memory, one of the prerequisites of survival in chemistry”

- Rolf Huisgen

“María, ¿cómo se llamaba esa cosa que ya sabes taca y filtras…?”

- Joan Miguel

Dedicat al meu germà

USC
UNIVERSIDADE DE SANTIAGO DE COMPOSTELA

USC
UNIVERSIDADE
DE SANTIAGO
DE COMPOSTELA

Table of contents

Abbreviations and acronyms..... 11

INTRODUCTION..... 15

1. Chemical biology 17

2. Bioorthogonal chemistry 18

2.1. What is bioorthogonal chemistry..... 18

2.2. The birth of bioorthogonal chemistry: Hydrazone ligations..... 20

2.3. Staudinger ligation..... 22

2.4. The azide-alkyne cycloaddition. The rise of click chemistry 25

2.5. Applications of the CuAAC in chemical biology..... 27

2.6. Strain-promoted azide-alkyne cycloadditions 31

2.7. Bioorthogonal ligations based on inverse electron demand diels-alder cycloadditions 33

2.8. Photochemical ligations..... 35

3. Transition metal-catalyzed transformations in biological settings 37

3.1. Organometallic catalysis. Reactions in aqueous media 37

3.2. Transition metal catalysis in biological habitats and living cells 40

4. Conclusions 48

GENERAL OBJECTIVES..... 49

CHAPTER 2. COPPER AZIDE-ALKYNE CYCLOADDITION IN MAMMALIAN CELLS..... 53

1. CuAAC inside live mammalian cells 55

2. Objectives..... 59

3. Results and discussion..... 60

3.1. CuAAC reactions with *in situ* prepared tristriazole complexes..... 60

3.2. Cellular experiments with *in situ* prepared tristriazole complexes..... 70

3.3. CuAAC reactions with predefined copper (I) complexes..... 72

3.4. Cellular experiments with predefined Cu(I) complexes 77

3.5. Quantification of the reaction inside living cells 78

4. Conclusion..... 81

CHAPTER 3. Ru [2+2+2] CYCLOADDITION IN BIOLOGICAL MEDIA AND MAMMALIAN CELLS..... 83

1. Transition metal-promoted cycloadditions..... 85

2. TM-promoted [2+2+2] cycloadditions in aqueous and biological media: antecedents 88

3. Objectives..... 90

4. Results and discussion 91

4.1. Ruthenium-promoted intramolecular [2+2+2] cycloadditions in aqueous and biological settings 91

4.2. Ruthenium-promoted intramolecular [2+2+2] cycloadditions in cellular settings 92

4.3. Ruthenium-promoted intermolecular [2+2+2] cycloadditions in aqueous and biological settings 94

4.4. Ruthenium-promoted intermolecular [2+2+2] cycloadditions in cellular settings 105

4.5. Detection of intracellular cycloaddition products by HPLC-MS 110

4.6. Localized ruthenium-promoted intermolecular [2+2+2] cycloadditions in specific organelles 114

5. Conclusions 116

Chapter 4: PHOTOREDOX CATALYSIS IN LIVE MAMAMALIAN CELLS 117

1. Introduction into visible-light photochemistry 119

2. Fundamentals of the photo-Meerwein arylation 121

3.Visible light photocatalysis in aqueous media 123

4. Photocatalysis in biological settings 124

5. Objectives 128

7. Results and discussion 129

7.1. Photocatalyzed arylations of unsaturated substrates in aqueous media 129

7.2. Photocatalytic formal-cycloadditions in aqueous and biological settings 132

7.3. Photocatalytic formal-cycloaddition in cellular settings 142

8. Conclusions 143

OVERALL CONCLUSIONS 145

RESUMO DA TESE DOCTORAL 149

EXPERIMENTAL SECTION 161

LIST OF PUBLICATIONS 260

USC
UNIVERSIDADE DE SANTIAGO DE COMPOSTELA

Abbreviations and acronyms

Ac_4ManNAz	*N*-Azidoacetyl mannosamine
ACPK	N^{ε}-(((1*R*,2*R*)-2-Azidocyclopentyloxy)-carbonyl)-L-lysine
ACQ	Aggregation-caused quenching
AHA	Azidohomoalanine
AIE	Aggregation-induced emission
AQ	Anthraquinone
Azido-dATP	7-Deaza-2'-deoxyadenosine
BARAC	Biarylazacyclooctynone
BBTE	4-((Bis([1-(phenylmethyl)-1*H*-1,2,3-triazol-4-yl)methyl)amino)methyl)-1*H*-1,2,3-triazole1-ethanol
BCN	Bicyclononyne
Bpin	Pinacol boronic ester
Bpy	Bipyridine
BSA	Bovine serum albumin
BTTAA	2-(4-((Bis((1-*tert*-butyl)-1*H*-1,2,3-triazol-4-yl)methyl)-1*H*-1,2,3-triazol-1-yl)acetic acid
BTTE	3-(4- ((Bis((1-*tert*-butyl-1H-1,2,3-triazol-4-yl)methyl)amino)methyl)-1H-1,2,3-triazol-1- yl)ethanol
BTTP	3-(4- ((Bis((1-*tert*-butyl-1H-1,2,3-triazol-4-yl)methyl)amino)methyl)-1H-1,2,3-triazol-1-yl)propanol
BTTPS	3-(4- ((Bis((1-*tert*-butyl-1H-1,2,3-triazol-4-yl)methyl)amino)methyl)-1H-1,2,3-triazol-1-yl)propyl hydrogen sulfate
C	Cu(I) predefined complex
CoA	Coenzyme A
Cp	Cyclopentadienyl
Cp*	Pentamethylcyclopentadienyl
CPP	Cell penetrating peptide
CTCF	Corrected total cell fluorescence
COD	1,5-Cyclooctadiene
CuAAC	Copper catalyzed azide-alkyne cycloaddition
Cys	Cysteine
Cz	Carbazole
DCE	1,2-Dichloroethane
DCM	Dichloromethane
DEPT	Distortionless Enhancement by Polarization Transfer
DIFO	Difluorobenzocyclooctyne
DIPEA	*N*,*N*-Diisopropylethylamine
DMAP	4-Dimethylaminopyridine
DMEM	Dulbecco's modified eagle medium
DMF	*N*,*N*-Dimethyl formamide
DMN	Dimethylnapthhalimide
DMP	Dess-Martin periodinane
DMSO	Dimethyl sulfoxide
DNA	Deoxyribonucleic acid
DNP	2,4-Dinitrophenol
EDC	1-Ethyl-3-(3-dimethylaminopropyl)carbodiimide
EDG	Electron donor group
EDTA	Ethylenediaminetetraacetic acid
EPR	Electron paramagnetic resonance
Equiv.	Equivalents
E_t	Energy transfer
EWG	Electron withdrawing group

USC UNIVERSIDADE DE SANTIAGO DE COMPOSTELA

FRET ---------- Föster resonance energy transfer
GFP ---------- Green fluorescent protein
GSH ---------- Glutathione
HAT ---------- Hydrogen atom transfer
Hpg ---------- Homopropargyl glycine
HPLC ---------- High-performance liquid chromatography
ICP-MS ---------- Inductively coupled plasma mass spectrometry
ICT ---------- Intramolecular charge transfer
IEDDAC ---------- Inverse electron demand Diels-Alder cycloaddition
L ---------- Ligand
LC-MS ---------- Liquid chromatography-mass spectrometry
Lys ---------- Cell lysates
ManLev ---------- *N*-levulinoyl mannosamine
Met ---------- Methionine
MOF ---------- Metal organic framework
MONP ---------- Metal-organic nanoparticle
MTT ---------- 3-(4,5-Dimethylthiazol-2-yl)-2,5-diphenyl-2H-tetrazolium bromide assay
NaAsc ---------- Sodium ascorbate
NADH ---------- Nicotinamide adenine dinucleotide
NB ---------- Norbornane
NCL ---------- Native chemical ligation
NMR ---------- Nuclear magnetic resonance
NP ---------- Nanoparticle
OCT ---------- Cyclooctyne
p-Az ---------- *p*-Aziophenylalanine
PBS ---------- Phosphate-buffered saline
PC ---------- Photocatalyst
PDT ---------- Photodynamic therapy
PEG ---------- Poly(ethylene glycol)
PTZ ---------- Phenothiazine
ROS ---------- Reactive oxygen species
r. t. ---------- Room temperature
RuAtAC ---------- Ruthenium-catalyzed azide-thioalkyne cycloaddition
RuPhos ---------- 2-Dicyclohexylphosphino-2′,6′-diisopropoxybiphenyl
SET ---------- Single electron transfer
siaNAz ---------- Azido sialic acid
SIMes ---------- 1,3-Bis(2,4,6-trimethylphenyl)-4,5-dihydroimidazol-2-ylidene
SPAAC ---------- Strain-promoted azide-alkyne cycloaddition
TBAB ---------- tetrabutylammonium bromide
TBTA ---------- Tris(benzoyl-triazolylmethyl)amine
TCEP ---------- Tris(carboxyethyl) phosphine
TCO ---------- Transcyclooctene
TFA ---------- Trifluoroacetic acid
THPTA ---------- Tris((1-hydroxy-propyl-1H-1,2,3-triazol-4-yl)methyl)amine
THF ---------- Tetrahydrofuran
TM ---------- Transition metal
TMB ---------- Trimethoxybenzene
TMS ---------- Trimethylsilyl
TPA ---------- Triphenylamine
TPE ---------- Tetraphenylethylene
Tpa* ---------- N-((Tris(3,5-dimethyl-1-H-pyrazol-1-yl)methyl)))
TPP ---------- Triphenylphosphonium
Tppts ---------- Tris(m-sulfonatophenyl)-phosphine
Trp ---------- Tryptophan

USC UNIVERSIDADE DE SANTIAGO DE COMPOSTELA

TrPE ---------- Triphenylethylene

Tyr ---------- Tyrosine

9-Az-NeuAc ---------9-Azido-9-deoxy-N-acetylneuraminic acid

USC UNIVERSIDADE DE SANTIAGO DE COMPOSTELA

USC
UNIVERSIDADE
DE SANTIAGO
DE COMPOSTELA

INTRODUCTION

USC
UNIVERSIDADE
DE SANTIAGO
DE COMPOSTELA

USC
UNIVERSIDADE
DE SANTIAGO
DE COMPOSTELA

1. Chemical biology

As the smallest unit of life, the cell has been widely studied.[1] However, ultimately, the cell is not more than a soup of molecules that are perfectly organized, and therefore chemists, the experts in molecules, have been increasingly involved in interrogating and manipulating cellular and biological systems. This field of Chemical Biology encompasses a variety of topics that goes from the study of life from a chemical point of view, to the synthesis of biomolecules, the introduction of small molecules in biological systems or even the discovery of new chemical processes by taking inspiration from biology.[2,3]

For instance, the development of innocuous probes that are able to specifically label biomolecules or organelles,[4] the synthesis of proteins by Native Chemical Ligation (NCL)[5] or the use of optimized enzymes by direct evolution[6,7] are some "recent" research topics within the field of chemical biology (figure 1).

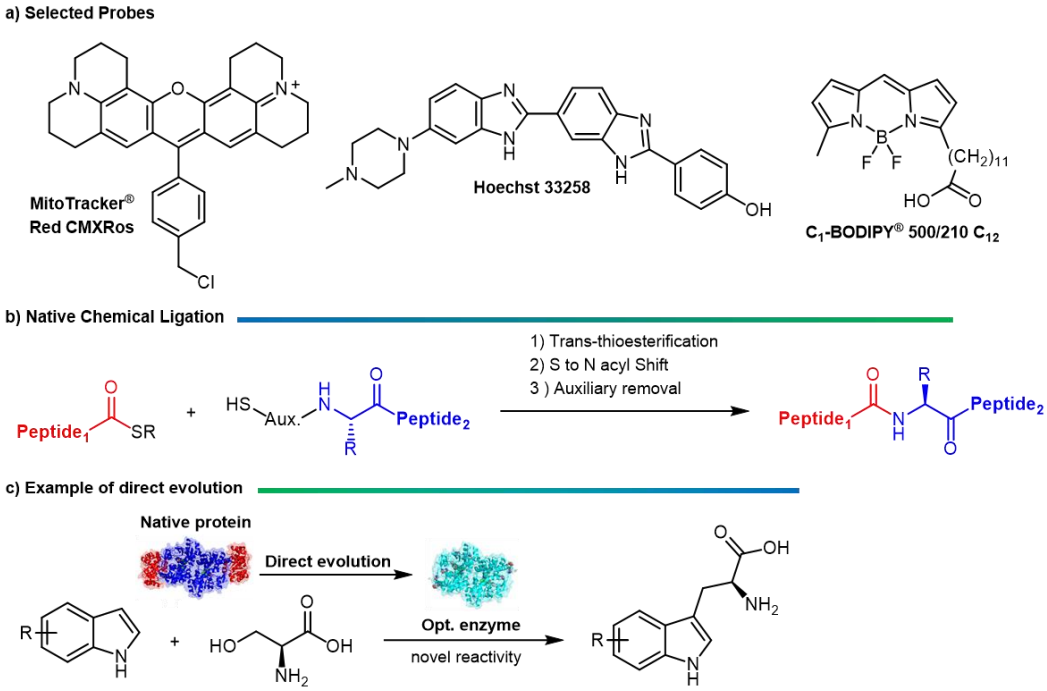

Figure 1. Some contributions of chemical biology to life science: a) Selected probes for organelle targeting and fluorescent staining: MitoTracker® as mitochondrial marker, Hoechst for nucleus staining and BODIPY® for lipids targeting. b) General scheme of a Native Chemical Ligation. c) Outline of an evolved enzyme to perform a specific reaction.[8]

[1] R. Hook, *Micrographia*, Royal Society, **1665**.
[2] *Nat. Chem. Biol.* **2015**, *11*, 363.
[3] K. L. Morrison, G. A. Weiss, *Nat. Chem. Biol.* **2006**, *2*, 3.
[4] I. Johnson, M. T. Z. Spence, The Molecular Probes Handbook 11th Ed, Molecular Probes, **2010**.
[5] S. S. Kulkarni, J. Sayers, B. Premdjee, R. J. Payne, *Nat. Rev.* **2018**, *2*, 0122.
[6] F. H. Arnold, *Acc. Chem. Rev.* **1998**, *31*, 125.
[7] K. Chen, F. H. Arnold, *Nat. Catal.* **2020**, *3*, 203.
[8] D. K. Romney, J. Murciano-Calles, J. E. Wehrmüller, F. H. Arnold, *J. Am. Chem. Soc.* **2017**, *139*, 10769.

2. Bioorthogonal chemistry

2.1. What is bioorthogonal chemistry

Despite the impressive progress of Chemical Biology over the last decades, there is still a lack of novel robust techniques and methodologies that contribute to the study of life in a harmless manner. In this sense, Bioorthogonal Chemistry was born as an approach to perform selected reactions in biological systems without perturbing the host metabolism (figure 2). Since its recent consolidation as an important branch of chemical biology, bioorthogonal chemistry has continued to grow in an exponential manner.[9] In the meantime, it has also contributed to revolutionize related fields such as cell imaging, drug development or biotechnology, due to its ability to manipulate small exogenous compounds in biological and living settings. Bioorthogonal tools supplement other biological post-translation modification strategies for protein tagging like "genetically encoded fluorescent proteins",[10] antibody recognition[11] or "avidine/streptavidine-biotin technology",[12,13] among others.

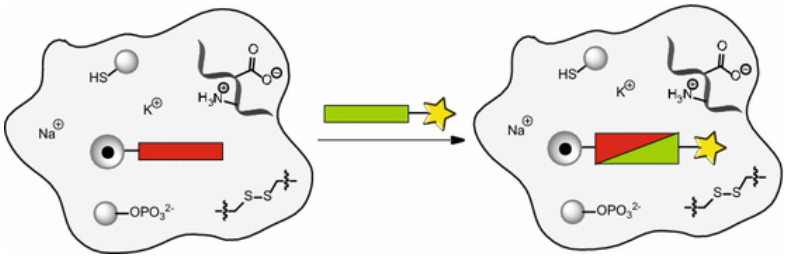

Figure 2. Simplified representation of a bioorthogonal modification in a living system.

Bioorthogonal reactions share some common features, such as: chemoselectivity, good performance under physiological conditions (that is, aqueous media, neutral pH, 37 ºC) and fast rates. The components of the transformations are generally exogenous to nature and consequently, should not be metabolized by the cell. They must be innocuous to the biological system and stable under physiological conditions.

Fast kinetics is one of the most important attributes since it allows not only to reduce the exposition time of the abiotic components to the biological system, but also to decrease the concentration of reagents. Along the years there has been intensive research on the development of fast bioorthogonal reactions based on the activation of substrates with strain, or by electronic tuning.[14] In contrast, the use of catalysts has been less explored.

[9] T. Cañeque, S. Müller, R. Rodriguez, *Nat. Rev. Chem.* **2018**, *2*, 202.
[10] G. U. Nienhaus, *Angew. Chem. Int. Ed.* **2008**, *47*, 8992.
[11] C. Milstein, G. Winter, *Nature* **1991**, *349*, 293.
[12] O. H. Laitinen, V. P. Hytönen, H. R. Nordlund, M. S. Kulomaa, *Cell. Mol. Life. Sci.* **2006**, *63*, 2992.
[13] Q. Le, V. Nguyen, S. Park, *Appl. Microbiol. Biotechnol.* **2019**, *103*, 7355.
[14] S. L. Scinto, D. A. Bilodeau, R. Hincapie, W. Lee, S. S. Nguyen, M. Xu, C. W. am Ende, M. G. Finn, K. Lang, Q. Lin, J. P. Pezacki, J. A. Prescher, M. S. Robillard, J. M. Fox, *Nat. Rev. Methods Primers* **2021**, *1*, 30.

Together with high reaction kinetics, chemoselectivity is the most pursued feature, since the reaction must be compatible with an important number of functional groups and biomolecules present in living systems.

Introducing other characteristics in the substrates, like soluble and lipophilic components to allow internalization, or targeting moieties to reach a specific location, are also important aspects to take into account when designing bioorthogonal tools.[15] Sometimes, a better biological assimilation is preferred rather than a very high reactivity.[16,17]

The most common strategy used in the application of bioorthogonal chemistry involves two main steps (figure 3). First, a molecule of interest is modified to bear a bioorthogonal functional tag (I), and is assimilated by the biological system (II). Second, a paired reacting partner bearing a probe (III) selectively reacts with the tag within the biological habitat (IV).[18,19] Although the focus of this research was initially set in bioconjugation approaches, bioorthogonal tools have been increasingly used for the controlled release of bioactive molecules,[20] or even for the synthesis of designed products.[21,22]

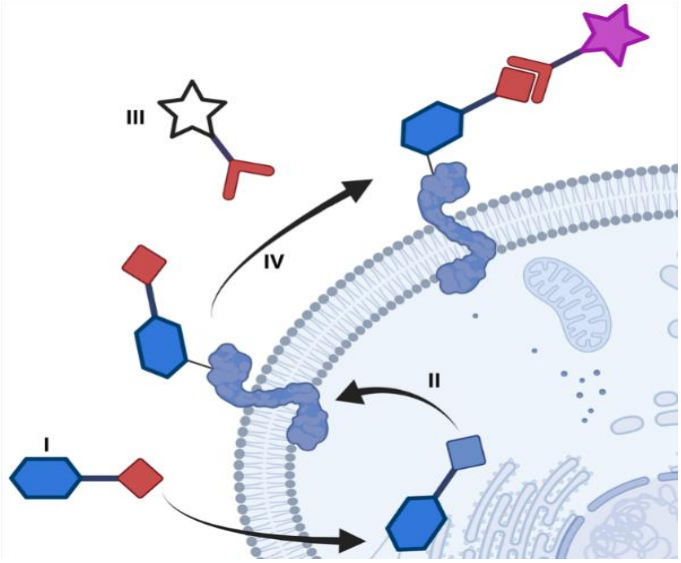

Figure 3. Bioorthogonal bioconjugation standard strategy. I = Molecule of interest (blue hexagon) bearing the bioorthogonal handle (red square); II = Assimilation by the biological system; III = Inactivated probe partner (colorless star), bearing the biorthogonal counterpart tag; IV = Bioorthogonal transformation that leads to the bioconjugation of the molecule of interest.

[15] Y. Tian, Q. Lin, *ACS Chem. Biol.* **2019**, *14*, 2489.
[16] C. P. Ramil, M. Dong, P. An, T. M. Lewandowski, Z. Yu, L. J. Miller, Q. Lin, *J. Am. Chem. Soc.* **2017**, *139*, 13376.
[17] J. Miguel-Ávila, M. Tomás-Gamasa, A. Olmos, P. J. Pérez, J. L. Mascareñas, *Chem. Sci.* **2018**, *9*, 1947.
[18] E. M. Sletten, C. R. Bertozzi, *Angew. Chem. Int. Ed.* **2009**, *48*, 6974.
[19] E. M. Sletten, C. R. Bertozzi, *Acc. Chem. Res.* **2011**, *44*, 666.
[20] J. Wang, X. Wang, X. Fan, P. R. Chen, *ACS Cent. Sci.* **2021**, 7, 929.
[21] M. O. N. van de L'Isle, M. C. Ortega-Liebana, A. Unciti-Broceta, *Curr. Opin. Chem. Biol.* **2021**, *61*, 32.
[22] D. P. Nguyen, H. T. H. Nguyen, L. H. Do, *ACS Catal.* **2021**, *11*, 5148.

2.2. The birth of bioorthogonal chemistry: Hydrazone ligations

The term Bioorthogonal Chemistry was coined for the first time in 2003 by Prof. Bertozzi.[23] Despite its recent birth, it is difficult to ensure which is the first real bioorthogonal reaction due to its close relation to the selective modification of proteins.[19] Nevertheless, a few reports from Rideout and coworkers between late 1980s and early 1990s can be considered among the first publications dealing with bioorthogonal principles.[24,25,26] In these articles the authors demonstrated the viability of performing hydrazine-aldehyde condensations in the presence of bacteria or cells (figure 4a). The efforts were focused on the design of substrates than can be internalized by cells where the reaction could take place efficiently (figure 4b). The ligation was applied for the selective generation of cytotoxicity in specific cells.

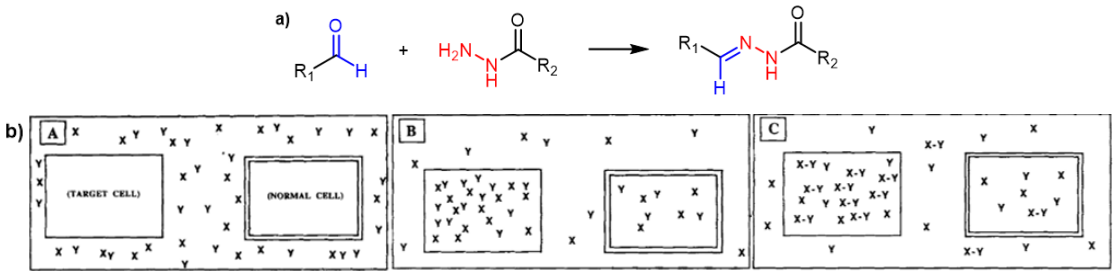

Figure 4. a) Reaction scheme by Rideout: hydrazine-aldehyde condensation. b) Representative description of a selective reaction inside cells by Rideout in 1990, before the definition of bioorthogonal chemistry. A) Incubation of normal and target cells, with both substrates X and Y. B) Selective internalization of X and Y in the target cell. C) Reaction inter and intracellular.[26]

This strategy was further improved by Bertozzi and coworkers in 1997 (figure 5). They succeeded in performing a similar type of condensation in Jurkat or HeLa cell surfaces, by expressing in excess, a mannose derivative (ManLev, 5 mM) bearing a ketone group in the cellular membrane. An exogenous hydrazine probe modified with biotin (1 mM) was used as coupling partner and allowed to react at room temperature for 2 h.[27,28]

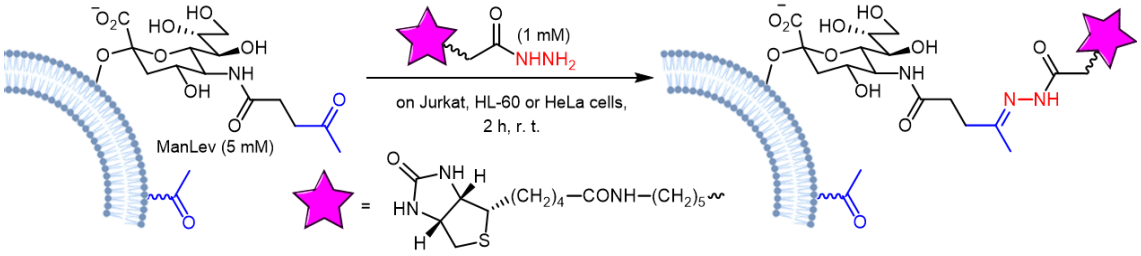

Figure 5. Ketone-acylhydrazine condensation on mammalian cell surface, by Bertozzi and coworkers in 1997.[27]

USC UNIVERSIDADE DE SANTIAGO DE COMPOSTELA

[23] H. C. Hang, C. Yu, D. K. Kato, C. R. Bertozzi, *Proc. Natl. Acad. Sci. U.S.A.* **2003**, *100*, 14846.
[24] D. Rideout, *Science* **1986**, *233*, 561.
[25] D. Rideout, J. Jaworski, R. Dagnino, *Biochem. Pharm.* **1988**, *37*, 4505.
[26] D. Rideout, T. Calogeropoulou, J. Jaworski, M. McCarthy, *Biopolymers* **1990**, *29*, 247.
[27] L. K. Mahal, K. J. Yarema, C. R. Bertozzi, *Science* **1997**, *276*, 1125.
[28] H. C. Hang, C. R. Bertozzi, *J. Am. Chem. Soc.* **2001**, *123*, 1242.

Since these pioneering examples, it was not until 2003 that the first intracellular bioorthogonal version saw the light. The Schultz's group described an intracellular condensation between N-acetyl-L-phenylalanine previously expressed in *E. coli* proteins and either a fluorescent or biotinylated hydrazine probe.[29] However, the first mammalian intracellular version of this type of coupling was reported by the Kool's group 10 years later. In this case, an exchange strategy that involves a hydrazone fluorescein derivative, coupled with a Föster Resonance Energy Transfer (FRET) fluorescence quencher (Q, figure 6), was designed. This inactive hydrazone (20 μM) was exchanged along 1 h, with the target aldehyde (100 μM) using 2,4-dimethoxyaniline as organic catalyst (10 mM, figure 6). The reaction promotes the release of the quencher as an aldehyde derivative, liberating a fluorescent hydrazone in the process.[30]

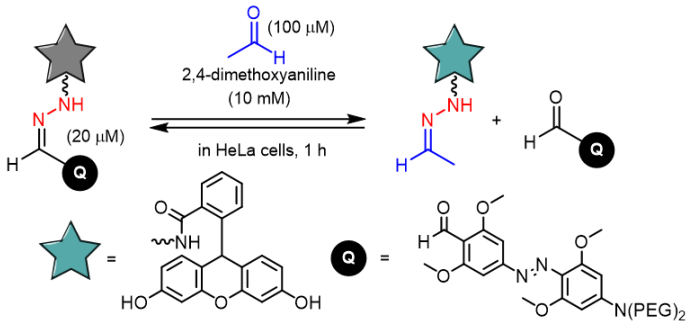

Figure 6. Hydrazone exchange in HeLa cells, developed by Kool and co-workers in 2016. PEG = poly(ethylene glycol) as flexible group for energy release.[30]

Despite the hydrazone condensation can be considered among the first bioorthogonal reactions, and a breakthrough in the field,[31] it was quickly set apart mainly due to selectivity problems (competition with endogenous aldehydes, ketones) or side reactions like hydrolysis. Thus, the research moved towards other transformations like the Staudinger ligation or the azide-alkyne cycloaddition.

USC UNIVERSIDADE DE SANTIAGO DE COMPOSTELA

[29] P. G. Schultz, Z. Zhang, B. A. C. Smith, L. Wang, A. Brock, C. Cho, *Biochemistry* **2003**, *42*, 6735.
[30] E. T. Kool, L. H. Yuen, N. S. Saxena, H. S. Park, K. Weinberg, *ACS Chem. Biol.* **2016**, *11*, 2312.
[31] E. T. Kool, D. K. Kölmel, *Chem. Rev.* **2017**, *117*, 10358.

2.3. Staudinger ligation

The Staudinger reduction was proposed by Meyer and Staudinger in 1919,[32,33] and involves the conversion of organic azides into amines through the formation of iminophosphoranes (figure 7).

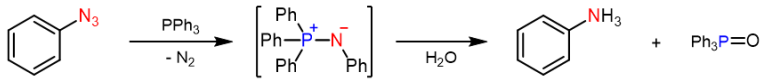

Figure 7. Transformation proposed by Meyer and Staudinger in 1919.[32,33]

This reaction was brought to the field of chemical biology in 2000 by Bertozzi and coworkers,[34] with the design of a ligation version to couple phosphines and azides (figure 8), which fits with the concept of a bioorthogonal transformation. These two functional groups, are totally abiotic and show an amazing orthogonality and biocompatibility.[19] The ligation involves an ortho-phosphine terephthalic acid analogue. After the reaction with the corresponding azide, and nitrogen loss, the aza-ylide **I** is trapped by the ester group, undergoing a cyclization to give the oxazaphosphetane **II**. In the aqueous environment, the intermediate **II** is hydrolyzed, affording a *p*-carbamoylbenzoic acid analogue, with a phosphine oxide in its structure, as a final product. Therefore, in this case the ligation entails the formation of an amide bond.[33]

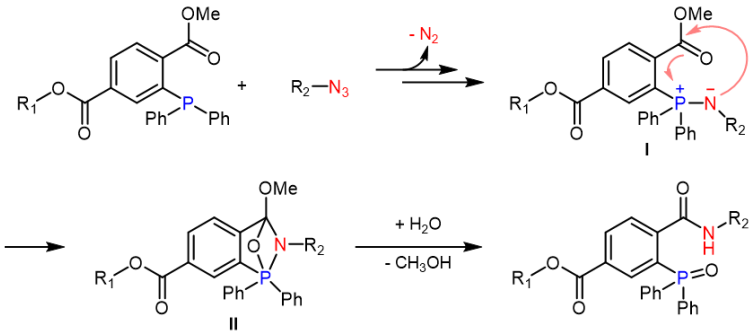

Figure 8. Mechanism of the Staudinger ligation designed by Bertozzi in 2000.[34]

These authors were able to metabolically incorporate azidosugars into the membrane of Jurkat or HeLa mammalian cells. The small size of the azide group is neglected by the biosynthetic machinery, allowing the assembly of glycoproteins bearing the azide function at specific points of the cell surface. The coupling partner (1 mM) containing the phosphine group was modified to exhibit a biotin for a posterior interaction with avidin, and allowed to react for one hour at room temperature in presence of incubated cells modified with azidosugar.

USC UNIVERSIDADE DE SANTIAGO DE COMPOSTELA

[32] H. Staudinger, J. Meyer, *Helv. Chim. Acta* **1919**, *2*, 635.
[33] C. Bednarek, I. Wehl, N. Jung, U. Schepers, S. Bräse, *Chem. Rev.* **2020**, *120*, 4301.
[34] C. R. Bertozzi, E. Saxon, *Science* **2000**, *287*, 2007.

The bioorthogonal coupling presented at least a two-fold improved efficiency, in comparation to the hydrazone ligation (figure 9).[34] Furthermore, the group of Bertozzi expanded this methodology through the years, to carry out the reactions in parallel with the hydrazone condensation,[35] or even in mice.[36]

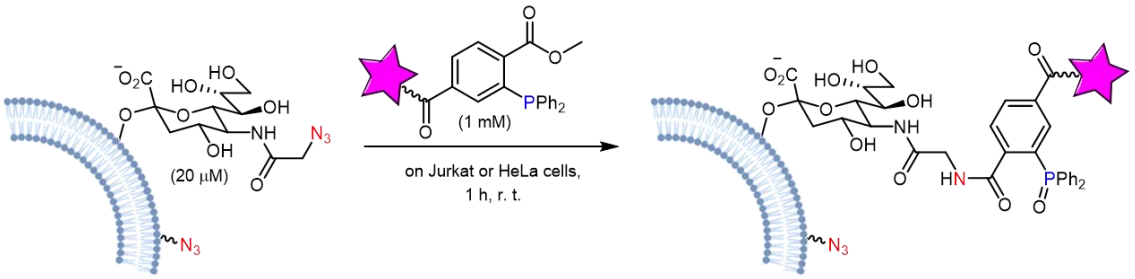

Figure 9. Staudinger ligation performed on mammalian cell surface by Bertozzi in 2000.[34]

These studies demonstrated the high level of bioorthogonality of the azide functionality, which has been widely used in the field. Its inertness, small size and unique reactivity that arises from its 1,3 – dipole character makes the azide a very appealing functional group for abiotic ligations in biological settings.[37] The azide moiety has been since then introduced into many other molecules that can be incorporated into biological polymers through metabolic pathways.[38,39] Some of them are indicated in figure 10: a) acetylated N-azidoacetylmannosamine (Ac_4ManNAz) which is metabolized into azido-sialic acid (siaNAz) and expressed on cell surface;[34] b) azidohomoalanine (AHA) which is metabolized by cells as a methionine (Met) analogue;[40] c) *p*-azidophenyalanine (*p*-Az) that has been introduced by genetic code expansion;[41] d) an azido 7-deaza-2'-deoxyadenosine (Azido-dATP) analogue that has been used for the modification of DNA.[42]

2546

[35] P. V. Chang, J. A. Prescher, M. J. Hangauer, C. R. Bertozzi, *J. Am. Chem. Soc.* **2007**, *129*, 8400.
[36] J. A. Prescher, D. H. Dube, C. R. Bertozzi, *Nature* **2004**, *430*, 873.
[37] M. F. Debets, C. W. J. Van der Doelen, F. P. J. T. Rutjes, F. L. Delft, *ChemBioChem* **2010**, *11*, 1168.
[38] N. J. Pedowitz, M. R. Pratt, *RSC Chem. Biol.* **2021**, *2*, 306.
[39] K. Lang, J. W. Chin, *Chem. Rev.* **2014**, *114*, 4764.
[40] K. L. Kiick, E. Saxon, D. A. Tirrell, C. R. Bertozzi, *Proc. Natl. Acad. Sci. USA* **2002**, *99*, 19.
[41] M. Tsao, F. Tian, P. G. Schultz, *ChemBioChem* **2005**, *6*, 2147.
[42] S. H. Weisbrod, A. Marx, *Chem. Commun.* **2007**, 1828

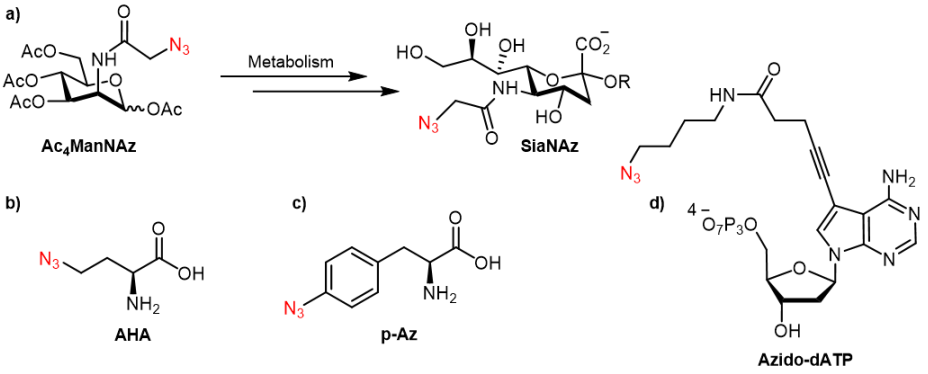

Figure 10. Some of the azido-biomolecules employed in the Staudinger ligation and further bioorthogonal transformations.

As important as the internalized azide-tagged biomolecule, is the reaction partner. On this regard, the group of Bertozzi explored the use of smart probes, compounds that are fluorescent only after the reaction takes place.[43] For this purpose, they developed a coumarin smart probe in which the fluorescence is quenched via an intramolecular charge transfer (ICT) pathway which involves the lone pair of electrons of a phosphine group. After the reaction with an AHA bearing protein (65 μg/mL) and 200 μM of coumarin, a 60-fold fluorescence increase was observed (figure 11).[44] Since then, the use of smart probes for bioorthogonal labeling has become each day more popular until turning into a standard strategy in bioorthogonal chemistry.

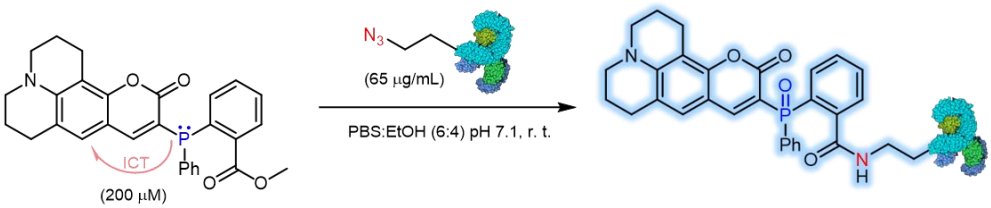

Figure 11. Staudinger ligation developed by Bertozzi using smart probes with intramolecular charge transfer quenching in 2003.[44]

Although the Staudinger reaction was the first bioorthogonal process that could be translated and widely used in cells and even in living systems, it presents important drawbacks. For instance, it is among the slowest bioorthogonal reactions.[45,46]

USC UNIVERSIDADE DE SANTIAGO DE COMPOSTELA

[43] P. Shieh, C. R. Bertozzi, *Org. Biomol. Chem.* **2014**, *12*, 9307.
[44] G. A. Lemieux, C. L. De Graffenried, C. R. Bertozzi, *J. Am. Chem. Soc.* **2003**, *125*, 4708.
[45] A. S. Cohen, E. A. Dubikovskaya, J. S. Rush, C. R. Bertozzi, *J. Am. Chem. Soc.* **2010**, *132*, 8563.
[46] B. L. Oliveira, Z. Guo, G. J. L. Bernardes, *Chem. Soc. Rev.* **2017**, *46*, 4895.

2.4. The azide-alkyne cycloaddition. The rise of click chemistry

Initially the term "click" chemistry was coined by Sharpless in 2001 for a type of reactions very simple to perform,[47] insensitive to water or oxygen, and fast kinetics. However, this definition has evolved along the years. Nowadays, the requirements of a transformation to be categorized as "click" should feature: modularity, broad scope, efficiency (high yielding), stability of the products under physiological conditions, generation of inoffensive byproducts (removed by non-chromatographic methods) or no generation at all, and stereospecificity. Besides that, the process must use simple reaction conditions, readily available starting materials and reagents, a benign solvent (preferably water), easy to remove or no solvent at all. These attributes described for click reactions overlap in great measure with those of bioorthogonal ligations. Both concepts reflect the same underlying chemical principles applied to different purposes, either to improve synthetic outcomes, or to perform selective transformations in biological media.[48]

Not surprisingly, the azide functional group is highly appealing for click-like transformations,[37] due to its intrinsic reactivity as 1,3 dipole.[49] However, the azide-alkyne cycloaddition require elevated temperatures and tend to give different mixtures of isomers (1,4 and 1,5-disubstituted-1,2,3-triazoles), which restricts their potential applications in the field (figure 12).[50,51] The situation completely changed in 2002, when Sharpless,[52] and Meldal[53] independently published the use of metal catalysts to speed up this transformation (more than 10000 citations each paper). Specifically, they observed that the addition of copper(I) salts had a tremendous impact in the course of the reaction, improving kinetics (100 million-fold), increasing yields and robustness, under smooth conditions (water became the preferred solvent). Furthermore, the Cu-catalyzed transformation selectively furnishes the 1,4-triazole isomer as the only product. As a result, the CuAAC (acronym for copper(I) catalyzed azide-alkyne cycloaddition) became on its own merits the paradigm of a click transformation.

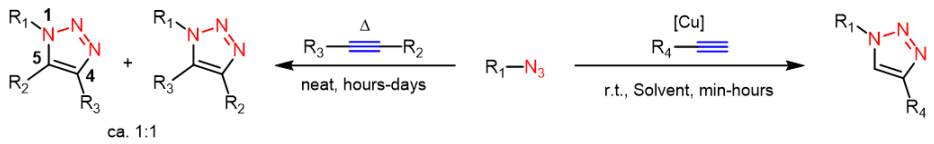

Figure 12. Both classical non catalyzed azide-alkyne cycloaddition (left), and the copper catalyzed azide-alkyne aycloaddition (CuAAC) (right).

[47] H. C. Kolb, M. G. Finn, K. B. Sharpless, *Angew. Chem. Int. Ed.* **2001**, *40*, 2004.
[48] C. S. McKay, M. G. Finn, *Chem. Biol.* **2014**, *21*, 1075.
[49] M. Breugst, H. Reissig, *Angew. Chem. Int. Ed.* **2020**, *59*, 12293.
[50] G. Szeimies, L. Moebius, R. Huisgen, *Chem. Ber.* **1967**, *100*, 2494.
[51] F. Himo, T. Lovell, R. Hilgraf, V.V. Rostovtsev, L. Noodleman, K. B. Sharpless, V. V. Fokin, *J. Am. Chem. Soc.* **2005**, *127*, 210.
[52] V. V. Rostovtsev, L. G. Green, V. V. Fokin, K. B. Sharpless, *Angew. Chem. Int. Ed.* **2002**, *41*, 2596.
[53] C. W. Tornoe, C. Christensen, M. Meldal, *J. Org. Chem.* **2002**, *67*, 3057.

Due to the importance of this reaction, its mechanism has been deeply studied and has evolved over the years. The currently accepted version entails the formation of dinuclear Cu intermediates as it is shown in figure 13.[54] The catalytic cycle would start with the formation of s-bound copper intermediate, followed by the interaction of a *p*-bound copper atom to form the copper acetylide (**I**). Then, coordination with the corresponding azide could occur in a reversible manner (**II**). Subsequently, a nucleophilic attack at the N-3 of the azide by the b-carbon of the acetylide would lead to the six-membered metallacycle **III**, that after a reductive elimination will afford the main triazole skeleton (**IV**). A final protonation step would yield the expected 1,4-triazole.[55]

Experimental evidence for the acetylide formation is strong, not only the isolation of this species,[56] but also because of the fail of internal alkynes to undergo the reaction. The pi-interaction of the copper with the alkyne would decrease the pKa helping in the acetylide formation. Meanwhile the formation of intermediate **III** is supported by isotopic experiments that show homologation of both copper atoms and by the isolation of acetylide and triazolide species bearing two copper atoms.[57] The final intermediate **IV** has also been isolated corroborating the last step.[54]

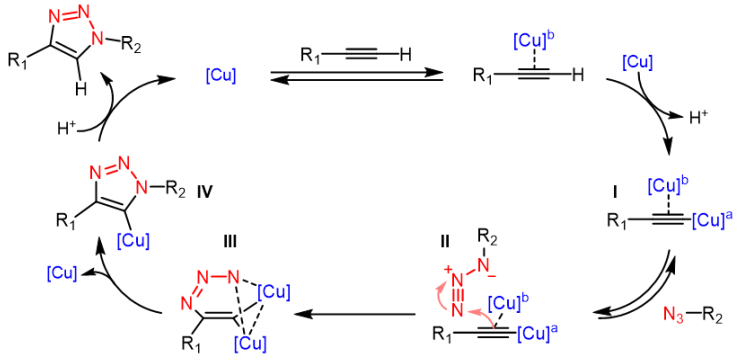

Figure 13. Currently accepted mechanism for the CuAAC.[54,55]

USC UNIVERSIDADE DE SANTIAGO DE COMPOSTELA

[54] H. B. E. Ayouchia, L. Bahsis, H. Anane, L. R. Domingo, S. Stiriba, *RSC Adv.* **2018**, *8*, 7670.
[55] B. T. Worrell, J. A. Malik, V. V. Fokin, *Science* **2013**, *340*, 457.
[56] C. Nolte, P. Meyer, B. F. Straub, *Angew. Chem. Int. Ed.* **2007**, *46*, 2101.
[57] L. Jin, D. R. Tolentino, M. Melaimi, G. Bertrand, *Sci. Adv.* **2015**, 1.

2.5. Applications of the CuAAC in chemical biology

The use of the CuAAC as a ligation tool in biological chemistry was initially oriented towards the modification of proteins[53,58] or other biopolymers like DNA,[59] or virus capsid.[60] These early CuAAC reactions were carried out in aqueous buffers like phosphate saline solution (PBS) or mixed with organic solvents, using $CuSO_4$ as copper source (1 equiv), and 4 equivalents of sodium ascorbate (NaAsc) as a reductant to ensure the formation of a Cu(I) complex. Very soon it was discovered that the reaction is better performed in the presence of external copper ligands. Common ligands are based on tris(triazolylmethyl)amine scaffolds (figure 14), which protect the copper atom from oxidation and improve the kinetics due to the increase of electron density on the metal center.[61] This type of complexes have evolved over the time and have been adapted to the bioorthogonal needs by the incorporation of bulky electron rich groups such as ^{t}Bu,[62] chelating substituents such as acids (BTTAA), alcohols (BTTP or THPTA) or soluble moieties like sulfonates (BTTPS).[63] In this regard, BTTAA has been until now the most efficient ligand,[64] meanwhile alcohol-based ligands added in excess are able to minimize the reactive oxygen species (ROS) generation.[65]

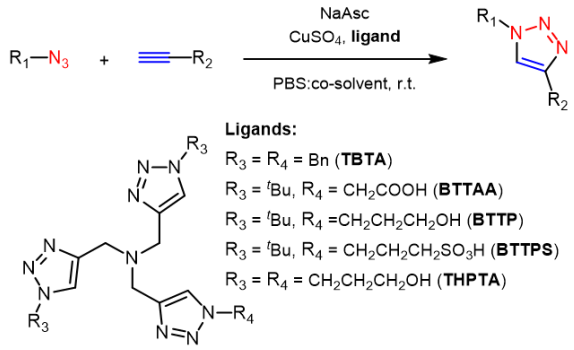

Figure 14. Typical CuAAC conditions for bioconjugation and common employed catalysts.

The knowledge acquired in the bioorthogonal studies of the Staudinger ligation, for the incorporation of azido groups in biological systems, favored a rapid translation of the CuAAC to the area of biological chemistry.

[58] A. E. Speers, G. C. Adam, B. F. Cravatt, *J. Am. Chem. Soc.* **2003**, *125*, 4686.
[59] H. Ruparel, Z. Li, T. S. Seo, J. Ju, *J. Org. Chem.* **2003**, *68*, 609.
[60] Q. Wang, T. R. Chan, R. Hilgraf, V. V. Fokin, K. B. Sharpless, M. G. Finn, *J. Am. Chem. Soc.* **2003**, *125*, 3192.
[61] T. R. Chan, R. Hilgraf, K. B. Sharpless, V. V. Fokin, *Org. Lett.* **2004**, *6*, 2853.
[62] W. Wang, S. Hong, A. Tran, H. Jiang, R. Triano, Y. Liu, X. Chen, P. Wu, *Chem. Asian J.* **2011**, *6*, 2796.
[63] D. Soriano del Amo, W. Wang, H. Jiang, C. Besanceney, A. C. Yan, M. Levy, Y. Liu, F. L. Marlow, P. Wu, *J. Am. Chem. Soc.* **2010**, *132*, 16893.
[64] C. Besanceney-Webler, H. Jiang, T. Zheng, L. Feng, D. Soriano del Amo, W. Wang, L. M. Klivansky, F. L. Marlow, Y. Liu, P. Wu, *Angew. Chem. Int. Ed.* **2011**, *50*, 8051.
[65] S. Li, H, Cai, J. He, H. Chen, S. Lam, T. Cao, Z. Zhu, S. J. Bark, C. Cai, *Bioconjugate Chem.* **2016**, *27*, 2315.

The first example of this reaction in living bacteria was published in 2003 by Tirrell and coworkers (figure 15). In this work, they overexpressed on the surface of *E. coli* a protein bearing an AHA aminoacid by genetic engineering, and demonstrated the viability of performing a CuAAC transformation using a biotinylated alkyne (16 h, 4 ºC). They used $CuSO_4$ as copper source (100 μM), tris(benzoyltriazolylmethyl)amine (TBTA, 200 μM) as ligand, and tris(carboxyethyl)phosphine (TCEP, 200 μM) as reductant to avoid the oxidation of copper and thiols.[66]

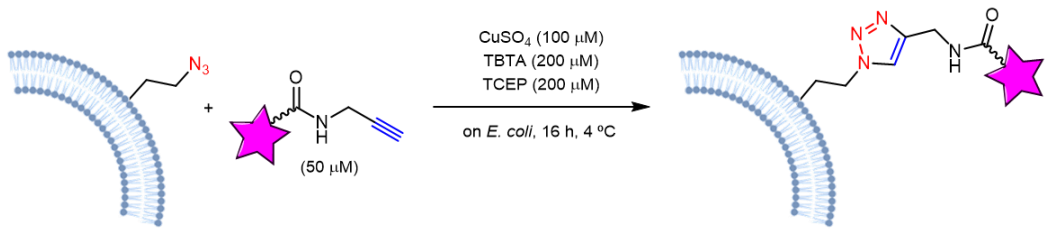

Figure 15. First CuAAC trasfromation performed on bacterial cell surface developed by Tirrell's group in 2003.[66]

A couple of years later, Tirrell's group changed the strategy and incorporated the alkyne moiety into the unnatural amino acid, instead of the azide functionality. Thus, they introduced an homopropargyl glycine (Hpg) as methionine (Met) analogue on the bacterial machinery[67] and later in mammalian cells (figure 16).[68] In both cases, they used a fluorogenic azido-coumarin probe as membrane permeable coupling partner. After the formation of the triazole, the lone pair of electrons from the azide gets delocalized, preventing an ICT, and as a consequence, there is a drastic increase of fluorescence.[43] However, the protocol required the fixation of cells with paraformaldehyde before the treatment with 200 μM $CuSO_4$, 400 μM TCEP, 200 μM TBTA and 25 μM of the probe. This strategy was further improved in 2010 by Wu's group, demonstrating that the transformation can be achieved in zebrafish embryos. The development of a sulfonate triazole ligand (BTTPS) allowed to decrease the cytotoxicity of Cu(I) complexes.[63]

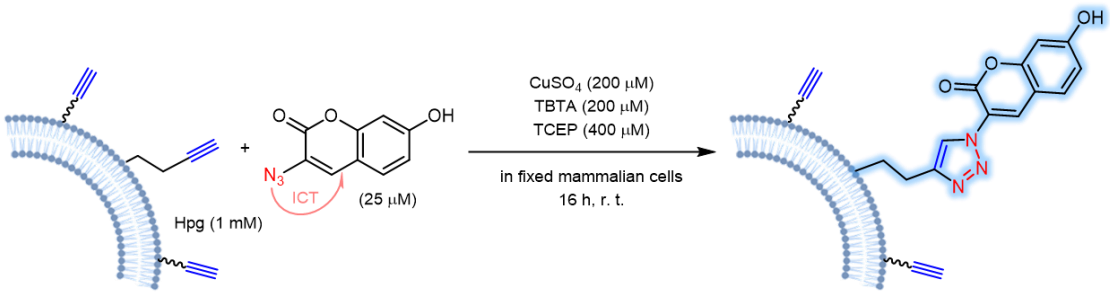

Figure 16. CuAAC performed in fixed mammalian cells with an intramolecular charge transfer quenched azide-coumarin developed by Tirrell and co-workers in 2006.[68]

[66] A. J. Link, A. Tirrell, *J. Am. Chem. Soc.* **2003**, *125*, 11164.
[67] K. E. Beatty, F. Xie, Q. Wang, D. A. Tirrell, *J. Am. Chem. Soc.* **2005**, *127*, 14150.
[68] K. E. Beatty, J. C. Liu, F. Xie, D. C. Dieterich, E. M. Schuman, Q. Wang, D. A. Tirrell, *Angew. Chem. Int. Ed.* **2006**, *45*, 7364.

One of the most important contributions in the area was described by Chen and co-workers. In 2012, the group made a first incursion into intracellular bacterial CuAAC reactions with unfixed cells, applying this transformation for intracellular pH detection.[69] Yet, the group optimized the protocol in 2014. They studied the bioconjugation between an azido-lysine (ACPK) containing GFP (Green Fluorescent Protein) expressed inside *E. coli* by means of genetic code expansion and an alkyne-dimethylnaphthalimide (DMN) probe (figure 17). They found that some aforementioned complexes based on BTTP or BTTAA ligands excelled in promoting the reaction, while others negative charged species, such BTTPS based complexes, were unable to enter the cell. As observed in previous works, under optimized conditions (100 μM $CuSO_4$, 200 μM ligand, 2.5 mM NaAsc and 300 μM of alkyne probe), the more common TBTA ligand was unable to mask copper toxicity, meanwhile BTTP was the best ligand for performing the process inside living bacteria.[70]

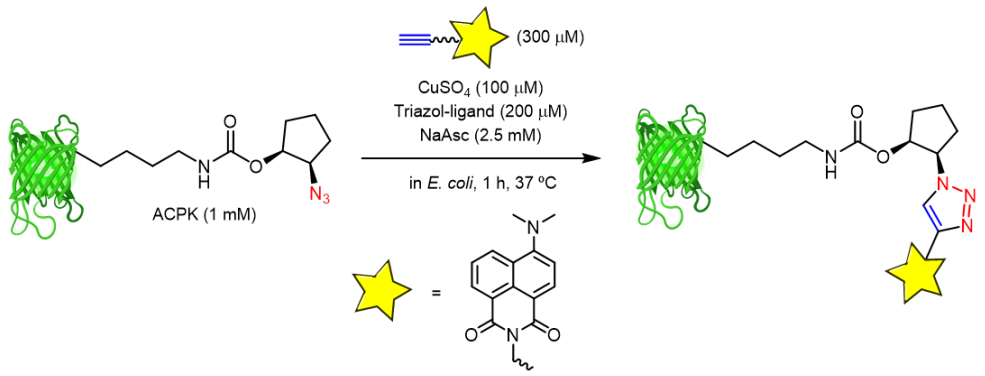

Figure 17. CuAAC performed on GFP within living bacteria cell by Chen and Co-workers in 2014.[70]

Cu nanoparticles (NP) have also been used as reagents for CuAAC. Therefore, in 2016 Bradley and coworkers reported that the use of environment protected Cu-NP located within a polymeric support, allow bioorthogonal ligations in the extracellular space of mammalian cells.[71]

USC UNIVERSIDADE DE SANTIAGO DE COMPOSTELA

[69] M. Yang, Y. Song, M. Zhang, S. Lin, Z. Hao, Y. Liang, D. Zhang, P. R. Chen, *Angew. Chem. Int. Ed.* **2012**, *51*, 7674.
[70] M. Yang, A. S. Jalloh, W. Wei, J. Zhao, P. Wu, P. R. Chen, *Nat. Commun.* **2014**, *5*, 4981.
[71] J. J. Mullins, J. Clavadetscher, S. Hoffman, A. Lilienkampf, L. Mackay, R. M. Yusop, S. A. Rider, M. Bradley, *Angew. Chem. Int. Ed.* **2016**, *55*, 15662.

This type of click biorthogonal cycloadditions can be also promoted by ruthenium complexes.[72,73,74] Therefore, the group of Mascareñas demonstrated in 2017 that thioalkynes react very efficiently with azides, using Ru(II) catalysts, in the presence of biomolecules or even bacteria cells.[75] More recently, the group reported a photo-triggered version of this transformation, that can be even applied to peptides (figure 18). Using different ruthenium arene sandwich complexes, they were able to activate the catalyst with light, improving the yields and decreasing the concentration of substrates required to perform the reaction to the micromolar range (500 μM peptide, 1 mM thioalkyne and 250 μM Ru catalyst). Interestingly, the group also showed that this process is compatible with a canonical CuAAC, which renders the ruthenium-catalyzed azide-thioalkyne cycloaddition (RuAtAC), as powerful and complementary tool in the field of bioorthogonal chemistry.[76]

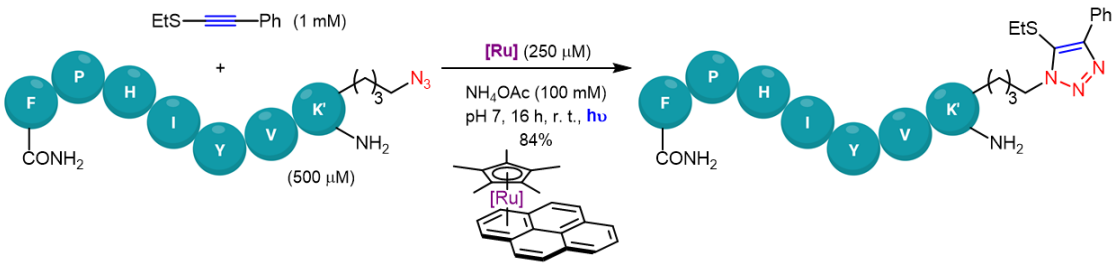

Figure 18. Photo-triggered RuAtAC applied to peptide modification developed by Mascareñas group in 2021.[76]

Despite the enormous biological potential of the CuACC reaction, examples of intracellular reactions are still very limited, owing to the instability of the copper, its potential cytotoxicity and its easy deactivation in the complex environment of a cell. For instance, copper atoms are regulated in cells and can be trapped by copper binding proteins.[77] Also, inner thiols can bind copper, inactivating the catalyst and generating oxidative stress. Nevertheless, these limitations differ among the complexes employed and therefore there's place for "upgrades".[78,79] The most recent contributions in this topic will be specifically discussed in chapter II.

[72] L. Zhang, X. Chen, P. Xue, H. H. Y. Sun, I. D. Williams, K. B. Sharpless, V. V. Fokin, G. Jia, *J. Am. Chem. Soc.* **2005**, *127*, 15998.
[73] T. Wang, F. Wu, G. Chiang, S. He, Y. Lo, J. Organomet. Chem. **2014**, *774*, 57.
[74] H. X. Siyang, H. L. Liu, X. Y. Wu, P. N. Liu, *RSC Adv.* **2015**, *5*, 4693.
[75] P. Destito, J. R. Couceiro, H. Faustino, F. López, J. L. Mascareñas, *Angew. Chem. Int. Ed.* **2017**, *56*, 10766.
[76] A. Gutiérrez-González, P. Destito, J. R. Couceiro, C. Pérez-González, F. López, J. L. Mascareñas, *Angew. Chem. Int. Ed.* **2021**, *60*, 16059.
[77] M. T. Morgan, D. Bourassa, S. Harankhedkar, A. M. McCallum, S. A. Zlatic, J. S. Calvo, G. Meloni, V. Faundez, C. J. Fahrni, *Proc. Natl Acad. Sci. USA* **2019**, *116*, 12167.
[78] D. C. Kennedy, C. S. McKay, M. C. B. Legault, D. C. Danielson, J. A. Blake, A. F. Pegoraro, A. Stolow, Z. Mester, J. P. Pezacki, *J. Am. Chem. Soc.* **2011**, *133*, 17993.
[79] L. M. Gaetke, C. K. Chow, *Toxicology* **2003**, *189*, 147.

2.6. Strain-promoted azide-alkyne cycloadditions

The use of metals for promoting bioorthogonal cycloadditions is appealing, because they don't require especially reactive substrates. However, in recent years there have been many advances in a different strategy based on the use of strained reactants, which avoids the employ of metals. Inspired by Huisgen,[80] but especially by the work of Wittig and Krebs with strained cycloalkynes,[81] the group of Bertozzi investigated the strain-promoted azide-alkyne cycloaddition (SPAAC), in parallel with the development of the Staudinger ligation. They needed activated alkynes to perform the reaction, and found that the cycloaddition of cyclootyne and azides take place at room temperature without the need of a catalyst (figure 19).

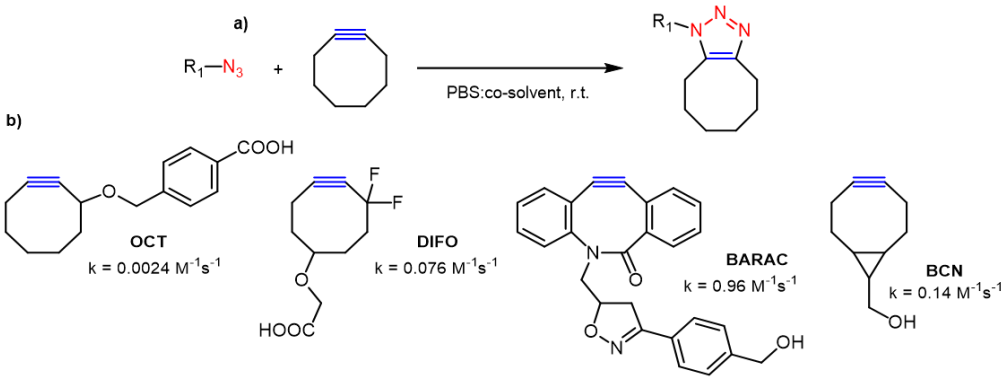

Figure 19. a) General conditions for SPAAC labeling. b) Common strained cyclooctynes and their kinetics.[19]

Other cycloalkynes with improved water solubility, or better kinetics due to a higher ring strain or the presence of electron withdrawing groups (EWG) such as fluorine atoms[82,83] and fused aryl rings, have been described.[84,85]

The first application of the SPAAC transformation in a biological context appeared in 2004. An azido-sugar was expressed on cell surface of CHO and Jurkat mammalian cells and the labeling with the cyclooctyne (OCT) was demonstrated.[86] Some years later, in 2007, Bertozzi and co-workers implemented a new difluorobenzocyclooctyne (DIFO) coupled with an Alexa Fluor 488 probe (100 μM), for the SPAAC reaction. At 37 ºC, they could observe, cell-binding in a matter of minutes (figure 20).[82]

[80] R. Huisgen, *Proc. Chem. Soc.* **1961**, 357.
[81] G. Wittig, A. Krebs, *Chem. Ber.* **1961**, *94*, 3260.
[82] J. M. Baskin, J. A. Prescher, S. T. Laughlin, N. J. Agard, P. V. Chang, I. A. Miller, A. Lo, J. A. Codelli, C. R. Bertozzi, *Proc. Natl. Acad. Sci. U.S.A.* **2007**, *104*, 16793.
[83] N. J. Agard, J. M. Baskin, J. A. Prescher, A. Lo, C. R. Bertozzi, *ACS Chem. Bio.* **2006**, *1*, 644.
[84] X. Ning, J. Guo, M. A. Wolfert, G. Boons, *Angew. Chem. Int. Ed.* **2008**, *47*, 2253.
[85] J. C. Jewett, E. M. Sletten, C. R. Bertozzi, *J. Am. Chem. Soc.* **2010**, *132*, 3688.
[86] N. J. Agard, J. A. Prescher, C. R. Bertozzi, *J. Am. Chem. Soc.* **2004**, *126*, 15046.

This new version was applied to the study of glycan recycle metabolism, where the labelled modified-sugars on the cell surface are internalized, and further detected in endosomes and in the Golgi apparatus. Some years later the transformation was achieved in zebrafish,[87] nematodes[88] and even mouses.[89]

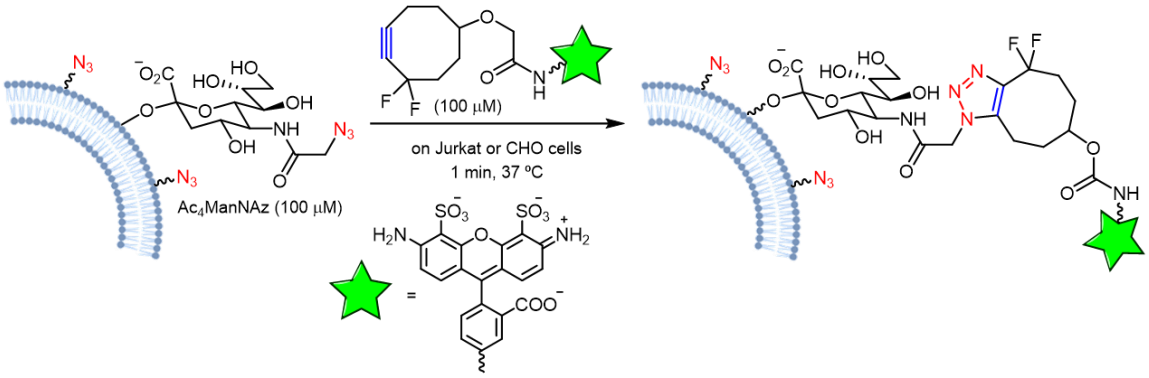

Figure 20. SPAAC coupling developed by Bertozzi and co-workers on cell surface in 2007.[89]

The first intracellular example came from a collaboration between Tirrel and Bertozzi groups, in 2010 (figure 21). Therein, the AHA aminoacid containing an azide group was metabolically incorporated after treatment with 1 mM of AHA. Afterwards, cells were supplied with 50 μM of DIFO-coumarin, noticing fluorescence after 10 min at 37 ºC.[90] The acquisition of three-dimensional microscopic images confirmed the intracellular reaction. Unfortunately, almost half of the fluorescence came from membrane proteins, and additionally, some intracellular fluorescence background caused by non-specific side reactions, owing to the side reactivity of the cyclooctyne. Remarkably, the transformation is still nowadays pretty used. For instance, although preliminary, recently Xi and co-workers were able to carry out the cycloaddition inside mitochondria of mammalian cells.[91]

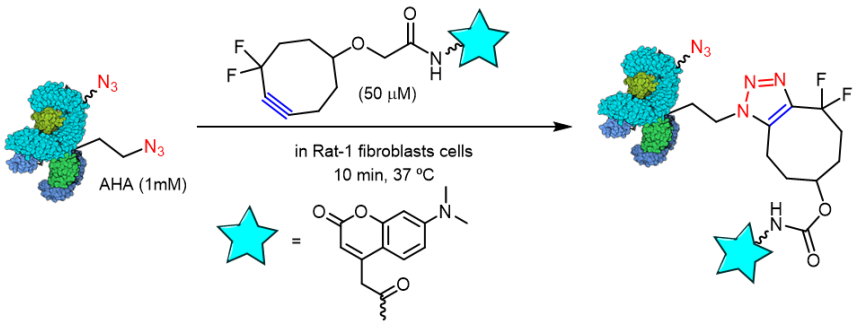

Figure 21. Intracellular version of SPAAC developed by Tirrel and Bertozzi in 2010.[90]

USC UNIVERSIDADE DE SANTIAGO DE COMPOSTELA

[87] S. T. Laughlin, J. M. Baskin, S. L. Amacher, C. R. Bertozzi, *Science*, **2008**, *320*, 664.
[88] S. T. Laughlin, C. R. Bertozzi, *ACS Chem. Biol.* **2009**, *4*, 1068.
[89] P. V. Chang, J. A. Prescher, E. M. Sletten, J. M. Baskin, I. A. Miller, N. J. Agard, A. Lo, C. R. Bertozzi, *Proc. Natl. Acad. Sci. U.S.A.* **2010**, *107*, 1821.
[90] K. E. Beatty, J. D. Fisk, B. P. Smart, Y. Y. Lu, J. Szychowski, M. J. Hangauer, J. M. Baskin, C. R. Bertozzi, D. A. Tirrel, *ChemBioChem* **2010**, *11*, 2092.
[91] L. Yi, X. Yang, X. Cai, D. Wang, Y. Gao, Z. Xi, *RSC Adv.* **2019**, *9*, 23.

The strained azide-alkyne cycloaddition is not exempt of problems. The kinetics are slower than those of CuAAC (10-100 times),[92] and usually suffers from non-specific reactions with nucleophiles of the biological media.[90] Moreover, the cyclooctyne group is not easy to prepare and can be considered as a "bulky" moiety in comparation with the standard triazole obtained in a CuAAC.

2.7. Bioorthogonal ligations based on inverse electron demand diels-alder cycloadditions

Given these problems, there has been an intense effort to develop new, more efficient alternatives to the strain-driven cycloadditions. In this context, the most popular bioorthogonal reaction nowadays is perhaps the inverse electron-demand diels-alder (IEDDA) or tetrazine ligation between a 1,2,4,5-tetrazine and an alkyne/alkene reaction. This [4+2] cycloaddition affords dihydropyridazine or pyridazine conjugates, showing the highest kinetics in the bioorthogonal reaction portfolio (figure 22).[46]

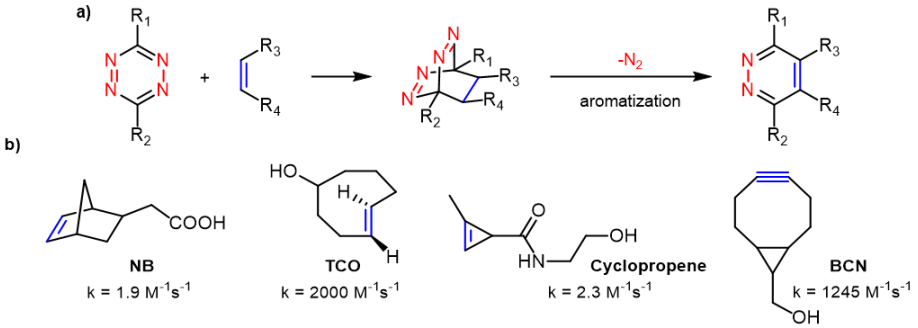

Figure 22. a) General scheme for the inverse electron demand diels-alder (IEDDA). b) Common cyclooctene-cyclooctynes employed nowadays for the IEDDA and some of their kinetics in methanol-water mixtures.[93,94,95,96]

The first relevant report appeared in 2008 when Fox and co-workers demonstrated the biocompatibility and efficiency of the reaction in the presence of nucleophiles, biological media or even mammalian cell lysates.[94] This was further confirmed by the group of Devaraj which performed the reaction on an antibody bearing a norbornane structure (NB) on pre-targeted cells.[93] The authors introduced the use of a smart probe in this transformation, taking advantage of the resonant energy transfer between the selected BODIPY employed fluorophore and the tetrazine. Additionally, they corroborated, by the first time, an intracellular IEEDA cycloaddition by incubation of mammalian cells with a taxol analogue, able to bind the microtubular network and posterior reaction with transcyclooctene (TCO) as dienophile.[97]

[92] S. I. Presolski, V. Hong, S. H. Cho, M. G. Finn, *J. Am. Chem. Soc.* **2010**, *132*, 14570.
[93] R. Weissleder, S. A. Hilderbrand, N. K. Devaraj, *Bioconjugate Chem.* **2008**, *19*, 2297.
[94] M. L. Blackman, M. Royzen, J. M. Fox, *J. Am. Chem. Soc.* **2008**, *130*, 13518.
[95] J. Yang, Y. Liang, J. S. K. N. Houk, N. K. Devaraj, *Chem. Eur. J.* **2014**, *20*, 3365.
[96] K. Lang, L. Davis, S. Wallace, M. Mahesh, D. J. Cox, M. L. Blackman, J. M. Fox, J. W. Chin, *J. Am. Chem. Soc.* **2012**, *134*, 10317.
[97] S. Hilderbrand, R. Upadhyay, R. Mazitschek, R. Weissleder, N. K. Devaraj, *Angew. Chem. Int. Ed.* **2010**, *49*, 2869.

The groups of Fox and Lemke demonstrated, almost simultaneously along 2012, that different dienophiles could be incorporated via genetic code expansion in bacteria[98] or even in mammalian cells[99,100] undergoing the reaction despite the size of the employed TCO, NB, or bicyclononyne (BCN). Prescher and co-workers designed a cyclopropene attached to a sugar analogue (9-Az-NeuAc) improving efficiency of metabolism incorporation and cell surface labeling. The prior treatment of cells with 1 mM of the modified sugar, allowed them to bioconjugate a tetrazine-biotin (100 μM) on mammalian Jurkat cell membrane after 1 h at 37 ºC (figure 23).[101]

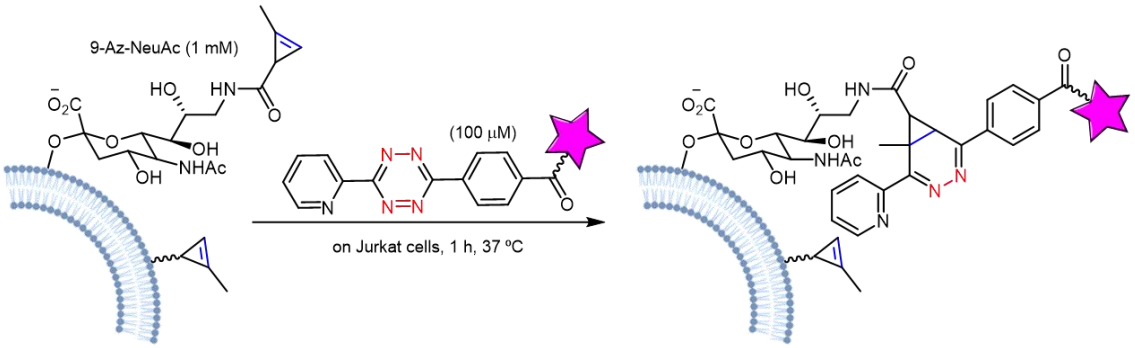

Figure 23. Inverse electron demand diels-alder on cell surface using cyclopropane as bioorthogonal handle developed by Prescher and co-workers in 2012.[101]

The IEEDA cycloadditions have been used for different type of exciting applications, ranging from super-resolution microscopy,[102,103] to the detection of radiotracers.[104,105]

Nonethelesss, this inverse Diels Alder cycloaddition also shown problems of side reactivity, because of the presence of the strained reactants, and the synthesis of some of the precursors is not trivial.[46]

[98] J. L. Seitchik, J. C. Peeler, M. T. Taylor, M. L. Blackman, T. W. Rhoads, R. B. Cooley, C. Refakis, J. M. Fox, R. A. Mehl, *J. Am. Chem. Soc.* **2012**, *134*. 2898.
[99] T. Plass, S. Milles, C. Koehler, J. Szymanski, R. Mueller, M. Wießler, C. Schultz, E. A. Lemke, *Angew. Chem. Int. Ed.* **2012**, *51*, 4166.
[100] J. W. Chin, K. Lang, L. Davis, S. Wallace, M. Mahesh, D. J. Cox, M. L. Blackman, J. M. Fox, *J. Am. Chem. Soc.* **2012**, *134*, 10317.
[101] D. M. Patterson, L. A. Nazarova, B. Xia, D. N. Kamber, J. A. Prescher, *J. Am. Chem. Soc.* **2012**, *134*, 18638.
[102] G. Beliu, A. J. Kurz, A. C. Kuhlemann, L. Behringer-Pliess, M. Meub, N. Wolf, J. Seibel, Z. Shi, M. Schnermann, J. B. Grimm, L. D. Lavis, S. Doose, M. Sauer, *Commun. Biol.* **2019**, *2*, 261.
[103] P. Werther, K. Yserentant, F. Braun, N. Klatwasser, C. Popp, M. Baalmann, D. Herten, R. Wombacher, *Angew. Chem. Int. Ed.* **2020**, *59*, 804.
[104] T. Läppchen, R. Rossin, T. R. van Mourik, G. Gruntz, F. J. M. Hoeben, R. M. Versteegen, H. M. Janssen, J. Lub, M. S. Robillard, *Nucl. Med. Biol.* **2017**, *55*, 19.
[105] J. L. Houghton, R. Membreno, D. Abdel-Atti, K. M. Cunanan, S. Carlin, W. W. Scholz, P. B. Zanzonico, J. S. Lewis, B. M. Zeglis, *Mol. Cancer Ther.* **2017**, *16*, 124.

2.8. Photochemical ligations

A few bioorthogonal, click-like reactions promoted by light have also been described. In 2008, Lin's group demonstrated that photo-induced 1,3 – dipolar cycloadditions can be made compatible with biological media, such as bacterial lysates.[106] This reaction, that was coined as "photoclick" later on,[107] relies on the generation of a highly reactive nitrile-imine dipole after UV irradiation of a 2,5 – diaryl tetrazole, and the subsequent release of N_2. This species, cyclizes spontaneously with a proper dipolarophile, either alkene or an electron deficient alkyne, to afford pyrazoline cycloadducts (figure 24).[108]

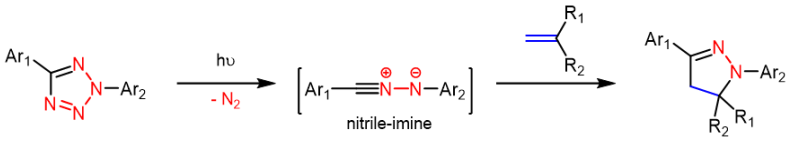

Figure 24. General scheme of the photoinduced 1,3-dipolar cycloaddition.

This group successfully translated this transformation into *E. coli* bacteria by genetically encoding,[109] or into mammalian cells by metabolic incorporation of homoallylglycine (HAG, 1 mM) as Met analogue (figure 25).[110] Thus, the alkenyl-tagged HeLa cells were treated with 100 μM of tetrazole, and set under 365 nm or two-photon IR laser irradiation along 2 min at 37 ºC. Nevertheless, despite the fluorogenic nature of the pyrazolines, the fluorescence obtained remained still low and controls showed background noise.

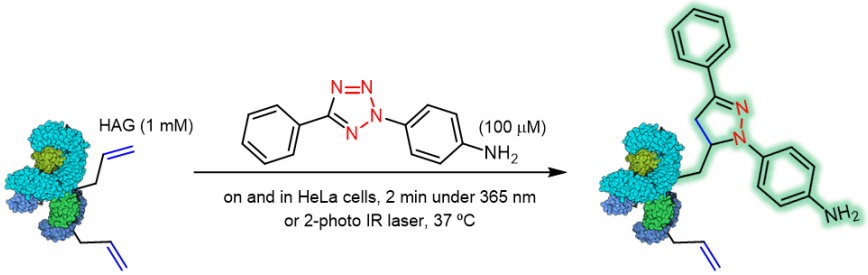

Figure 25. Intracellular version of the "photo-click" reaction developed by Lin in 2010.[110]

USC
UNIVERSIDADE DE SANTIAGO DE COMPOSTELA

[106] J. S. Clovis, A. Eckell, R. Sustmann, R. Huisgen, *Chem. Ber.* **1967**, *100*, 60.
[107] R. K. V. Lim, Q. Lin, *Acc. Chem. Res.* **2011**, *44*, 828.
[108] W. Song, Y. Wang, J. Qu, M. M. Madden, Q. Lin, *Angew. Chem. Int. Ed.* **2008**, *47*, 2832.
[109] W. Song, Y. Wang, J. Qu, Q. Lin, *J. Am. Chem. Soc.* **2008**, *130*, 9654.
[110] W. Song, Y. Wang, Z. Yu, C. I. R. Vera, J. Qu, Q. Lin, *ACS Chem. Biol.* **2010**, *5*, 875.

The "photo-click" also faces important limitations: (i) selectivity issues (the nitrile-imine intermediate has shown to react with any kind of nucleophile, even with solvents); (ii) slower kinetics than those of CuAAC; (iii) the requirement of UV light.[111]

Photochemistry has recently gained attention again, with the incorporation of hindered tetrazoles, the development of photo-triggered versions of other bioorthogonal transformations such as the SPAAC[112] or IEDDAC[113] as well, or more recently, the development of reactions in cellular settings.[114,115]

[111] Z. Li, L. Qian, L. Li, J. C. Bernhammer, H. V. Huynh, J. Lee, S. Q. Yao, *Angew. Chem. Int. Ed.* **2016**, *55*, 2002.
[112] A. A. Poloukhtine, N. E. Mbua, M. A. Wolfert, G. Boons, V. V. Popik, *J. Am. Chem. Soc.* **2009**, *131*, 15769.
[113] S. V. Mayer, A. Murnauer, M. von Wrisberg, M. Jokisch, K. Lang, *Angew. Chem. Int. Ed.* **2019**, *58*, 15876.
[114] Z. Yao, X. Xu, X. Zhang, Q. Xiong, S. Jiang, Z. Yu, *Org. Biomol. Chem.* **2019**, *17*, 6777.
[115] J. Li, H. Kong, L. Huang, B. Chen, K. Qin, M. Zheng, Z. Yan, Y. Zhang, *J. Am. Chem. Soc.* **2018**, *140*, 14542.

3. Transition metal-catalyzed transformations in biological settings

3.1. Organometallic catalysis. Reactions in aqueous media

As shown in the introduction, among the different bioorthogonal reactions so far developed, the CuAAC, one of the most prominent transformations, is catalyzed by transition metals (TM, mainly copper). This process follows a typical organometallic mechanism based on elementary steps indicated in figure 26.[116,117] This suggests that other organometallic catalyzed processes could be also compatible with biological conditions. However, despite organometallic catalysis is a powerful tool for a broad range of reactivity including redox transformations, cross-couplings, isomerizations or formal cycloadditions,[118] it is yet underexplored in the biological field. This is in great part due to the established view that organometallic pathways are incompatible with water and oxygen, and also with biological components.[119]

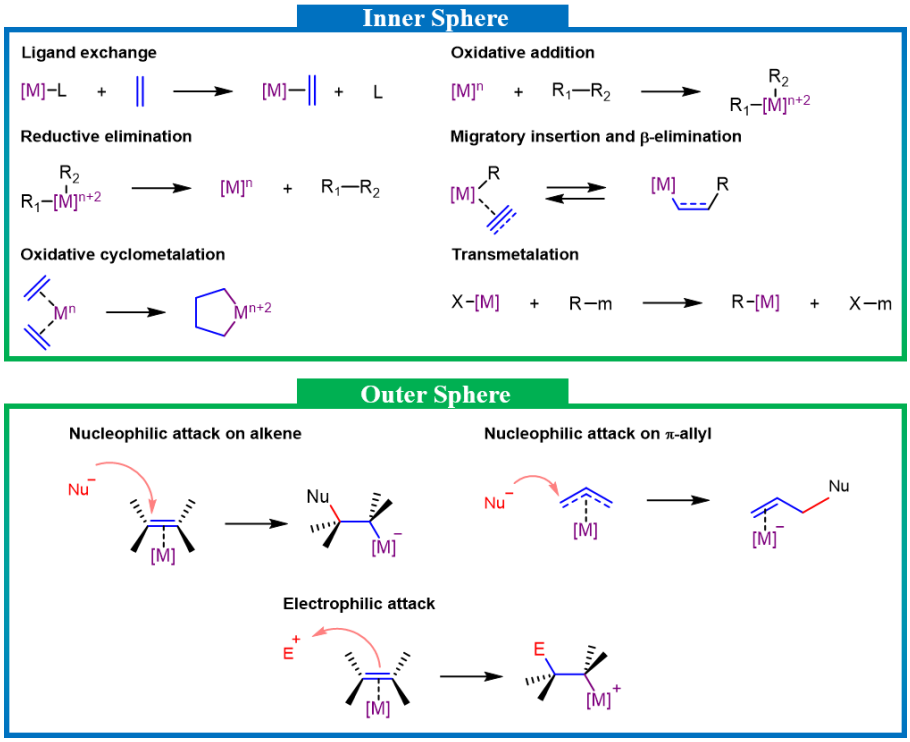

Figure 26. Typical elementary organometallic steps, involving either inner or outer sphere mechanisms.

USC UNIVERSIDADE DE SANTIAGO DE COMPOSTELA

[116] A. K. Å. Persson, PhD thesis, Palladium (II)-Catalyzed Oxidative Cyclization Strategies.
[117] P. Destito, PhD thesis, Transition metal-promoted bioorthogonal transformations in biological media.
[118] R. H. Crabtree, *The Organometallic Chemistry of the Transition Metals*, 6th Edition, Wiley, **2014**.
[119] A. Chanda, V. V. Fokin, *Chem. Rev.* **2009**, *109*, 725.

However, in recent years a number of TM-catalyzed transformations have been demonstrated to tolerate water and the presence of air.[120] This is the case of the Suzuki's reaction, one of the most popular cross coupling transformations (figure 27).[121,122] It has not only been performed in water but also in the presence of biological mixtures. It is worth to mention that the Sonogashira and Heck cross couplings have followed a similar evolution along the years.[123,124,125]

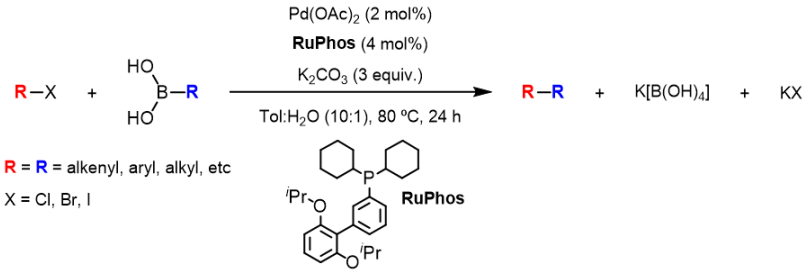

Figure 27. Standard conditions for Suzuki cross coupling.[126] RuPhos: 2-Dicyclohexylphosphino-2'-6'-diisopropoxybiphenyl.

The Suzuki cross-coupling starts with the oxidative addition of an organohalide to a palladium(0) (Pd^0) complex. The resulting Pd^{II} complex reacts with an organometallic species by transmetalation, giving as a result a Pd^{II} intermediate bearing the two organic coupling partners. At this point, a reductive elimination step provides the desired organic compound containing the new C-C bond, recovering Pd^0, able to re-enter into the catalytic cycle (figure 28).[121,127]

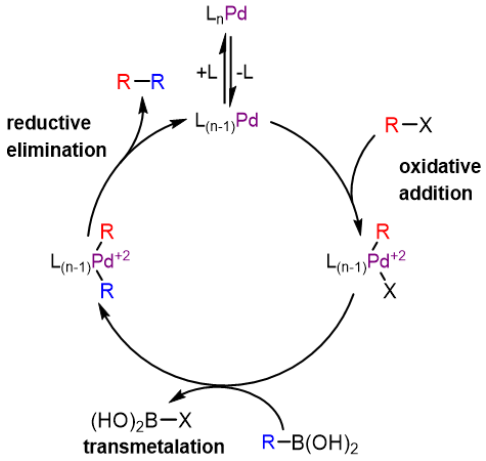

Figure 28. Suzuki-Miyaura mechanism.[121,127]

[120] B. Cornils, W. A. Herrman, *Aqueous-Phase Organometallic Catalysis*, 2nd Edition, Wiley, **2004**.
[121] C. C. C. J. Seechurn, M. O. Kitching, T. J. Colacot, V. Snieckus, *Angew. Chem. Int. Ed.* **2012**, *51*, 5062.
[122] D. G. Hall, *Boronic acids Volume 2*, 2nd Edition, Wiley, **2011**.
[123] P. G. Isengger, B. G. Davis, *J. Am Chem. Soc.* **2019**, *141*, 8005.
[124] A. L. Satz, J. Cai, Y. Chen, R. Goodnow, F. Gruber, A. Kowalczyk, A. Petersen, G. Naderi-Oboodi, Lucja Orzechowski, Q. Strebel, *Bioconjugate Chem*. **2015**, *26*, 1623.
[125] K. Kodama, S. Fukuzawa, H. Nakayama, T. Kigawa, K. Sakamoto, T. Yabuki, N. Matsuda, M. Shirouzu, K. Takio, K. Tachibana, S. Yokoyama, *ChemBioChem* **2006**, *7*, 134.
[126] S. D. Dreher, S. E. Lim, D. L. Sandrock, G. A. Molander, *J. Org. Chem.* **2009**, *74*, 3626.
[127] A. De Meijere, F. Diederich, *Metal-Catalyzed Cross-Coupling Reactions Volume 1*, 2nd Edition, Wiley, **2004**.

Using water soluble ligands like dpdbs, it is possible to carry out the couplings even in pure water (figure 29).[128]

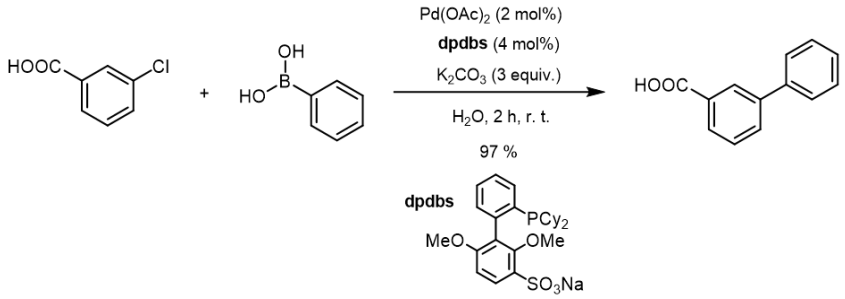

Figure 29. Suzuki-Miyaura reaction developed in aqueous media by Buchwald and coworkers in 2005.[128] Dpdbs: Sodium 2-Dicyclohexylphosphino-2',6'-dimethoxybiphenyl-3'-sulfonate.

The groups of Schultz and Davis explored the application of the Suzuki coupling for the modification of biomacromolecules in aqueous solvents.[129] Therefore, Davis and co-workers demonstrated that it is possible to perform efficient bioconjugations to proteins in phosphate aqueous buffers after 30 min at 37 ºC, using 50 equivalents of palladium complex, and 500 equivalents of the corresponding phenylboronic acid (figure 30).[130] Notably, the buffer solution employed (pH~8) is basic enough to allow the key transmetalation step to occur in the biological media, without addition of any other base.

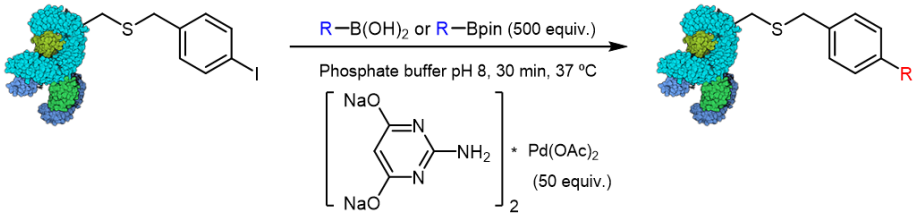

Figure 30. Biocompatible Suzuki's version reported by Davis and co-workers in 2009.[130] Bpin: Pinacol boronic ester.

In addition to the Suzuki coupling other type of transition metal catalyzed cross couplings, like Sonogashira or metathesis transformations, have been also demonstrated to work in aqueous media, and in bioconjugation reactions. And more recently, the range of reactions has been expanded to include redox process, isomerizations, cyclizations and of course, cycloadditions, like the CuAAC or the RuAtAC.[131,132]

USC UNIVERSIDADE DE SANTIAGO DE COMPOSTELA

[128] K. W. Anderson, S. L. Buchwald, *Angew. Chem. Int. Ed.* **2005**, *44*, 6173.
[129] E. Brustad, M. L. Bushey, J. W. Lee, D. Groff, W. Liu, P. G. Schultz, *Angew. Chem. Int. Ed.* **2008**, *47*, 8220.[130] J. M. Chalker, C. S. C. Wood, B. G. Davis, *J. Am. Chem. Soc.* **2009**, *131*, 16346.
[130] J. M. Chalker, C. S. C. Wood, B. G. Davis, *J. Am. Chem. Soc.* **2009**, *131*, 16346.
[131] P. Destito, C. Vidal, F. López, J. L. Mascareñas, *Chem. Eur. J.* **2021**, *27*, 4789.
[132] P. H. Dixneuf, V. Cadierno, *Metal-Catalyzed Reactions in Water*, Wiley-VCH Verlag GmbH & Co. KgaA, **2013**.

3.2. Transition metal catalysis in biological habitats and living cells

Translating organometallic reactions from water to biological mixtures is especially challenging owing to the presence of numerous components that can deactivate the catalyst or trap the intermediates of the reaction mechanism. However, as previously indicated for the CuAAC, this transition is possible.

Initial examples demonstrating the viability of carrying out metal-promoted processes in biological environments appeared in 1985, when Cséplö and co-workers reported the hydrogenation of unsaturated fatty acids in presence of mesophyll protoplast plant cells using a water-soluble ruthenium catalyst, although the reaction generated toxicity.[133]

It took time until other organometallic processes could be performed in biological settings. I will now summarize some of the most relevant contributions, organized by reaction types.

3.2.1. Bond cleavage (uncaging) transformations

In 2006, the Meggers group noticed the ability of the commercially available ruthenium(II) Cp*Ru(COD)Cl to promote the cleavage of allylcarbamates into their corresponding amines, in the presence of water, at open air, with the aid of external thiols. Moreover, a caged rhodamine 110 exhibiting no fluorescence, was used to check the viability of the methodology inside living mammalian cells. A 10-fold increase was observed in the cytoplasm of the cells, after cell treatment with 100 μM of the allocated probe, 20 mol% of ruthenium catalyst and 5 equivalents of thiophenol for 15 min (figure 31). This value decreased to a 3.5-fold increase if no external thiol was added.[134] This report, which was unnoticed for several years, is now considered, together with the CuAAC, a pioneering contribution demonstrating the viability of performing transition metal catalysis inside living mammalian cells. In 2014, the group of Mascareñas employed the uncaging reaction for the controlled release of DNA binders inside mammalian cells.[135]

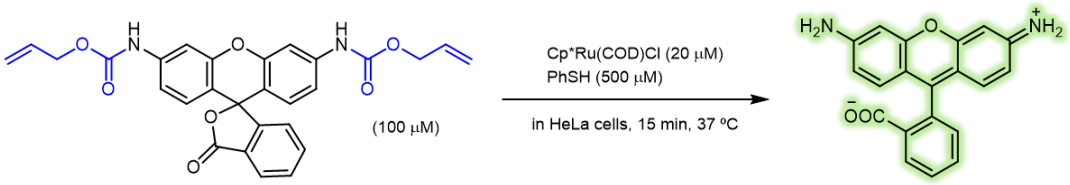

Figure 31. Allylcarbamate deprotection of rhodamine 110, inside HeLa cells reported by Meggers and co-workers in 2006.[134]

USC UNIVERSIDADE DE SANTIAGO DE COMPOSTELA

[133] L. Vigh, F. Joó, A. Cséplö, *J. Biochem.* **1985**, *146*, 241.
[134] C. Streu, E. Meggers, *Angew. Chem. Int. Ed.* **2006**, *45*, 5645.
[135] M. I. Sánchez, C. Pernas, E. Vázquz Sentís, J.L. Mascareñas, *Chem. Sci.* **2014**, *5*, 1901.

Later on, the same group found out that 2-carboxyquinoline based Ru complexes are more efficient catalysts for similar uncaging reactions.[136] The group of Mascareñas demonstrated that derivatizing the quinoline ligand with a pyrene-diphenylphosphonium moiety, the metallic resulting species can be targeted to mitochondria, where it can perform the desired deprotection processes, also of allyl protected phenols.[137,138] Indeed, the strategy was also used for the localized release of 2,4-dinitrophenol (DNP), a well-known mitochondrial depolarizing agent, which exhibited no biological effects in its caged allyl-DNP form, even at high concentrations (500 μM).[139] The transformation not only proceeded in a controlled manner, but interestingly, the incubation of cells with 50 μM of the Ru-quinoline catalyst and 150 μM of allyl-DNP, showed improved performance in comparison with the direct incubations of the cells with the drug. These results suggested a potential advantage of confining catalysis in specific cellular organelles.

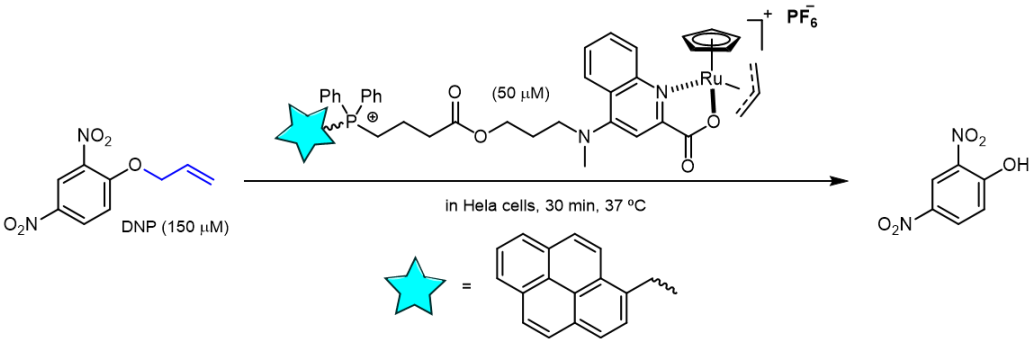

Figure 32. Allyl deprotection of DNP inside mitochondria using pyrenephosphonium-Ru catalyst reported by Mascareñas and co-workers in 2016.[139] DNP: 2,4-dinitrophenol.

This type of metal catalyzed uncaging is very powerful for the generation of molecules with biological activity inside cells, organelles or even animals in a controlled manner, and therefore, many other versions have been investigated.

For instance, the group of Sasmal (former Meggers' student) reported an Ir-catalyzed version of the allyl removal reaction inside HeLa cells.[140] On the other hand, Pd-catalyzed deallylation and depropargylation reactions have demonstrated to be compatible with biological and cellular habitats, despite palladium complexes can be readily inactivated by biological components.

USC UNIVERSIDADE DE SANTIAGO DE COMPOSTELA

[136] T. Völker, F. Dempwolff, P. L. Graumann, E. Meggers, *Angew. Chem. Int. Ed.* **2014**, *53*, 10536.
[137] R. A. J. Smith, R. C. Hartley, H. M. Cochemé, M. P. Murphy, *Trens Pharmacol. Sci.* **2012**, *33*, 341.
[138] J. G. McCarron, M. P. Murphy, S. Chalmers, S. T. Caldwell, C. Quin, T. A. Primer, A. M. James, A. G. Cairns, R. C. Hartley, *J. Am. Chem. Soc.* **2012**, *134*, 758.
[139] M. Tomás-Gamasa, M. Martínez-Calvo, J. R. Couceiro, J. L. Mascareñas, *Nat. Commun.* **2016**, *7*, 12538.
[140] N. Sing, A. Gupta, P. Prasad, P. Mahawar, S. Gupta, P. K. Sasmal, *Inorg. Chem.* **2021**, *60*, 12644.

The groups of Chen[141,142] and Mascareñas[143] have reported palladium-based strategies for the intracellular activation of small molecules or the uncaging of lysine from allyl or propargyl protected derivatives.

In order to avoid a rapid deactivation, the group of Rotello made gold NP with trapped Pd-catalysts, and demonstrated that they can promote the intracellular activation of the antitumoral 5-fluorouracil.[144] In a recent contribution, Mascareñas and P. del Pino employed a metal organic framework (MOF) architecture to stabilize Pd-nanocube cores that acted as efficient catalysts for the release of several probes inside mammalian cells.[145]

Another relevant recent contribution in the area, is the construction of catalytic metallopeptides that can work in biological settings. The group of Mascareñas prepared a miniprotein derivative containing palladium attached to two histidine residues, and demonstrated that the hybrid system can be internalized and promote depropargylation reactions inside mammalian cells. The system can be extended to small RGD peptides.[146]

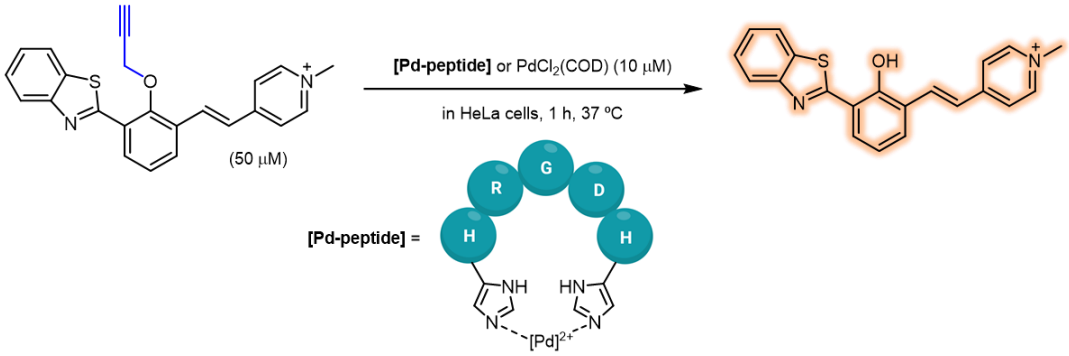

Figure 33. Propargyl deprotection in mammalian cells mediated by Pd-peptide reported by Mascareñas group in 2020.[146]

In addition to the Pd or Ru mediated deprotection processes, there are other alternatives based on gold catalysis, and the ability of gold to bind and carry out alkyne activation.[147,148]

---

[141] J. Li, J. Yu, J. Zhao, J. Wang, S. Zheng, S. Lin, L. Chen, M. Yang, S. Jia, X. Zhang, P. R. Chen, *Nat. Chem.* **2014**, *6*, 352.
[142] J. Wang, B. Cheng, J. Li, Z. Zhang, W. Hong, X. Chen, P. R. Chen, *Angew. Chem. Int. Ed.* **2015**, *54*, 5364.
[143] M. Martínez-Calvo, J. R. Couceiro, P. Destito, J. Rodríguez, J. Mosquera, J. L. Mascareñas, *ACS Catal.* **2018**, *8*, 6055.
[144] G. Y. Tonga, Y. Jeong, B. Duncan, T. Mizuhara, R. Mout, R. Das, S. T. Kim, Y. Yeh, B. Yan, S. Hou, V. M. Rotello, *Nat. Chem.* **2015**, *7*, 597.
[145] R. Martínez, C. Carrillo-Carrión, P. Destito, A. Alvarez, M. Tomás-Gamasa, B. Pelaz, F. López, J. L. Mascareñas, P. del Pino, *Cell. Rep. Phys. Sci.* **2020**, *1*, 1.
[146] S. Learte-Aymamí, C. Vidal, A. Gutiérrez-González, J. L. Mascareñas, *Angew. Chem. Int. Ed.* **2020**, *59*, 9149.
[147] A. Kumar, S. Kumar, N. Kumari, S. H. Lee, J. Han, I. J. Michael, Y. Cho, I. S. Lee, *ACS Catal.* **2019**, *9*, 977.
[148] M. Jbara, E. Eid, A. Brik, *J. Am. Chem. Soc.* **2020**, *142*, 8203.

3.2.2. Cross couplings

Curiously, in contrast to the above deprotection schemes, bond forming transformations have been scarcely explored in cells.[21,22] In this sense, cross coupling reactions like the Sonogashira or the Suzuki-Miyaura (introduced in section 3.1), are among the most important synthetic methodologies. Due to their smooth conditions, their tolerance to water together with the importance of the construction of carbon-carbon bonds,[121,127] it was just a matter of time that some groups succeeded in the development of biocompatible versions.

In 2011, Lin *et al.* modified bacteria cells, expressing cells ubiquitin containing an Hpg in substitution of methionine, and demonstrated that using 1 mM of a palladium pyrimidine complex in presence of 5 mM NaAsc, they could perform a Sonogashira coupling type between the alkyne of the resulting protein and iodofluorescein (100 μM).[149] This methodology was translated to the mammalian cell surface some years later.[150] In 2013, Chen and co-workers reported an efficient manner to perform the Sonogashira coupling, using commercial $Pd(NO_3)_2$ and Na_2PdCl_4 sources, inside bacteria cell instead of soluble Pd pyrimidine complexes.[151] They suggest that the reaction is indeed catalyzed by *in situ* formed Pd(0) NP.[152]

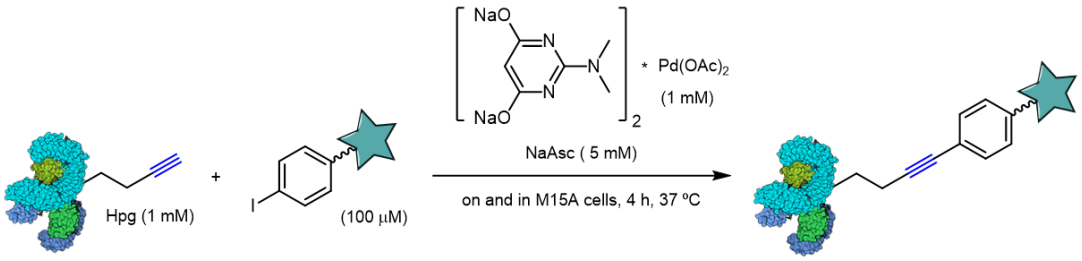

Figure 34. Copper-free Sonogashira reaction carried out inside living bacteria by Lin and co-workers in 2011.[149]

With regard to Suzuki couplings, in 2011 Bradley, Uniciti-Broceta and co-workers indicated that Pd(0)-NPs can promote the coupling of boronic esters and a fluoresceine derivative exhibiting a triflate group and a triphenylphosphonium (TPP, to help internalization) tag, inside HeLa cells. However, a detailed inspection of the information included in the article raises doubts on the full rigor of the claim.[153] In 2018, Qu proposed the use of Pd-NP embedded in microporous silica nanostructures, that one, functionalized with an azobenzene-cyclodextrin association, acting as photosensitive responsive catalysts.[154]

[149] N. Li, R. K. V. Lim, S. Edwardraja, Q. Lin, *J. Am. Chem. Soc.* **2011**, *133*, 15316.
[150] N. Li, C. P. Ramil, R. K. V. Lim, Q. Lin, *ACS Chem. Biol.* **2015**, *10*, 379.
[151] J. Li, S. Lin, J. Wang, S. Jia, M. Yang, Z. Hao, X. Zhang, P. R. Chen, *J. Am. Chem. Soc.* **2013**, *135*, 7330.
[152] W. D. Windt, P. Aelterman, W. Verstraete, *Environ. Microbiol.* **2005**, *7*, 314.
[153] R. M. Yusop, A. Unciti-Broceta, E. M. V. Johansson, R. M. Sánchez-Martín, M. Bradley, *Nat. Chem.* **2011**, *3*, 239.
[154] F. Wang, Y. Zhang, Z. Du, J. Ren, X. Qu, *Nat. Commun.* **2018**, *9*, 1209.

3.2.3. Olefin metathesis

Olefin cross metathesis, along with the Suzuki and Sonogashira transformations, is among the most relevant ways to generate new C-C bonds. In general terms, the reaction consists in the exchange of substituents between alkene partners through a catalytic process of cleavage and reassembling of the double bonds.[155,156]

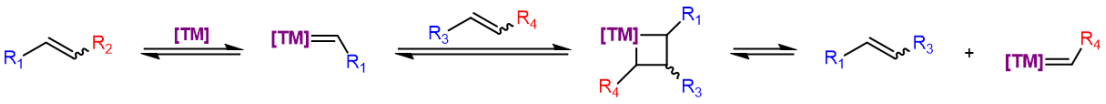

Figure 35. Olefin metathesis mechanism.[156]

In 2018, the group of Michel reported an olefin metathesis in different cells lines, using discrete second generation Hoveyda-Grubbs catalysts attached to a BODIPY-based fluorophore. The system (2 μM) reacts with freshly bubbled ethylene for 10 min at 37 ºC, releasing the fluorophore and consequently, activating its fluorescence (figure 36).[157] Albeit control experiments showed some background noise, and therefore side reactions seem to take place, the process presents selectivity towards ethylene or allyl alcohols. However, the use of stochiometric amounts of Ru limits its synthetic applicability.

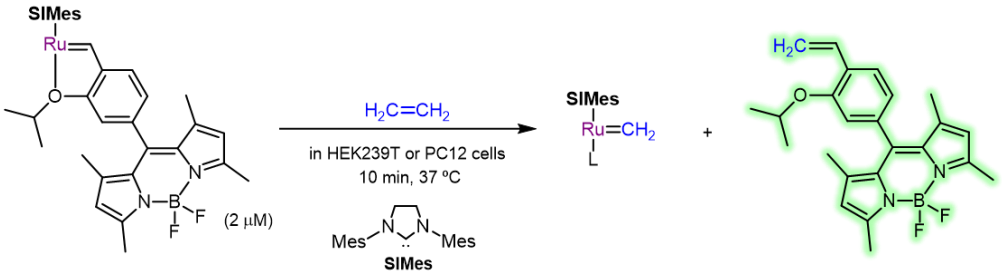

Figure 36. Olefin metathesis with ethylene carried out inside BEP-4 cells by Michel and co-workers in 2018.[157] *SIMes: 1,3-Bis(2,4,6-trimethylphenyl)-4,5-dihydroimidazol-2-ylidene.*

More recently, in 2019 the group of Prof. Tanaka addressed the catalyst passivation issue by developing a new artificial metalloenzyme in which the ruthenium catalyst is well embedded inside the protein coat. They attached the Ru complex to a coumarin that locates the catalyst in the hydrophobic pocket of a bovine serum albumin (BSA) protein. The resulting hybrid can catalyze the reaction in different mammalian cell lines such HeLa or A549, without disturbing endogenous biomolecules, and can even be used for the controlled generation of the drug Umbelliprenin.[158]

USC
UNIVERSIDADE DE SANTIAGO DE COMPOSTELA

[155] N. Calderon, *Acc. Chem. Res.* **1972**, *5*, 127.
[156] R. H. Grubbs, D. J. O'Leary, *Handbook of Metathesis, Volume 2: Applications in Organic Synthesis*, 2nd ed., Wiley-VCH, Weinheim, **2015**.
[157] S. N. W. Toussaint, R. T. Calkins, S. Lee, B. W. Michel, *J. Am. Chem. Soc.* **2018**, *140*, 13151.
[158] S. Eda I. Nasibullin, K. Vong, N. Kudo, M. Yoshida, A. Kurbangalieva, K. Tanaka, *Nat. Catal.* **2019**, *2*, 780.

3.2.4. Redox processes

The cell has a controlled redox environment, and therefore, performing exogenous reduction or oxidation processes inside biological systems is extremely complicated. Nevertheless, Sadler demonstrated in 2012 that pyruvate could be transformed into lactate by means of Ru or Ir catalysts, using the endogenous NADH reductant as a hydride source, opening the door to intracellular redox transformations using cell native reductants.[159] The group of Do report a reduction of aldehyde to alcohols in NIH-3T3 cells, using Cp*Ir complexes as catalysts.[160,161] In 2018, Sadler and coworkers replaced Ru or Ir complexes by biocompatible *p*-cymene osmium catalyst, and used sodium formate as exogenous reductant. This strategy allowed them to transform pyruvate into L- or D-lactate inside A2780 living cells (figure 37).[162] The final configuration of lactate was dependent on the catalyst configuration, representing the first enantioselective transformation by a synthetic catalyst inside living cells. Interestingly, sodium formate could be directly added or generated inside the cells from *N*-formylmethionine, substrate of the peptide deformylase, overexpressed in cancer cells such as PC3 cells. Unfortunately, both Do's and Sadler's processes presented very low efficiencies (≈ 1% in aqueous media) and then, *in cellulo* fluorescence experiments only showed a small increase of intensity.

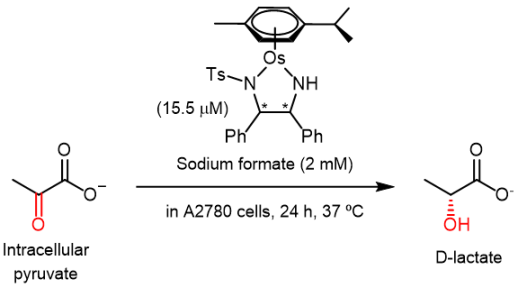

Figure 37. Enantioselective synthesis of D-Lactate in A2780 mammalian cells by Sadler and co-workers in 2018.[162]

USC
UNIVERSIDADE DE SANTIAGO DE COMPOSTELA

[159] S. Betanzos-Lara, Z. Liu, A. Habtemariam, A. M. Pizarro, B. Qamar, P. J. Sadler, *Angew. Chem. Int. Ed.* **2012**, *51*, 3897.
[160] A. H. Ngo, M. Ibañez, L. H. Do, *ACS Catal.* **2016**, *6*, 2637.
[161] S. Bose, A. H. Ngo, L. H. Do, *J. Am. Chem. Soc.* **2017**, *139*, 8792.
[162] J. P. Coverdale, I. Romero-Canelón, C. Sánchez-Cano, G. J. Clarkson, A. Habtemariam, M. Wills, P. J. Sadler, *Nat. Chem.* **2018**, *10*, 347.

The group of Mascareñas demonstrated the viability of performing a ruthenium-catalyzed redox neutral isomerization of allylic alcohols, instead of a hydrogenation. As in the case of the reduction reactions indicated above, the reaction involves a hydride transfer from the metal complex to the substrate. The process proved to be highly efficient not only in aqueous solvents, but also in different complex biological media and even inside diverse cell lines, without the use of external additives (only 10 mol% Ru catalyst, 100 μM of smart probe). Liquid chromatography – mass spectrometry (LC-MS) techniques allowed to monitor the process and revealed a turnover of 22, confirming the catalytic nature of the reaction.

Besides, the strategy was applied to the intracellular generation of bioactive products, such as glutathione (GSH) depleting α,β-unsaturated ketones, which promoted stronger effect than that obtained with the direct incubation of the product.[163]

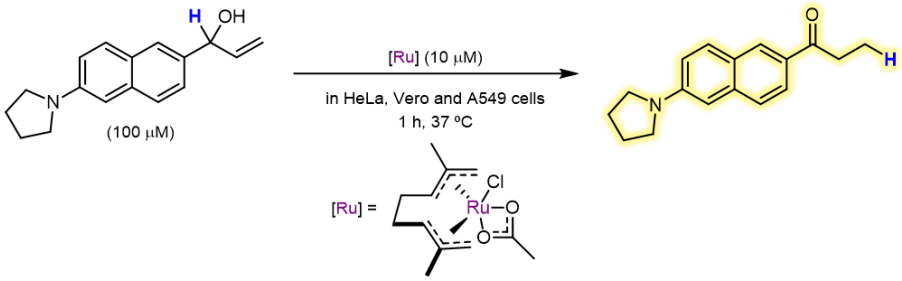

Figure 38. Redox neutral isomerization inside mammalian cells by Mascareñas and co-workers in 2019.[163]

More recently, Qu and co-workers reported the use of mesoporous silica-Pd NP with chiral modifiers for the enantioselective synthesis of Ibuprofen, a well-known anti-inflammatory drug (pharmacological activity is manly attributed to S-enantiomer),[164,165] through an asymmetric transfer hydrogenation, using sodium formate as hydride source (ca. 75% ee). Remarkably, the reduction took place intracellularly in mammalian cells or even mice, observing that the biological effect, for instance, an anti-inflammatory action, depends on the use of the correct Pd-NP chirality.[166]

USC
UNIVERSIDADE DE SANTIAGO DE COMPOSTELA

[163] C. Vidal, M. Tomás-Gamasa, A. Gutiérrez-González, J. L. Mascareñas, *J. Am. Chem. Soc.* **2019**, *141*, 5125.
[164] N. Aslam, R. Bushra, *Oman Med. J.* **2010**, *25*, 155.
[165] K. D. Rainsford, *Int. J. Clin. Pract. Suppl.* **2013**, *67*, 9.
[166] Z. Du, C. Liu, H. Song, P. Scott, Z. Liu, J. Ren, X. Qu, *Chem.* **2020**, *6*, 2060.

3.2.5. Cycloisomerizations

Gold complexes are well known π acids capable of activating alkynes. This activation can be used to promote cycloisomerization processes, even in cellular media.

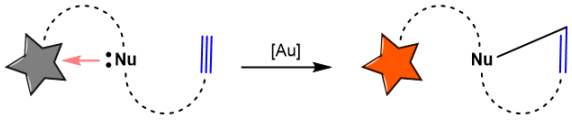

Figure 39. General scheme for the activation of gold sensitive probes.

For instance, Tae and co-workers reported in 2009 the synthesis of an oxazole-TAMRA after cyclization with Au(III) of propargyl amide-TAMRA. The concurrent increase of fluorescence from the oxazole generation was used for Au detection in cells.[167] Similar strategies were designed by Yoon,[168,169] Ahn and co-workers.[170] Another annulation strategy was published by Patra's group. Therein, a fluorescein probe was derivatized with a 2-ethynylbenzoic acid moiety, with its consequent fluorescence quenching. The presence of Au(I) or Au(III) triggers an intramolecular cyclization, that would release an active fluorescein and the new created isochromene skeleton.[171] In the same way as previous works, it was claimed to be performed inside mammalian cells, although only one preliminary experiment was shown.

In these articles, the main objective was the creation of Au detection probes. In 2018, the group of Mascareñas reported a gold mediated cycloisomerization in mammalian cells. They demonstrated that gold chloride complexes can be activated in aqueous media without the need of a chloride scavenger, allowing phenylpropyonates to cycle and build fluorescent coumarins.[172] Remarkably, the reaction can be also carried out concurrently and orthogonally with the previously mentioned ruthenium promoted allyl deprotection. This was the first time that two metals promoted bioorthogonal transformations inside living cells in a total independent manner, working in parallel, without observing cross reactivities.

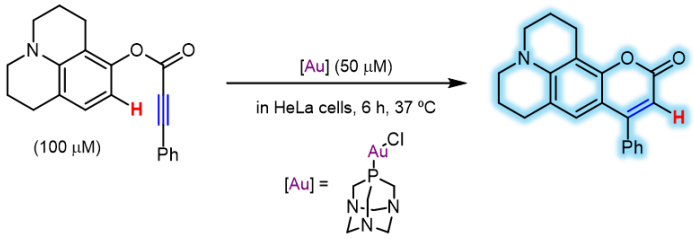

Figure 40. Cycloisomerization inside HeLa cells performed by Mascareñas group in 2018.[172]

USC UNIVERSIDADE DE SANTIAGO DE COMPOSTELA

Y. Yang, S. Lee, [167] J. Tae, *Org. Lett.* **2009**, *11*, 5610.
[168] M. J. Jou, X. Chen, K. M. K. Swamy, H. N. Kim, H. Kim, S. Lee, J. Yoon, *Chem. Commun.* **2009**, 7218.
[169] J. H. Do, H. N. Kim, J. S. Kim, H. J. Kim, J. Yoon, *Org. Lett.* **2010**, *12*, 932.
[170] O. A. Egorova, H. Seo, A. Chatterjee, K. H. Ahn, *Org. Lett.* **2010**, *12*, 401.
[171] N. T. Patil, V. S. Shinde, M. S. Thakare, P. H. Kumar, P. R. Bangal, A. K. Barui, C. R. Patra, *Chem. Commun.* **2012**, *48*, 11229.
[172] C. Vidal, M. Tomás-Gamasa, P. Destito, F. López, J. L. Mascareñas, *Nat. Commun.* **2018**, *9*, 1913.

3.2.6. Carbene-mediated transformations

Recently, our group demonstrated that carbene insertions can also be carried out inside mammalian cells, provided the substrates are appropriately engineered. Metal-carbene complexes had been previously used for the modification of biomolecules, especially with Rh,[173] but had been never explored in a living system. In the current work, the group was able to assemble complex structures such as benzoquinoxalines, starting from alpha-keto diazocarbenes, ortho-amino arylamines and benign Cu(II) salts.[174] Interestingly, this process could discriminate between different cell lines thanks to the derivatization of a copper ligand with an integrin-targeting motif, that could be further used for the cell selective generation of a bioactive benzoquinoxaline with mitochondria depolarizing properties (figure 41). Due to the wide reactivity of carbenoids, the authors foresee novel future applications of the carbene transfer chemistry into the field of bioorthogonal chemistry.

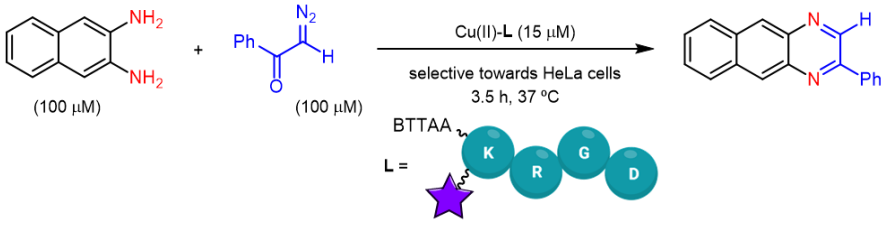

Figure 41. Carbene mediated N-H insertion in selectively directed mammalian cells by Mascareñas group in 2021.[174]

4. Conclusions

In summary, despite the well-established belief that transition metal catalysis was incompatible with biological systems, an increasing number of evidences indicate that this hypothesis is wrong, and that transition metal catalyzed reactions can be performed in complex biological media and even in living contexts. It is true, however, that most of the transformations are very poor in terms of catalytic efficiency, in great part owing to the deactivation of the catalyst or catalytic intermediates, but also because of transport, localization and toxicity problems. The field is in its infancy, and much remains to be progressed until we can truly add this abiotic chemistry to the armory of reactions that can be performed in cells and organisms.

USC
UNIVERSIDADE DE SANTIAGO DE COMPOSTELA

[173] K. A. Mix, M. R. Aronoff, R. T. Raines, *ACS Chem. Biol.* **2016**, *11*, 3233.
[174] S. Gutiérrez, M. Tomás-Gamasa, J. L. Mascareñas, *Angew. Chem. Int. Ed.* **2021**, *60*, 22017.

GENERAL OBJECTIVES

USC
UNIVERSIDADE
DE SANTIAGO
DE COMPOSTELA

USC
UNIVERSIDADE
DE SANTIAGO
DE COMPOSTELA

Considering all precedents and the current challenges in the field of bioorthogonal chemistry, this doctoral thesis aims the study and improvement of existing bioconjugation techniques, and the development of novel biocompatible transformations in native settings, relaying on the power of transition metal catalysis for the synthesis of complex structures. Specifically, we focus on:

1) Translation of CuAAC into mammalian cells: Previous works have been mainly focused on cell surface bioconjugation with some coy contributions inside cells with the use of non-conventional methodologies such as cell fixation or the use of azide-chelating copper complexes. The limitations have raised the question if a simpler process involving discrete substrates is plausible with the use of predefined Cu(I) complexes in absence of exogenous reductants. We have approached this goal, and the results are discussed in chapter II.

2) Novel cycloadditions in biological media: As described before, our group has gained some expertise in synthetic protocols in biological media and cellular settings based mainly in ruthenium catalysts. Thus, the transition metal has demonstrated to be a biocompatible and flexible for a diverse kind of reactivity. In chapter III, we expand the bioorthogonal reaction pool with a metal-promoted [2+2+2] cycloaddition, carried out for the first time inside mammalian cells. Therein, this transformation is applied for the one-step synthesis of the core skeleton of important biomolecules and fluorophores.

3) Synthetical photoredox catalysis approximation in native settings: Visible light photocatalysis has recently gained attention for biological purposes due to its biocompatibility and the spatiotemporal control it provides. Nevertheless, synthetic applications in cell environment are unknown until date. In chapter IV, we explore some photo-Meerwein arylations in aqueous and biological media investigating the bioorthogonality of these synthetic photoredox transformations.

USC
UNIVERSIDADE
DE SANTIAGO
DE COMPOSTELA

USC
UNIVERSIDADE
DE SANTIAGO
DE COMPOSTELA

CHAPTER 2. COPPER AZIDE-ALKYNE CYCLOADDITION IN MAMMALIAN CELLS

This chapter includes work published in Chemical Science as:

J. Miguel-Ávila,[a] M. Tomás-Gamasa,[a] A. Olmos,[b] Pedro J. Pérez,[b] J. L. Mascareñas,[a] *Chem. Sci.* **2018**, *9*, 1947.

[a]Centro Singular de Investigación en Química Biolóxica e Materiais Moleculares (CIQUS) and Departamento de Química Organica, Universidad de Santiago de Compostela, 15782, Santiago de Compostela, Spain.

[b]Laboratorio de Catálisis Homogénea, Unidad Asociada al CSIC, CIQSO-Centro de Investigación en Química Sostenible, Departamento de Química, Universidad de Huelva, Campus de El Carmen s/n, 21007 Huelva, Spain.

DOI: 10.1039/C7SC04643J, Open Acces article (RSC, Most impactful Chemical Biology articles of 2018)

USC UNIVERSIDADE DE SANTIAGO DE COMPOSTELA

USC
UNIVERSIDADE
DE SANTIAGO
DE COMPOSTELA

1. CuAAC inside live mammalian cells

As mentioned in the introduction, the copper azide-alkyne aycloaddition, known as CuAAC, that could be considered as a Nobel Prize-like discovery, has been key to trigger the field of bioorthogonal chemistry. Even now, after years of progress in this area, the CuAAC, together with the emergence of the IEDDA, can be considered as the more relevant bioorthogonal transformation so far discovered.[46] The simplicity of the substrates in terms of synthesis and handling, its intrinsic chemoselectivity and the compatibility with aqueous media, makes this reaction a priority choice for performing bioorthogonal ligations.[14,37] However, translating this process to living cells and organisms is very challenging, mostly because of the instability of the copper complex, its potential sequestration by biological components and its presumable toxicity.[77,78] As indicated in the introduction, most significant advances in this topic were carried out only in bacteria, that is much less complex than a mammalian cell.

Initial attempts to carry out CuAAC reactions in mammalian cells were reported in 2006, using HeLa and HEK293T cell lines,[68] and some years later, in 2008, employing mice derived cells.[175] However, fixation of cells with paraformaldehyde before their treatment with substrates and the copper source was mandatory in both cases to observe reaction. Hence, this example cannot be considered a real *in cellulo* application of the click reaction. In 2012, the group of Ting relied on the smart concept of using "Cu chelating azides", where the combination of copper salts with different 2-methylazidopyridines resulted in an improvement of several orders of magnitude on kinetics with respect to the use of other azides (figure 42c).[176,177] The reason behind this acceleration of the CuAAC is the enhancement of electrophilicity that experiences the azido group once the neighbor pyridine is chelated with the metal. This is also an advantage in terms of orthogonality, owing to the preference of the copper to be chelated by a bidentate ligand.

The group of Ting demonstrated that the reaction can be performed on HEK cells, incorporating an Hpg (200 μM) aminoacid on the membrane. The reaction was carried with 200 μM of pycolil azide, 40 μM of $CuSO_4$ as copper source, 5 equivalents of BTTAA or THPTA ligand, 2.5 mM of NaAsc for 5 min at 37 ºC in PBS as cellular media. Albeit it was also reported to be performed inside A375 cells with metabolic incorporated Hpg and ethynyl-uridine (50 and 200 μM, respectively), the expriments were carried out with fixed cells prior to substrate incubation, and conditions were forced with the use of 2 mM of $CuSO_4$, 4 equivalents of THPTA and 5 equivalents of NaAsc for 1 h.

USC DE SANTIAGO DE COMPOSTELA

[175] A. Salic, T. J. Mitchison, *Proc. Natl. Acad. Sci. USA* **2008**, *105*, 2415.
[176] U. Sing, P. Slade, K. R. Gee, A. Y. Ting, *Angew. Chem. Int. Ed.* **2012**, *51*, 5852.
[177] C. Uttamapinant, M. I. Sánchez, D. S. Liu, J. Z. Yao, K. A. White, S. Grecian, S. Clarke, K. R. Gee, A. Y. Ting, *Nat. Protoc.* **2013**, *8*, 1620.

The first report of an intracellular mammalian cell CuAAC had to wait until 2014. Taran developed a different version of the same concept, modifying the standard tristriazole ligands with a chelating azide into its structure (figure 42d). These substrates underwent the reaction with alkynes with very good rates and efficiencies, using micromolar concentrations, and in presence of cell lysates.[178]

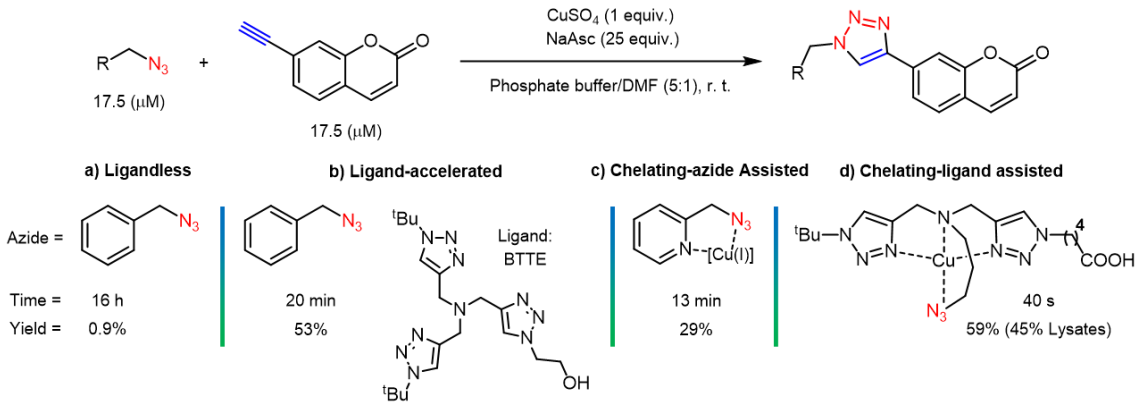

Figure 42. Comparison of CuAAC methodologies under diluted conditions.

The chelating-azide substrate developed by Taran's group (figure 42c) was implemented in HuH-7 human cells, using a microtubule skeleton tracker modified with an alkyne moiety and the Cu chelating azide precursor conjugated to a TAMRA fluorophore. For this purpose, $CuSO_4$ was incubated with one equiv. of the chelating azide and 50 equiv. of NaAsc. The mixture was added to a final concentration of 50 μM into cells incubated with 62.5 nM of the alkyne probe at 37 ºC. After 2 h, the cells were fixed with paraformaldehyde, and a second incubation with Oregon green-tubulin tracker was performed to confirm the intracellular reaction and the colocalization with the generated red fluorophore (figure 43).

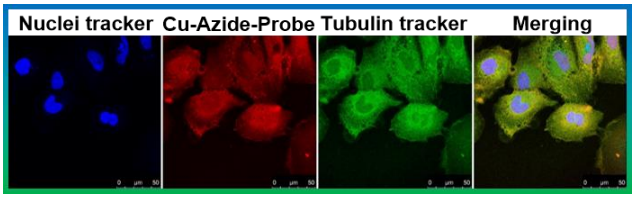

Figure 43. Imaging experiments from Taran's work. From left to right: blue channel for the DAPI-nuclei tracker probe, red channel for the product of the reaction with TAMRA, green channel for the Oregon green-tubulin tracker, and merging of pictures. Yellow color resulting from merging between red and green channel corroborates co-localization between the product and the tubulin tracker.[178]

A major disadvantage of these latter chelating azide strategies is that the copper catalyst has to be used in stoichiometric amounts, as it is trapped in the final adduct.

[178] V. Bevilacqua, M. King, M. Chaumontet, M. Nothisen, S. Gabillet, D. Buisson, C. Puente, A. Wagner, F. Taran, *Angew. Chem. Int. Ed.* **2014**, *53*, 5872.

In 2016, the group of Zimmerman built metal-organic nanoparticle (MONP) by incubating 5 μM of polymers and 50 μM of $CuSO_4$ for 15 h at room temperature, and demonstrated that the resulting Cu-MONP conferred water stability and solubility, while retaining affinity for organic substrates. Indeed, these heterogenous, polymeric constructs were able to promoted CuAAC reactions with good efficiencies, in aqueous buffers. Experiments in cells, either bacteria or mammalian cells, with 0.5 μM of Cu-MONP and 2 mM of NaAsc showed impressive results in promoting the cycloaddition of a fluorogenic azidocoumarin and ethynylanisole, as probed by fluorescence microscopy (figure 44c).[179] Importantly, they demonstrated that the Cu-MONP polymer presents an acceptable toxicity index. In the weak side, the system is not well defined at the molecular level; and it is not clear which is the final copper species that is promoting the reaction.

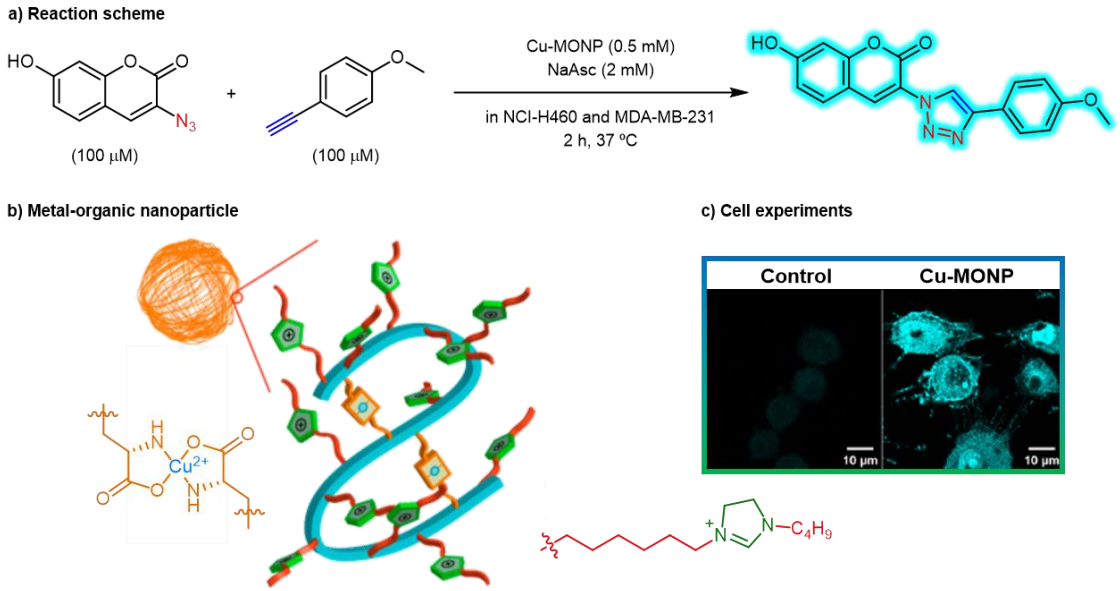

Figure 44. a) Reaction scheme employed for the intracellular transformation in NCI-H460 (human cell lung). b) Zimmerman's metal-organic nanoparticle (MONP), and c) cell experiments. Control: cell incubation with azide and alkyne. Cu-MONP: cell incubation with azide, alkyne and Cu-MONPs.[179]

USC UNIVERSIDADE DE SANTIAGO DE COMPOSTELA

[179] Y. Bai, X. Feng, H. Xing, Y. Xu, B. K. Kim, N. Baig, T. Zhou, A. A. Gewirth, Y. Lu, E. Oldfield, S. C. Zimmerman, *J. Am. Chem. Soc.* **2016**, *138*, 11077.

In 2017, Cai and co-workers suggested that tristriazole ligands such as BTTAA linked to cell penetrating peptides (CPPs) as copper ligands could promote not only the formation of active copper catalysts but also their cellular internalization (up to 15 fold respect to the conventional ligand).[180] These complexes were active in the CuAAC, in mixtures Dulbecco's modified eagle medium (cellular media, DMEM) and PBS, and also were able to promote the reaction in OVCAR5 cells, using external azidocoumarin derivatives with Hpg aminoacid analogue metabolically incorporated in proteins (figure 45).

However, the efficiency of the reactions was very low, and manly localized on the cell membrane (18% yield) with an almost negligible intracellular yield (0.8%), according to the calculations of the authors. The group associated this low yield inside the cell to the presence of endogenous thiols that passivated the catalyst, especially GSH, which presents a high intracellular concentration.

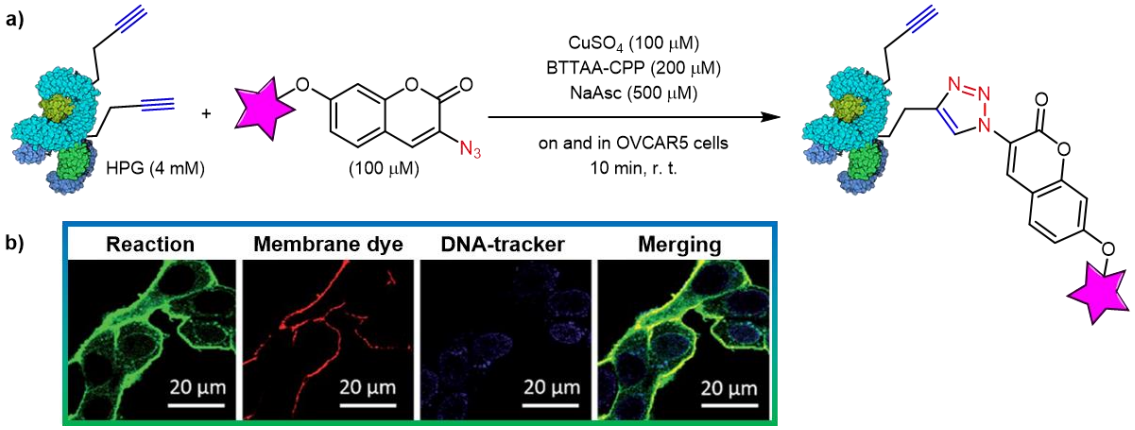

Figure 45. a) Cell imaging scheme strategy followed by the group of Cai. b) Imaging cell experiments. Reaction: green fluorescence from product formation plus avidin-fluorescein conjugation with biotin (pink star). Merging: Picture overlapping of reaction with, membrane dye or DNA-tracker, which confirms membrane and cytosolic CuAAC, but not inside the nucleus.

Overall, at the outset of my PhD work, the progress in the development of CuAAC inside mammalian cells, without fixing the cells, was very limited. Main issues to be addressed are, besides the supposed cytotoxicity, were the low activities and presumable decomposition of the catalyst, the intracellular transport of the Cu complex, or the need to use reductants to convert Cu(II) into Cu(I).

USC UNIVERSIDADE DE SANTIAGO DE COMPOSTELA

[180] S. Li, L. Wang, F. Yu, Z. Zhu, D. Shobaki, H. Chen, M. Wang, J. Wang, G. Qin, U. J. Erasquin, L. Ren, Y. Wang, C. Cai, *Chem. Sci.* **2017**, *8*, 2107.

2. Objectives

As commented, the CuACC is an extraordinary reaction in terms of rate and orthogonality, and has been used in many biological contexts. However, its application in intracellular mammalian settings has been very limited.

We hypothesized that the transformation would be feasible using predefined Cu(I) complexes featuring appropriately designed tris triazole ligands. The idea behind the project, is that the ligand not only protects and stabilizes the Cu(I) species required for the reaction, but the use of predefine Cu(I) complexes, also avoids the need of ascorbate, which is known to be toxic to the cells, and facilitates the intracellular transport.

We therefore proposed the *in situ* synthesis of a variety of copper (I) complexes exhibiting well defined tristriazole ligands, and the investigation of their ability to catalyze CuAAC in biological mixtures and more importantly, in mammalian cells, in the absence of added ascorbate.

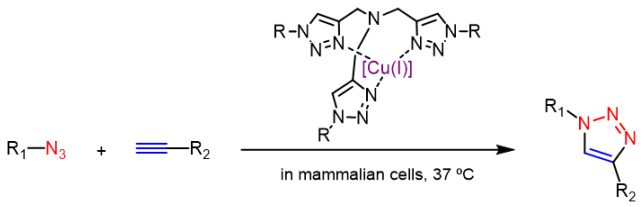

USC
UNIVERSIDADE DE SANTIAGO DE COMPOSTELA

3. Results and discussion

3.1. CuAAC reactions with *in situ* prepared tristriazole complexes

3.1.1. Synthesis of the ligands

Using as ligand of reference the most common ligand, TBTA, we first focused our efforts on the synthesis of a variety of tris-triazole ligands, named **L1-L4**, which are indicated in figure 46, that exhibit different characteristics. The first ligand **L1** is called BTTAA, previously used with good results in other CuAAC.[64] It presents *tert*-butyl groups, therefore increasing steric bulkiness, and very likely, hydrophobicity. BBTE (**L2**) and BTTE (**L3**), hydroxyl analogues of TBTA and BTTA ligands, respectively, could be easily derivatized through the hydroxyl group. Indeed, the introduction of a triphenylphosphonium moiety in the BTTE structure (BTTE-P, **L4**), could allow us to target the final copper complex to the mitochondria, or at least to ease the cell uptake, while providing extra solubility.[137,138]

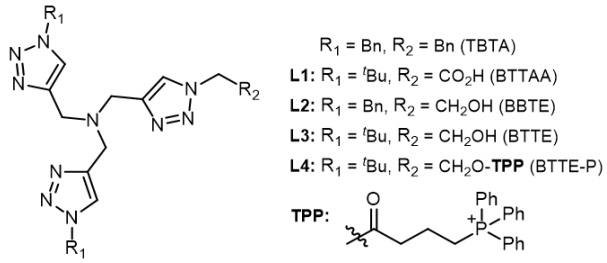

Figure 46. Tristriazolyl ligands explored in this project.

The synthesis of ligands **L1**, **L2** and **L3** was carried out using a protocol adapted from a reported procedure in 4 steps,[64] as indicated in figure 47. Firstly, the triazolyl scaffold was built through a CuAAC reaction between a selected azide (either benzylazide (**1**) or ^{t}Bu-azide (**2**)) and 3,3-diethoxyprop-1-yne. Standard conditions using $CuSO_4$ as copper source, NaAsc as reductant for Cu activation in water and ^{t}BuOH as co-solvent for substrate solubilization, led to the triazoles **3** or **4** in almost quantitative yields. Afterwards, the acetal was hydrolyzed to yield the aldehydes **5** or **6** (85%), which undergo a reductive amination with propargyl amine and $Na(AcO)_3BH$ as reductant, leading to bistriazole alkynes **7** and **8** in excellent yields (80%). At this point, the second triazolyl substituent group was introduced by means of a CuAAC with the second selected azide (ethanolazide (**9**) or azido acetic acid (**10**)) to give the corresponding tristriazole systems **L1** in a 40% yield, or **L2** and **L3** in excellent yields (87 and 93% respectively).

USC UNIVERSIDADE DE SANTIAGO DE COMPOSTELA

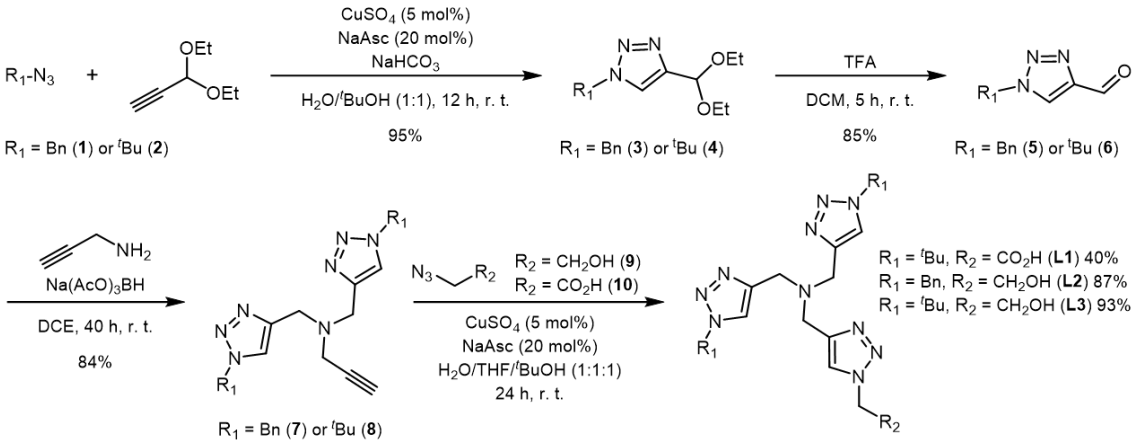

Figure 47. Synthesis of tristriazole ligands employed.

The moderated yield obtained in the synthesis of **L1** could be due the coordination of the azido acetic acid (**10**) to the copper. This was overcome with the use of $CuBr(PPh_3)_3$ as catalyst, although deoxygenation, inert atmosphere and heating were also needed to increase the yield to 80%.

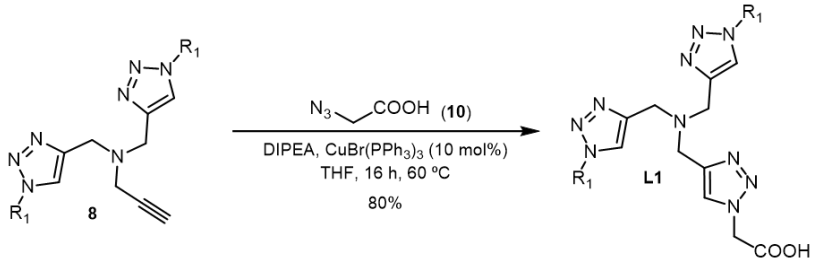

*Figure 48. Alternative **L1** synthesis.*

Further derivatizations included the esterification of **L3** with the TPP acid derivative **12** using EDC as coupling agent, treatment which led to **L4** in 55% yield.

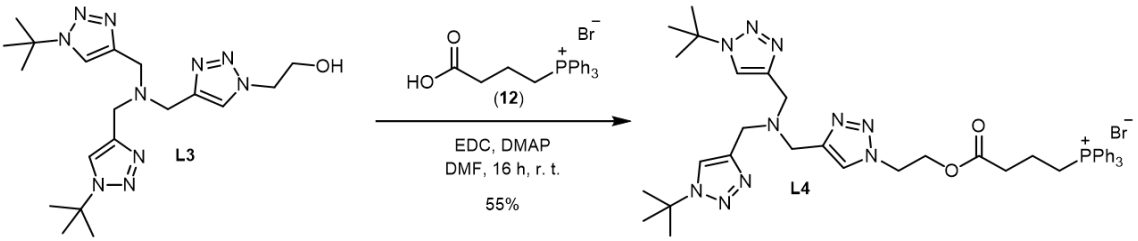

*Figure 49. Synthesis of **L4** from **L3**.*

USC UNIVERSIDADE DE SANTIAGO DE COMPOSTELA

3.1.2. Selection and probes synthesis

With these ligands in hand, we studied their performance in CuAAC reactions using as probe (the fluorogenic 3-azido-7-hydroxycoumarin (**13**)),[43] as since exhibits an increase in blue fluorescence after the cycloaddition. This coumarin could be prepared through a two-step synthetic route (figure 50).[181] The first step combines the Claisen condensation of N-acetylglycine with 2,4-dihydroxy benzaldehyde and esterification of the acid with the alcohol in the meta position. After filtration, the acetyl groups were hydrolyzed in acid media, the diazonium salt was formed with $NaNO_2$, which was converted into the final azide with NaN_3, presumably by an addition-elimination process. [182,183] Overall, the product **13** was isolated with a 10% yield.

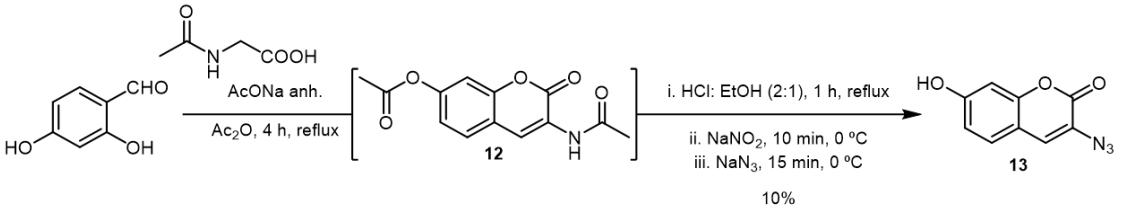

*Figure 50. Synthesis of the probe azido-hydroxycoumarin **13**.*[181]

The cycloaddition product of azide **13** with propargyl alcohol was made using $CuSO_4$ as catalyst and NaAsc as reducing agent in a H_2O/^{t}BuOH mixture. Despite the azide **13** was not totally solubilized, the reaction afforded the triazole **14** in 84% after 48 h at room temperature.

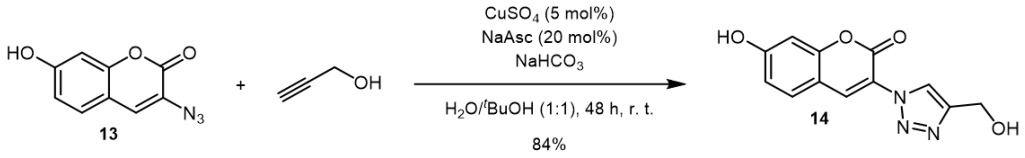

*Figure 51. Synthesis of the fluorescent triazole **14**.*

The product was used to build a calibration curve, key to easily quantify its formation in the reaction screening experiments shown later.

USC UNIVERSIDADE DE SANTIAGO DE COMPOSTELA

[181] K. Sivakumar, F. Xie, B. M. Cash, S. Long, H. N. Barnhill, Q. Wang, *Org. Lett.* **2004**, *6*, 4603.
[182] A. Fox, S. Collier, L. A. Burke, R. N. Butler, *J. Chem. Soc., Perkin Trans.* **1998**, *2*, 2243.
[183] S. M. Joshi, A. de Cózar, V. Gómez-Vallejo, J. Koziorowski, J. Llop, F. P. Cossío, *Chem. Commun.* **2015**, *51*, 8954.

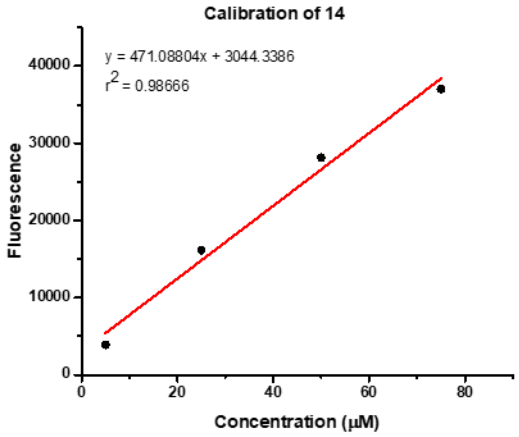

*Figure 52. Calibration of the coumarin probe **14**.*

Additionally, we also prepared the azido-benzothiazole **18**, that after undergoing CuAAC it exhibits green-red fluorescence (figure 53). This would open the door for future orthogonal reactions using both probes in parallel. This azide was obtained in 2 steps.[184] The first step relays in the addition of an *in situ* prepared methyl carbanion of the benzothiazole **15**, to the aldehyde **16,** resulting in the alcohol **17** in a moderate 44% yield. Then, the hydroxyl group is eliminated under acidic conditions to yield the probe **18** (37%).

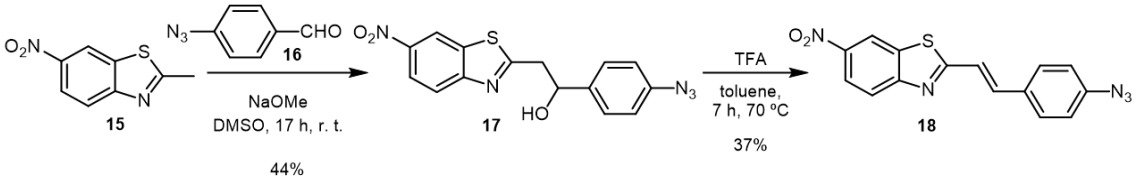

*Figure 53. Synthesis of the probe azido-benzothiazole **18**.[184]*

This azide reacts with propargylic alcohol using $CuSO_4$ and NaAsc in a mixture 1:1 of water-ethanol, albeit with low yield. We later found that while the cycloaddition product **19** is fluorescent, the reacting azide also presents some fluorescence background, which somewhat complicates the use of this chemistry for monitoring the transformation by fluorescence.

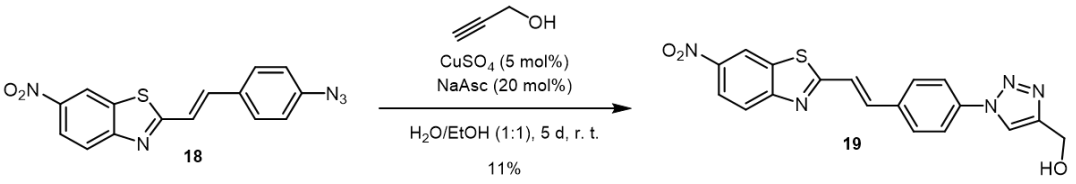

*Figure 54. Synthesis of the fluorescent triazole **19**.*

USC
UNIVERSIDADE DE SANTIAGO DE COMPOSTELA

[184] A. Herner, I. Nikic, M. Kállay, E. A. Lemke, P. Kele, *Org. Biomol. Chem.* **2013**, *11*, 3297.

3.1.3. CuAAC reactions with azides 13

The initial CuAAC experiments were carried out in a plate reader (96 wells), what allows us to perform reactions by triplicate. The procedure consistes of first preparing a 2.5 mM solution of the **Cu(II)**-tristriazole complexes just before each use, by mixing a fresh water solution of $CuSO_4$ and an aqueous solution of the corresponding ligand **L** (5% DMSO, 2 equiv. respect Cu) for 10 minutes in a 0.5 mL Eppendorf, at room temperature under air. Concurrently, a mixture containing 115 μM of azide and 230 μM propargyl alcohol in H_2O or PBS is prepared in a 2 mL Eppendorf tube starting from fresh azide solution in DMSO and aqueous fresh solution of propargyl alcohol. 87 μL of the solution with the substrates is added into the corresponding well, followed by 3 μL of the **Cu(II)-L** solution. Finally, 10 μL of a 25 mM NaAsc is added into the wells, thus promoting the formation of the Cu(I) species and eventually triggering the cycloaddition under air at room temperature. In summary, the final conditions are 100 μM of azide, 200 μM of alkyne, 75 μM of the **Cu(II)-L** complex (75 mol%) and 2.5 mM of NaAsc (if present) in H_2O (0.5% of final DMSO content).

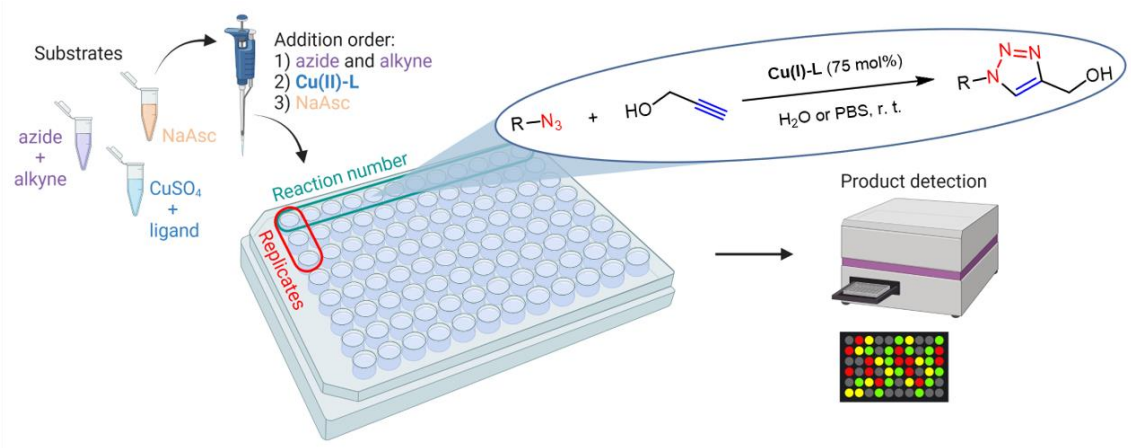

Figure 55. Schematic representation of the reaction screening methodology employed in this work.

As expected from previous reports, initial cycloaddition experiments with the probe **13** gave good results using H_2O as solvent. All ligands were able to promote the reaction in 20 min (table 1), but practically no fluorescence increase was found when no ligand was used. The yields were calculated using the calibration curve previously shown (figure 55), and are indicated in table 1.

USC
UNIVERSIDADE DE SANTIAGO DE COMPOSTELA

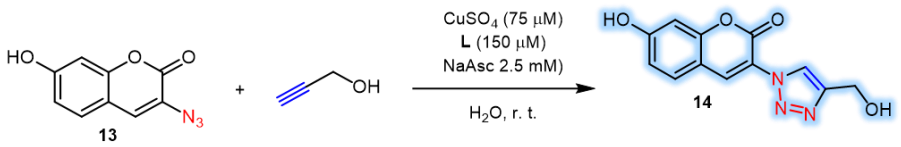

Entry	Ligand	Time (min)	Yield (%)
1	**L1**	20	56
2	**L2**	20	47
3	**L3**	20	49
4	**L4**	20	61
5	-	20	-
6	**L1**	30	56
7	**L2**	30	48
8	**L3**	30	50
9	**L4**	30	61
10	-	30	-

*Table 1. Catalytic activity of the different **Cu(I)-L** complexes (considering the complete reduction) with the hydroxicoumarin **13**. Conditions: 100 μM of azido-probe **13**, 200 μM of propargyl alcohol, 75 μM of **Cu(I)-L** (from $CuSO_4$, and **L** preincubation), 2.5 mM NaAsc, in water at 25 ºC for 20 or 30 min.*

As shown in the table 1, the new designed Cu(I)-**L4** complex affords the product in 61% yield, slightly better than when **L1** is employed, the more commonly used in bioorthogonal experiments. No further increase in yields was detected after 30 min of reaction.

These results, that confirms the water tolerance of the reaction, led us to carry out a preliminary test of the viability of performing these reactions in mammalian cells. The complex of **Cu(I)-L4** was freshly prepared in a similar way to that used in the experiments in the plate reader. More in detail, both the copper salt ($CuSO_4$) and the ligand were mixed in a 1:2 stoichiometry in H_2O for 1 h to ensure the complete complexation of the copper, to a final concentration of 2.5 mM (**Cu(II)-L**). Then 6.25 equiv. of NaAsc were added and the mixture was kept for 30 min, to ensure the reduction of the copper (**Cu(I)-L**).

A solution of this mixture (12 μL) in 388 μL of DMEM was added to a culture of cells (HeLa, 400.000), for a final concentration of 75 μM. After 30 min incubation, cells were thoroughly washed with DMEM twice to ensure that the extracellular copper was removed. Afterwards, cells were treated with a solution of 100 μM of probe **13** and 200 μM of propargyl alcohol, in 400 μL of DMEM. After 1 h, the cells were washed with DMEM (x2) and observed under the microscope. This protocol, that is quite general for the cellular experiments, minimizes extracellular reactions, because of the washing steps.

USC DE SANTIAGO DE COMPOSTELA

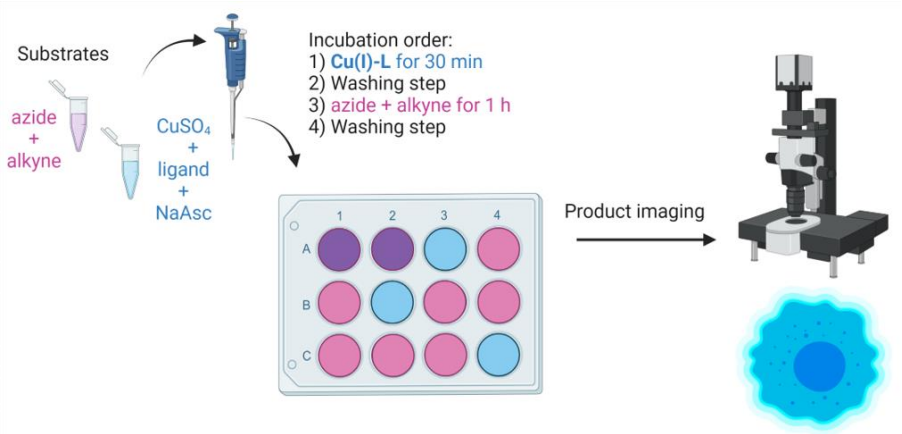

Figure 56. Schematic representation of the methodology employed in cellular experiments in this work.

Unfortunately, we didn't observe the appearance of blue fluorescence at all, characteristic of the product (figure 57). We hypothesized that this failure, might be related to the formation of a very low amount of the product, which is not particularly highly fluorescent, or perhaps with internalization problems of the azide probe.

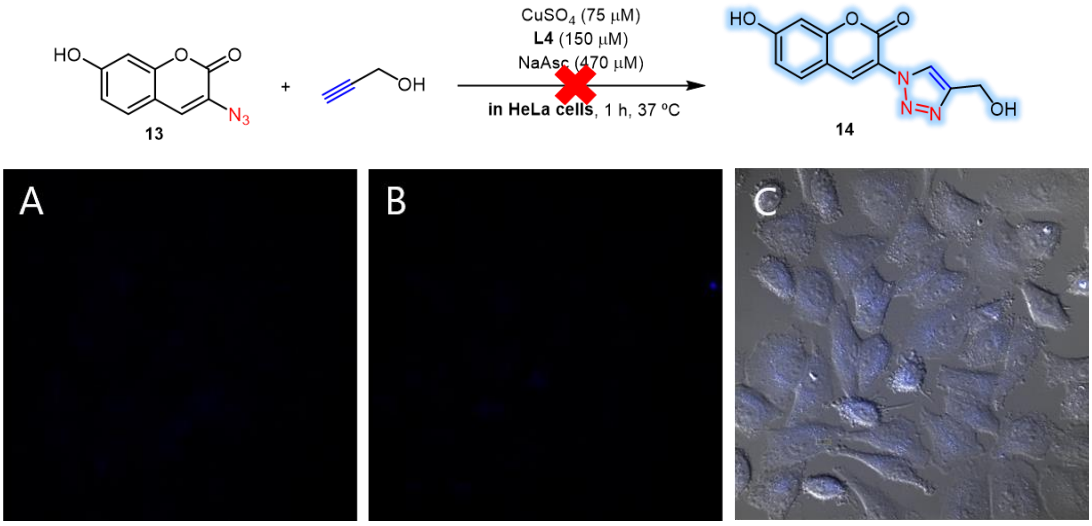

*Figure 57. Fluorescence micrographies of HeLa cells with probe **13** and the in situ made **Cu(I)-L4** complex. Protocol: cells were incubated with 75 μM of **Cu(I)-L4** complex (from $CuSO_4$, L and NaAsc preincubation), washed and then incubated with 100 μM probe **13**, and 200 μM propargyl alcohol at 37 ºC for 1 h. A) incubation of cells with probe **13** and propargyl alcohol. B) Incubation of cells with substrates, and freshly prepared **Cu(I)-L4** complex. C) Bright-field from B. Fluorescence obtained in the blue channel (λ_{exc} = 385 nm, λ_{em} = 410-480 nm).*

USC
UNIVERSIDADE DE SANTIAGO DE COMPOSTELA

3.1.4. Selection of probe 20

In view of previous results and having in mind the higher stability of alkyl azides when compared to aryl azides,[185] we considered to test the behavior of 9-(azidomethyl)-anthracene **20**, that was easily prepared by reaction of the corresponding bromide with NaN_3. In addition, its partial hydrophobicity could favor the cellular internalization.

We were glad to confirm that this probe undergoes the CuAAC annulation with propargyl alcohol to give the expected triazole **21**, when treated with $CuSO_4$ and NaAsc in a H_2O-^{t}BuOH mixture (1:1, not totally solubilized, 1.18 M). The product was isolated in a 41% yield (figure 58a). The triazole **21** is 155-fold more fluorescent than the azide precursor **20**, which facilitates monitoring the process by fluorescence (figure 58b and c).

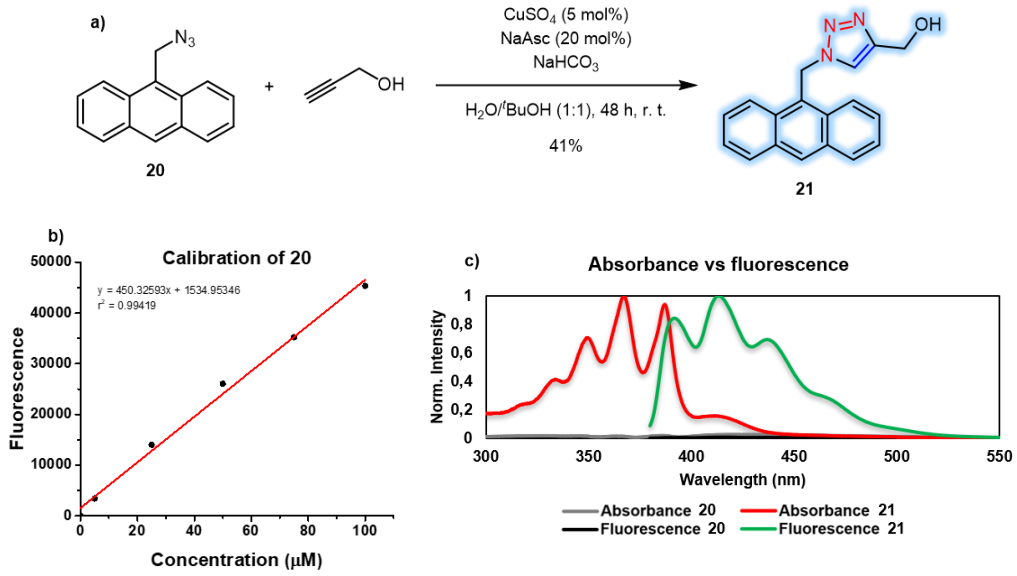

*Figure 58. a) Synthesis of triazole **21**, b) Fluorescence calibration curve. c) Absorbance and fluorescence spectra.*

USC UNIVERSIDADE DE SANTIAGO DE COMPOSTELA

[185] J. H. Boyer, F. C. Canter, *Chem. Rev.* **1954**, *54*, 1.

3.1.5. CuAAC reactions with anthracenyl azide 20

With this new probe **20** in hand, we performed a detailed study of the CuAAC at a scale of 100 μM in water and PBS, using 2 equiv. of propargyl alcohol, 75 μM of Cu(I)-L complexes (75 mol%) and 33 equiv. of NaAsc to trigger the reaction, following the stablished methodology developed with the coumarin **13** (plate reader).

In the absence of ligands, *i.e.*, when only $CuSO_4$ and NaAsc were employed, the reaction gaves poor yields even after 24 h. Similarly, if no NaAsc was used to trigger the reaction, no fluorescence enhancement was observed, independently of the ligand employed. Gratifyingly, using the preformed and reduced complex of the Cu(II) salt with **L4** we observed a 55% yield in water and 54% in PBS after 10 min of reaction, while with **Cu(I)-L1** and **Cu(II)-L3** led to lower yields (around 30%). After 20 minutes, **Cu(I)-L4** provided almost 70% yield in both water and PBS. These results were further corroborated by HPLC-UV, where similar outcomes were found after 1 h in H_2O. Besides, full conversion of the azide was corroborated (see experimental section, Chapter II S4).

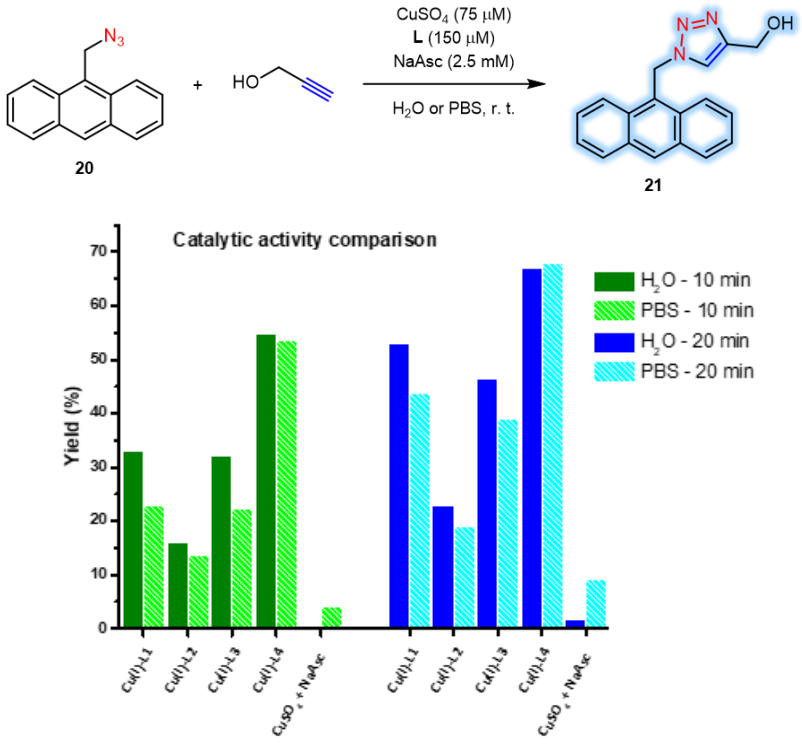

*Figure 59. Catalytic activity of the different **Cu(I)-L** complexes (considering the complete reduction, **L**) with the antracenyl azide probe **20**. Conditions: 100 μM of azido-probe **20**, 200 μM of propargyl alcohol, 75 μM of **Cu(I)-L** (from $CuSO_4$ and **L** preincubation), 2.5 mM NaAsc, in water or PBS at 25 ºC for 10 or 20 min.*

We next performed studies along time for comparing the activities of the different **Cu(I)-L** complexes (figure 60). When the reaction was carried out with **Cu(I)-L4**, the plateau was reached in 20 min, while with **Cu(I)-L1** full conversion required around 10 minutes extra, and **Cu(I)-L3** other additional 20 minutes. Therefore, the best results were obtained using **L4** as ligand. We then checked the influence of the catalyst loading, finding out that we can go down to 25 mol% (25 μM) and the yield is not specially affected. Meanwhile, in the case of **L1** or **L3**, decreasing the catalyst loading below 50 mol% (50 μM) entailed a drastic decrease in the reactivity.

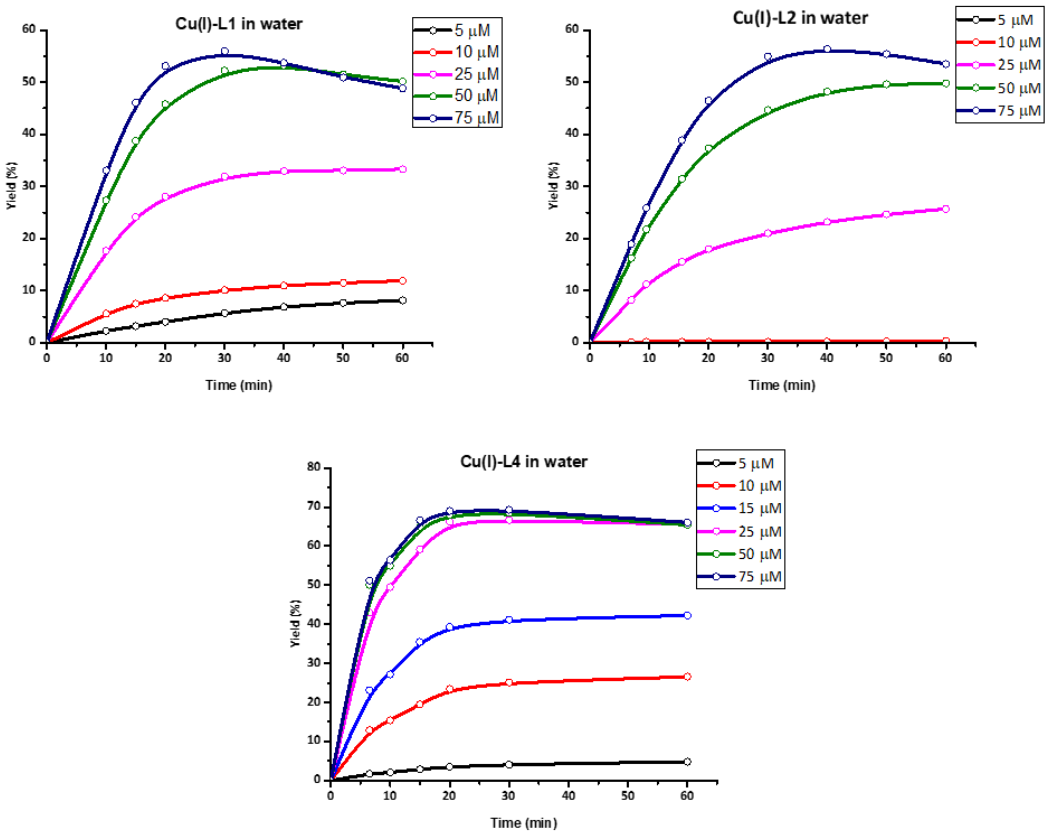

*Figure 60. Experiments along time with **Cu(I)-L1**, **Cu(I)-L3** and **Cu(I)-L4**. Conditions: 100 μM of azido probe **20**, 200 μM of propargyl alcohol, the corresponding amount of **Cu(I)-L** (from $CuSO_4$ and **L** preincubation), 2.5 mM NaAsc, in water or PBS at 25 ºC along the time.*

USC UNIVERSIDADE DE SANTIAGO DE COMPOSTELA

3.2. Cellular experiments with *in situ* prepared tristriazole complexes

Cellular experiments were carried out with the anthracenyl azide **20**, using similar conditions than described before: 100 μM of azide **20**, 2 equiv. of propargyl alcohol and 75 μM of the corresponding **Cu(I)-L** complex, previously prepared from the incubation of $CuSO_4$, the selected ligand and NaAsc. In contrast with previous experiments in HeLa cells using probe **13**, we did observe the rise of fluorescence (figure 61) across the cytoplasm and in vesicles, with cells showing an unaltered morphology, which was more intense when the experiment was carried out with ligand **L4** (figure 61, panel F), although with other ligands we also observed reactivity. Extracellular reactivity could be discarded due to the extensive washing protocols. In addition, this was further confirmed by the observation of a total lack of reactivity in control experiments using extracellular media.

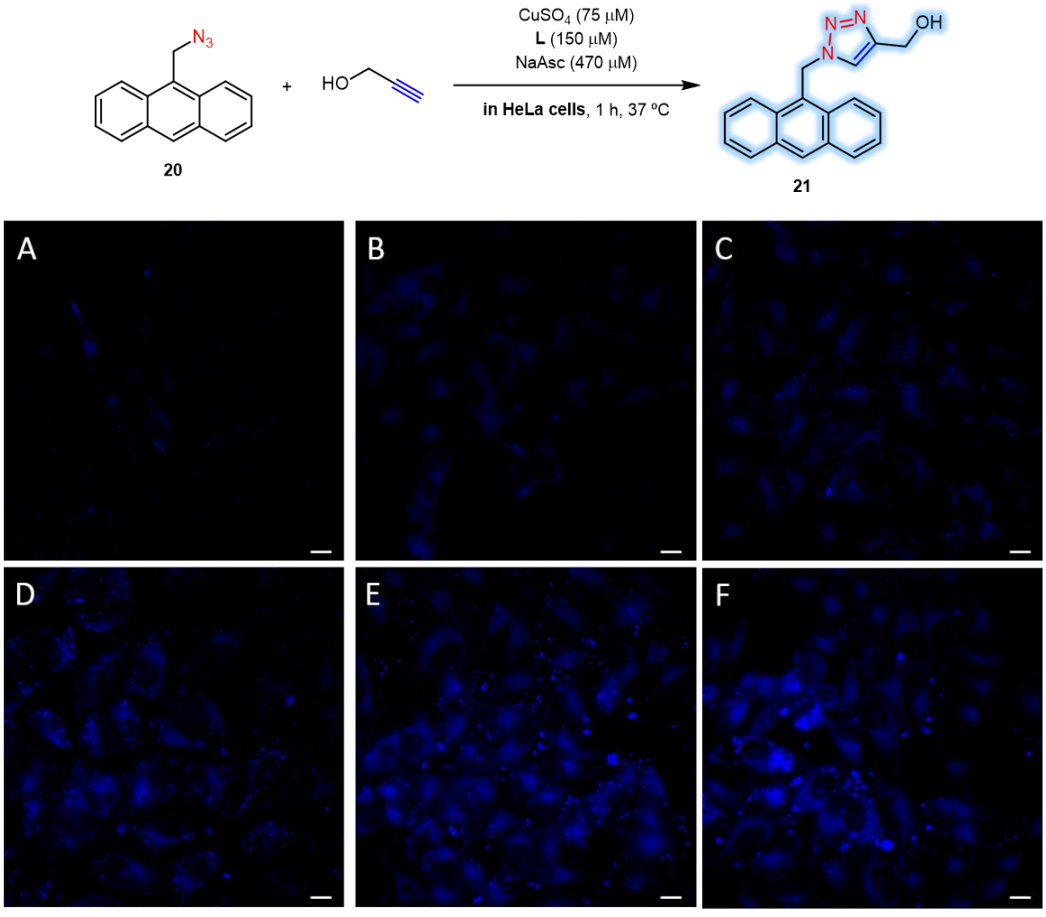

*Figure 61. Fluorescence micrographies of HeLa cells with different **Cu(I)-L** complexes. Protocol: cells were incubated with 75 μM of **Cu(I)-L** (from $CuSO_4$, Ln and NaAsc preincubation), washed and then incubated with 100 μM of azide **20**, and 200 μM of propargyl alcohol at 37 ºC for 1 h. A) Control without Cu. B) Ligandless Cu(I). C) **Cu(I)-L2**. D) **Cu(I)-L3**. E) **Cu(I)-L1**. F) **Cu(I)-L4**. Fluorescence obtained in the blue channel (λ_{exc} = 385 nm, λ_{em} = 410-480 nm).*

USC DE COMPOSTELA

It is well known that the cell presents a reductive environment.[186,187] Thus, we wondered whether the **Cu(II)-L** complex could be directly reduced inside cells to the active Cu(I) complexes. In fact, as it can be observed in figure 62, panel A, in experiments carried out with **Cu(II)-L3** without preforming the reduction of Cu(II) complex with NaAsc, there is some residual fluorescence, that can be slightly increased with the subsequent addition of NaAsc to the cell incubation media (figure 62, panel B). The addition of well-known Cu chelators such EDTA in the cellular media didn't affect the fluorescence outcome (figure 62, panel C). Nonetheless, the intensity of the signals is clearly lower than that obtained when the **Cu(II)-L** complexes were pretreated with NaAsc.

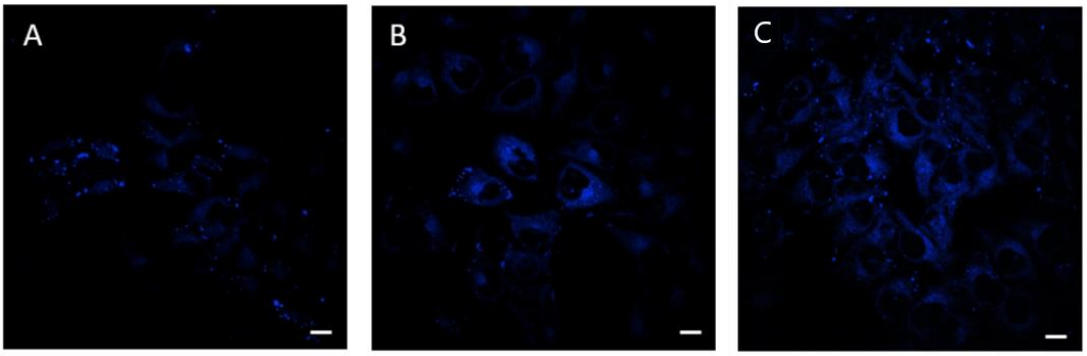

*Figure 62. Fluorescence micrographies of additional experiments in HeLa cells. Protocol: cells were incubated with 75 μM of the chosen Cu catalyst, washed and then incubated with 100 μM of azide **20**, and 200 μM of propargyl alcohol at 37 ºC for 1 h. A) **Cu(II)-L3** (from $CuSO_4$ and **L3** preincubation without NaAsc). B) **Cu(II)-L3** (from $CuSO_4$ and **L3** preincubation) plus posterior incubation with 6.25 equiv. NaAsc, with respect to Cu content. C) **Cu(I)-L3** (from $CuSO_4$, **L3** and NaAsc preincubation) and 2 equiv. EDTA with respect to Cu content. Fluorescence obtained in the blue channel (λ_{exc} = 385 nm, λ_{em} = 410-480 nm)*

It is important to indicate that in the above cellular experiments we didn't not observe signs of toxicity, and cell shapes observed in brightfield microscope were the natural cell morphology (see MTT assays later).

USC
UNIVERSIDADE DE SANTIAGO DE COMPOSTELA

[186] H. J. Forman, J. Fukuto, M. Torres, *Signal Transduction by Reactive Oxygen and Nitrogen Species: Pathways and Chemical Principles* **2003**, Kluwer Academic Publishers.
[187] B. A. Wagner, V. G. J. Rodgers, G. R. Buettner, *Cell Biochem. Biophys.* **2013**, *67*, 477.

3.3. CuAAC reactions with predefined copper (I) complexes

In the previous experiments, the copper(I) complexes were made by *in situ* reduction of the corresponding Cu(II) precursors, which requires the use of a reductant, and doesn't ensure how much of the Cu(I) is produced. It would be highly desirable to use well-defined Cu(I) complexes instead.

For this goal, we selected some several copper(I) complexes that have been previsouly described: $[Cu(Tpa^*)]PF_6$[188] (**C1**), the commercially available phosphinite $CuI\{P(OEt)_3$[189] (**C2**), a carbene containing catalyst $[Cu(IAd)_2]PF_6$[190] (**C3**) and a phosphite $CuBr\{PPh_2(OPh\text{-}2\text{-}OMe)\}$[191] (**C4**) (figure 63).

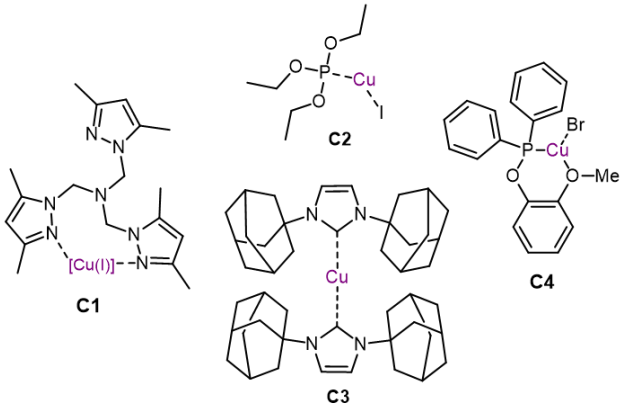

Figure 63. Representation of the different complexes employed in this section.

Complex **C1** $[Cu(Tpa^*)]PF_6$**,** was prepared in a dry box by mixing $[Cu(NCMe)_4]PF_6$ with 1 equivalent of trispyrazol ligand (Tpa*) (2 h).

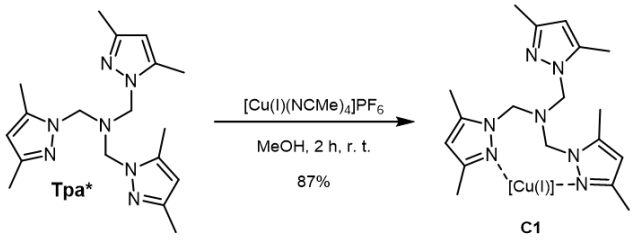

*Figure 64. Synthesis of **C1**.*

C3 complex was synthetized through the formation of the carbene ligand IAd from the $IAdBF_4$ salt and ^{t}BuONa, in presence of $[Cu(NCMe)_4]PF_6$.

[188] E. Haldón, M. Delgado-Rebollo, A. Prieto, E. Álvarez, C. Maya, M. C. Nicasio, P. J. Pérez, *Inorg. Chem.* **2014**, *53*, 4192.

[189] Before testing the phosphinite **C2**, Bromotris(triphenylphosphonie)copper(I) $Cu(PPh_3)_3Br$, and $Cu(phen)PPh_3Br$ were tried. However, in conjunction with the azide, it gave an absurd high amount of background fluorescent noise. Likely the Staudinger reduction took place, activating the probe. Then, an oxidized phosphine was tested in order to avoid the Staudinger process.

[190] S. Díez-González, S. P. Nolan, *Angew. Chem. Int. Ed.* **2008**, *47*, 8881.

[191] S. Lal, J. McNally, A. J. P. White, S. Díez-González, *Organometallic* **2011**, *30*, 6225.

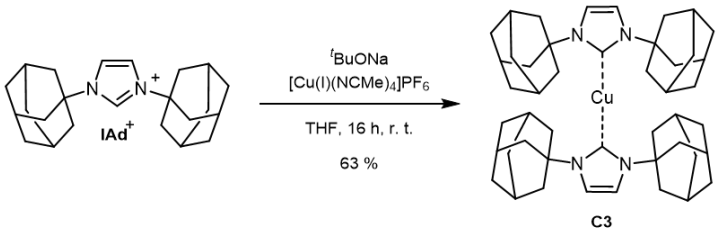

*Figure 65. Synthesis of **C3**.*

The phosphite complex **C4** was synthetized in two steps, which involved the phosphorylation of o-methoxyphenol with Ph_2PCl followed by the formation of the complex using CuBr as copper source (21% yield).

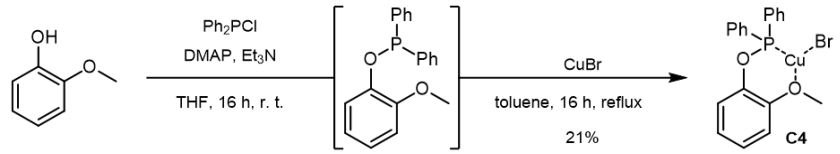

*Figure 66. Synthesis of **C4**.*

We also made complex **C5** $[Cu(BTTE)]PF_6$, prepared in a dry box by mixing $[Cu(NCMe)_4]PF_6$ with 1 equivalent of **L3** (2 h).

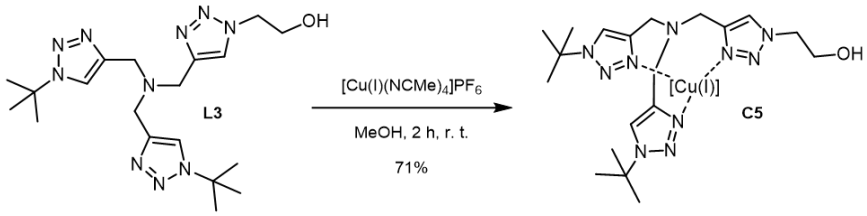

*Figure 67. Synthesis of complex **C5**.*

USC
UNIVERSIDADE DE SANTIAGO DE COMPOSTELA

The cycloaddition experiments were carried out by adding 3 µL of a fresh stock 2.5 mM of the corresponding predefined Cu(I) complexes to a well containing the same amounts of substrates as in the previous experiments (87 µL of the substrate mixture: 115 µM of azide **20** and 230 µM of propargyl alcohol) in H_2O or PBS. The assays were performed in the absence or presence of NaAsc (10 µL of a 25 mM NaAsc solution). Accordingly, the final concentrations were 100 µM of the azide, 2 equivalents of propargyl alcohol, 75 µM of the predefined Cu complex (and 2.5 mM of NaAsc if used).

In absence of reductant, the yields were low, less than 10% after 20 min at room temperature (figure 68). The yield observed with **C1** could be improved up to ca. 15% in H_2O by raising the temperature to 37 ºC (physiological temperature). Importantly, the addition of NaAsc led to much better yields, especially for **C1** that reached a 50% of yield. These results suggest that under open air conditions the Cu(I) species are readily oxidized to Cu(II). Using **C5** and NaAsc, performing the reaction at 37 ºC, we observed a yield of 43% in H_2O and 57% in PBS, after 20 min. Similar results were obtained by the analysis of the reaction by HPLC-UV after 1 h in H_2O (see experimental section, Chapter II S4).

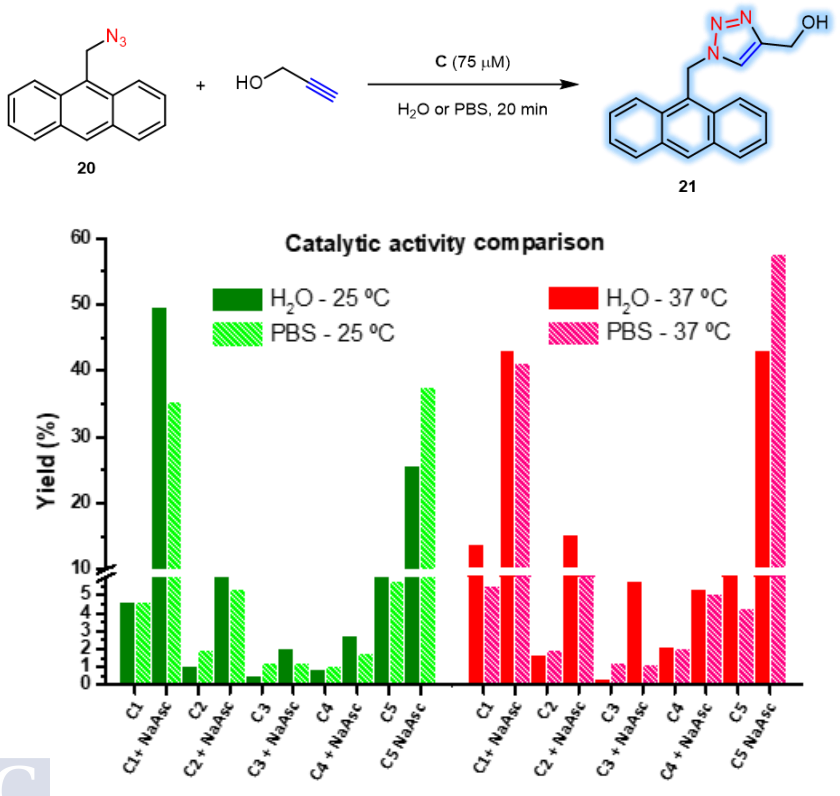

*Figure 68. Catalytic activity of the different predefined Cu(I) complexes (**C**) with the antracenyl azide probe **20**. Conditions: 100 µM of azide **20**, 200 µM of propargyl alcohol, 75 µM of the predefined complex **C**, 25 equiv. of NaAsc (if added), in water or PBS at 25 or 37 ºC for 20 min.*

We then performed a more detailed monitoring of the reaction promoted by the complexes with the best activity, **C1** and **C5,** in absence or presence of NaAsc. We also checked the effect of the catalyst loading (figure 69). With **C1** the reaction reached a plateau in 20 min, with no big differences between a catalyst concentration of 50 or 75 μM. Meanwhile, **C5** required the double amount of time at 25 ºC, being even problematic to decrease the concentration below 75 μM. However, at 37 ºC, both in water and PBS, **C5** reached the plateau between 10 and 20 min, with only a slight decrease when catalyst loading was decreased up to 50 μM. No yield improvement was observed after 20 min and in absence of NaAsc for **C1** either **C5**.

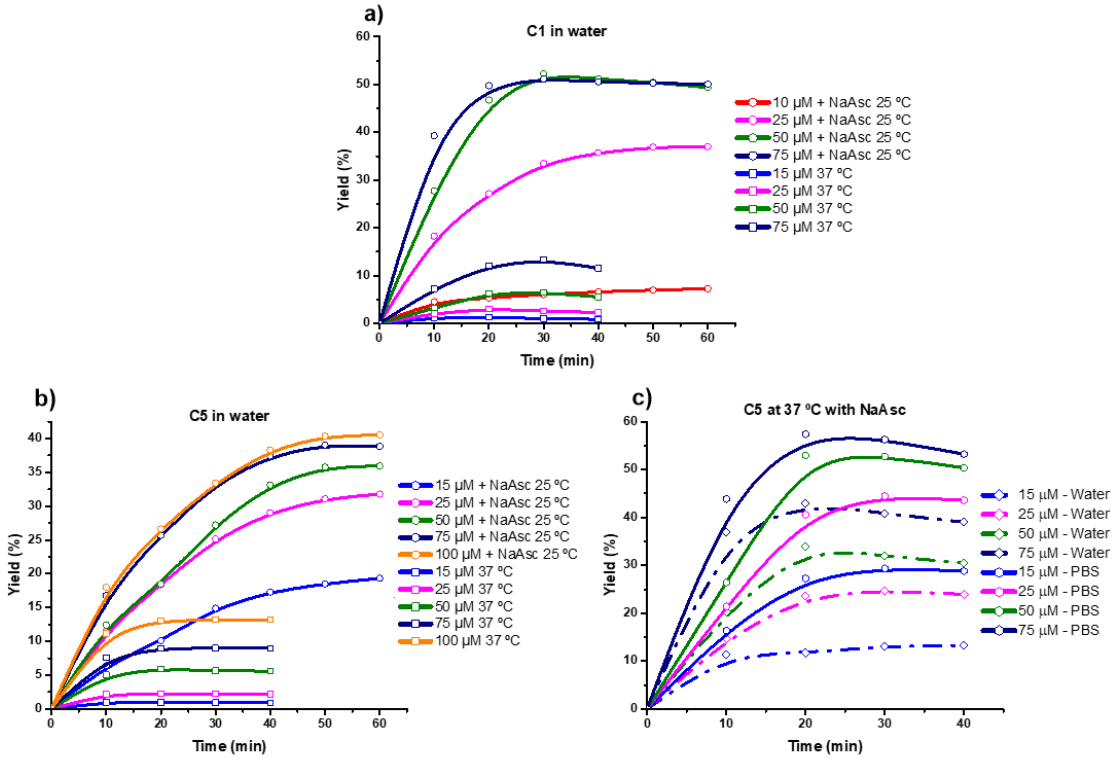

*Figure 69. Experiments along time of **C1** and **C5**. Conditions: 100 μM of azide **20**, 200 μM of propargyl alcohol, the corresponding amount of the predefined Cu(I) complex **C**, plus 25 equiv. (if added) of NaAsc, in water or PBS at 25 or 37 ºC.*

USC UNIVERSIDADE DE SANTIAGO DE COMPOSTELA

In order to test the stability of the copper complexes **C1** and **C5**, we performed Electron Paramagnetic Resonance (EPR) measurements to study the Cu oxidation state with time (figure 70). The EPR showed a fast oxidation of a 10 mM solution of **C1** (up to 81% after 10 min) in DMSO. **C5** was more stable, keeping its reduced form for more than 40 minutes (25% of oxidation, figure 70c).

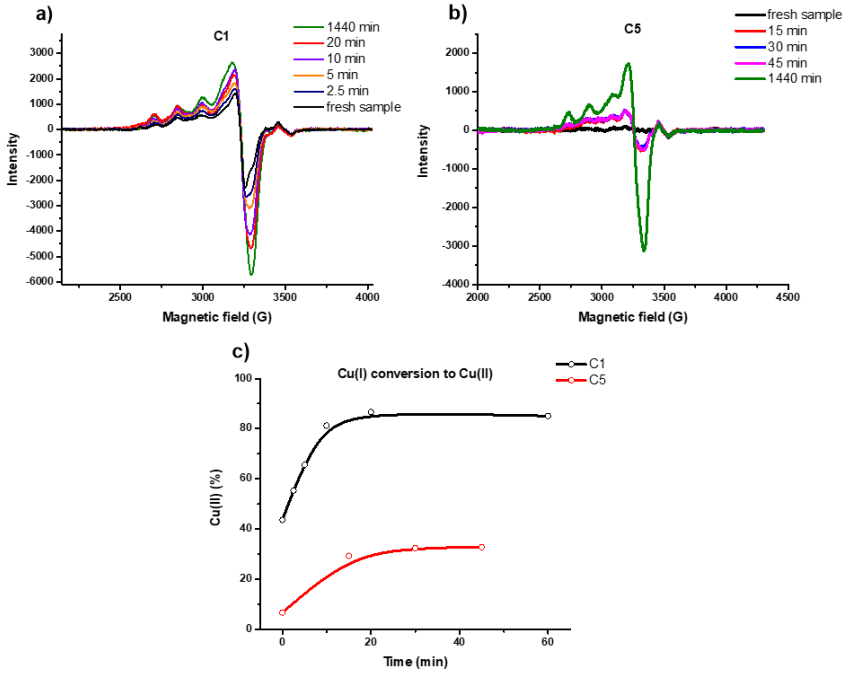

*Figure 70. EPR experiments for a) **C1** and b) **C5**. c) Cu(II) sample quantification. A fresh sample was considered "time 0", while a sample of 24 h under air was considered, and later confirmed by NMR, to be 100% oxidized Cu(II) complex.*

USC UNIVERSIDADE DE SANTIAGO DE COMPOSTELA

3.4. Cellular experiments with predefined Cu(I) complexes

The higher stability exhibited by **C5** suggested that it might be able to work in cellular experiments, keeping its reduced state in the cell environment for the reaction time. This prompted us to test its activity, compare it with the rest of Cu(I) complexes. These experiments were carried out as follows: cells were treated with 400 μL of DMEM containing 50 μM of the proper predefined Cu(I) complex (from a 10 mM stock DMSO solution) for 30 min. Then, cells were thoroughly washed with DMEM twice to ensure that no extracellular copper was present, and then incubated with a solution of 100 μM of probe **20** and 200 μM of propargyl alcohol, in 400 μL of DMEM. After 1 h, cells were washed again with DMEM (x2) and observed under the microscope.

Not surprisingly, when **C3** was used, no fluorescence was detected. However, with **C**5 we observed a bright fluorescence enhancement, not only in HeLa cells, but also in a different cell line such as A549 (figure 71, panel B). Interestingly, the phosphite complex **C2** and phosphonite **C4** were also able to promote some fluorescence (figure 71, panels D and E), although much lower in comparation with **C1** (figure 71, panel C).

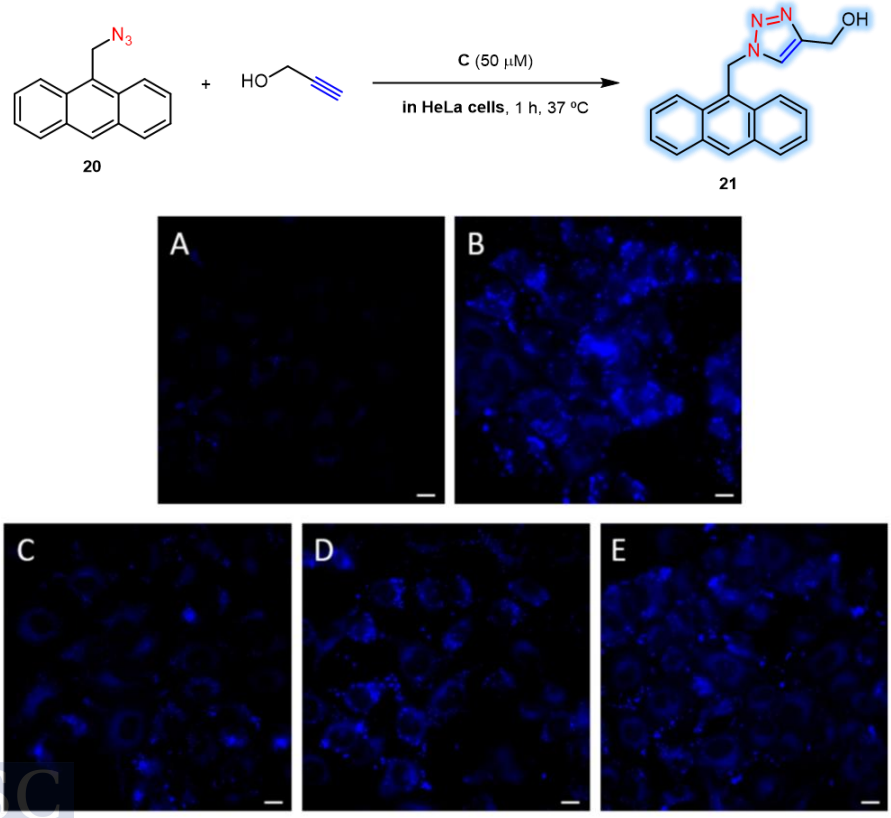

*Figure 71. Experiments in A549 cells with predefined Cu(I) complexes. Protocol: cells were incubated with 50 μM of the predefined Cu(I) complex, washed and then incubated with 100 μM of azide **20** and 200 μM of propargyl alcohol at 37 ºC for 1 h. A) Control without Cu. B) **C5**. C) **C1**. D) **C2**. E) **C4**. Fluorescence obtained in the blue channel (λ_{exc} = 385 nm, λ_{em} = 410-480 nm)*

Overall, **C1** and **C5** highlighted the potential of this kind of predefined complexes to generate similar, or even better intracellular results than the standard *in situ* prepared tristriazole complexes (**Cu(I)-L**). In this sense, we performed flow cytometry assays to mesure the cell fluorescence, thus allowing a more precise comparation among employed catalysts (figure 72). In consonance with previous experiments, the *in situ* prepared **Cu(I)-L3** (from $CuSO_4$, L3 and NaAsc preincubation) and the predefined complexes **C1** and **C5**, were the ones giving the best results.

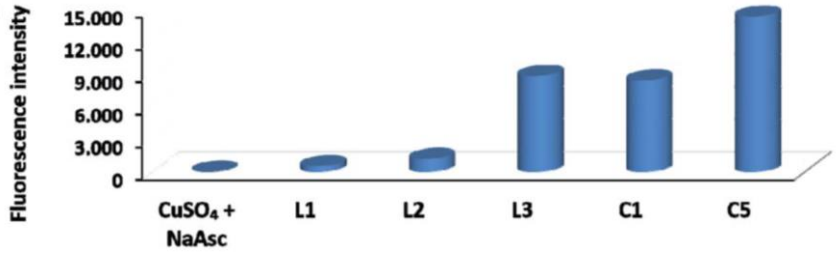

*Figure 72. Compared cellular fluorescence measured by flow cytometry of experiments with in situ prepared **Cu(I)-L** (75 μM), or the predefined complexes **C1** and **C5** (50 μM) in absence of NaAsc.*

3.5. Quantification of the reaction inside living cells

Furthermore, this protocol could be also adapted to calculate the reaction yields of the intracellular transformations with the plate reader. First the amount of substrate internalized was calculated as follows. The content of cells incubated in 4 mL DMEM with 100 μM substrate **20** for 1 hour (100000 cells/well) was extracted with a solution of 1 mL MeOH/H_2O (8:2). This sample was analyzed by HPLC-UV using coumarin as internal standard. Whit the calibration curve of **20** (figure 73), we could determine a 15% of internalization of substrate **20**.

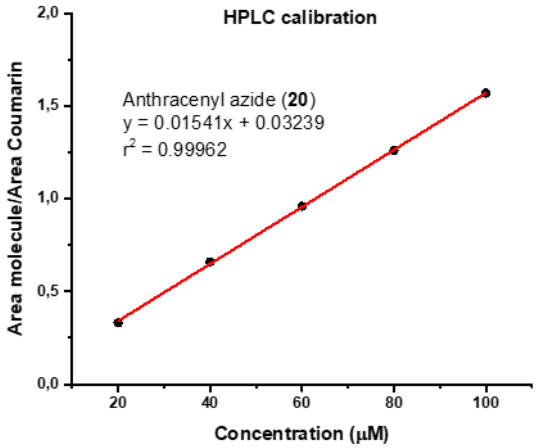

*Figure 73. HPLC-UV calibration curve of **20**.*

For the quantification of **21**, we used fluorescence spectrometry. Fluorescence calibration of triazole probe **21** at low concentration (figure 74) and normalization respect the total number of cells is key to determine the amount of product intracellularly generated after reaction incubation and the posterior methanolic extraction.

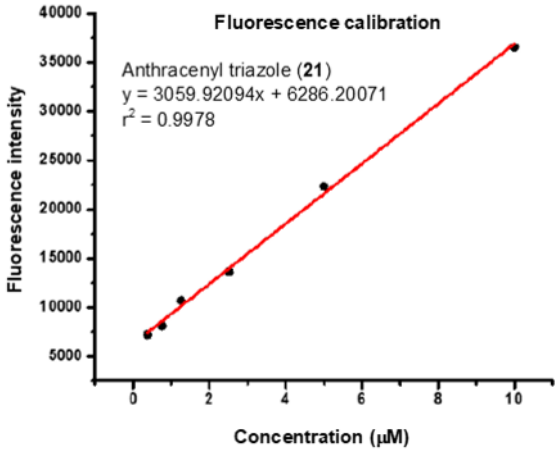

*Figure 74. Fluorescence calibration of triazole **21***

Then, we compared the performance of the two complexes bearing the BTTE ligand (**L3**), the predefined **C5**, and the *in situ* prepared **Cu(I)-L3**, at a concentration of 50 μM (table 2). In fact, **Cu(I)-L3** furnished 0.41 μM of product, what corresponds to 2.7% yield, an impressive result in comparation to Cai's protocol, taking into account that we made no efforts to decrease the GSH presence inside the cell. More thought-provoking was the formation of 2.71 μM of product when **C5** was employed, which is traduced into an astonishing 18% yield. Moreover, this complex still performs well at 25 μM, reaching a 10.4% of yield with no apparent cytotoxicity.

Catalyst	Cat. concentration (μM)	Product formation (μM)	Product formation/cell (μM/cell)	Yield (%)
Cu(I)-L3	50	0.41	$2.39 \cdot 10^{-06}$	2.7
C5	50	2.71	$1.58 \cdot 10^{-05}$	18
C5	25	1.57	$9.16 \cdot 10^{-06}$	10.4

*Table 2. Yield quantification of CuAAC reaction inside HeLa cells. Protocol: cells were incubated with the chosen amount of **Cu(I)-L3** (from $CuSO_4$, **L3** and NaAsc preincubation) or **C5** (in absence of NaAsc), washed and then incubated with 100 μM of azide **20** and 200 μM of propargyl alcohol at 37 ºC for 1 h. Extraction of cell content with MeOH and fluorescence experiments led to the quantification of intracellular concentration of **21**.*

It cannot be discarded that the performance of the catalysts (*in situ* and predefined) could be associated to different cellular uptake. Using ICP-MS experiments we could measure the amount of intracellular copper, which is indicated in figure 75a. These data confirm that the predefined Cu(I) complex **C5** was internalized 3 times better than its *in situ* generated equivalent **Cu(I)-L3**. The TPP analogue **Cu(I)-L4** was also efficiently internalized. Interestingly, in all the cases we observed that the predefined complexes (**C1-C4**) are better internalized than the *in situ* made tristriazole complexes using NaAsc (**Cu(I)-L**). These results, which confirm the good internalization of **C4**, are in consonance with its good performance in cellular experiments, despite the yields we had observed previously were low. In addition, the ICP analysis also corroborated the intracellular location of Cu as it can be observed in figure 75b.

USC DE SANTIAGO DE COMPOSTELA

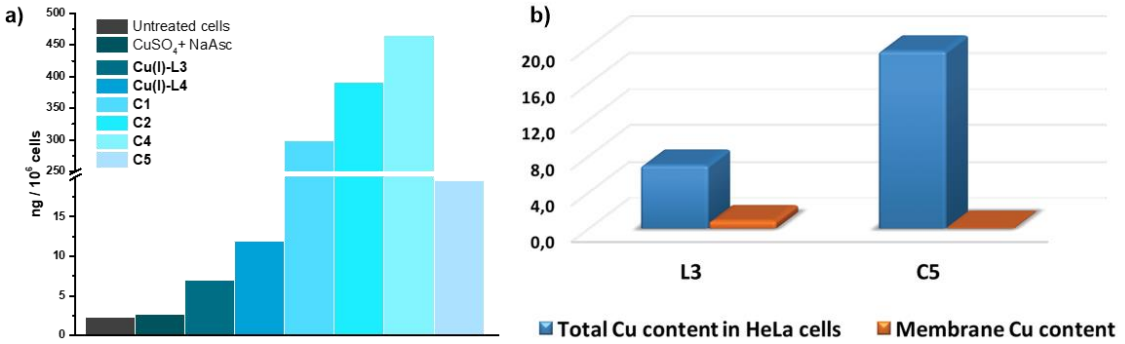

Figure 75. a) ICP-MS experiments for the quantification of the cellular uptake of copper catalyst. b) ICP-MS results of the copper accumulated in the membrane of HeLa cells. Protocol: HeLa cells were incubated with 75 μM of ***Cu(I)-L*** *complexes (from* $CuSO_4$*,* ***L*** *and NaAsc preincubation) and 50 μM of* ***C*** *complexes (absence of NaAsc).*

Of course, key to complete the cellular studies is the study of cytotoxicity of the copper complexes. Remarkably, under our reaction conditions, we observed no substantial cytotoxicity with most of them. We performed the colorimetric MTT (3-(4,5-dimethylthiazol-2-yl)-2,5-diphenyl-2H-tetrazolium bromide) assays (figure 76) to evaluate the cytotoxicity of the complexes employed in this study in a range between 25-150 μM. We found that the predefined complexes **C1-C4** presented toxicity at concentration above 50 μM. In contrast, the tristriazoles prepared *in situ* (**Cu(I)-L**) were less toxic, even after 12 h. Importantly, cells incubated with 50 μM of the most active predefined catalysts, **C1** and **C5**, showed a viability of ca. 85% and 70% after 2h respectively. Satisfactorily, a concentration of 25 μM of C5 led to a survival over 80%.

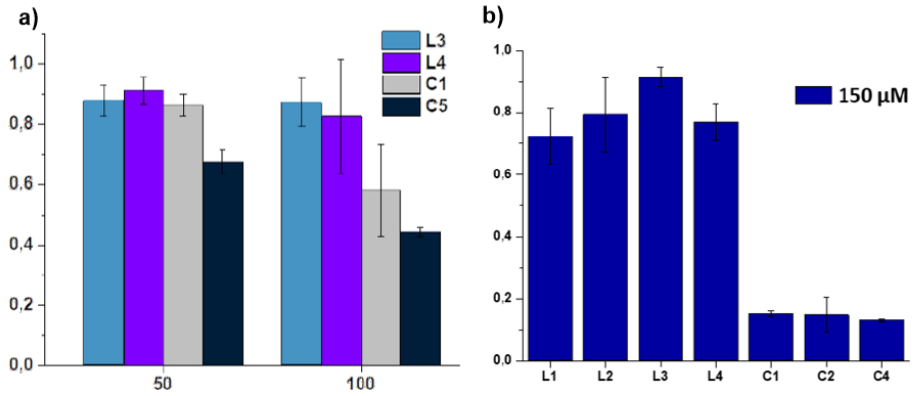

Figure 76. a) Cytotoxicity study of the most significant Cu(I) complexes in the range of 50 and 100 μM, after 2h. b) Cytotoxicity study at 150 μM after 12 h.

USC
UNIVERSIDADE DE SANTIAGO DE COMPOSTELA

4. Conclusion

In conclusion, we have demonstrated that water soluble copper(I) complexes featuring designed ligands can readily enter mammalian cells and promote intracellular CuAAC annulations of small, abiotic and freely diffusible molecules. Our results indicate that using appropriate ligands, it is possible to tune the cell uptake and reactivity of Cu(I) complexes, and importantly, confirm the viability of using discrete copper species to promote efficient CuAAC annulations in the challenging interior of mammalian cells. Indeed, an independently isolated Cu(I)–tris(triazolylmethyl)amine complex, **C5**, that can be stored without degradation when kept under nitrogen, is capable of promoting the intracellular transformation even in the absence of NaAsc. This new complex displays better cellular uptake and better intracellular reactivity than that observed for the in situ made **Cu(I)-L3** complex. This complex is therefore working as an "off-the-shelve" catalyst to promote challenging intermolecular annulations inside mammalian cells. The copper complex **C5** circumvents some of the actual limitations of the "in vivo" CuAAC chemistry, since it avoids the use of excess of ligands or the use of reductants such as ascorbate.

USC
UNIVERSIDADE DE SANTIAGO DE COMPOSTELA

USC
UNIVERSIDADE
DE SANTIAGO
DE COMPOSTELA

CHAPTER 3. Ru [2+2+2] CYCLOADDITION IN BIOLOGICAL MEDIA AND MAMMALIAN CELLS

This chapter includes work published in Chemical Science as:

J. Miguel-Ávila,[a] M. Tomás-Gamasa,[a] J. L. Mascareñas,[a] *Angew. Chem. Int.* **2020**, *59*, 17628.

[a]Centro Singular de Investigación en Química Biolóxica e Materiais Moleculares (CIQUS) and Departamento de Química Organica, Universidad de Santiago de Compostela, 15782, Santiago de Compostela, Spain.

DOI: 10.1002/anie.202006689, Open Acces articles (Very Important Paper)

USC
UNIVERSIDADE DE SANTIAGO DE COMPOSTELA

USC
UNIVERSIDADE
DE SANTIAGO
DE COMPOSTELA

1. Transition metal-promoted cycloadditions

As shown in the introduction and in the previous chapter, the queen mothers of bioorthogonal chemistry are cycloaddition reactions, including the strain-derived cycloadditions or the CuACC.[192] These reactions have been manly used for bioconjugations, and in some cases for biological interrogation,[14,20] but usually not for synthetic purposes, namely, the synthesis of complex structures with potential biological properties. This is surprising, as cycloaddition reactions are extremely appealing form a synthetic point of view, owing to the intrinsic complexity increase they achieve, fact that is already exemplified with the parent Diels-Alder reaction.

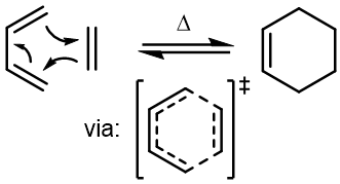

Figure 77. General scheme for a Diels-Alder reaction.

Despite its intrinsic synthetic interest, the Diels-Alder reaction present important limitations, such as the need of specific substrates with tuned electronic properties.[193,194] In this context, the development of metal-catalyzed cycloadditions is especially attractive, as it allows a much wider range of reactivity.

Coordination of the π-electrons of unsaturated systems to transition metals change the electronic properties of the former, and therefore its reactivity, that can engage in different type of reactions, including cycloadditions. Pd, Rh, Ru, Ni, Co and Ir are common metals used in different type of catalytic processes, including formal cycloadditions.[195,196,197,198] Importantly, in many cases, these reactions can be tuned by playing with the metal ligands.

[192] S. S. Nguyen, J. A. Prescher, *Nat. Rev. Chem.* **2020**, *4*, 476.
[193] F. A. Carey, R. J. Sundberg, Advanced Organic Chemistry 5th Ed, Springer, **2008**.
[194] J. Clayden, N. Greeves, S. Warren, Organic Chemistry 2nd Ed, Oxford, **2012**.
[195] A. Roglans, A. Pla-Quintana, M. Solà, *Chem. Rev.* **2021**, *121*, 3, 1894. (for 2+2+2)
[196] B. M. Trost, Z. Zuo, J. E. Schultz, *Chem. Eur. J.* **2020**, *26*, 15354. (7 membered rings)
[197] M. Gulías, A. Collado, B. Trillo, F. López, E. Oñate, M. A. Esteruelas, J. L. Mascareñas, *J. Am. Chem. Soc.* **2011**, *133*, 7660. (for 2+2)
[198] M. Gulías, F. López, J. L. Mascareñas, *Pure Appl. Chem.* **2011**, *83*, 495. (for 3+2)

Ruthenium, is one of the metals that has demonstrated a better performance to catalyze formal cycloadditions. This is also of particular interest for potential bioorthogonal applications, as it has shown high tolerance in biological environments.

Commercially available ruthenium complexes like Cp*Ru(COD)Cl or $[CpRu(NCMe)_3]PF_6$, have demonstrated to be very effective to promote different type of synthetically relevant cycloadditions.[199,200] Some mentionable examples are collected in figure 78: a) a [2+2] reactionreported by the group of Mitsudo in 1994;[201] b) a [4+2] process described by Trost and co-workers in 2000;[202] c) a [2+2+2] cycloaddition published by Itoh's group in 2003.[203]

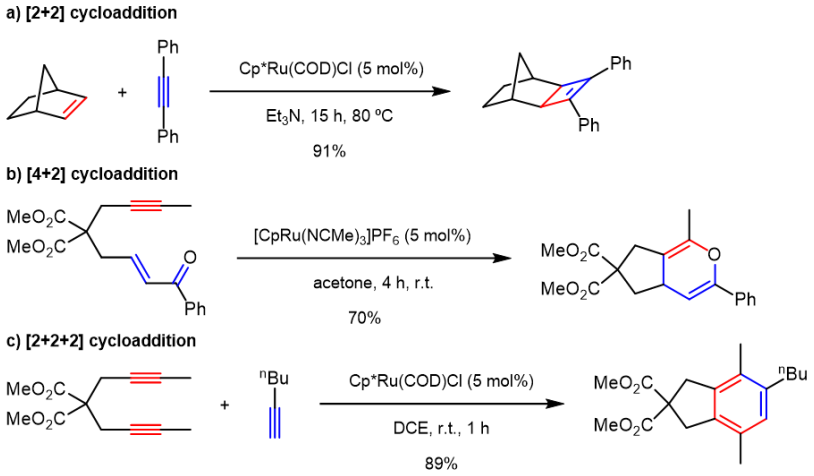

Figure 78. Ruthenium catalyzed cycloadditions. a) [2+2] Cycloaddition reported by Mitsudo in 1994.[201] b) [4+2] Cycloaddition reported by Trost in 2000.[202] c) [2+2+2] Cycloaddition reported by Itoh in 2003.[203]

This last type of reaction, the [2+2+2] cycloaddition, is highly attractive from the constructive and complexity increase point of view, as from very simple substrates it is possible to build aryl rings, generating very interesting structures.

USC UNIVERSIDADE DE SANTIAGO DE COMPOSTELA

[199] L. Severa, J. Vávra, A. Kohoutová, M. Cízková, T. Sálová, J. Hývl, D. Saman, R. Pohl, L. Adriaenssens, F. Teplý, Tetrahedron Lett. **2009**, *50*, 4526.
[200] J. Palaniraja, S. M. Roopan, *Chem. Sci. Rev. Lett.* **2014**, *3*, 93.
[201] T. Mitsudo, H. Naruse, T. Kondo, Y. Ozaki, Y. Watanabe, *Angew. Chem. Int. Ed. Engl.* **1994**, *33*, 580.
[202] B. M. Trost, R. E. Brown, F. D. Toste, *J. Am. Chem. Soc.* **2000**, *122*, 5877.
[203] Y. Yamamoto, T. Arakawa, K. Itoh, *J. Am. Chem. Soc.* **2003**, *125*, 12143.

The reaction has been proposed to take place through the following general mechanism: the catalytic cycle starts with the coordination of the two alkynes to the Ru(II) complex. Subsequently, and oxidative cycloametallation, which is the rate-determining step, gives a ruthenacyclopentatriene and its tautomeric ruthenacyclopentadiene form (**II**). After the coordination of the external alkyne (**III**), subsequent [2+2] cycloaddition yields a ruthenabicycloheptratriene (**IV**), that quickly suffers a rearrangement, triggering the ring opening and forming a ruthenacycloheptatetraene (**V**). Finally, a reductive elimination step leads to the formation of the corresponding arene (**VI**) that is displaced, completing the cycle.[195,204]

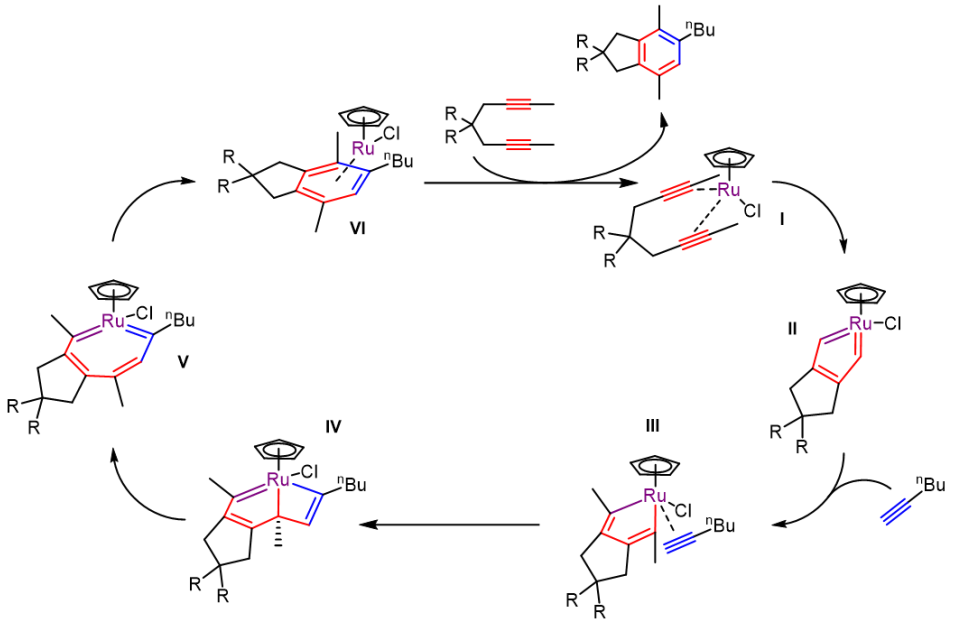

Figure 79. Mechanism for the ruthenium promoted [2+2+2] rerported by Itoh in 2003.[203] R = CO_2Me. Colors represent electron movement in the different compounds.

USC
UNIVERSIDADE DE SANTIAGO DE COMPOSTELA

[204] K. Tanaka, *Transition-Metal-Mediated Aromatic Ring Construction*, Wiley, **2013**.

2. TM-promoted [2+2+2] cycloadditions in aqueous and biological media: antecedents

Alkynes are well-established bioorthogonal reactants, and key partners for instance for the CuAAC. Therefore, they might be used for other type of reactions in biological environments. Considering the synthetic relevance of the above commented metal-promoted [2+2+2] cycloadditions, one could wonder about the viability of performing this transformation in biological media. A few examples that demonstrate their water compatibility have been described, not only with ruthenium,[205] but also with rhodium or cobalt catalysts.[206,207,208] However, solubility issues tend to be a problem. The groups of Oshima and Wan demonstrated that using a tris(*m*-sulfonatophenyl)-phosphine (tppts) as ligand,[209] the reaction is more efficient and can be carried out in mixtures with high water proportion.[210,211]

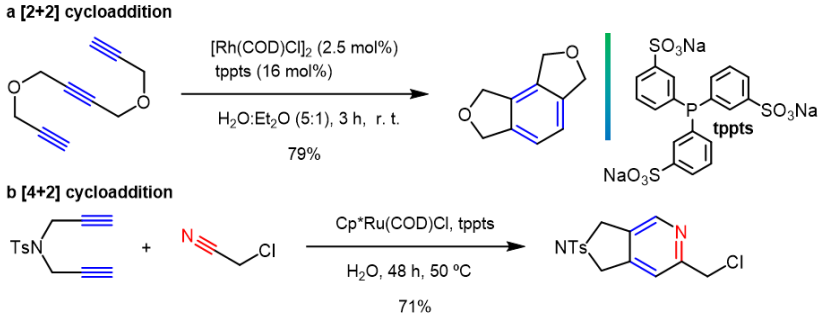

Figure 80. TM [2+2+2] reaction performed in water using soluble ligands.[210,211]

In terms of bioorthogonality, and considering the possibility of carrying out this type of cycloadditions in complex biological media, there is a nice contribution by Teplý and collaborators in 2009. Herein, they reported an intramolecular [2+2+2] cycloaddition of designed triynes in bacteria cell lysates, at room temperature (figure 81).[212] This result suggest that the multicomponent cycloaddition can be carried in complex aqueous media, at least in an intramolecular form.

[205] V. Cadierno, S. E. García-Garrido, J. Gimeno, *J. Am. Chem. Soc.* **2006**, *128*, 15094.
[206] L. Yong, H. Butenschön, *Chem. Commun.* **2002**, *23*, 2852.
[207] B. Heller, B. Sundermann, H. Buschmann, H. Drexler, J. You, U. Holzgrabe, E. Heller, G. Oehme, *J. Org. Chem.* **2002**, *67*, 4414.
[208] Y. Wang, S. Huang, T. Lin, F. Tsai, *Tetrahedron* **2010**, *66*, 7136.
[209] Complex preformed in situ at 100 ºC under deoxygenated conditions
[210] F. Xu, C. Wang, X. Li, B. Wan, *ChemSusChem*, **2012**, *5*, 854.
[211] H. Kinoshita, H. Shinokubo, K. Oshima, *J. Am. Chem. Soc.* **2003**, *125*, 7784.
[212] L. Adriaenssens, L. Severa, J. Vávra, T. Sálová, J. Hývl, M. Cízkova, R. Pohl, D. Saman, F. Teplý, *Collect. Czech. Chem. Commun.* **2009**, *74*, 1023.

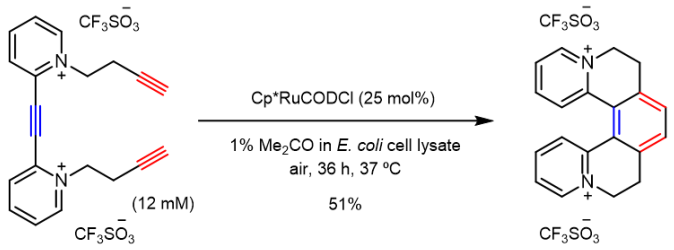

Figure 81. Ruthenium promoted [2+2+2] cycloaddition to afford diquats reported by Teplý in biological media.[212]

More recently, the group of Young introduced a Rh promoted [2+2+2] formal cycloaddition used as bioconjugation tool (figure 82). For this purpose, a GFP bearing an aminoacid with a dipropargyl functionalization was genetically expressed and isolated from *E. coli* bacteria.[213] This dialkyne reacts with Fluorescein 488-alkyne as probe, in the presence of a water-soluble Rh-biphenylcarboxylate catalyst. The procedure allows to perform efficient bioconjugations at room temperature, with a minimal protein degradation after 2 h. Nevertheless, the protocol requires high amounts of catalyst loading and NaAsc.

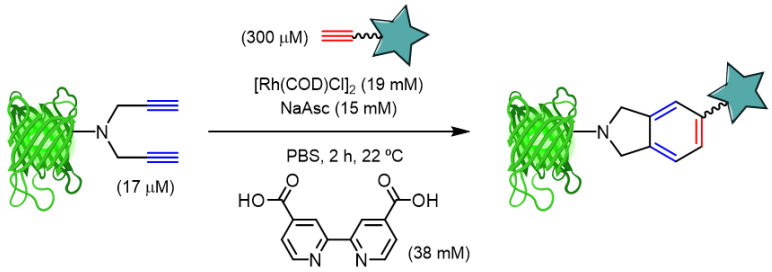

Figure 82. Biocompatible Rh [2+2+2] cycloaddition on GFP reported by Young.[213]

USC UNIVERSIDADE DE SANTIAGO DE COMPOSTELA

[213] C. R. Travis, E. A. King, G. H. Gaunt, D. D. Young, *ChemBioChem* **2020**, *21*, 310.

3. Objectives

In view of the precedents on the use of the CuAAC in biological settings, and the antecedents (scarce) presented above on metal promoted [2+2+2] cycloadditions, we considered worthy to test the viability of this type of cycloadditions in biological relevant mixtures and even live cells. We reasoned that the presence of the dialkyne might provide for bioorthogonal "fishing" of low valence transition metals reagents. An ensuing oxidative cyclometallation would give a metallacycle that could trap the alkyne partner leading to the corresponding aromatic cycloadduct.

We considered the use of ruthenium (II) complexes, owing to their low toxic nature and the precedents of the group on other Ru mediated processes,[135,139,163] and using as reference the work of Teply.

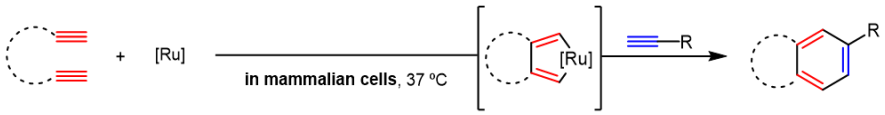

While our first experiments will be focused to fully intramolecular processes, we also plan to test intermolecular variants that could provide for the synthesis of relevant products.

USC
UNIVERSIDADE DE SANTIAGO DE COMPOSTELA

4. Results and discussion

4.1. Ruthenium-promoted intramolecular [2+2+2] cycloadditions in aqueous and biological settings

Considering that the helquat products obtained by Teply and coworkers using a ruthenium formal [2+2+2] cycloaddition can be fluorescent, our initial studies were focused on employing the triyne **24** as starting material, that upon Ru promoted cycloaddition should give the cycloadduct **25**.

The probe **24** was synthetized following reported procedures.[214] The synthetic route involves two consecutive Sonogashira reactions. The first coupling between 2-bromopyridine and 2-methyl-3-buten-2-ol using $PdCl_2(PPh_3)_2$ as catalyst affords the alkyne **22** in 91% yield. This alkyne **22** undergoes a second Sonogashira reaction with another equivalent of 2-bromopyridine, in basic media to deprotect the alkyne, and Pd/C as catalyst. The dipyridine-ethyne **23**, obtained in 78% yield, reacts with an *in situ* prepared but-3-ynyl-triflate leading to the final triyne **24** (83% yield). This triyne undergoes the desired formal [2+2+2] cycloaddition when treated with Cp*Ru(COD)Cl (**Ru1**) under reflux in H_2O/DMSO mixture. As seen previously along the section 2. of this chapter, the reaction is feasible at 37 ºC and in bacteria lysates, but in a slower rate.[212]

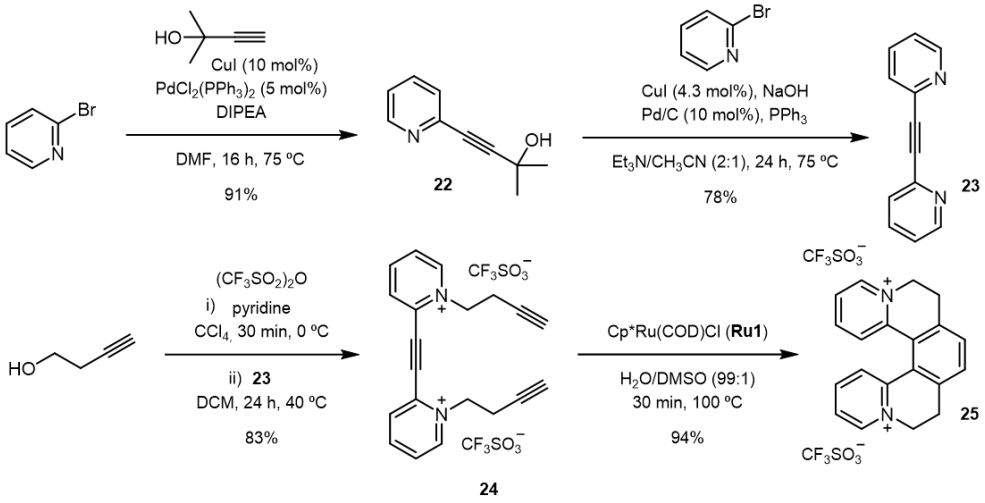

*Figure 83. Synthesis of the triyne **24** and its cycloaddition to provide helquat **25**.*

USC UNIVERSIDADE DE SANTIAGO DE COMPOSTELA

[214] L. Adriaenssens, L. Severa, T. Sálová, I. Císarová, R. Pohl, D. Saman, S. V. Rocha, N. S. Finney, L. Pospísil, P. Slavícek, F. Teplý, *Chem. Eur. J.* **2009**, *15*, 1072.

This good result encouraged us to explore this transformation in more complex biological settings under diluted conditions. We tested the reaction in different media, such as PBS, DMEM or HeLa lysates (6 mg/mL), using 1 mM concentrations, at room temperature for 24 h, without any precaution to avoid oxygen (figure 84). Yields were determined by NMR using trimethoxybenzene (TMB) as internal standard. Gratifyingly, using 25 mol% of **Ru1** we obtained a 52% yield in PBS. In DMEM the yield was 41%, while in presence of cell lysates it was slightly lower (32%).

*Figure 84. Intramolecular Ru promoted [2+2+2] cycloaddition. Conditions: 1 mM of triyene **24** and 25 mol% of **Ru1** at room temperature for 24 h.*

4.2. Ruthenium-promoted intramolecular [2+2+2] cycloadditions in cellular settings

Despite the yields were relatively modest, the process seems to be compatible with aqueous and biological environments. Thus, we decided to check the viability of the reaction inside live mammalian cells. The experiments were initiated with the incubation of HeLa mammalian cells with the selected concentration of the Ru complex (20-50 μM, added from DMSO stock) in DMEM for 30 min. After the proper washing steps (2xDMEM), cells were incubated with 100 μM of the substrate (added in a DMSO stock) for 1 h. Finally, cells were washed again prior to microscopy visualization.

USC UNIVERSIDADE DE SANTIAGO DE COMPOSTELA

Preliminary results in HeLa cells are shown in figure 84. While substrate **24** doesn't present fluorescent properties, the helquat **25** is a fluorophore that exhibits intense blue fluorescence (λ_{em} = 400 nm when excited at 330 nm). Adding triyene **24** to the cells, as expected, didn't raise any appreciable fluorescence (figure 85, panel A). However, if the cells were previously treated with **Ru1** (50 μM) and then with the substrate **24** (100 μM), and kept for 1 h, a slight blue fluorescent signal appears, that albeit pallid, suggests that the intracellular reaction is taking place (figure 85, panel B). Remarkably, using the quinoline-Ru complex **Ru2** as ruthenium catalyst (50 μM),[139] we observed a much higher increase in fluorescence intensity (figure 85, panels C). Posterior fluorescence quantification by CTFC (corrected total cell fluorescence) revealed a three-fold higher increment when **Ru2** is employed in comparison with that observed with commercial **Ru1**.

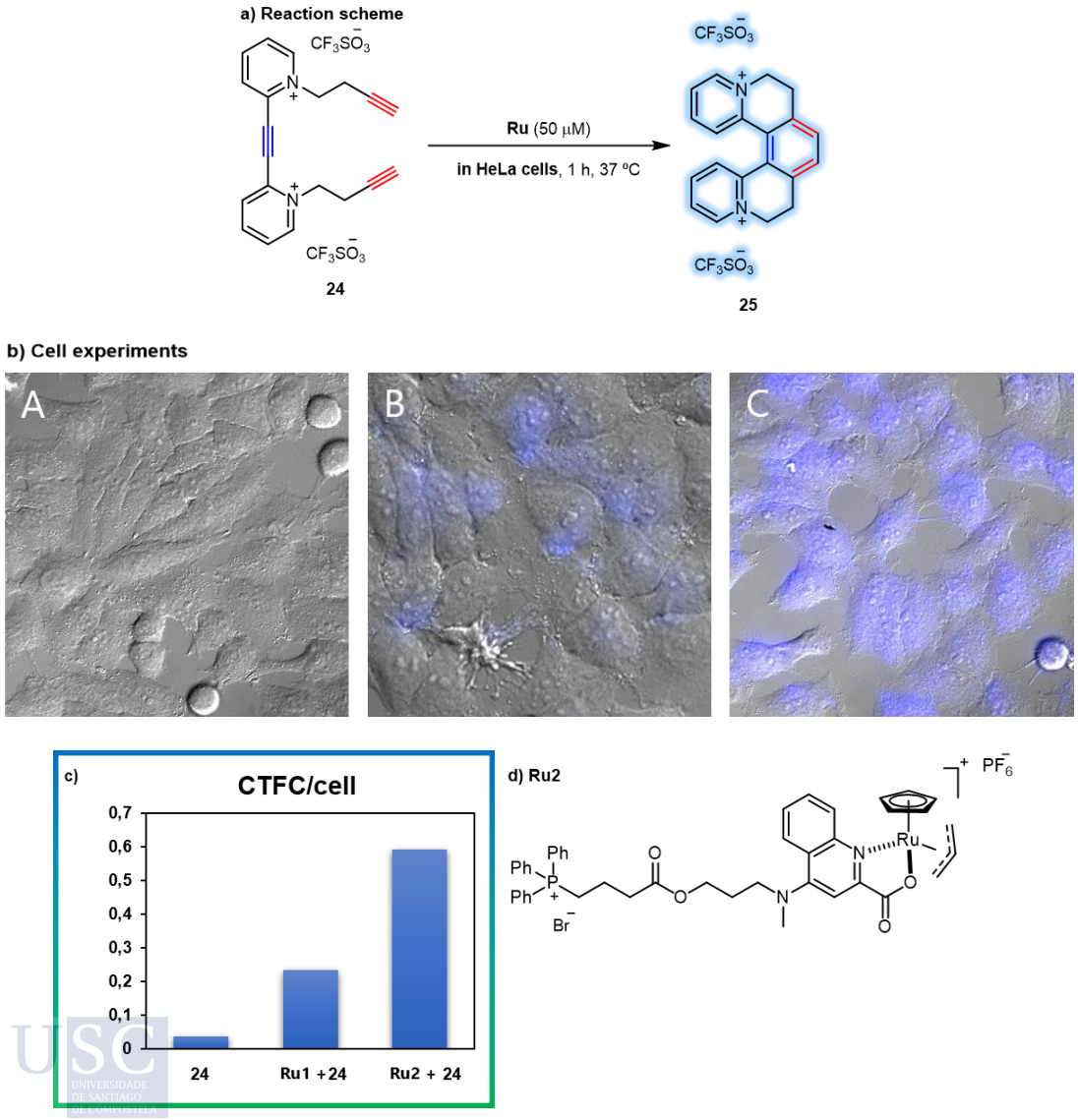

*Figure 85. a) Reaction scheme. b) Fluorescence micrographies of experiments with HeLa cells. Protocol: cells were incubated with 50 μM **Ru1** or **Ru2**, then cells were washed and incubated with 100 μM of **24** at 37 ºC for 1 h. Fluorescence obtained in the blue channel (λ_{exc} = 385 nm, λ_{em} = 410-480 nm). A) Control without **Ru**. B) **Ru1**. C) **Ru2**. c) CTCF measurements (corrected total cell fluorescence). d) **Ru2** catalyst structure.*

4.3. Ruthenium-promoted intermolecular [2+2+2] cycloadditions in aqueous and biological settings

Once demonstrated the viability of performing the cycloadditions in native settings, we questioned whether it would be possible to move into intermolecular reactions. Albeit the intramolecularity of the process favored the cycloaddition of **24**, we envisioned that once a ruthenacycle intermediate is formed from the diyne, it can be trapped efficiently using external alkynes. We first selected the propargyl ether **26** as diyne, due to its commercial availability. Moreover, it has been previously used by Itoh as a precursor to synthesize phtalanes in dichloroethane under smooth conditions (figure 86).[203] Importantly, the final structures are biorelevant scaffolds.[215]

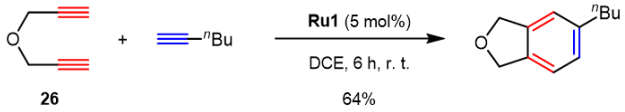

Figure 86. Synthesis of phtalanes reported by Itoh in 2003.[203]

As alkyne partners we selected the phenylacetylene compounds **27** and **28** which contain and EDG/EWG in the structure, respectively. The formation of the products **29** and **30** could be easily identify by NMR spectroscopy, using TMB as internal standard.

Under Itoh' conditions, ruthenium complex **Ru1** (5 mol%) the reaction of alkyne **27** with **26** gave the expected cycloadduct **29** in 75% yield (table 3, entry 1), that prompted us to decrease the concentration from 166 mM to 1 mM, and move towards the use of aqueous solvents. Thus, mixing diyne **26** with 25 mol% of **Ru1**, 4 equivalents of anisole **27** in MilliQ water resulted in a slightly cloudy mixture, obtaining the product in 60% yield after 2h.

Using a buffered PBS solution, the product was formed in 94% yield (entry.4). The use of DMEM or even lysates were also tolerated leading to 95% and 89% yields, respectively. Curiously, an excess of ruthenium (50 mol%) went in detriment of the reaction, decreasing substantially the yield, especially in water (entries 3 and 5). Curiously, alkyne **28** led to lower yields, with only traces in H_2O (entries 10 and 11).

USC UNIVERSIDADE DE SANTIAGO DE COMPOSTELA

[215] G. Lin, S. S. K Chan, H. S. Chung, S. L. Li, *Stud. Nat. Prod. Chem.* **2005**, *32*, 611.

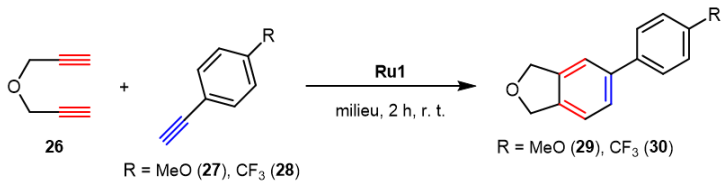

Entry	Alkyne	**Ru1** (mol%)	Milieu	Yield (%)[4]
1[1]	27	5	DCE	75[5]
2	27	25	H_2O	60
3	27	50	H_2O	43
4	27	25	PBS	94
5	27	50	PBS	78
6	27	25	DMEM	95
7	27	50	DMEM	95
8	27	25	Lysate[2]	62
9	27	25	Lysate[3]	89
10	28	25	H_2O	traces
11	28	25	PBS	63

*Table 3. Milieu scope for the [2+2+2] reaction to obtain phtalanes. Conditions: 1 mM propargyl ether **26**, 4 equiv. alkyne **27** or **28**, the proper amount of **Ru1** in the chosen solvent at r. t. for 2 h. [1]Standard conditions used by Itoh. [2]Cells lysates 2 mg/mL prepared from water dilution. [3]Cells lysates 2 mg/L prepared from PBS dilution. [4]Yields were determined by NMR using TMB as internal standard [5]Isolated yield.*

We next explored the performance of other type of ruthenium complexes, which have previously shown to compatible with biological settings. In this sense, we prepared the quinoline containing complexes **Ru3** and **Ru4**,[136,139] the bis-allyl-Ru dimer (**Ru5**), and its acetate-Ru monomer (**Ru6**).[172] We also considered the commercially available [Cp*Ru(NCMe)$_3$]PF$_6$ (**Ru7**)[76].

The quinoline-ruthenium complexes were prepared following reported procedures.[136] Starting from kynurenic acid, the alcohol is brominated with P_2O_5 and tetrabutylammonium bromide (TBAB) to give **31** in a 10% of yield. Allylation of the carboxylic acid and coupling with N-methyl-3-aminopropanol led to ligand **32** in 65% yield. Finally, the complex **Ru3** is formed in 70% yield by mixing the ligand **32** with [CpRu(NCMe)$_3$]PF$_6$

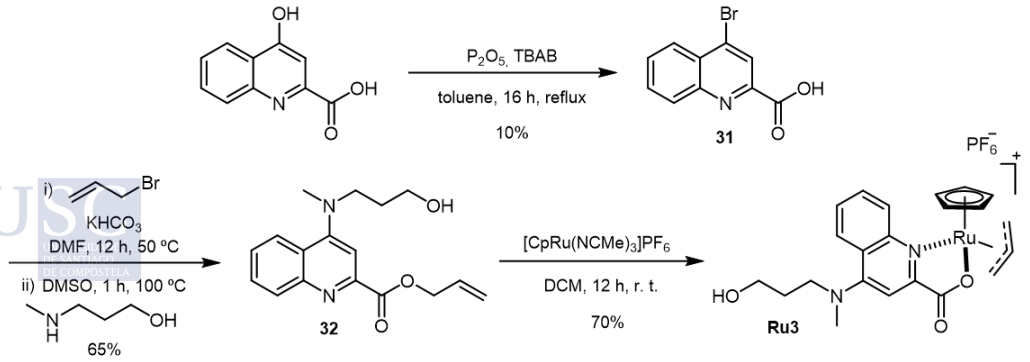

*Figure 87. Synthesis of **Ru3**.*

Ru2 can be synthetized from the ligand **32** by coupling it with 4-tryphenylphosphinobutanoic acid (30% of yield), using EDC as activating agent, and its posterior treatment with $[CpRu(NCMe)_3]PF_6$, leading to the complex **Ru2** in 65% of yield.

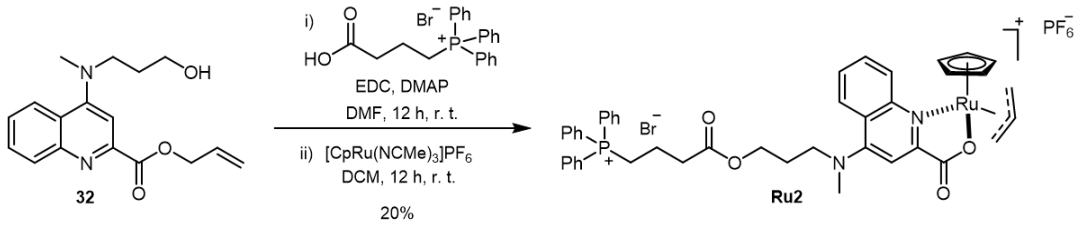

*Figure 88. Synthesis of **Ru2**.*

The complex **Ru4** was also prepared according to literature protocols.[216] 3-Amino-4-hydroxybenzoic acid is condensed in acid media with acrolein to construct the quinoline core (**33**) in quantitative yields. Its posterior allylation to give **34**, and hydrolysis affords the quinoline acid **35** in good yields. **Ru4** is formed by mixing the ligand **35** with $[CpRu(NCMe)_3]PF_6$ in 74% yield.

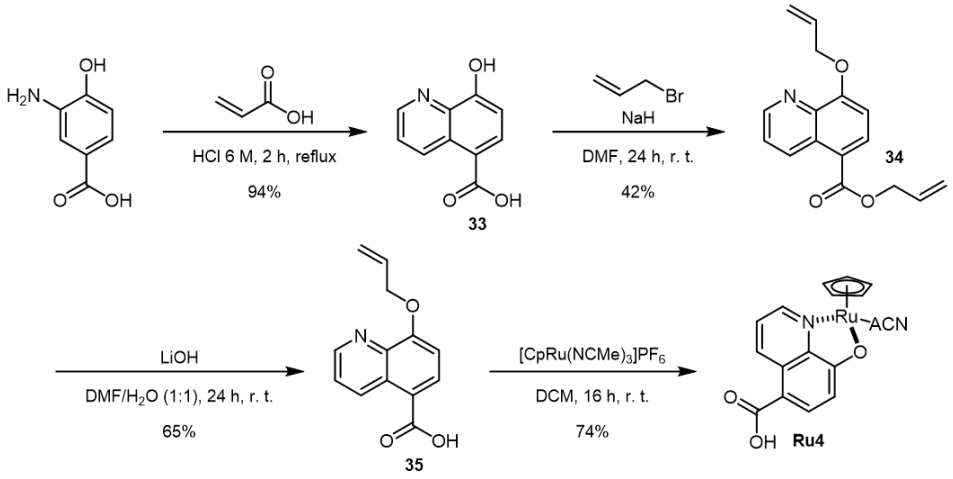

*Figure 89. Synthesis of **Ru4**.*

The bisallyl Ru(IV) complex **Ru5** was obtained following a procedure previously developed in the group by mixing $RuCl_3$, isoprene and 2-methoxyethanol (38% yield). **Ru6** was synthetized from **Ru5** and silver acetate in a 60% of yield.[172] The formation of the complexes was corroborated by HPLC-MS.

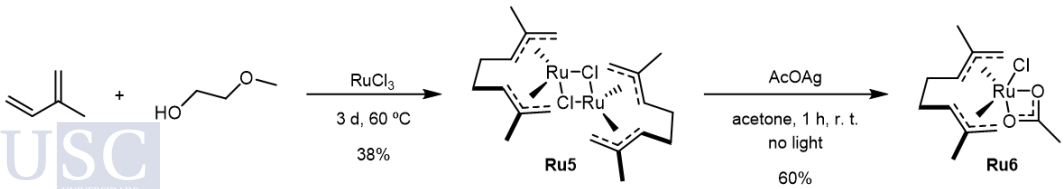

*Figure 90. Synthesis of ruthenium (IV) complexes **Ru5** and **Ru6**.*

[216] T. Völker, E. Meggers, *ChemBioChem* **2017**, *18*, 1083.

We then tested the different complexes under the standard conditions: 1 mM of **26**, 4 equivalents of **27** and 25 mol% of the chosen ruthenium catalyst in PBS for 2 h. However, when **Ru2** was tested, we didn't observe the formation of the desired cycloadduct (table 4, entry 1).

It is known that this kind of Ru(IV) quinoline-catalysts are activated by nucleophilic addition of exogenous,[136] or endogenous nucleophiles,[139] such as PhSH or GSH to the allyl ligand, leading to an active Ru(II) species. Therefore, we tested the reaction with **Ru2** in presence of different nucleophilic species, such as PhSH, aniline or 2-phenylethanol (PhEtOH), observing the formation of the product in 6, 10 and 14% of yield respectively (entry 3-5). When PhSH and **Ru3** were combined, only a 5% of product was obtained (entry 6). We also tested the performance of a ruthenium(II) complex, such as **Ru4**. In this case, an increase of the yield up to 25% was observed (entry 6). Furthermore, we explored **Ru5** and its monomer **Ru6**, as they were recently applied by the group for redox isomerization processes in HeLa cells. Pleasingly, both furnished over 70% yield with a 50 mol% of catalyst loading (entry 8-10).

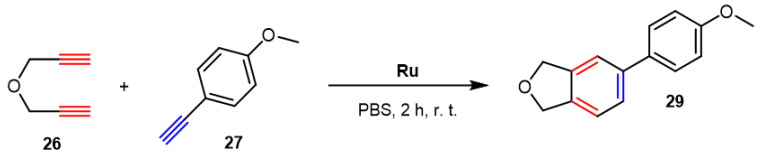

Entry	**Ru**	Cat. loading (mol%)	Additive	Yield (%)[5]
1[1]	**Ru2**	25		-
2	**Ru2**	25	NaAsc[3]	-
3	**Ru2**	25	PhSH[4]	6
4	**Ru2**	25	Aniline[4]	10
5	**Ru2**	25	PhEtOH[4]	14
6	**Ru3**	50	PhEtOH[4]	5
7[1]	**Ru4**	25		25
8	**Ru5**	25[2]		73
9	**Ru5**	12[2]		59
10	**Ru6**	50		80
11	**Ru7**	25		38

*Table 4. Catalysts with bioorthogonal potential under study. Conditions: 1 mM of propargyl ether **26**, 4 equiv. of **27**, the chosen Ru catalyst in PBS for 2 hours. [1]Allowed to react for 24 h. [2]The amount of ruthenium is the double due the dimeric nature of the complex. [3]Concentration of 25 μM. [4]1equiv. of the additive was employed. [5]Yields were determined by NMR using TMB as internal standard.*

All the above results confirm the viability of the intermolecular cycloaddition. However, the product of these reactions is not fluorescent, which made difficult their translation and monitoring in more complex settings, especially under biological and living conditions.

USC DE SANTIAGO DE COMPOSTELA

4.3.1. [2+2+2] Intermolecular cycloadditions that give fluorescent products

Anthraquinones (AQ) are fascinating secondary metabolites that some organisms such plants, fungi insects or bacteria are able to synthesize. Similarly to phtalanes, these structures are synthesized from acetylCoA and malonylCoA by the multidomain polyketide synthase, following an elaborated multistep pathway, where the main transformation consist in a consecutive decarboxylative Claisen thioester condensation (figure 91).[217] An enormous number of different post-translational modifications can take place, leading to a large family of biomolecules,[218] which involves a great variety of bioactive compounds, and importantly, some of them with fluorescent properties.[219]

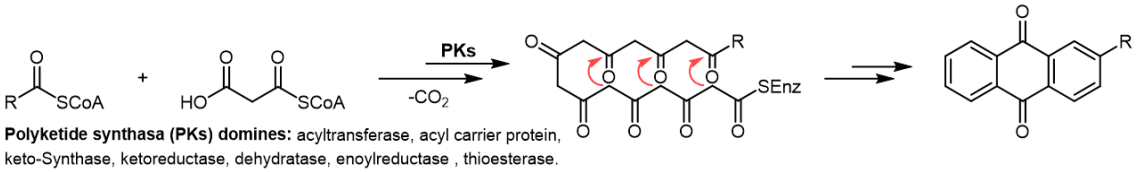

Figure 91. Plausible biological pathway for the synthesis of anthraquinones.

Remarkably, mammalian cells lack the metabolic machinery to make these polyketide products. Thus, we considered that a fruitful translation of the above [2+2+2] to intracellular environment would provide mammalian cells a way to have access to these metabolites.

In 2003, Itoh and co-workers reported a smooth synthesis of anthraquinones (AQ) starting from bispropargylic ketones, [220] based on a a ruthenium-catalyzed [2+2+2] cycloaddition. The reaction takes places in DCE, at 60 mM, using 4 equiv. of the partner alkyne, and 5 mol% of **Ru1** (65% yield).

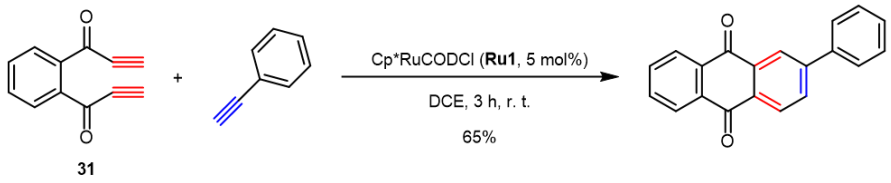

Figure 92. Synthesis of anthraquinones reported by Itoh in 2003.[220]

USC UNIVERSIDADE DE SANTIAGO DE COMPOSTELA

[217] C. Hertweck, *Angew. Chem. Int. Ed.* **2009**, *48*, 4688.
[218] C. Olano, C. Méndez, J. A. Salas, *Nat. Prod. Rep.* **2010**, *27*, 571.
[219] G. M. Ziarani, R. Moradi, N. Lashgari, H. G. Kruger, *Metal-Free Synthetic Organic Dyes* 1st Ed, Elsevier, **2018**.
[220] Y. Yamamoto, K. Hata, T. Arakawa, K. Itoh, *Chem. Commun.* **2003**, 1290.

On the basis of this reaction, and considering the cycloaddition studies described in the previous section, we decided to investigate the synthesis of AQs in the presence of biological media. The required diyne precursors were prepared by addition of selected Grignard reagents (ethynylmagnesium bromide or equivalent) to the corresponding dialdehydes, followed by oxidation with Dess-Martin periodinane (DMP) to afford the desired ketones (figure 93).

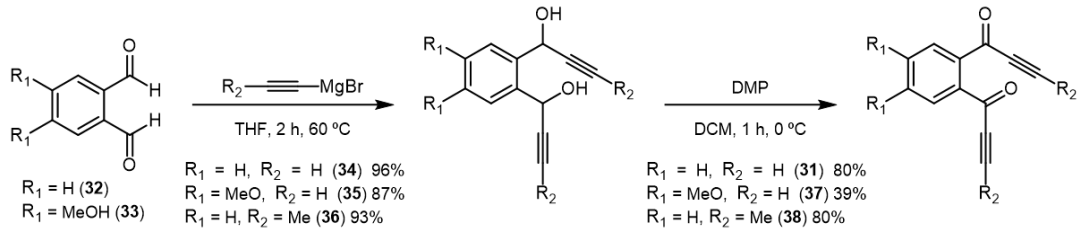

Figure 93. Synthesis of diynes employed in this work.

While o-phthalaldehyde is commercially available, the other aldehydes were easily synthesized as indicated in the following scheme:

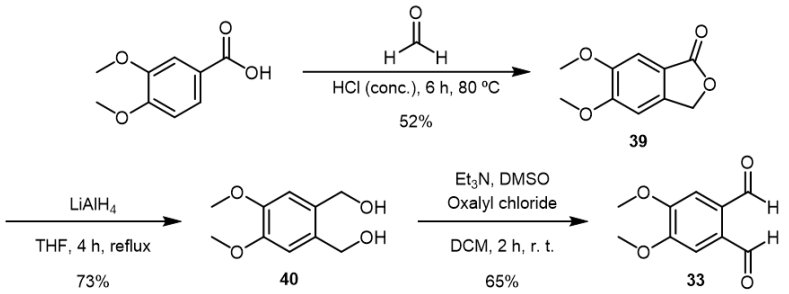

*Figure 94. synthesis of aldehyde **33**.*

With the diynes in hand, we tested the cycloaddition chemistry. Employing Itoh's conditions in DCE, with diyne **31** and 1-ethynyl-4-methoxybenzene (**27**), we observed the formation of the anthraquinone **41**, which was isolated in 55% (table 5, entry 1). Importantly, we confirmed that this product exhibits a very good blue fluorescence (λ_{exc} = 430 nm, λ_{em} = 536 nm).

We then moved to aqueous and biologically relevant conditions, using 1 mM concentrations of the diyne **31**, 4 equivalents of **27**, and TMB as NMR internal standard to determine the yields. As shown in table 5, with 25 mol% of the catalyst **Ru1**, **41** was obtained in 59% yield in water. This mixture is slightly heterogeneous, mainly because of the low solubility of **31**, suggesting that it is an "on water" reaction. With 50 mol% of the catalyst the yield increased to 79%, recovering the unreacted diyne (see experimental section, Chapter III S4). Curiously, reactions performed under stoichiometric conditions suffered an important decrease in yield.

USC UNIVERSIDADE DE SANTIAGO DE COMPOSTELA

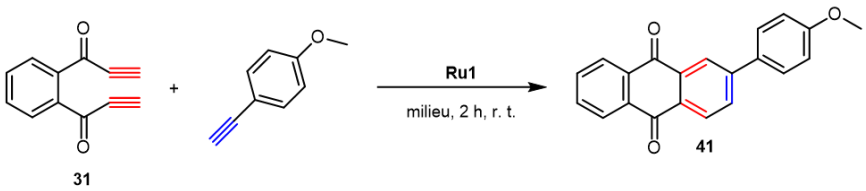

Entry	**Ru1** (mol%)	Milieu	Yield (%)[3]
1[1]	5	DCE	55[4]
2	5	H_2O	6
3	10	H_2O	25
4	25	H_2O	59
5	50	H_2O	79
6	100	H_2O	68
7	25	H_2O[2]	27
8	25	H_2O/ACN	20

*Table 5. Milieu scope for the ruthenium promoted [2+2+2] cycloaddition to obtain anthraquinones **41**. Conditions: 1 mM of **31**, 4 equiv. of alkyne **27**, **Ru1**, at room temperature for 2 h. [1]Itoh standard conditions. [2]Deoxygenated solvent. [3]Yields were determined by NMR using TMB as internal standard. [4]Isolated yield.*

The transformation tolerates more complex biological media such as PBS, DMEM and cell lysates (65, 37, 28% respectively with 25 mol% of **Ru1**). These results could be improved by increasing the catalyst loading to 50 mol%, leading to acceptable yields of 59 and 43% when DMEM and HeLa lysates were used, respectively.

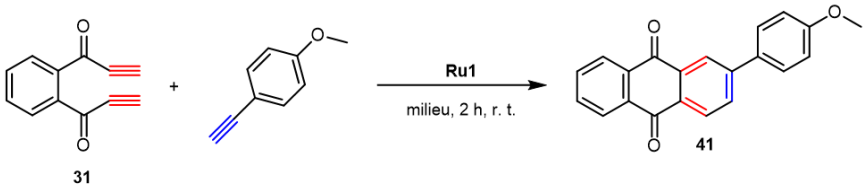

Entry	**Ru1** (mol%)	Milieu	Yield (%)[1]
1	5	PBS	13
2	10	PBS	23
3	25	PBS	65
4	50	PBS	67
5	25	DMEM	37
6	50	DMEM	59
7	25	Lys	28
8	50	Lys	43

*Table 6. Milieu scope for the ruthenium promoted [2+2+2] cycloaddition to obtain anthraquinone **41**. Conditions: 1 mM of **31**, 4 equiv. of alkyne **27**, **Ru1** in different milieu at room temperature for 2h (4 hours for lysates). [1]Yields were determined by NMR using TMB as internal standard.*

USC DE SANTIAGO DE COMPOSTELA

The reaction was also studied along time. As can be notice in figure 95, plateau was reached between 30 min and 1 h, when water, PBS or even DMEM were employed, and independently of the amount of catalyst employed. However, in lysates the process was slower.

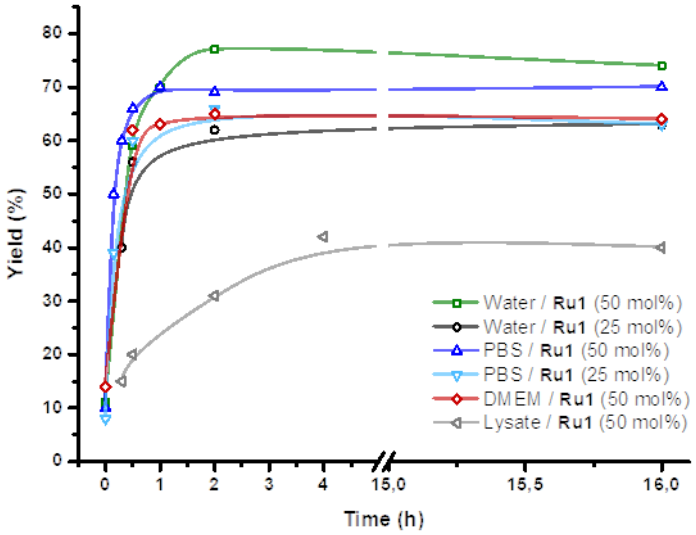

*Figure 95. Experiments along time of the ruthenium promoted [2+2+2] cycloaddition of **31** and **27**. Conditions: 1 mM of **31**, 4 equiv. of alkyne **27**, **Ru1** in different milieu at room temperature. Yields were determined by NMR using TMB as internal standard.*

Lowering the concentration of the diyne **31** led to a decrease in the yield (from 59 to 36%, table 7, entry 1). By using higher catalyst loadings (50 mol%), the yield was raised to 53% (entry 2), although still below the value of 79% obtained at 1 mM. On the other hand, varying the equivalents of the alkyne partner was also translated into a significant yield decay, although with 2 equiv. the yield was still acceptable (entries 5 and 6). The catalyst was not active after 2 h of reaction, as proved by adding additional substrate and observing no further reaction (entry 7).

USC UNIVERSIDADE DE SANTIAGO DE COMPOSTELA

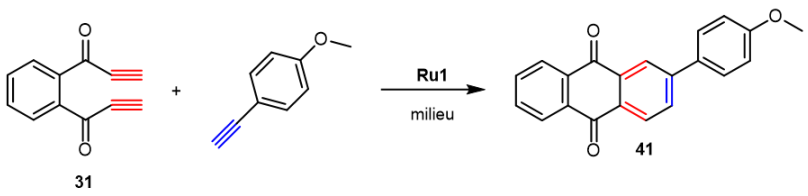

Entry	**Ru1** (mol%)	Deviation from standard conditions	Milieu	Yield (%)[1]
1	25	**31** (0.5 mM)	H_2O	36
2	50	**31** (0.5 mM)	H_2O	53
3	25	1 equiv. **27**	H_2O	30
4	50	1 equiv. **27**	H_2O	32
5	25	2 equiv. **27**	H_2O	43
6	50	2 equiv. **27**	H_2O	49
7	50	+1 equiv. **31** after 2 h	PBS	63
8	50	+4 equiv. **31** after 2 h	PBS	68
9	50	+ 50 mol% **Ru1** after 2 h	PBS	70
10	25	37 ºC	PBS	40
11	50	37 ºC	PBS	64

*Table 7. Effect on the deviation of the standard conditions to the Ru promoted [2+2+2] transformation. Standard conditions: 1 mM of **31**, 4 equiv. of **27**, 25 or 50 mol% of **Ru1**, in water or PBS at room temperature for 2 h. [1]Yields were determined by NMR using TMB as internal standard.*

Finally, other ruthenium complexes employed in the studies of section 5.1, were also tested. In general, they were less efficient in PBS, than the parent complex Ru1 (table 8). In particular, **Ru2**, **Ru3** and **Ru4** failed to promote the transformation.

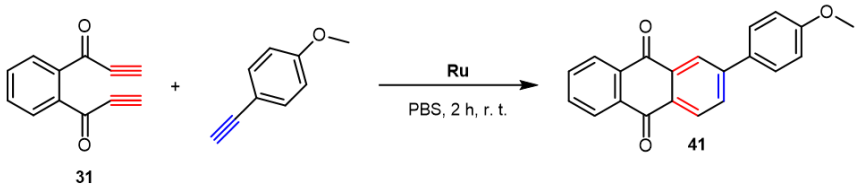

Entry	Ru1 (mol%)	Catalyst	Yield (%)[1]
1	50	**Ru6**	5
2	25	**Ru5**	12
3	50	**Ru5**	10
4	25	**Ru7**	30
5	50	**Ru7**	33

*Table 8. Scope of other Ruthenium catalysts. Conditions: 1 mM of **31**, 4 eq of **27**, 25 or 50 mol% of the selected **Ru** catalyst, PBS, at room temperature for 2 h. [1]Yields were determined by NMR using TMB as internal standard.*

USC UNIVERSIDADE DE SANTIAGO DE COMPOSTELA

All-around, these experiments suggest that cellular experiments will require 50 mol% or even up to 1 equiv. of Ru catalysts, because the concentration in that crowded media will be much lower, and the reactions will be performed at physiological temperature (37 ºC).

As previously mentioned, the anthraquinone **41** obtained through the ruthenium promoted [2+2+2] cycloaddition displays excellent fluorescent properties, exhibiting a bright emission between 450-750 nm, when excited at 385 nm. However, both the reactants and the ruthenium catalysts don't present fluorescence at all (figure 96). Hence, this system can be considered as adequate for our cellular experiments, and allowing us to monitor the progress of the reactions in real time using fluorescence microscopy.

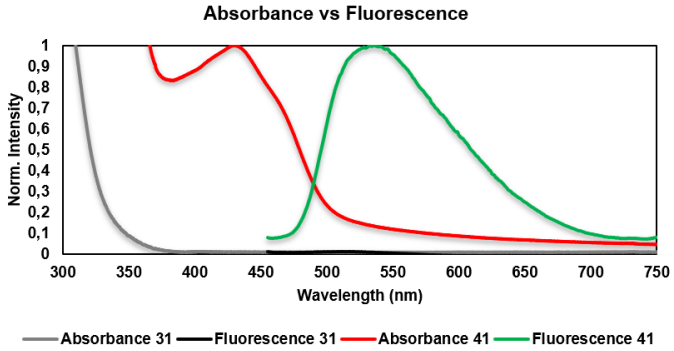

*Figure 96. Absorbance vs fluorescence spectra of the diyene **31** and anthraquinone **41**. Absorbance experiments were carried out in water at 100 μM and fluorescence at 20 μM with excitation at λ_{em} = 385 nm.*

In addition, we decided to extend the scope, and explore some other substrates, either modifying the substituents of the mono or the diyne. When dimethoxy-bearing diynes **37** or the internal diynes **38** were submitted to the reaction conditions, products **42** or **43** were obtained in modest yields. These lower values could be attributed to the deactivation of the dieynes by EDGs, but also to the lower solubility (at least of **38**). Indeed, this diyne demonstrated to perform better when acetonitrile was added as co-solvent (table 9, entry 5 and 6). The reaction of trifluoromethylphenylacetylene **28** with **31** afforded the product **44** in yields over 80% (entry 8).

USC UNIVERSIDADE DE SANTIAGO DE COMPOSTELA

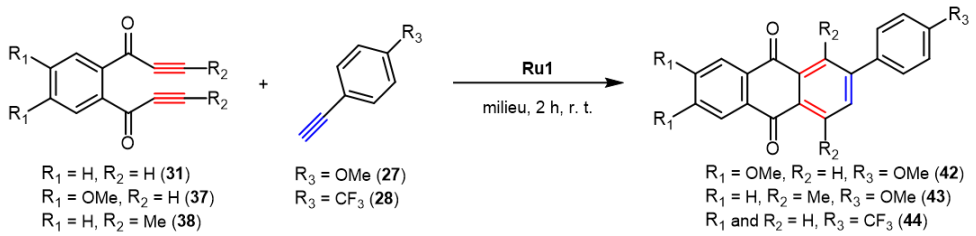

Entry	Diyne	Alkyne	**Ru1** (mol%)	Milieu	Yield (%)[2]
1	38	27	25	H_2O	24
2	38	27	50	H_2O	45
3	38	27	25	PBS	40
4	38	27	50	PBS	48
5	38	27	25	H_2O/MeCN[1]	43
6	38	27	50	H_2O/MeCN[1]	59
7	37	27	50	H_2O	40
8	31	28	25	PBS	81

*Table 9. Substrate scope for the ruthenium promoted [2+2+2] cycloaddition to obtain anthraquinones. Conditions: 1 mM of the diyne, 4 equiv. of the alkyne, 25-50 mol% of **Ru1**, in water, PBS or [1]a mixture H_2O/MeCN (8:2) at r t. for 2 h, without any precaution to avoid oxygen. [2]Yields were determined by NMR using TMB as internal standard.*

Nevertheless, the fluorescent properties of these anthraquinone are not as good as the one shown by product **41**, and therefore we didn't further check their reactivity in cells.

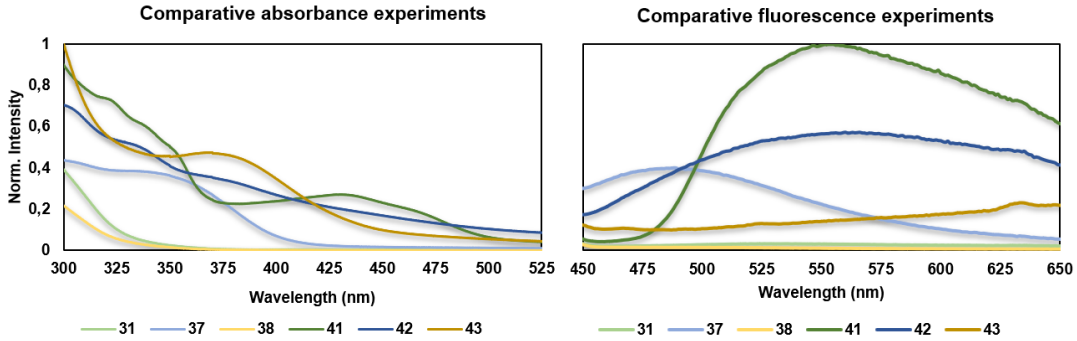

*Figure 97. Absorbance and fluorescence comparison among diynes **31**, **37**, **38** and anthraquinones **41, 42, 43**. Absorbance experiments were performed at 100 μM in water, and fluorescence at 40 μM using λ = 385 nm as excitation wavelength.*

USC UNIVERSIDADE DE SANTIAGO DE COMPOSTELA

4.4. Ruthenium-promoted intermolecular [2+2+2] cycloadditions in cellular settings

The viability of the intracellular reactions was studied in HeLa and A549 mammalian cells, using **Ru2** as catalytic complex, due to the good intracellular performance shown in the previous intramolecular reaction described in section 4. The reactions were carried out by incubating the cells with 50 μM of the ruthenium complex in DMEM for 30 min, followed by two washing steps with DMEM and then treatment with the substrates (50 μM of **31** and 150 μM of **27**) for different reaction times. Prior to the visualization under fluorescence microscopy, 2 washing steps in DMEM were performed to eliminate extracellular background.

Gratifyingly, we observed the appearance of an intense fluorescent signal after only 15 minutes of incubation (figure 98, panels B, C). Moreover, the concentration of the ruthenium could be decreased to 25 μM, with a very good performance (see experimental section, Chapter III S7). Complex **Ru1** was able to promote the intracellular transformation, although under the same conditions the intensity of the fluorescence was lower, perhaps because of its poorer cell penetration. (see experimental section, Chapter III S10).

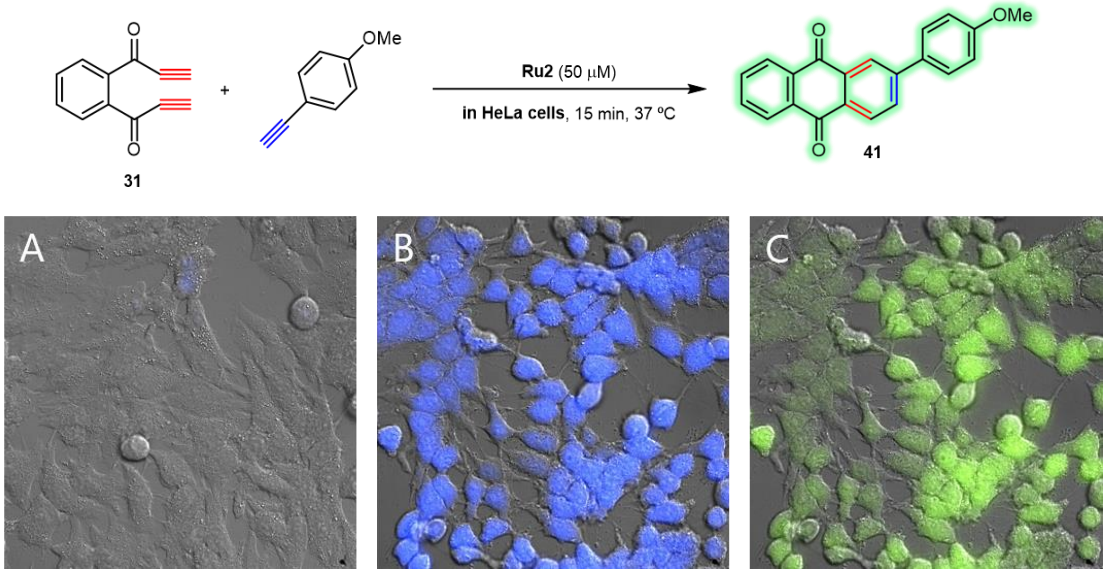

*Figure 98. Fluorescence micrographies in HeLa cells. Protocol: cells were incubated with 50 μM of **Ru2**, then washed and incubated with 50 μM of **31** and 150 μM of alkyne **27** at 37 ºC for 15 min. A) Control without **Ru**. B) **Ru2**, fluorescence obtained in the blue channel (λ_{exc} = 385 nm, λ_{em} = 410-480 nm). C) **Ru2**, fluorescence obtained in the green channel (λ_{exc} = 470 nm, λ_{em} = 490-580 nm).*

USC UNIVERSIDADE DE SANTIAGO DE COMPOSTELA

4.4.1. Anthraquinones as AIEgen motifs

AIEgens are fluorogens with aggregation-induced emission, exhibiting week or non-fluorescence in a molecular state, but high and stable emission in the aggregate state (figure 99a). In other words, this new kind of probes are not active in solution, and only show their properties when enough amount of AIEgen precipitates. This solves the main drawbacks of classic fluorophores: sensitivity, stability, and lack of effectiveness due to the aggregation-caused quenching (ACQ), limiting the concentration able to be used in biological setting (figure 99b). AIEgens are grounded in polyaromatic structures with rotor moieties that lead to a non-radiative decay in solution. After precipitation, the restriction of the molecular motion and the incapability to perform intermolecular π-π stacking (what would accelerate non-radiative decay) due to a non-planar structure, yields to bright and stable emission.[221,222] A number of biological applications for sensing and imaging are increasingly found in literature.[223,224,225] For instance, Tang and co-workers reported in 2010 the use of a tetraphenylethylene (TPE)-maleimide as a cysteine sensitive smart probe (figure 99c).[226]

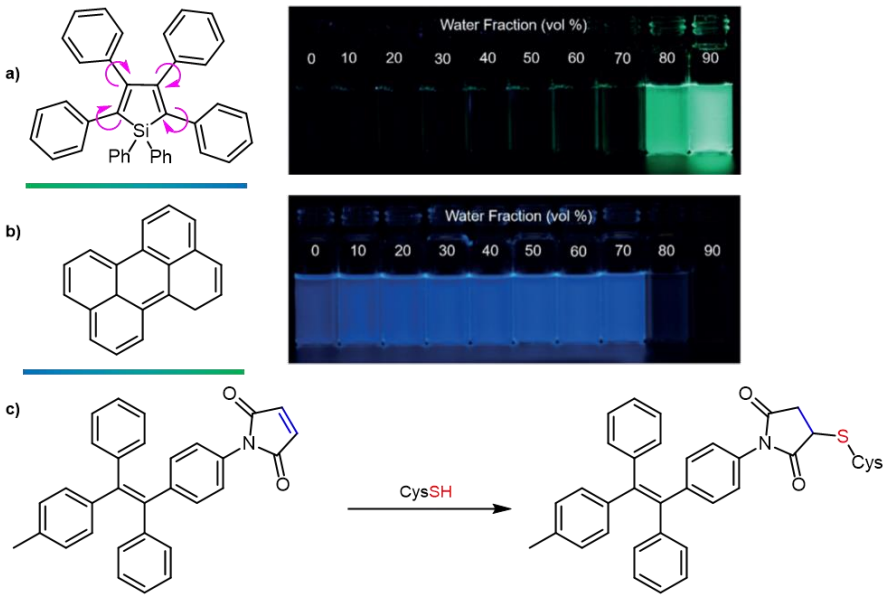

Figure 99. a) Hexaphenylsilole structure, its molecular rotors (pink arrows) and AIE behavior from THF-Water solutions. High water proportion induces the probe precipitation and the fluorescence enhancement. b) Perylene structure and its behavior as classic fluorophore. High water proportion induces the probe precipitation and fluorescence inhibition. c) Cysteine AIE-probe developed by Tang's group. Maleimide group inhibits fluorescence by PET.[226]

USC UNIVERSIDADE DE SANTIAGO DE COMPOSTELA

[221] S. Suzuki, S. Sasaki, A. S. Sairi, R. Iwai, B. Z. Tang, G. Konishi, *Angew. Chem. Int. Ed.* **2020**, *59*, 9856.
[222] Z. Zhao, H. Zhang, J. W. Y. Lam, B. Z. Tang, *Angew. Chem. Int. Ed.* **2020**, *59*, 9888.
[223] D. Ding, K. Li, B. Liu, B. Z. Tang, *Acc. Chem. Res.* **2013**, 46, 2441.
[224] X. Cai, B. Liu, *Angew. Chem. Int. Ed.* **2020**, *59*, 9868.
[225] X. Gao, J. Z. Sun, B. Z. Tang, *Isr. J. Chem.* **2018**, *58*, 845.
[226] Y. Liu, Y. Yu, J. W. Y. Lam, Y. Hong, M. Faisal, W. Z. Yuan, B. Z. Tang, *Chem. Eur. J.* **2010**, *16*, 8433.

The formation of an AIEgen inside live cells could provide advantages over other types of fluorophores, such as fluorescence amplification and specific localization, avoiding the diffusion through the cellular membrane. We therefore considered the synthesis of AQ's that could display AIGen properties (figure 100). The carbazole-AQ (Cz-AQ) and the triphenylamino-AQ (TPA-AQ) were reported by the group of Sun in 2017,[227] while the phenothiazine-AQ (PTZ-AQ) was described by Lee's and co-workers.[228] Albeit all of them displayed a nice AIE character and quantum yield, at outset we thought that TPA-AQ could be easily prepared through our Ru promoted [2+2+2] cycloaddition.

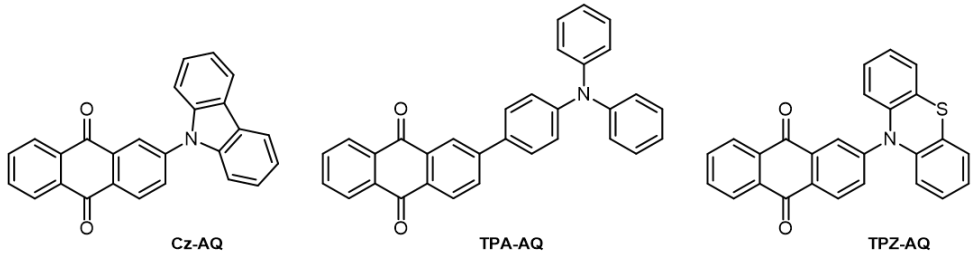

Figure 100. Some anthraquinones found in the literature that display AIE character.[227,228]

For this, we use TPA-alkyne **45**, obtained through a Sonogashira's cross coupling, shown in figure 101.

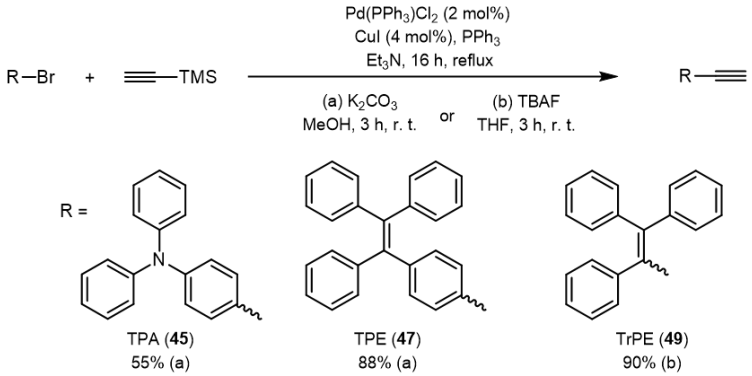

*Figure 101. General protocol for the synthesis of alkynes **45**, **47** and **49**.*

Oddly, following Itoh's protocol,[220] the product **46** was obtained in only a 15% yield, being difficult to purify, and recovering the substrate (figure 102a). In parallel, we decided to synthesize the alkyne-TPE derivative **47**, envisioning that upon the [2+2+2], the product TPE-AQ (**48**) could exhibit relevant AIE properties.

USC UNIVERSIDADE DE SANTIAGO DE COMPOSTELA

[227] B. Huang, Y. Ji, Z. Li, N. Zhou, W. Jiang, Y. Feng, B. Lin, Y. Sun, *J. Lumin.* **2017**, *187*, 414.
[228] B. Huang, W. Chen, Z. Li, J. Zhang, W. Zhao, Y. Feng, B. Z. Tang, C. Lee, *Angew. Chem. Int. Ed.* **2018**, *57*, 12473.

In this case, the cycloaddition in DCE furnished 40% of the expected anthraquinone **48**. However, preliminary assays demonstrated that this product already presents low AIE properties. Indeed, the precursor **47** is a much better dye, and blue emitting fluorophore. For our purposes, it would be much better to use a cycloaddition precursor that is not an AIGen by itself. Therefore, we prepared the triphenylethylene-alkyne (TrPE-alkyne, **49**). Gratifyingly, in this case the cycloaddition reaction affords the anthraquinone **50** took place in an excellent 73% yield. More importantly, this product exhibited an astonishing bright fluorescence (with a 22-fold-increase in comparison with **49**, substrate that lacks any kind of AIE properties) (figure 102b). A fluorescence comparison among H_2O/THF mixtures of compound **50** confirmed the good behavior as AIE. When the proportion of water increases the anthraquinone displays higher fluorescence, due to a higher amount of compound **50** precipitated and thus, more emitting anthraquinone in the solid state (figure 102c).

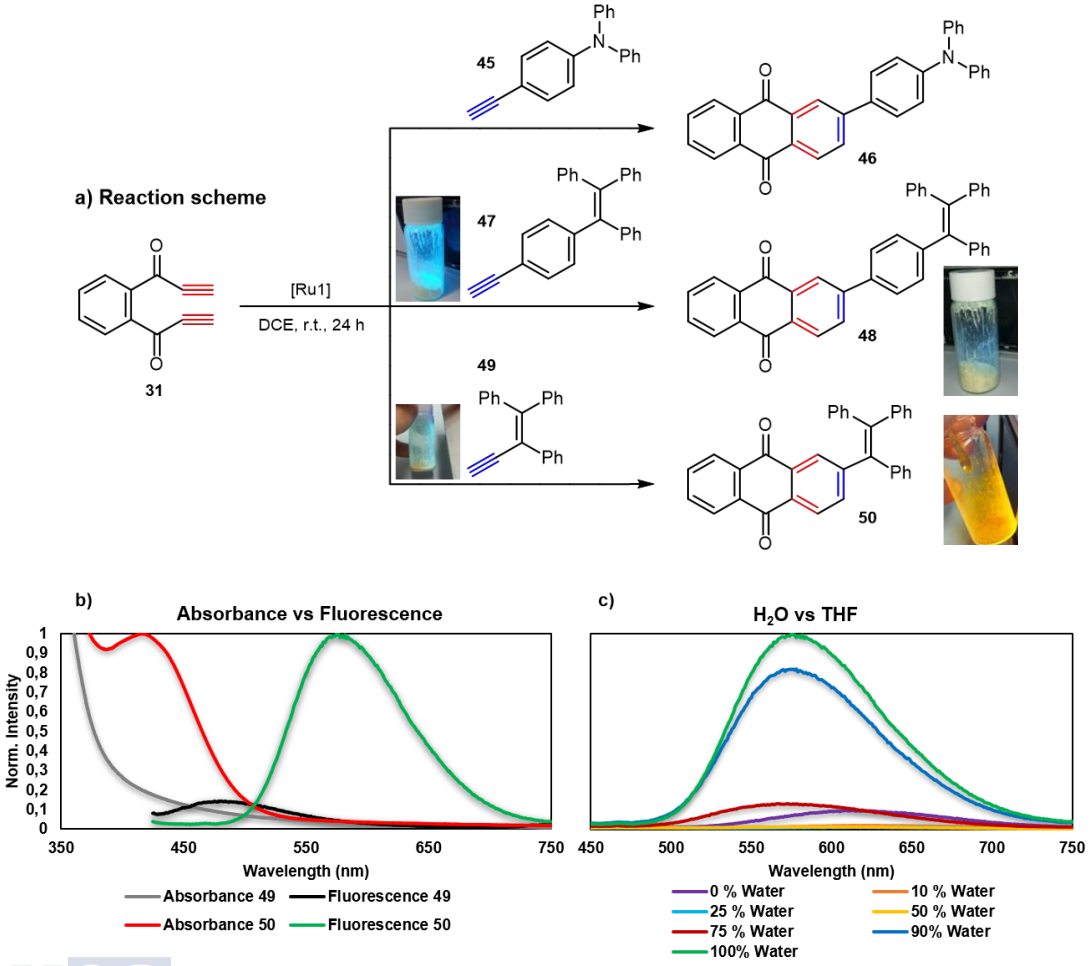

*Figure 102. a) Synthesis of AIE-anthraquinones **46**,**48**,**50** and representative pictures of their AIE character. b) Absorbance vs fluorescence spectra of alkyne **49** and anthraquinone **50**. Absorbance experiments were carried out in water at 100 μM and fluorescence at 20 μM with an excitation at λexc = 385 nm. c) Fluorescence experiments in H_2O/THF mixtures with 20 μM of AQ **50**.*

4.4.2. Cellular experiments with AIEgen motifs

We then moved to live mammalian cells. As expected, when cells were incubated directly with AQ **48**, low levels of fluorescence were observed, further discarding the use of this probe. In the case of AQ **46**, cells treated with this product displayed aggregates of concentrated fluorescence, only slightly higher than **48**, being difficult to differentiate between that of the substrate **45** and the product AQ **46**.

In contrast, incubation of cells with AQ **50** (50 μM, added from a DMSO stock) led to an intense and bright fluorescent signal. However, this product is concentrated in extracellular sites, meaning that it forms instantly aggregates once added into the well plate (figure 103, panel B). The product can only be inefficiently internalized after permeabilization of the membrane using digitonin (see experimental section, Chapter III S9).

The reaction protocol for the cellular experiments is similar to that previously used for other bioorthogonal reactions: addition of a solution of **Ru2** (20 mM in DMSO) for a final concentration of 50 μM, after 30 min of cell incubation, extensive washing with DMEM, and addition of a solution of diyne **31** (50 μM) and the alkyne **49** (150 μM). After 3 h, we observed a low fluorescence increase. This could be due to a poor internalization of the alkyne **49**, and for that reason, we decided to add it in several portions (1/3 each 30 min). In this case, we did observe the appearance of an intense intracellular red fluorescent signal in form of intracellular aggregates through all the cell (figure 103, panel C).

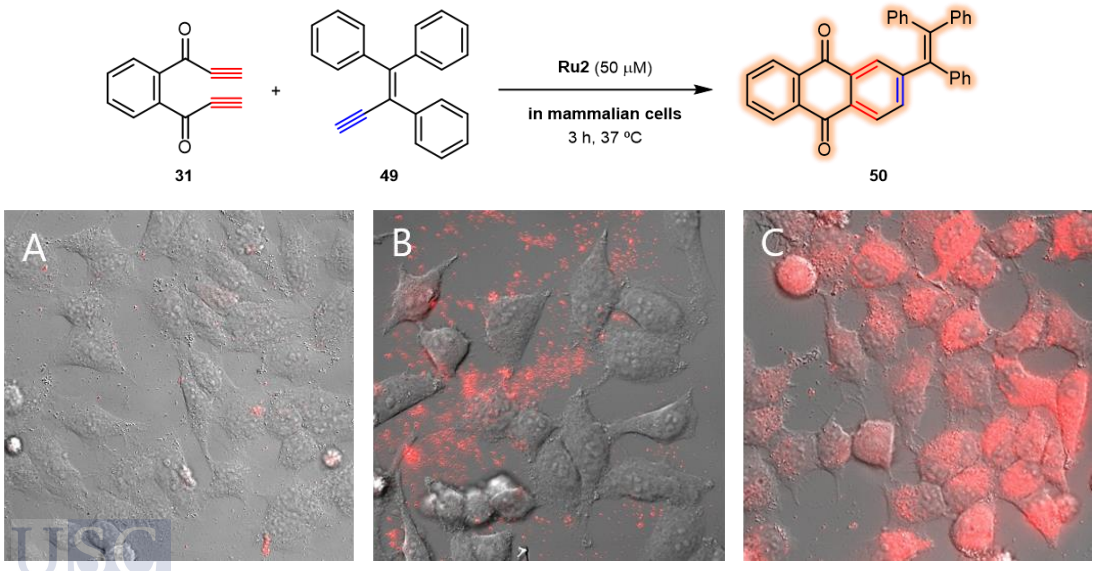

*Figure 103. Fluorescence micrographies in HeLa cells. Protocol: cells were incubated with 50 μM of **Ru2**, then washed and incubated with 50 μM of **31** and 150 μM of **49** at 37 ºC for 3 h. Fluorescence obtained in the red channel (λ_{exc} = 550 nm, λ_{em} = 570-690 nm). A) Control without **Ru2**. B) Incubation of cells with 50 μM of **50**. C) Reaction in cells.*

4.5. Detection of intracellular cycloaddition products by HPLC-MS

The observation of a bright intracellular fluorescence only when the cell had been previously treated with the ruthenium complex, and the lack of internalization of the product **50**, is highly supportive of an intracellular [2+2+2] cycloaddition.

Nonetheless, we wondered whether we could further confirm the reaction by detecting the presence of the product by Electrospray ionization-Mass spectrometry (ESI-MS). Therefore, to further facilitate the detection of the cycloadduct, we synthetized an alkyne containing phosphonium group, which is a very useful tag for MS (**53**). The nucleophilic addition of 4-iodophenol to dibromopropane affords the ether **51** in a 75% yield. The trimethylsilyl alkyne moiety is introduced through a Sonogashira's cross coupling, followed by a TMS deprotection to provide the 1-(3-bromopropoxy)-4-ethynylbenzene **52** in a 78% yield. Finally, reaction with PPh_3 leads to the desired alkyne-TPP **53** in an excellent yield.

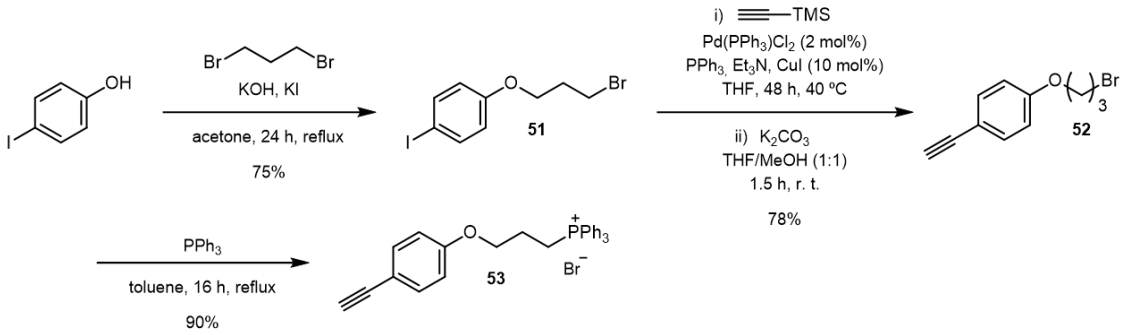

*Figure 104. Synthesis of the alkyne-TPP **53**.*

This alkyne **52** engaged well in the cycloaddition with diyne **31** in DCE, using **Ru1** as catalyst, to give the expected product **54**. The resulting AQ can react with PPh_3 to give the desired derivative AQ-TPP (**55**) in 48% yield. Although cycloaddition among **31** and **53** could afford the product **55** in one step, the low solubility of the TPP-alkyne in organic solvents prevented this route. The same reasoning was followed in the synthesis of **53**, where the incorporation of the TPP moiety was left to the last step.

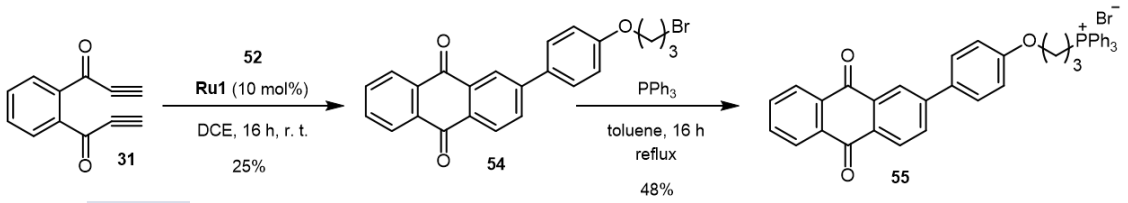

*Figure 105. Synthesis of anthraquinone-TPP **55**.*

USC UNIVERSIDADE DE SANTIAGO DE COMPOSTELA

We then explored the cycloaddition under aqueous conditions (1 mM diyne **31**, 4 equivalents of **53** or **52**, 25 mol% of **Ru1** in water mixtures for 2 h). The yields were determined by NMR using TMB as internal standard.

The results are summarized in table 10, When the bromo derivative **52** was employed, we were able to observe the product in reasonable yields (around 40%) either with H_2O or with an organic co-solvent. However, with the phosphonium derivative, the reaction mixture presented a slightly turbid aspect when ran in pure H_2O, and the process was less efficient, recovering most of the starting diyne.

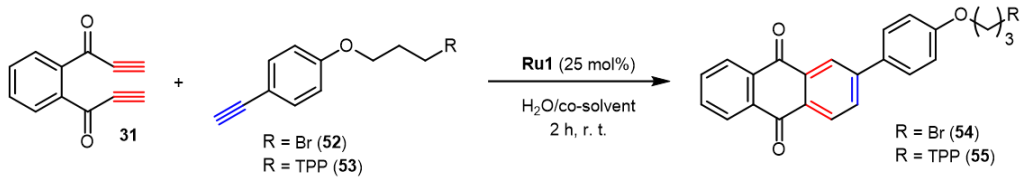

Entry	Alkyne	Milieu	Yield (%)[1]
1	52	H_2O	40
2	52	H_2O/MeCN (8:2)	42
3	52	H_2O/MeOH (8:2)	39
4	52	H_2O/MeOH (5:5)	40
5	53	H_2O	trace
6	53	H_2O/MeCN (9:1)	17
7	53	H_2O/MeCN (8:2)	47
8	53	H_2O/MeCN (5:5)	50
9	53	H_2O/MeOH (5:5)	54

*Table 10. Co-solvent screening for Ru promoted [2+2+2] cycloaddition to obtain TPP-Anthraquinones. Conditions: 1 mM of the diyne **31**, 4 equiv. of the proper alkyne, 25-50 mol% of **Ru1**, at r.t. for 2 h. [1]Yields were determined by NMR using TMB as internal standard.*

Although the reaction with the TPP-alkyne **53** gave modest yields, likely because of physical solubility problems, we considered that it would be sufficient for its detection inside cells. Consequently, we moved to cellular experiments which were carried using standard protocols with alkyne **53** (150 μM diyne **31** (50 μM) and **Ru2** (50 μM)), and allowing the reaction to take place for 4 hours to maximize the formation of product. Afterwards, the cellular content soluble in methanol was extracted and treated for its posterior HPLC-MS detection.

USC UNIVERSIDADE DE SANTIAGO DE COMPOSTELA

Gratifyingly, we were able to detect the compound AQ-TPP (**55**) in these extracts confirming the intracellular formation of the product (figure 106a), although the intensity of the extracted ion chromatogram was quite low, and difficult to quantify. Remarkably, some product in the reaction media could be also appreciated in lower intensity (figure 106b).

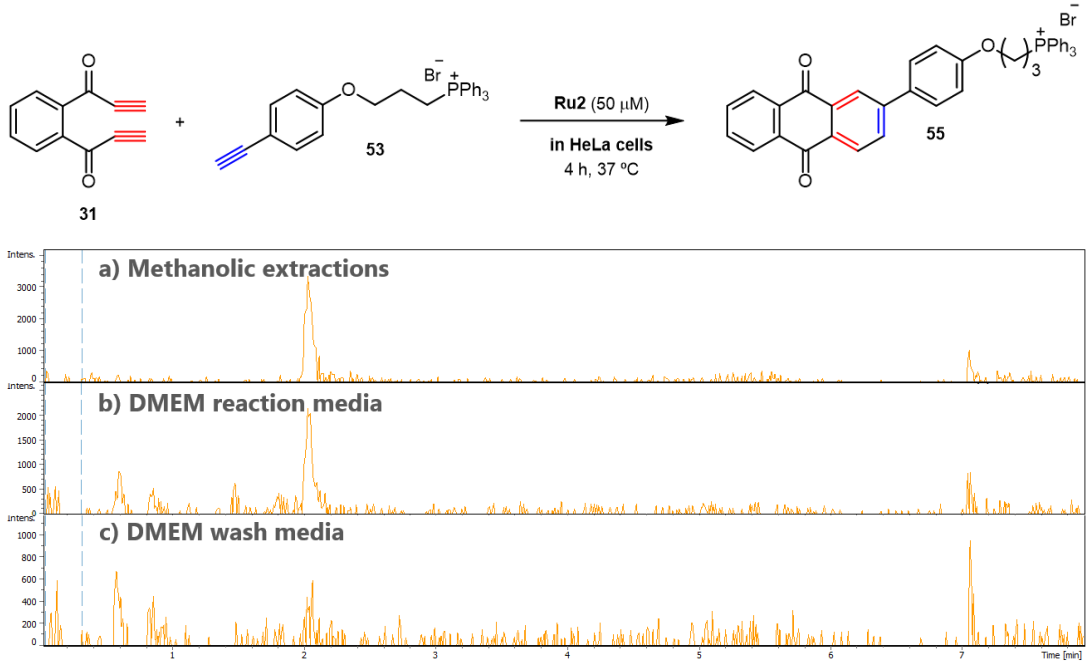

*Figure 106. Extracted ion chromatogram of the formation of **55** in cellular experiments. Protocol: cells were incubated with 50 μM **Ru1** for 30 min, after the washes steps, cells were incubated with 50 μM of **31** and 150 μM of **53**, at 37 ºC for 4 h. a) Chromatogram of the methanolic extract. b) Chromatogram of the DMEM reaction media. c) Chromatogram of the wash media prior cellular extraction.*

In view of these results, we decided to check whether non-fluorescent products, like the phthalans, could also be formed and detected in cells by MS following the same approach, the diyne **26** and the alkyne **53** bearing the TPP moiety for the detection, were subjected to the reaction conditions. Accordingly, a representative amount of product **56** was detected in the methanol extract (figure 107a). In this case, we also detected product in the washings steps performed prior to methanol extraction, what could mean that some product can diffuse outside the cell.

USC UNIVERSIDADE DE SANTIAGO DE COMPOSTELA

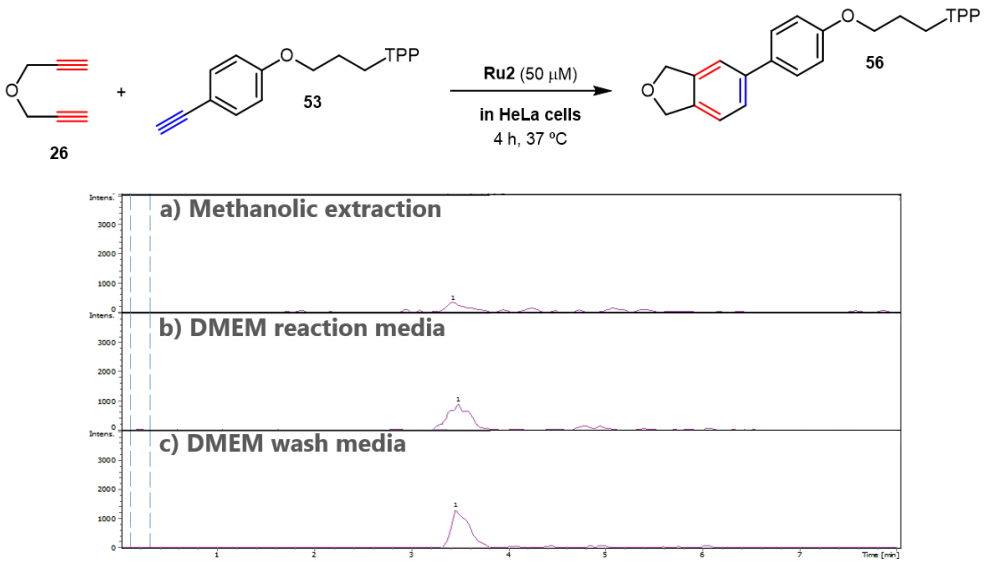

*Figure 107. Extracted ion chromatogram of the formation of **56** in cellular experiments. Protocol: cells were incubated with 50 μM **Ru2** for 30 min, after the washes steps, cells were incubated with 50 μM of **26** and 150 μM of **53**, at 37 ºC for 4 h. a) Chromatogram of the methanolic extract. b) Chromatogram of the DMEM reaction media. c) Chromatogram of the wash media prior cellular extraction.*

Curiously, in this case when we ran the same experiments in cells using R**u1** instead of **Ru2**, a higher amount of product **56** was formed inside the cell (figure 108, a). Moreover, the levels of final product detected in the reaction media and wash media, were always very low (figure 108, b and c).

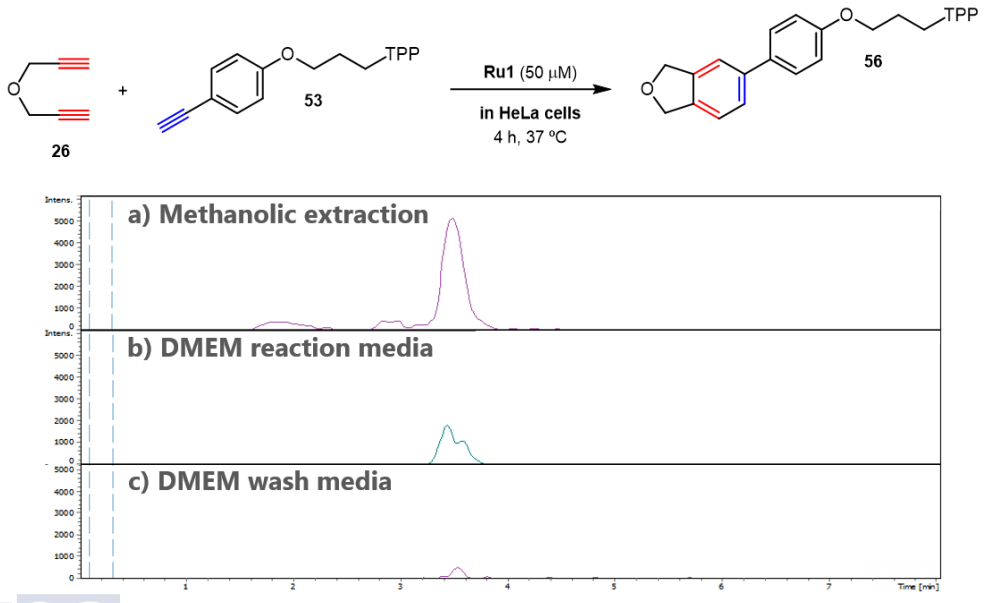

*Figure 108. Extracted ion chromatogram of the formation of **56** in cellular experiments. Protocol: cells were incubated with 50 μM **Ru1** for 30 min, after the washes steps, cells were incubated with 50 μM of **26** and 150 μM of **53**, at 37 ºC for 4 h. a) Chromatogram of the methanolic extract. b) Chromatogram of the DMEM reaction media. c) Chromatogram of the wash media prior cellular extraction.*

4.6. Localized ruthenium-promoted intermolecular [2+2+2] cycloadditions in specific organelles

In previous work of the group, a **Ru2** derivative (**Ru8**, figure 109) was demonstrated to accumulate in mitochondria, performing its catalytic activity (uncaging reactions) in this organelle.[139] This new complex provided a colocalization with the organelle of around 88%.[229] Thus, we found appealing to test if this complex is also active in the intracellular [2+2+2] cycloadditions and if it can express its activity in the mitochondria surroundings . We selected the optimized cycloaddition that provides the product AIE-AQ (**50**). Experiments were performed incubating the cells with of **Ru8** (50 μM) for 1 h. After two washing steps, cells were treated with 50 μM of **31** and 150 μM of the triphenylethylene-alkyne **49** for 3 h at 37 ºC. As negative control, some cells were treated with **Ru1**, that lack the localization tag. In order to confirm the mitochondrial localization of the product, a green fluorescent mitochondrial marker (mitotracker^{MT}) was also used. As can be observed in figure 105, when **Ru1** was employed, the product fluorescence spread through the cell (figure 109, panel A). The absence of overlay with the fluorescent signal of the mitotracker confirms the lack of colocalization. In contrast, transformations that were promoted by **Ru8** exhibited a localized fluorescence (figure 109, D), predominantly matching with the mitochondrial dye (figure 109, panel F).

USC UNIVERSIDADE DE SANTIAGO DE COMPOSTELA

[229] 0.88 of Mander's coefficient M_1 (385-500 nm)

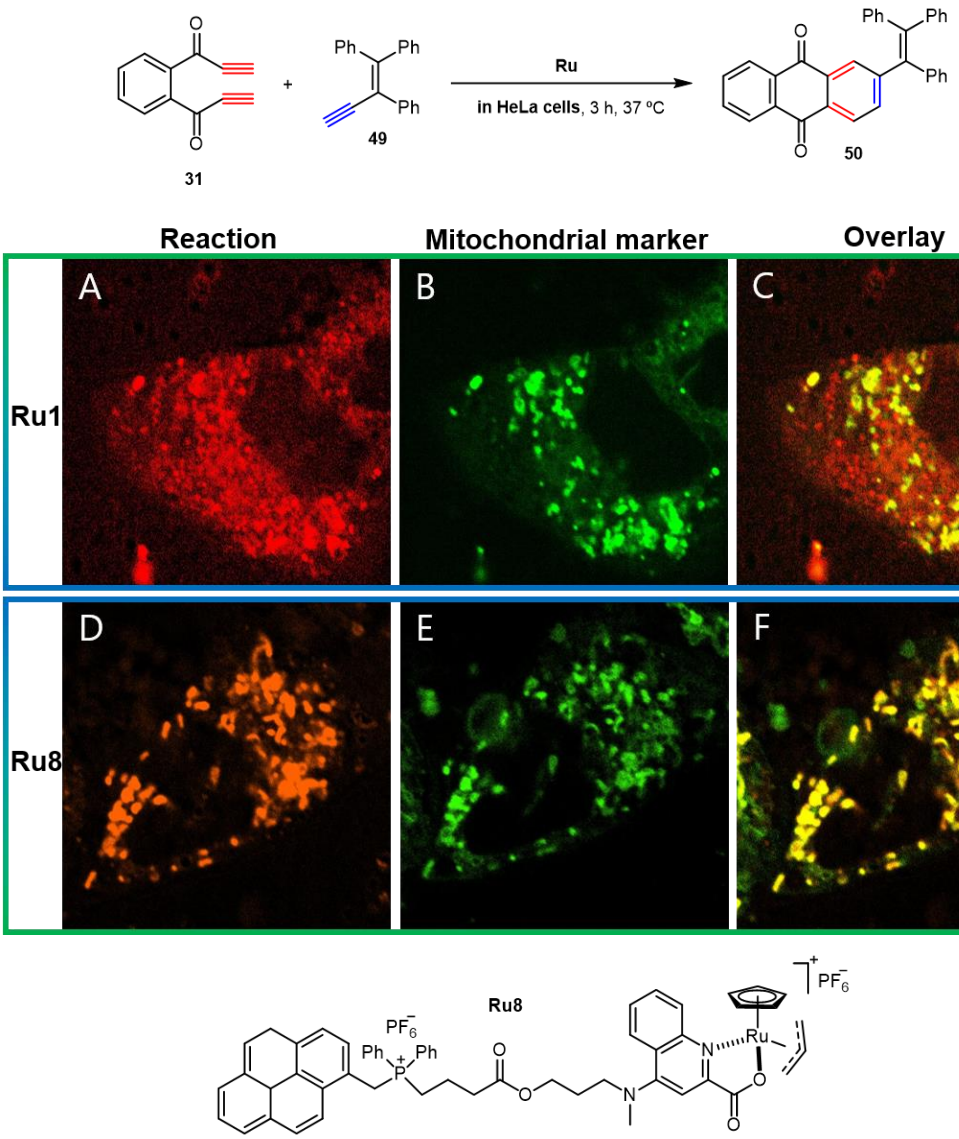

Figure 109. Fluorescence micrographies of co-localization experiments in HeLa cells. Protocol: cells were incubated with 50 μM ***Ru1*** *or* ***Ru8*** *for 3 h, then were washed and incubated with 50 μM of* ***31*** *and 150 μM of* ***49****, at 37 ºC for 1 h. A and D: Red channel (*λ_{exc} *= 550 nm,* λ_{em} *= 570-690 nm) corresponding to intracellular transformation with cells incubated with* ***31****,* ***49*** *and* ***Ru8****. B and E: Green channel (*λ_{exc} *= 470 nm,* λ_{em} *= 490-580 nm) corresponding to mitochondrial marker fluorescence. C and F: merging of A and B, and D and E. A, B and C were performed with* ***Ru1*** *and D, E and F with* ***Ru8****.*

USC UNIVERSIDADE DE SANTIAGO DE COMPOSTELA

In previous works of the group, the cytotoxicity of different Ru catalysts were already analyzed, with **Ru2** and **Ru8** showing no remarkable cytotoxicity.[139] So, we performed an MTT assay to evaluate the cytotoxicity of **Ru1**, diyne **31**, the alkyne **49** and the resulting AIEgen **50** in a range of 10-100 μM for 12 h as shown in figure 110. Importantly, no remarkable cytotoxicity was observed with any component below 100 μM. At this concentration, a moderate cytotoxicity was noticeable for **Ru1**, and only a slight decrease in cell viability was displayed for **31**, which still kept over 80%.

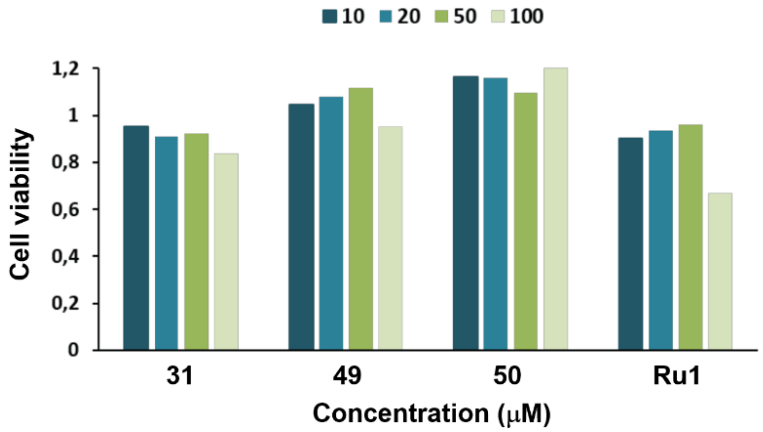

*Figure 110. Cell viability of cells treated with **31**, **49**, **50** and **Ru1** compounds between 10-100 μM for 12 h.*

5. Conclusions

As conclusion, our results demonstrate that transition metals can promote challenging [2+2+2] multicomponent cycloadditions in live mammalian cells. The use of abiotic reactants with bidentate metal coordination abilities (diyne) seems instrumental for the success of the process. In addition to provide a cutting-edge addition to the palette of cell-compatible metal-mediated transformations, our work demonstrates the viability of synthesizing complex, biorelevant polycycles inside cells from simple precursors, and therefore goes beyond the more common uncaging or ligation reactions. Our intracellular synthetic strategy allows to generate products that otherwise cannot be delivered to the cell, as well as controlling their spatial distribution by using suitable ruthenium reagents. Indeed, the possibility of generating the desired products in specific subcellular locations, just by changing the targeting characteristics of the reagents, is exciting. While further work to increase the efficiency of the reactions is needed, our discoveries should further foster this young field of intracellular metal catalysis, and trigger important applications in chemical and synthetic biology, and in biomedicine.

USC
UNIVERSIDADE DE SANTIAGO DE COMPOSTELA

Chapter 4: PHOTOREDOX CATALYSIS IN LIVE MAMAMALIAN CELLS

USC
UNIVERSIDADE
DE SANTIAGO
DE COMPOSTELA

USC
UNIVERSIDADE
DE SANTIAGO
DE COMPOSTELA

1. Introduction into visible-light photochemistry

Photochemical transformations rely on the use of light to trigger reactions that otherwise cannot take place under normal thermal conditions (figure 111a). In some cases, light promoted reactions can be carried out with the assistance of catalysts, that are called photocatalysts, (PC) that absorb light and transfer the energy to a substrate, that is not able to absorb the light *"per se"* (or requires a higher energetic light source). Thus, they act as intermediates between light and substrates, in a process called "sensitization", that finishes with the excited substrate, in a higher energy position, and ready to trigger the corresponding reaction. So, a good photocatalyst must be not only a good light absorber but also be able to state in the excited state without suffering important changes in its structure. In figure 111b, it can be observed the internal electronic reorganization that suffers the photocatalyst before its quenching, which can be radiative, non-radiative or undergo a reaction.[230,231]

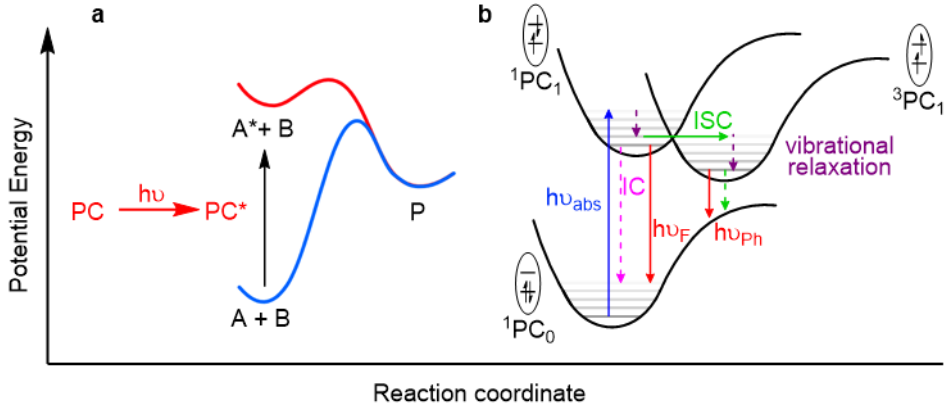

Figure 111. a) Simplified representation of potential energy surface along the course of the reaction. In red the photochemical pathway, in blue the thermal pathway. B) Simplified representation of the potential energy surface for a photocatalyst electronic rearrangement.

Since the late 2000s there has been a drastic increase in the number of contributions in the field of photocatalysis and nowadays a huge amount of photocatalysts can be found, from cheap and green organic photocatalysts to organometallic complexes, mainly based on Ru and Ir metals.[232]

USC UNIVERSIDADE DE SANTIAGO DE COMPOSTELA

[230] B. König, *Chemical Photocatalysis* 2nd Ed, De Gruyter, **2020**.
[231] J. K. McCusker, *Chem. Soc. Rev.* **2016**, *45*, 5803.
[232] M. H. Shaw, J. Twilton, D. W. C. MacMillan, *J. Org. Chem.* **2016**, *81*, 6898.

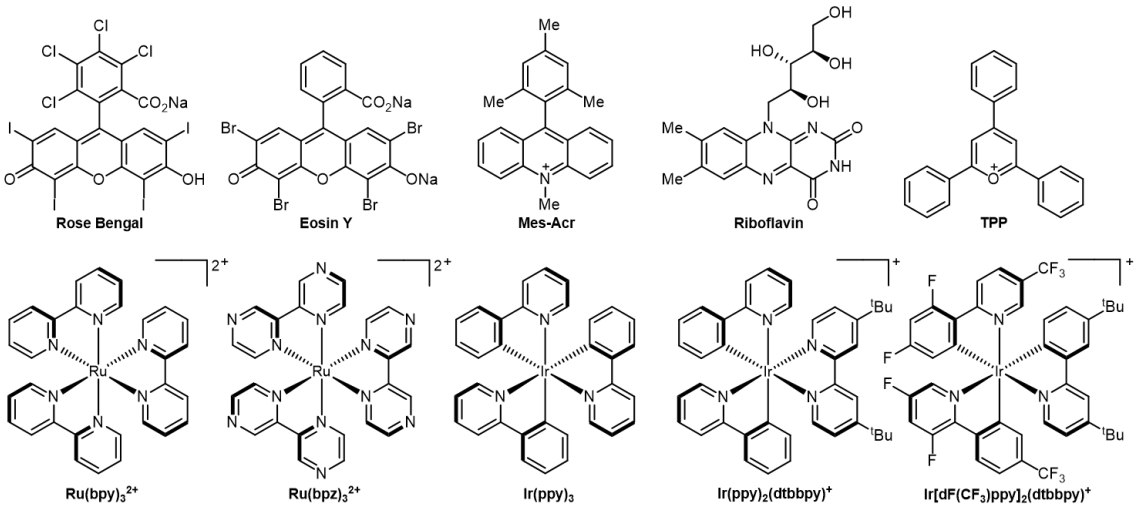

Figure 112. Compendium of common photocatalysts. Upper par; some of the most common organic photocatalysts.[233] *Below; some of the most common organometallic photocatalysts.*[234]

Within the plausible bimolecular quenching of the PC by a chemical reactant, we can distinguish two different mechanisms. One of them is known as photoredox catalysis, and relies on the concept that the excited triplet state of the catalyst can perform single electron transfer processes (SET),[235,236] leading to high energy radical intermediates (figure 113). The other mechanism, far less explored, is named energy transfer (E_t), which is based in the direct transference of the energy gathered in the excited triplet state ($^3PC_1$). In this process, PC will act as energy donor and the corresponding substrate as energy acceptor, leading to the excited substrate after molecular orbitals overlapping, and electron exchange (Dexter mechanism).[237]

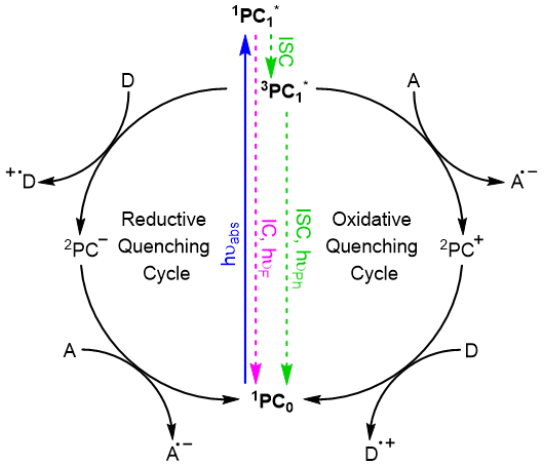

Figure 113. Oxidative and reductive quenching cycle for a PC. D: electron donor. A: electron acceptor.

USC UNIVERSIDADE DE SANTIAGO DE COMPOSTELA

[233] N. A. Romero, D. A. Nicewicz, *Chem. Rev.* **2016**, *116*, 10075.
[234] K. Teegardin, J. I. Day, J. Chan, J. Weaver, *Org. Process Res. Dev.* **2016**, 20, 1156.
[235] J. W. Tucker, C. R. J. Stephenson, *J. Org. Chem.* **2012**, *77*, 1617.
[236] C. K. Prier, D. A. Rankic, D. W. C. MacMillan, *Chem. Rev.* **2013**, *113*, 5322.
[237] F. Strieth-Kalthoff, M. J. James, M. Teders, L. Pitzer, F. Glorius, *Chem. Soc. Rev.* **2018**, *47*, 7190.

Although many times considered as chaotic or uncontrollable, radicals have grown with chemists since the nineties and, actually, reactions involving radicals can be nowadays rationalized, giving access to hindered regions and avoiding undesired reactivity of functional groups such hydroxyl or amino.[238,239] Nowadays, some classic radical reactions like Birch reduction,[240] Meerwein arylation,[241,242] Pschorr cyclation[243] are well established. Indeed, the last two transformations have recognized diazonium salts as excellent radical precursors.[244,245] Moreover, the latter forementioned combined diazonium salts with light for the first time.

2. Fundamentals of the photo-Meerwein arylation

The study of the Meerwein arylation was initiated with the use of Cu (and later stochiometric amounts of Ti[246] or Fe[247]) in order to generate aryl radicals from diazonium salts and to couple them with alkenes (figure 114). However, important drawbacks like limited scope, formation of side products and moderate yields, have restricted its usage.[248]

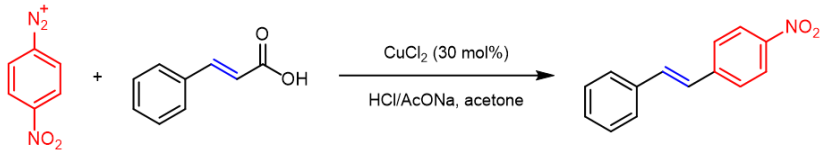

Figure 114. Classic Meerwein arylation catalyzed by Cu, developed by Meerwein in 1939.[248]

This situation changed drastically in 2012 with the impressive work developed by König's group. They reported a photocatalyzed Meerwein reaction under mild conditions that occurred via visible-light photocatalysis. Therein, arylation of different heteroarenes was achieved with yields normally over 70%, using 1 mol% of ruthenium-tris(2,2'-bipyridyl) ($Ru(bpy)_3$) or 7.5 mol% of Eosin Y as catalyst, DMSO as solvent for 2 h and no extra additives.[249] Following this first contribution, other related transformations, such as the synthesis of stilbenes or the arylation of benzoquinones and coumarins, were also described.[250] More interestingly, alkynes also suffered radical aryl additions, expanding thus the scope of the transformation from Csp^2-Csp^2 to Csp^2-Csp carbons.

[238] M, Yan, J. C. Lo, J. T. Edwards, P. S. Baran, *J. Am. Chem. Soc.* **2016**, *138*, 12692.
[239] N. E. S. Tay, D. Lehnherr, T. Rovis, *Chem. Rev.* **2021**, *122*, 2487.
[240] P. W. Rabideau, *Org. React.* **1992**, *42*, 1.
[241] H. Meerwein, E. Buchner, K. van Emsterk, *J. Prakt. Chem.* **1939**, *152*, 237.
[242] S. Kindt, M. R. Heinrich, *Synthesis* **2016**, *48*, 1597.
[243] H. Cano-Yelo, A. Deronzier, *J. Photochem.* **1987**, *37*, 315.
[244] T. Sandmeyer, *Ber. Dtsch. Chem. Ges.* **1884**, *17*, 1633.
[245] M. Gomberg, W. E. Bachmann, *J. Am. Chem. Soc.* **1924**, *46*, 2339.
[246] M. R. Heinrich, O. Blank, S. Wöefel, *Org. Lett.* **2006**, *8*, 3323.
[247] M. R. Heinrich, O. Blank, D. Ullrich, M. Kirschstein, *J. Org. Chem.* **2007**, *72*, 9609.
[248] D. P. Hari, B. König, *Angew. Chem. Int. Ed.* **2013**, *52*, 4734.
[249] D. P. Hari, P. Schroll, B. König, *J. Am. Chem. Soc.* **2012**, *134*, 2958.
[250] P. Schroll, D. P. Hari, B. König, *ChemistryOpen* **2012**, *1*, 130.

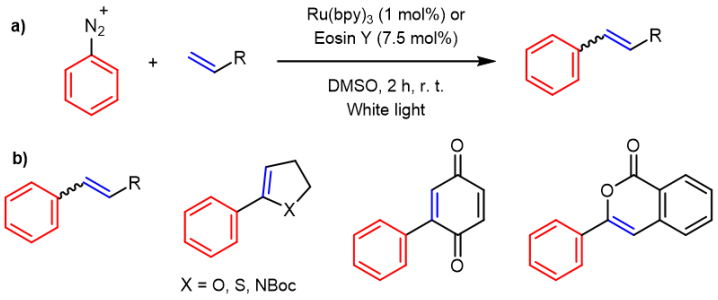

Figure 115. a) General Photo-Meerwein conditions. b) First arylated products reported by König's group.[249,250]

A plausible mechanism proposed by König is shown in figure 116. The diazonium salt presents a reduction potential near to 0 (reduction potential $E_{1/2}$ = 0.05 V vs SCE), and therefore can be reduced by an excited PC with moderate potential reduction like $Ru(bpy)_3$ ($E_{1/2}$ Ru(III)/Ru(II)* = -0.81V vs SCE)[234] or Eosin Y ($E_{1/2}$ PC^+/PC^* = -1.15 V vs SCE).[233] Hence a first SET step would lead to an aryl radical **I** with evolution of N_2. The addition of the aryl radical **I** to the corresponding alkene generates the key radical intermediate **II**, that requires a stabilization through EWG or resonance in order to evolve to the intermediate **III** by means of a radical scavenger. This could be either the metal complex in the classical version, the diazonium salt itself in a propagation way, or the cationic radical PC regenerating the catalyst. At this point, addition of a nucleophile or the deprotonation would lead to the arylation-addition product or the arylation-coupling product, respectively.[251,252]

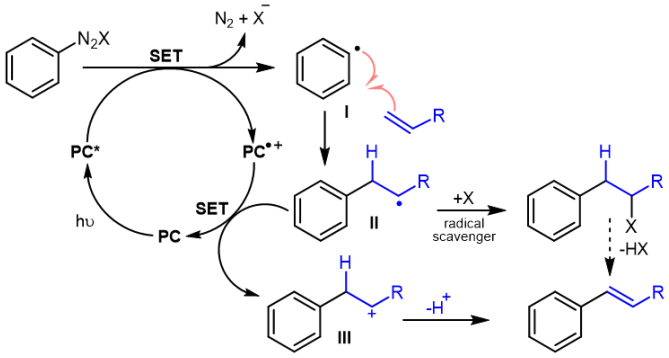

Figure 116. General mechanism for the photo-Meerwein reaction.[251,252]

USC UNIVERSIDADE DE SANTIAGO DE COMPOSTELA

[251] I. Ghosh, L. Marzo, A. Das, R. Shaikh, B. König, *Acc. Chem. Res.* **2016**, *49*, 1566.
[252] F. Mo, D. Qiu, L. Zhang, J. Wang, *Chem. Rev.* **2021**, *121*, 5741.

3.Visible light photocatalysis in aqueous media

Chemists are reticent to make reactions in water, as it can be a non-innocent solvent and, in many cases, introduces solubility problems. Despite that, alcohols or even water are not prone to react with radicals,[253] PC are commonly cationic[233,234] and aqueous solvent can be beneficial for kinetics.[254] However, there is a trend to avoid water also in the field of photocatalysis. Indeed, the examples of photocatalytic reactions in water media are scarce.[255] Nevertheless, some recent reports evidence that photocatalysis in water is not only plausible, but also allows to synthetize complex structures using mild conditions, sustainability that is even further enhanced if the reaction is triggered by visible light.

For instance, Xiao and co-workers reported in 2014 a photo-Meerwein reaction catalyzed by $Ru(bpy)_3$ for the arylation of different N-heteroaromatic hydrochloride salts such as pyridines, pyrazines, pyridazine, thiazoles or even different xanthines, like caffeine, and carried out by irradiation with blue light. The facility of the diazonium salt activation, coupled with their good water solubility, further facilitates the process. The reaction proceeds under smooth conditions leading to high yields of the coupled products, around 80%.[256] Despite the long rection times (60-80 h) and the poor selectivity between ortho- and para- position, the transformation set a precedent for future works.

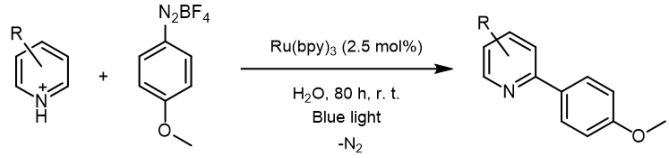

Figure 117. Photo-Meerwein of heteraromatic compounds in water proposed by Xiao in 2014.[256]

Another interesting contribution is the dimerization of *o*-phenyldiamines or *o*-aminophenol catalyzed by the organic PC Eosin Y, that leads to phenazines and phenoxazinones, respectively, in aqueous buffers. Remarkably, the transformation uses O_2 as key reagent in several reaction steps, although with air atmosphere is enough to. observe reactivity. Besides, temperature changes or reaction in non-buffered water is also plausible with only a slight yield decrease. Overall, the excellent yields (over 80%), reaction times (6-8 h), together with the simplicity of the substrate that contrasts with the complexity of the final product, shows clearly the potential of these transformations.[257]

USC UNIVERSIDADE DE SANTIAGO DE COMPOSTELA

[253] J. Hioe, H. Zipse, *Org. Biomol. Chem.* **2010**, *8*, 3609.
[254] S. Narayan, J. Muldoon, M. G. Finn, V. V. Fokin, H. C. Kolb, K. B. Sharpless, *Angew. Chem. Int. Ed.* **2005**, *44*, 3275.
[255] K. Sun, Q. Lv, X. Chen, L. Qu, B. Yu, *Green Chem.*, **2021**, *23*, 232.
[256] D. Xue, Z. Jia, C. Zhao, Y. Zhang, C. Wang, J. Xiao, *Chem. Eur. J.* **2014**, *20*, 2960.
[257] A. K. Dhara, S. Maity, B. B. Dhar, *Org. Lett.* **2021**, *23*, 3269.

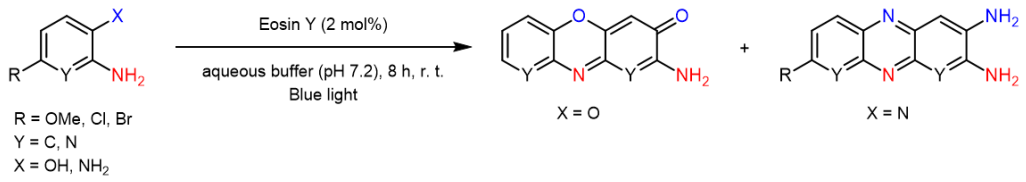

Figure 118. Dimerization of o-amino/hydroxy substituted anilines in water proposed by Dhar in 2021.[257]

4. Photocatalysis in biological settings

Light interacts everyday with life in different ways. It is well-known that bacteria and plants employ light to produce energy, in a process that involves transport of electrons. Moreover, light can also be used for promoting bioorthogonal chemical reactions in biological contexts.

Recently, the "photoclick" conjugation,[107] or photoactivable versions of SPAAC[112] or IEDDA,[113] have become quite popular due to their excellent properties for bioconjugation.[258,259] However, the use of photocatalysis in biological media is still anecdotic, and mainly restricted to the modification of biopolymers such as proteins (usually in Tyr or Cys residues) or DNA.[260,261] Photocatalysis can be also used for photodynamic therapy (PDT), that has been very useful for achieving a localized generation of cytotoxicity, usually by sensitizing oxygen and producing oxidizing reagents.[262]

The number of reports dealing with biological and cellular applications of photocatalytic processes, also using visible light, are increasing. For instance, the groups of Sadler, and more recently of Peng, have demonstrated that Ir photocatalysts can drive intracellular reduction processes, that affect the redox equilibrium of cells.[263,264]

In 2019 Chen and co-workers demonstrated a TMRE-photosensitized production of H_2O_2 from oxygen, and the ensuing application of this oxidant to produce phenol derivatives from boron precursors in mammalian cells.[265] Additionally, as can be appreciated in figure 119b, the use of this commercially mitochondria tracker, used as photosensitizer, allowed the reaction to take place specifically on mitochondria, exposing the potential of photocatalysis versus non-catalyzed photochemistry.

---

[258] J. Li, H. Kong, L. Huang, B. Cheng, K. Qin, M. Zheng, Z. Yan, Y. Zhang, *J. Am. Chem. Soc.* **2018**, *140*, 14542.
[259] Z. Yao, X. Wu, X. Zhang, Q. Xiong, S. Jiang, Z. Yu, *Org. Biomol. Chem.* **2019**, *17*, 6777.
[260] C. Bottecchia, T. Noël, *Chem. Eur. J.* **2019**, *25*, 26.
[261] V. M. Lechner, M. Nappi, P. J. Deneny, S. Folliet, J. C. K. Chu, M. J. Gaunt, *Chem. Rev.* **2022**, *122*, 1752.
[262] G. Gunaydin, M. E. Gedik, S. Ayan, *Front. Chem.* **2021,** *9*, 686303.
[263] H. Huang, S. Banerjee, K. Qiu, P. Zhang, O. Blacque, T. Malcomson, M. J. Paterson, G. J. Clarkson, M. Staniforth, V. G. Stavros, G. Gasser, H. Chao, P. J. Sadler, *Nat. Chem.* **2019**, *11*, 1041.
[264] M. Li, K. H. Gebremedhin, D. Ma, Z. Pu, T. Xiong, Y. Xu, J. S. Kim, X. Peng, *J. Am. Chem. Soc.* **2022**, *144*, 163.
[265] H. Wang, W. Li, K. Zeng, Y. Wu, Y. Zhang, T. Xu, Y. Chen, *Angew. Chem. Int. Ed.* **2019**, *58*, 561.

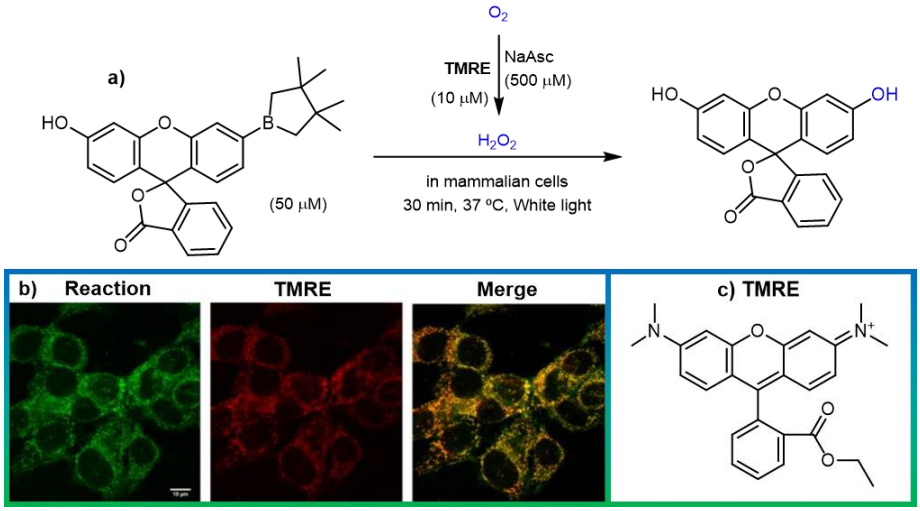

Figure 119. a) Alcohol unmasking in mammalian cells carried out by Yinyun's group in 2019. b) Microscopy imaging of MCF-7 cells. c) TMRE photocatalyst structure.[265]

Also, photo-promoted deprotection methodologies based on azide or pyridinium reductions have been an important hit in the field (figure 120). The group of Winssinger employed this technology for the release of AIE fluorophores, through a self-inmolative mechanism, in the cell membrane, in the nucleus of mammalian cells or even zebrafish without noticing cytotoxicity.[266] For this purpose, they focused on tailored Ru-photocatalyst bearing a proper directing group, or even attached to single strand DNA/RNA or PNA (Peptide Nucleic Acid) motif for its complementary chain recognition.[267,268]

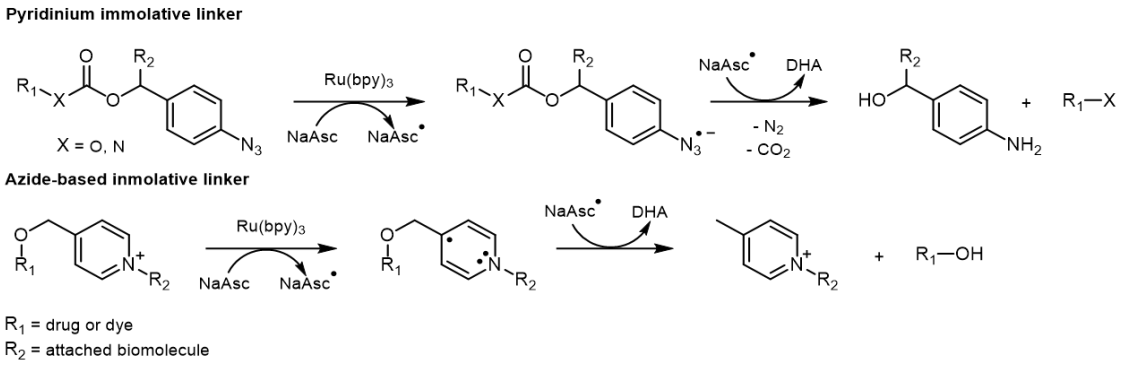

Figure 120. Photoreduction mechanism of azides and pyridinium for molecule release, via self-inmolative linkers.[266,267,268]

USC
UNIVERSIDADE DE SANTIAGO DE COMPOSTELA

[266] K. K. Sadhu, E. Lindberg, N. Winssinger, *Chem. Commun.* **2015**, *51*, 16664.
[267] K. K. Sadhu, N. Winssinger, *Chem. Eur. J.* **2013**, *19*, 8182.
[268] L. Holtzer, I. Oleinich, M. Anzola, E. Lindberg, K. K. Sadhu, M. Gonzalez-Gatian, N. Winssinger, *ACS Cent. Sci.* **2016**, *2*, 394.

However, the use of photocatalytic reactions with synthetic purposes in complex biological media remains unexplored. Chen and coworkers reported the alkynylation of primary, secondary, and tertiary alkanes in presence of different biomolecules. The generation of alkane radical was achieved via oxidation of trifluoroboronates (deboronative process) or reduction of N-acyloxyphthalimides (decarboxylative process) using $Ru(bpy)_3$ as PC (figure 121). In the first case, the radical is added into a benzidoxole (Bi)-alkyne. The benzidoxole group is eliminated as radical, which acts as PC regenerator, leading to a redox neutral process.

In contrast, in the decarboxylative process, addition of the alkane radical into alkynyl phenylsulfones generates a sulfinyl radical unable to regenerate the PC. Hence, addition of an external reductant such as DIPEA is needed. Importantly, the use of endogenous reductants like NADH or NaAsc provides almost identical yields.

Satisfactorily, the photo promoted reactions works over 80% of yield, at micromolar range, in biological buffers containing aminoacids such as cysteine or tyrosine, doble stranded DNA, BSA protein, or even in presence of a carbonic anhydrase enzyme, without disturbing its activity.[269,270] However, no further exploration of the transformation in the presence of living bacteria o mammalian cells has been performed, and high doses of additive are still needed, leaving place for further explorations.

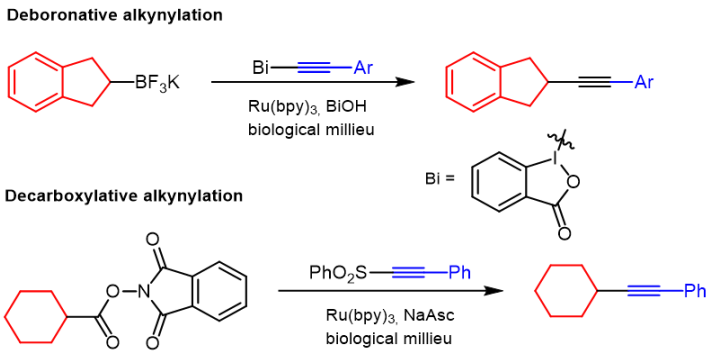

Figure 121. Deboronative and decarboxylative alkynylations reported by Chen in 2014 and 2015.[269,270]

USC UNIVERSIDADE DE SANTIAGO DE COMPOSTELA

[269] H. Huang, G. Zhang, L. Gong, S. Zhang, Y. Chen, *J. Am. Chem. Soc.* **2014**, *136*, 2280.
[270] J. Yang, J. Zhang, L. Qi, C. Hu, Y. Chen, *Chem. Commun.* **2015**, *51*, 5275.

In 2018, Ward and Wenger reported a concurrent photoredox and enzymatic catalytic process for the obtention of enantioenriched amines using a water-soluble Ir photocatalyst coupled to the bacteria machinery that recycles the non-desired enantiomer, leading to a high enantiomeric excess after several cycles.[271]

Very recently, a number of photocatalytic processes to generate reactive intermediates for protein mapping have been reported. Most of them rely on the generation of carbenes or nitrenes.[272,273]

USC UNIVERSIDADE DE SANTIAGO DE COMPOSTELA

[271] X. Guo, Y. Okamoto, M. R. Schreier, T. R. Ward, O. S. Wenger, *Chem. Sci.* **2018**, *9*, 5052.
[272] J. B. Geri, J. V. Oakley, T. Reyes-Robles, T. Wang, S. J. McCarver, C. H. White, F. P. Rodriguez-Rivera, Dann L. Parker, Jr, E. C. Hett, O. O. Fadeyi, R. C. Oslund, D. W. C. MacMillan, *Science* **2020**, *367*, 1091.
[273] H. Wang, Y. Zhang, K. Zeng, J. Qiang, Y. Cao, Y. Li, Y. Fang, Y. Zhang, Y. Chen, *JACS Au* **2021**, *1*, 1066.

5. Objectives

There is clearly an increasing interest in the use of photocatalytic processes for bioorthogonal chemistry and for biological purposes. However, the number of applications, especially in mammalian cells, is very small, and in particular, the use of photocatalytic processes for synthetic purposes in biological and cellular media is essentially unknown.

Considering the previous results of the photo-Meerwein transformation carried out in water by the Xiao's group, we questioned whether a similar photoredox process could be performed in the presence of complex biological mixtures. We hypothesized that the diazonium reagent could be more efficiently activated than other biological components, ensuring selectivity, in native settings. The resulting carbon radical might react with an appropriately designed acceptor, like a quinone, more efficiently that with other components, which would ensure bioorthogonality.

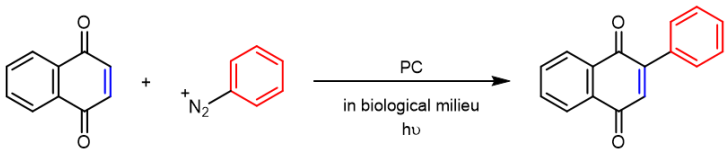

USC
UNIVERSIDADE DE SANTIAGO DE COMPOSTELA

7. Results and discussion

7.1. Photocatalyzed arylations of unsaturated substrates in aqueous media

In order to investigate if this aryl radical chemistry can be performed in biological complex environments, we considered the use of quinones as coupling partners owing to their well-known radical trapping properties.[274] Although König had previously reported the arylation of benzoquinone with diazonium salts in DMSO, (90% yield, 2 h),[250] we decided to study the arylation of naphthoquinones because of their interesting properties as secondary metabolites and their relation with anthraquinones.[275]

We explored the ability of 1,4-naphtoquinone **57** to act as a radical trapping agent of anisole diazonium salt **58** (table 11) producing the naphtoquinone **59a**. Reactions were carried out weighing the solids in Schlenk flasks. After the purge with Ar, the corresponding deoxygenated solvent is added, gently stirred and set under irradiation for the chosen reaction time with fan refrigeration. After extraction, yields were quantified by NMR using trimethoxybenzene as internal standard. The formation of the product of the double addition (**59b**) was also detected. Delightfully, initial experiments at 200 mM of diazonium salt **58** and 5 equivalent of **57** in DMSO as solvent, reflected the excellent behavior of compound **57** as radical scavenger, observing full conversion of the diazonium salt **58**, after 2 h of reaction under blue light source and using 1 mol% $Ru(bpy)_3(PF_6)_2$, from now on $Ru(bpy)_3$, as PC (68% of the monoaddition product **59a**, entry 1). Eosin Y was also tested as PC in a 7.5 mol% and white-light as well, yielding 80% yield (entry 2). Gratefully, the reaction also tolerates water as reaction media, obtaining 50% of **59a** in a mixture DMSO/H_2O (8:2). Nevertheless, higher amount of water led to precipitation of substrate **57**. Water solubility studies demonstrated that a combination of THF/H_2O 1:1 provided a homogeneous crude, and an excellent 85% yield. Moreover, under more complex biological media such as PBS the reactivity was maintained (74%, entries 6 and 7).

USC UNIVERSIDADE DE SANTIAGO DE COMPOSTELA

[274] O. Fónagy, E. Szabó-Bárdos, O. Horváth, *J. Photochem. Photobiol. A.* **2021**, *407*, 113057.
[275] P. Babula, V. Adam, L. Havel, R. Kizek, *Curr. Pharm. Anal.* **2009**, 5, 47.

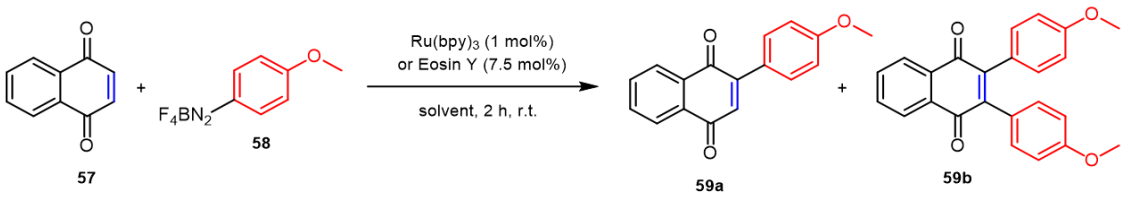

Entry	Catalyst	Cat. loading (mol%)	Milieu	Yield (%)[1]
1	$Ru(bpy)_3$	1	DMSO	68/32[2]
2	Eosin Y	7.5	DMSO	80/20[2]
3	$Ru(bpy)_3$	1	DMSO/H_2O 1:1	50/8
4	$Ru(bpy)_3$	1	DMSO/H_2O 8:2	40/traces
5	$Ru(bpy)_3$	1	DMSO/PBS 1:1	21/traces
6	$Ru(bpy)_3$	1	THF/H_2O 1:1	85/15
7	$Ru(bpy)_3$	1	THF/PBS 1:1	74/24

*Table 11. Preliminary experiments for the naphthoquinone arylation. Conditions: 200 mM of **58**, 5 equiv. of **57**, $Ru(bpy)_3$ at the chosen concentration under 32 W blue-light, in different solvents at room temperature for 2 h.* white-light was *employed. [1]Yields were determined by NMR using nitromethane as internal standard. [2]Isolated yield.*

In contrast, under more diluted conditions such as 10 mM (table 12), the use of THF was not beneficial, leading to dirty reaction crude and low yields. However, at this concentration the reaction took place satisfactorily in a mixture 1:1 DMSO/H_2O (73% yield of **59a**, entry 3) and DMSO/PBS (70% yield of **59a**, entry 6). Unfortunately, in the absence of a cosolvent yields were poor in both, water and PBS solvents (below 20%), mainly due to solubility issues of quinone **57** (entries 7 and 8).

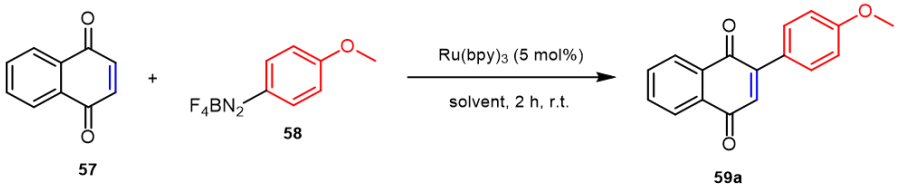

Entry	Cat. loading (mol%)	Milieu	Yield (%)[3]
1	5	THF/H_2O 1:1	32
2	5	THF/PBS 1:1	35
3	5	DMSO/H_2O 1:1	73
4[1]	5	DMSO/H_2O 1:1	34
5	5	DMSO/H_2O 8:2	38
6	5	DMSO/PBS 1:1	70
7	5	H_2O	20
8	5	PBS	16
9[2]	10	H_2O	19

*Table 12. Preliminary experiments for the naphthoquinone arylation. Conditions: 10 mM of **58**, 5 equiv. of **57**, $Ru(bpy)_3$ at the chosen concentration under 32 W blue-light irradiation, in different solvents at room temperature for 2 h. [1]1 equiv. of **57** was employed. [2]Reaction at 5 mM of **58**. [3]Yields were determined by NMR using nitromethane as internal standard.*

USC UNIVERSIDADE DE SANTIAGO DE COMPOSTELA

In view of these promising results and considering the excellent fluorescent properties of AIE derived anthraquinones developed in Chapter III, we explored the possibility of synthetizing a fluorescent product based on this skeleton. We anticipated that the addition of an aryl radical into triphenylethylene would be feasible, leading to the formation of a well-known AIEgen (figure 122).

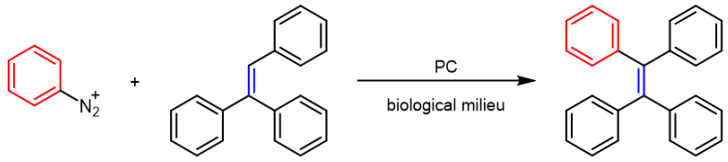

Figure 122. Our proposal for the formation of tetraphenylethylene.

The addition of an aryl radical into diphenylethylene was already reported by König using ethyl-2-(4-bromophenyl)acetate as source of aryl radical in DMSO, using his "conPET" strategy. This strategy allows the catalyst to accumulate two photons of different wavelength through a first excitation step, then reduction and a second excitation, emulating the photosynthesis pathway.[276] They obtained a mixture of saturated and unsaturated product (2.8:1) in good yields (64%, figure 123).[277]

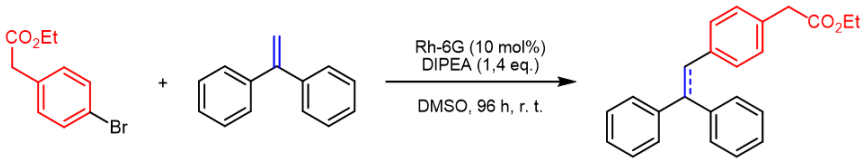

Figure 123. König's reported version of aryl addition into diphenylethylene.[277]

Initial experiments were performed at 200 mM of **58** with 5 equiv. of triphenylethylene, using 1 mol% of ruthenium complex in DMSO. The tetraphenyl product **60** was isolated in 54% yield after 2 h. When a mixture of DMSO/PBS 9:1 was used, a 27% of final compound was obtained. However, only traces were detected in a 1:1 mixture of DMSO/PBS. Despite these are preliminary results, they already underscore the potential of this approach, confirming a significative reactivity in aqueous media or buffered solutions, what stresses the viability of performing bioorthogonal photochemistry.

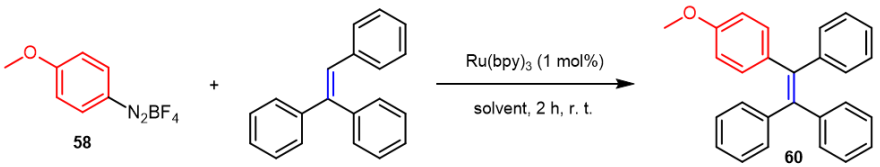

Figure 124. Diazonium salt addition into triphenylethylene.

USC UNIVERSIDADE DE SANTIAGO DE COMPOSTELA

[276] I. Ghosh, T. Ghosh, J. I. Bardagi, B. König, *Science* **2014**, *346*, 725.
[277] I. Ghosh, B. König, *Angew. Chem. Int. Ed.* **2016**, *55*, 7676.

7.2. Photocatalytic formal-cycloadditions in aqueous and biological settings

Considering our results in the previous sections on metal-catalyzed intermolecular cycloadditions we wondered whether it would be possible using photoredox catalysis, to make aqueous and biocompatible formal cycloadditions. Towards this objective, we took as reference a formal [4+2] benzannulation of biaryldiazonium salts with alkynes, reported by the group of Zhou in organic solvents.[278] This reaction likely proceeds by reduction of diazonium salt by the excited photocatalyst, and posterior addition into the alkyne. They performed the reaction at 330 mM of 2-biphenyldiazonium salt **61**, adding 5 equiv. of methyl propiolate (or 3 equiv. if diazonium salt is added fractionated), under visible-light irradiation in acetonitrile for 12 h, provides the final product **62** in 74% yield (figure 125). The process excels displaying a high quantum yield of 0.35, which lead us to presuppose some selectivity in complex environments.[279]

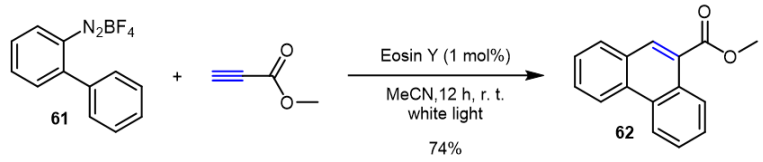

Figure 125. Standard conditions for [4+2] photo-cycloaddition developed by Zhou and co-workers in 2012.[278]

We considered that if this reaction works in water, it could be adapted to bioorthogonal environments as the radical chain that leads to the cycloadduct should occur in preference to other secondary processes. The mechanism can be seen as an expansion of the one proposed by König for the intermolecular couplings. In this case, the key radical intermediate **II** generated by the radical addition into the alkyne, would undergo a ring closing evolving to the new radical intermediate **III**. The stabilized radical would be oxidized, regenerating the PC and leading to the intermediate **IV**. A final re-aromatization step would provide the corresponding phenanthrene product.

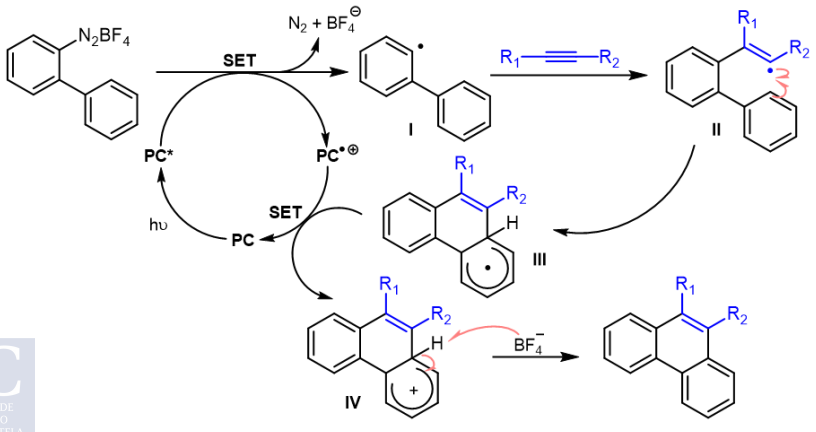

Figure 126. Proposed mechanism by the group of Zhou.[278]

[278] T. Xiao, X. Dong, Y. Tang, L. Zhou, *Adv. Synth. Catal.* **2012**, *354*, 3195.
[279] M. Majek, F. Filace, A. Jacobi von Wangelin, *Beilstein J. Org. Chem.* **2014**, *10*, 981.

In our hands, the replication of Zhou's conditions for the reaction of 2-biphenyldiazonium salt (**61**) with methyl propiolate in organic solvents to yield methylcarboxylatephenanthrene (**62**), provided almost the same results when 5 equiv. of methyl propiolate were employed (70%, table 13, entry 1). The solvent must be deoxygenated to avoid the quenching of the photocatalyst (entry 2). However, this behavior might have no consequences inside cells, due to their reductant and controlled environment.

Since the methyl propiolate is a liquid, the previous established protocol had to be adapted as follows. In the Schlenk flask, the solids were weighted, purged with Ar, and dissolved with the chosen deoxygenated solvent to a final concentration of 330 mM of **61** and 1 mol% of Eosin Y. At this point the mixture is gently stirred and 5 equivalents of the oil-liquid alkyne methyl propiolate is added and set under irradiation and fan refrigeration for the selected reaction time, and finally quantified by NMR using nitromethane as internal standard. The reaction was successfully performed in PBS, using 20% of DMSO as cosolvent to obtain a homogeneous mixture, obtaining the product in 66% of yield after 12 h (entry 4), although after only 30 min a big amount of precipitate corresponding to the product was observed.

Gratifyingly, the reaction run in pure PBS led to a 62% yield, thus confirming that a cosolvent is not needed. When non deoxygenated PBS is employed only a 10% of decrease was observed in contrast to MeCN (entry 2, 6), in consonance with a lower oxygen concentration in H_2O than MeCN.[280] Using a mixture of PBS/DMSO 8:2 as a solvent, a precipitate was quickly formed in 30 min. Furthermore, in the case of pure PBS, a biphasic mixture was observed in a few seconds, suggesting that the activation of the diazonium salt is drastically faster in water than MeCN, under these conditions. On this wise, we could decrease the reaction time from 12 to 2 h, reaching the same results in a robust way (entries 7 and 8). In further experiments we will study the kinetics of the reaction with more detail.

USC
UNIVERSIDADE DE SANTIAGO DE COMPOSTELA

[280] M. Quaranta, M. Murkovic, I. Klimant, *Analyst*, **2013**, *138*, 6243

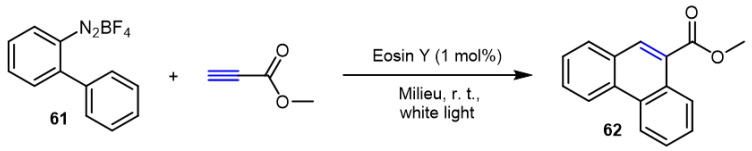

Entry	Milieu	Variation	Time (h)	Yield (%)[1]
1	MeCN		12	70[2]
2	MeCN	Non-deoxygenated	12	15
3	MeCN		24	62
4	PBS	20% DMSO	12	66
5	PBS		12	62
6	PBS	Non-deoxygenated	12	51
7	PBS	20% DMSO	2	66
8	PBS		2	62
9	Neat		12	34
10	Neat		2	37

*Table 13. Solvent and reaction time screening. Conditions:330 mM of diazonium salt **61**, 5 equiv. of methyl propiolate, $EosinYNa_2$ 1 mol%, under 32 W white light irradiation, in MeCN, PBS or in neat at room temperature for 2, 12 or 24 h. [1]Yields were determined by NMR using nitromethane as internal standard. [2]Isolated yield.*

In view of the results reported, we investigated other biocompatible photocatalysts. Specially, $Ru(bpy)_3$ was selected, due the considerable higher excited state lifetime, in comparison with Eosin Y.[233,234] Besides, as mentioned along the introduction, this type of bipyridine or phenantroline ruthenium catalysts have been employed in uncaging experiments reporting good results even in cells.

Initial results in MeCN as solvent showed similar catalytic activity of $Ru(bpy)_3$, with only a slight decrease in the yield (table 14, entry 1). However, carrying out the reaction in water or PBS resulted in excellent yields up to 84%. Indeed, this catalyst showed better performance than Eosin Y under these conditions after 2 h (entries 4 and 5).

Additionally, Riboflavin, an intracellular biomolecule with photoredox properties, was tested to check its ability to catalyze the reaction. This catalyst has been already studied in both organic photocatalysis and bioorthogonal applications.[281,282] But in this case, only a small amount of product was detected under blue irradiation (entry 6).

USC UNIVERSIDADE DE SANTIAGO DE COMPOSTELA

[281] S. A. Castro, E. Ruggiero, A. Ruiz-de-Angulo, E. Rezabal, J. C. Mareque-Rivas, X. Lopez, F. López-Gallego, L. Salassa, *Chem. Sci.* **2017**, *8*, 4619.
[282] J. Gurruchaga-Pereda, V. Martínez-Martínez, E. Rezabal, X. Lopez, C. Garino, F. Mancin, A. L. Cortajarena, L. Salassa, *ACS Catal.* **2020**, *10*, 187.

Some iridium complexes have been also employed for protein modification.[272,273] In this regard, we tested the commercially available tris[2-phenylpyridinate-C^2,N]iridium (III) ($Ir(ppy)_3$, but only 19% of yield was obtained (entry 7). Rhodamine and TMRE has been also reported by Chen and co-workers for alcohol unmasking inside mammalian cells.[265] Nevertheless, TMRE wasn't able to promote the cycloaddition and Rhodamine B led to a 20% of **61** (entries 8-9).

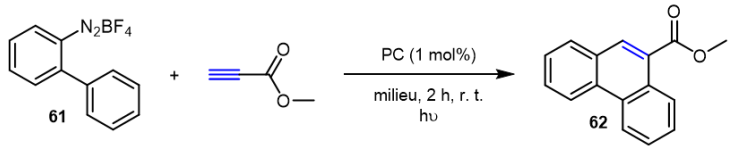

Entry	Catalyst	Milieu	Light	Variations	Yield (%)[1]
1	$Ru(bpy)_3$	MeCN	Blue		66
2	$Ru(bpy)_3$	MeCN	Blue	PC 0.5 mol%	56
3	$Ru(bpy)_3$	PBS	Blue	24 h	75
4	$Ru(bpy)_3$	PBS	Blue		84
5	$Ru(bpy)_3$	H_2O	Blue		84
6	Riboflavin	MeCN	Blue		11
7	$Ir(ppy)_3$	MeCN	Blue		19
8	Rhodamine B	PBS	White		20
9	TMRE	PBS	White		traces

*Table 14. Catalyst screening. Conditions: 330 mM of diazonium salt **61**, 5 equiv. of alkyne, 1 mol% of the chosen PC, under 32 W light irradiation, in MeCN or PBS at room temperature for 2h. [1]Yields were determined by NMR using nitromethane as internal standard.*

With these results in hand, we made a quick analysis of the scope using some selected alkynes and $Ru(bpy)_3$ as PC in MeCN or PBS as solvent. The use of the internal alkyne diphenylacetylene led to a modest isolated yield of 27% of **63** in MeCN, but no reaction in PBS was observed, consequence of the poor solubility. Similar, reaction with TMS protected acetylene gave 50% of yield in MeCN of the deprotected phenanthrene **64**, but failed in PBS. In contrast, with the use of the water-soluble propiolic acid the reaction achieves the formation of product **65** in an excellent 82% yield in PBS, in absence of an organic cosolvent. The use of other alkynes with strong EWGs such as 1-ethynyl-4-fluorobenzene and ethynyltrifluorotoluene (**28**) provided compounds **66** and **67** in 60% and 82% yield, respectively, which is in concordance with a better radical stabilization after the aryl radical addition.

USC UNIVERSIDADE DE SANTIAGO DE COMPOSTELA

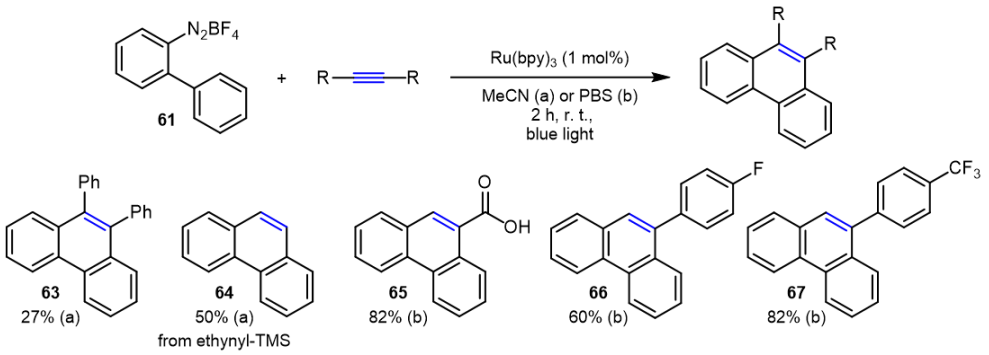

*Figure 127. Alkyne scope. Conditions: 330 mM of diazonium salt **61**, 5 equiv. of alkyne, 1 mol% Ru(bpy)$_3$, under 32 W blue light irradiation, in MeCN (a) or PBS (b) at room temperature for 2h. Isolated yields.*

Along the study of the reaction, several control experiments were concurrently performed. As expected, with no light irradiation no reaction took place, even when no special precautions in order to avoid environmental light were applied (table 15, entries 1-4). When reactions were performed under light irradiation without a catalyst, moderate yields could be obtained. Depending on the reaction conditions, the yield could drastically vary. For instance, the use of ACN as solvent (entries 5-7), or green as light source (entry 9), only provided traces of product. However, a 50% yield was obtained in reaction performed in H_2O (entry 13) or without any control of the temperature (entry 11). Thankfully, under standard conditions in PBS and blue light this problem was more subtle, obtaining around 24% of yield at room temperature (entry 17) or 36% when the reaction was performed at a physiological temperature of 37 ºC (entry 21).

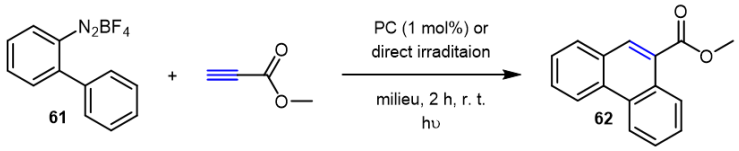

Entry	Catalyst	Milieu	Light	Variations	Yield (%)[2]
1		PBS		Dark[1]	-
2		PBS			-
3	Ru(bpy)$_3$	PBS		Dark[1]	-
4	Ru(bpy)$_3$	PBS			-
5		MeCN	Blue		trace
6		MeCN	Green		trace
7		MeCN	White		trace
8		PBS	Blue		24
9		PBS	Green		trace
10		PBS	White		36
11		PBS	Blue	No fan	52
12		PBS	Blue	37 ºC	36
13		H_2O	Blue		48

*Table 15. Solvent and reaction time screening. Standard conditions: 330 mM of diazonium salt **61**, 5 equiv. of alkyne, 1 mol% Ru(bpy)$_3$ if used, under 32 W light irradiation in ACN, PBS or water at room temperature for 2h. [1]Covered with black polyethylene plastic. [2]Yields were determined by NMR using nitromethane as internal standard.*

USC UNIVERSIDADE DE SANTIAGO DE COMPOSTELA

Nevertheless, these problems from uncatalyzed reactivity could be addressed by selecting the proper light source. Besides, we wondered if this effect would be still important in more diluted conditions. Hence, we started decreasing the concentration by half using Eosin Y as PC, with no important changes in the yield (table 16, entry 1). An additional dilution by half reported also similar results (entry 2). We decided to go some steps further, decreasing up to 20 mM and 10 mM (entries 3 and 4). At these concentrations, a sudden decrease of the yield was observed even at larger period of time. Besides at 1 mM the yield only reaches a 10% (entry 5). Increasing the catalyst loading to 5, 10 and 15 mol% and performing the transformations at longer period of time (entries 7-9) led to an increment in the yields. Pleasingly, the reaction performed at 10 mM without the presence of PC provided only product traces under white, blue light irradiation, or even heating at 37 ºC together with the light irradiation (entries 10-12).

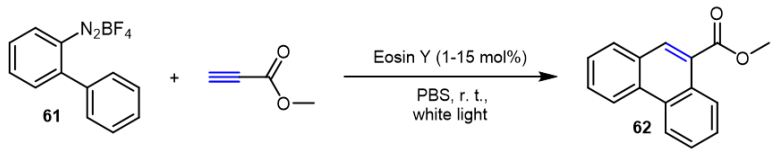

Entry	[**61**] (mM)	Catalyst	Cat. loading (mol%)	Time (h)	Yield (%)[4]
1	165	Eosin Y	1	2	60
2	83	Eosin Y	1	2	58
3	20	Eosin Y	1	24	27
4	10	Eosin Y	1	2	26
5	1	Eosin Y	1	2	10
6	10	Eosin Y	5	2	33
7	10	Eosin Y	5	24	48
8	10	Eosin Y	10	24	48
9	10	Eosin Y	15	24	54
10[1]	10			2	trace
11[2]	10			2	trace
12[3]	10			2	trace

*Table 16. Eosin Y catalyst optimization. Conditions: the selected concentration of diazonium salt **61**, 5 equiv. of alkyne, the proper amount of Eosin YNa_2, under 32 W white light irradiation, in PBS at room temperature for 2 or 24 h. [1]Control experiment without catalyst and irradiating with white light. [2]Control experiment irradiation with blue light. [3]Control experiment with blue light and 37 ºC. [4]Yields were determined by NMR using nitromethane as internal standard.*

USC UNIVERSIDADE DE SANTIAGO DE COMPOSTELA

A similar trend was found by using $Ru(bpy)_3$ as PC but with a higher performance, in terms of yields and kinetics. In this way, it was possible perform the reaction at 10 mM with high reproducibility, obtaining excellent yields after 2 h of reaction (table 17, entries 1-3). Even at shorter reaction times (5 min) a 25% of product was already detected (entry 5). Additionally, good yields were obtained at 5 mM after 2 h (entries 9 and 10), or moderated yields at 1 mM after 24 h (entry 12). Nevertheless, in contrast with Eosin Y, an excess of catalyst loading can inhibit the reaction, mainly attributable to the higher efficiency of the $Ru(bpy)_3$ and an excess of radical generation (entry 8).

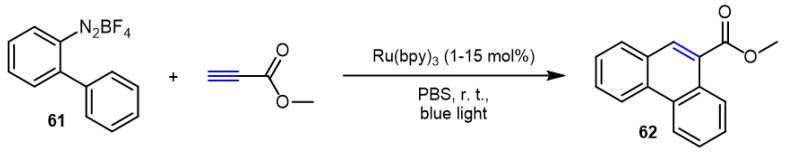

Entry	[**61**] (mM)	Cat. loading (mol%)	Time (h)	Yield (%)[2]
1	10	1	24	51
2	10	5	24	70
3	10	5	2	72
4	10	5	1	53
5	10	5	0.083	28
6	10	5	0.016	25
7	10	10	24	63
8	10	15	24	-
9	5	5	24	68
10	5	5	2	66
11	1	5[1]	2	trace
12	1	10[1]	24	54
13	1	15[1]	24	58
14	1	20[1]	24	48

*Table 17. Ruthenium catalyst optimization. Conditions: the selected concentration of diazonium salt **61,** 5 equiv. of alkyne, the proper amount of $Ru(bpy)_3$ under 32 W blue light irradiation, in PBS at room temperature for the selected time. [1]Catalyst added from a fresh stock of DMSO. [2]Yields were determined by NMR using nitromethane as internal standard.*

USC UNIVERSIDADE DE SANTIAGO DE COMPOSTELA

7.2.1. Influence of the fractionated addition of diazonium salt 61

During the optimization process at high concentration (330 mM), we decided to avoid the fractionated addition of the diazonium salt by adding more equivalents of the alkyne, in order to ease the process. However, since the reactions carried out at more diluted concentrations led to moderate yields, we considered the possibility of performing the slow addition of the diazonium salt.

We started to explore the addition of diazonium salt in fractions at 10 mM. In a practical manner, this means the addition of the diazonium salt in five portions, for an addition period of 5, 25 or 75 minutes. However, no increase of the yields was found after 2 h of reaction (table 18, entries 1-3), but a slight decrease could be observed instead. Curiously, stirring the reaction mixture for longer reaction times, afforded the quantitative formation of the product, likely due to a more controlled generation of radicals. Pleasingly, this behavior still remains at 1 mM, with the formation of the product in 90 % yield (entry 7-9), improving again drastically the yields previously achieved.

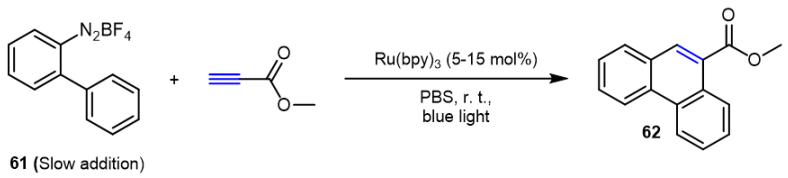

Entry	[**61**] (mM)	Fraction addition (min)[1]	Catalyst loading (mol%)	Time (h)	Yield (%)[2]
1	10	1	5	2	62
2	10	5	5	2	67
3	10	15	5	2	66
4	10	1	5	24	99
5	10	5	5	24	99
6	10	15	5	24	99
7	1	1	15	24	86
8	1	5	15	24	89
9	1	15	15	24	92

*Table 18. Experiments with addition of diazonium salt **61** in portions. Conditions: 10 mM or 1 mM of diazonium salt **61**, 5 equiv. of alkyne, 5-15 mol% of Ru(bpy)$_3$ as PC under blue light in PBS at room temperature. [1]Five additions of 0.004 mmol (0.2 eq each) at the specified time. [2]Yields were determined by NMR using nitromethane as internal standard.*

USC UNIVERSIDADE DE SANTIAGO DE COMPOSTELA

7.2.2. Exploring the biorthogonality of the reaction

At this point, we decided to explore the behavior of the reaction in the presence of biomolecules or in more complex biological media. Interestingly, at high concentration (330 mM), Eosin Y provided similar yields in DMEM or HeLa cells lysates to those obtained in PBS (table 19, entry 1-4). Although slightly lower yields were obtained with DMEM, this could be attached to the presence of the fluorophore phenol red competing with the Eosin Y in the reaction media, rather than the presence of biomolecules. Likewise, ruthenium catalyst exceled in this media at high concentration (entries 5 and 6). Yet, $Ru(bpy)_3$ retains this reactivity in lysates even at 10 mM (entries 7 and 8).

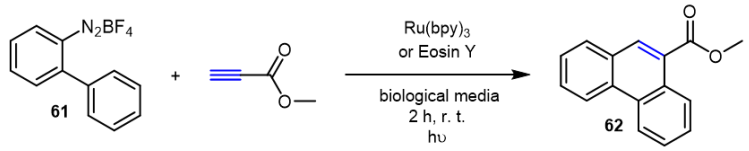

Entry	[**61**] (mM)	PC	Catalyst loading (mol%)	Milieu	Yield (%)[3]
1	330	Eosin Y	1	DMEM[1]	54
2	330	Eosin Y	1	DMEM	58
3	330	Eosin Y	1	Lysate[1,2]	67
4	330	Eosin Y	1	Lysate[2]	63
5	330	$Ru(bpy)_3$	1	DMEM	58
6	330	$Ru(bpy)_3$	1	Lysate[2]	59
7	10	$Ru(bpy)_3$	5	DMEM	42
8	10	$Ru(bpy)_3$	5	Lysate[2]	60

*Table 19. Experiments in biological medias. Conditions: 10 or 330 mM of diazonium salt **61**, 5 equiv. of alkyne, 1-5 mol% $Ru(bpy)_3$, under 32 W blue light or Eosin YNa2 32 W white light irradiation, in biological medias at room temperature for 2 h. [1]20% of DMSO as co-solvent. [2]2 mg protein/mL. [3]Yields were determined by NMR using nitromethane as internal standard.*

The transformation was also tested in the presence of BSA protein or some selected aminoacids that could react with the diazonium salt.[283] Gratifyingly, the reactions proceeded smoothly, with only a slight decay on the yield (table 20, entries 1-6). In contrast, in the presence of 1 equivalent of NADH, the reaction was inhibited and 45% of biphenyl was obtained as side reaction consequence of a hydrogen atom transfer (HAT) into the aryl radical. Nevertheless, use of 0.1 equivalents instead, the reaction was able to take place (entry 8), and yet the concentration of NADH employed is much higher than the expected in cells (168-97 μM).[284] Even more stimulating, the reaction was able to take place in a suspension of mammalian cells in PBS with similar yields than those obtained in the presence of biomolecules (entry 9).

[283] S. Sengupta, S. Chandrasekaran, *Org. Biomol. Chem.* **2019**, *17*, 8308.
[284] N. Ma, M. A. Digman, L. Malacrida, E. Gratton, *Biomed. Opt. Express* **2016**, *7*, 2441.

Some selected endogenous reductants were also tested to see if they can promote the reaction in absence of light. Only NaAsc was able to achieve modest yields with the use of 10 mol% (entries 10-13), similarly to NADH, the concentration used is several times higher than the reported in mammalian cells (50-80 μM).[285] Overall, the reaction showed promising bioorthogonal behavior and encouraged us for future intracellular experiments.

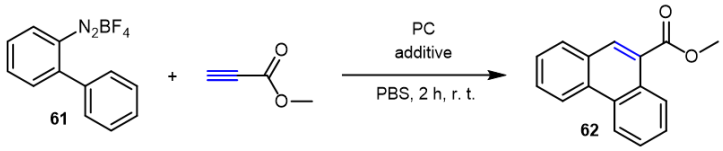

Entry	PC	Additive (equiv.)	Yield (%)[4]
1	$Ru(bpy)_3$	BSA[2]	52
2	$Ru(bpy)_3$	Cys (1)	47
3	$Ru(bpy)_3$	Trp (1)	42
4	$Ru(bpy)_3$	Tyr (1)	48
5	$Ru(bpy)_3$	GSH (1)	34
6	$Ru(bpy)_3$	GSH (0.1)	50
7	$Ru(bpy)_3$	NADH (1)	traces
8	$Ru(bpy)_3$	NADH (0.1)	50
9	$Ru(bpy)_3$	Cells[3]	53
10[1]		NaAsc (0.1)	30
11[1]		NADH (0.1)	trace
12[1]		L-DOPA (0.1)	10
13[1]		B-carotene (0.1)	traces

*Table 20. Ruthenium catalyst optimization. Conditions: 10 mM of diazonium salt **61**, 5 equiv. of alkyne, 5 mol% of $Ru(bpy)_3$, under 32 W blue light irradiation (if PC is used) at room temperature for 2 h. [1]With no light irradiation. [2]20 % of DMSO as co-solvent. [2]Performed with 2 mg BSA/mL in the media. [3]Perfomed in the presence of $1 \cdot 10^6$ HeLa cells/mL. [4]Yields were determined by NMR using nitromethane as internal standard.*

USC UNIVERSIDADE DE SANTIAGO DE COMPOSTELA

[285] M. Przbylo, M. Langner, *Cell. Mol. Biol. Lett*, **2020**, *25*, 32.

7.3. Photocatalytic formal-cycloaddition in cellular settings

Once demonstrated that the reaction tolerates biological components, we decided to evaluate the possibility of translating this transformation to living mammalian cells. In order to detect the formation of the product, we selected HPLC-MS, which provides not only detection, but there is potential to quantify the product formed too.

For this approach we went on with the optimized system. Thus, HeLa cells were treated in a similar manner to the previous chapters. This involves the incubation of cells in a sequential manner, first with the catalyst (50 μM) for 30 min and then with the substrates (100 μM) for another additional 30 min. Each step comprises two final washing steps in order to avoid extracellular reactions. Then cells were irradiated at room temperature with the appropriate source of light (controlling different parameters such as distance and power) for different reaction times. In order to measure the product being formed intracellularly, the intracellular content was extracted with MeOH and analyzed by ESI-MS spectrometry. Satisfactorily, analysis (extracted ion chromatogram) of methanolic extracts of cells treated with $Ru(bpy)_3$ and then with **61** and methyl propiolate, revealed the presence of the phenanthrene structure **62** after 30 min of irradiation with blue light. Thus, these results corroborate not only the intracellular formation of the cyclization product but also that the process needs light and a ruthenium complex to successfully take place. Indeed, in the experiments irradiated with no PC in the reaction media no product was detected. Same results were obtained for reactions performed in the presence of the PC without irradiation. Finally, in cells incubated with only the substrates, in the absence of light and ruthenium photocatalyst, there was no formation of the product. Important to mention, that this last section is still on going.

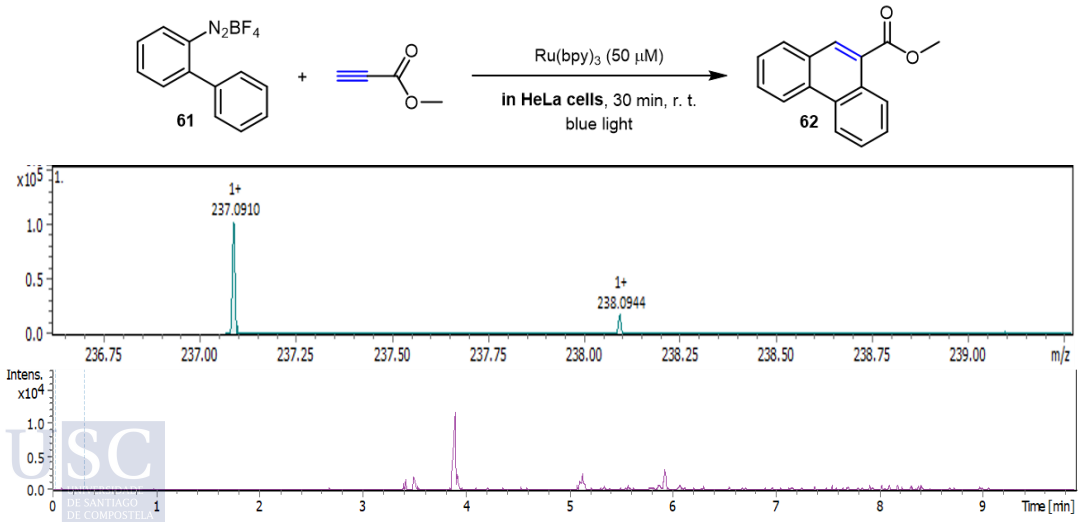

*Figure 128. Extracted ion chromatogram of the formation of **62** in cellular experiments. Protocol: cells were incubated with 50 μM $Ru(bpy)_3$ for 30 min, after the washsing steps, cells were incubated with 100 μM of **61** and methyl propiolate, for additional 30 min. Then, samples were irradiated with blue light at room temperature for 30 min.*

8. Conclusions

As conclusion, our results exemplified the first example of a photocatalyzed Meerwein transformation in live mammalian cells. We show that a rationalized design of the reaction components allows to generate aryl radicals, that can be efficiently trapped in a chemoselective manner to generate aromatic cycloadducts in a smooth manner, in presence of biomolecules, biological media, or cells without disturb the reaction. LC-MS experiments verify the intracellular and photochemical generation of the phenanthrene **62**, while no product was detected in absence of light or PC. We are aware that additional cellular experiments must be done to fully characterize the transformation, yet, we are excited with the results obtained, and the group is investigating the potential of photocatalysis in biological settings.

USC
UNIVERSIDADE DE SANTIAGO DE COMPOSTELA

USC
UNIVERSIDADE
DE SANTIAGO
DE COMPOSTELA

OVERALL CONCLUSIONS

USC
UNIVERSIDADE
DE SANTIAGO
DE COMPOSTELA

USC
UNIVERSIDADE
DE SANTIAGO
DE COMPOSTELA

This PhD work has aimed at the development of formal cycloaddition reactions promoted by transition metals or by photochemical means that can be carried out in aqueous and biological media, and even in the interior of live mammalian cells.

General conclusions:

1) We have demonstrated that well-defined water-soluble copper (I) complexes featuring designed ligands, can be efficiently internalized into mammalian cells and promote intracellular CuAAC of designed abiotic substrates. Remarkably, we have proven that predefined Cu(I) complexes are also able to promote the intracellular transformation, even at lower catalyst loadings, while avoiding the use of exogenous reductants such as ascorbate, and hence, improving the biocompatibility of the methodology.

2) We have described the first multicomponent [2+2+2] formal cycloaddition in live mammalian cells. The combination of ruthenium as transition metal catalyst and designed diynes or triynes with adequate coordination abilities, ensure the formation of key ruthenacycles that can be trapped by external alkynes even inside mammalian cells. Importantly, we have used the technology to build polyketide-derived secondary metabolites, from simple precursors, inside cells that lack the corresponding biological pathway to make them. This strategy goes beyond the most common uncaging or ligations reactions, providing for one of the more complex abiotic reactions so far carried out in live settings.

3) We have also used the methodology to build products showing aggregation-induced emission (AIE) properties, which overcome the concentration quenching of fluorescence characteristic of classical fluorophores. By definition, this type of compounds is highly insoluble, and hence experience a poor cellular uptake. We have proved that Ru promoted [2+2+2] cycloaddition can intracellularly generate the AIE product, that otherwise cannot be delivered into the cell. In addition, we have demonstrated that the use of tailored ruthenium reagents provides a spatial control over the product generation.

4) We have presented the first example of an intracellular photoredox formal cycloaddition, specifically a visible light-driven Meerwein reaction. We show that a rationalized design of the reaction components allows to generate aryl radicals, that can be efficiently trapped in a chemoselective manner to generate aromatic cycloadducts in a smooth manner. Further research to broaden the scope of the transformation to include novel functional groups and fluorescent products or the use of irradiation of higher wavelength, is highly desirable for future applications in native cellular environments.

USC UNIVERSIDADE DE SANTIAGO DE COMPOSTELA

USC
UNIVERSIDADE
DE SANTIAGO
DE COMPOSTELA

RESUMO DA TESE DOCTORAL

USC
UNIVERSIDADE
DE SANTIAGO
DE COMPOSTELA

USC
UNIVERSIDADE
DE SANTIAGO
DE COMPOSTELA

A química bioortogonal naceu recentemente como unha ferramenta para a investigación celular, revolucionando campos próximos como a microscopia, o desenvolvemento de fármacos ou a biotecnoloxía debido á súa capacidade para manipular compostos esóxenos dentro dos sistemas biolóxicos sen perturbar o metabolismo do hóspede. A pesar do seu éxito, o descubrimento de novas reaccións bioortogonais segue sendo un reto hoxe en día, debido a natureza das mesmas: os compoñentes deben ser inocuos e solubles en medios biolóxicos, facilmente interiorizables, reactivos en condicións fisiolóxicas e capaces de interactuar rápida e especificamente nun ambiente tan complexo como os medios biolóxicos.

O **capítulo I** serve de introdución ao campo da química bioortogonal e a súa evolución ao longo dos anos, poñendo en contexto os logros acadados paralelamente ao desenvolvemento desta tese de doutoramento. En primeiro lugar, preséntase un breve resumo das contribucións da química biolóxica, tales como a síntese de sondas, ligazón nativa de péptidos ou a evolución dirixida de proteínas, para a continuación facer énfase no uso de reaccións bioortogonais como ferramenta de bioconxugación. Finalmente, introdúcense as transformacións máis influentes neste campo, diferenciando claramente as reaccións realizadas na superficie das células ou as que se desenvolven no interior das células, o que supón un gran reto científico. A data de comezo da química bioortogonal establécese entre os anos 1980 e 1980, co traballo do grupo de Rideout baseado na condensación de hidracinas, previa acumulación dos substratos no interior da célula. Non obstante, non se falou oficialmente da bioortogonalidade ata 2003, ano no que o grupo de Bertozzi, que co paso do tempo se convertería nun referente no campo da química bioortogonal na superficie das células, acuñou o termo por primeira vez. Curiosamente, a condensación de hidracinas viu o seu verdadeiro potencial no campo das glicoproteínas presentes na membrana celular, polo que os azucres modificados con cetonas poderían bioconxugarse facilmente en ausencia de aldehidos ou outras cetonas no exterior da célula.

Actualmente, unha das reaccións que mellor cumpre os requisitos da química bioortogonal é a redución de Staudinger, unha transformación que foi redescuberta por Bertozzi no ano 2000, quen a utilizou para levar a cabo procesos de bioconxugación. Ademais, esta reacción supuxo un punto de partida para o uso de sondas intelixentes. Estas sondas son compostos cuxa fluorescencia está enmascarada pola presenza dun grupo funcional cun par de electróns libres que poden participar nunha transferencia de electróns intramoleculares promovida por luz (PET). Esta transformación utilizouse con gran éxito na superficies celulares, aínda que a súa aplicación no interior das células permaneceu esquiva.

USC UNIVERSIDADE DE COMPOSTELA

No seguinte apartado preséntase o concepto de química "click" e a súa relación coa química bioortogonal. Coméntanse as súas características tales como: la estabilidade dos substratos, modularidade e velocidade da reacción, condicións de reacción suaves, e incluso en condicións fisiolóxicas. Neste campo, as cicloadicións 1,3 – dipolar entre azidas – alquino para dar triazoles destacan sobre todas as demais, especialmente a versión catalizada polo cobre (I).

Esta versión desenvolta por Sharpless, Fokin e Medal en 2002, e trasladada posteriormente ao campo da química biolóxica en 2003 polo grupo de Tirrell, converteuse na reacción bioortogonal por excelencia, coa mellor cinética, substratos estables, esóxenos, pero sobre todo simples e pequenos, facilmente sintetizables e incorporables á maquinaria biolóxica. Por todo isto, no capítulo II ponse o foco na versión promovida polos catalizadores de cobre, tamén coñecida como CuAAC (cicloadición catalizada por cobre de azidas e alquinos).

A sección de bioconxugación remata presentando os exemplos máis recentes da química bioortogonal: as reaccións de cicloadición Diels - Alder con demanda inversa de electróns (IEDDAC) e os procesos fotoclick. Ambas transformacións presentan unha cinética comparable á cicloadición entre azida-alquino catalizada por cobre e, polo tanto, teñen o potencial necesario para levar a cabo as reaccións a concentracións moi baixas. Desafortunadamente, nestes procesos tamén se producen reaccións laterais, o que limita as súas posibles aplicacións.

A continuación, entra en escena a química organometálica, destacando o seu achegamento á química en auga xunto coa súa recente contribución á química biolóxica, cos traballo dos grupos de Schultz e Davis, ou a conxugación de proteínas mediante acoplamentos tipo Suzuki. Por último, discútese o gran impacto da química organometálica na expansión da química bioortogonal. Neste apartado faise énfase nas técnicas de liberación de moléculas activas, destacando o uso de catalizadores de metais de transición como rutenio, paladio ou mesmo ouro, para a desprotección de grupos alilo, alilcarbamato ou propargilo. A contribución do grupo de Meggers en 2006, que conseguiu levar a cabo estas reaccións en células vivas de mamíferos, foi pioneira e promotora deste tipo de procesos. Non obstante, o foco principal desta sección sobre a química organometálica reside no inexplorado campo da química bioortogonal sintética que, a día de hoxe, ten un número moi reducido de aplicacións en ambientes celulares.

A conclusión inmediata que se extrae deste capítulo é que a química bioortogonal é unha rama moi nova da química biolóxica cun gran potencial aínda por explorar. Por exemplo, os procesos bioortogonais baseados no uso de metais de transición apenas foron estudados, probablemente debido á crenza de que son incompatibles coa auga ou tóxicos para o ambiente celular ou, en definitiva, para a vida. É certo que estas reaccións presentan eficiencias menores que as das transformacións utilizadas para a bioconxugación, pero a existencia da CuAAC, xunto cun amplío abanico de reactividade da química organometálica, pon de manifesto o enorme potencial do uso

de metais de transición para realizar química bioortogonal sintética no interior de sistemas biolóxicos.

No **capítulo II** recollese o primeiro exemplo dunha cicloadición 1,3 - dipolar entre azida-alquino catalizada por cobre desenvolta no interior de células de mamíferos, utilizando moléculas discretas e abióticas. Demostrouse que a modificación de ligandos tristriazol consegue mellorar a actividade e a internalización dos complexos de cobre(I). Estas especies prepáranse mediante a redución *in situ* dos complexos de Cu(II). Así mesmo, o uso de complexos de cobre (I) predefinidos e illados con ligandos de trispirazol ou tristriazol, evita o uso de redutores externos e, polo tanto, aseguramos que o proceso reduza a súa citotoxicidade.

En primeiro lugar, introdúcense as diferentes estratexias que permitiron levar a cabo a realización da cicloadición entre azida-alquino catalizada por cobre no interior de células de mamíferos como HeLa ou A549, entre outras lineas celulares. Non obstante, estas achegas anteriores á esta tesede doutoramento, presentaban certos inconvenientes, como o uso de cantidades estequiométricas de cobre, distintos sistemas de nanopartículas complexos ou o uso de substratos metabólicamente incorporados que dan lugar a unha bioconxugación inespecífica.

A continuación, preséntase a síntese das sondas intelixentes empregadas neste traballo, destacando a antracenilazida (**1**) que xera o produto antraceniltriazol (**2**) despois da reacción de cicloadición con o alcohol proparxílico, así como os ligandos de tristriazol. Os ligandos estudados elixíronse polo seu amplo uso na bibliografía, e pola súa demostrada contribución ao aumento da actividade catalítica dos complexos de cobre(I) preparados *in situ* mediante a redución das correspondentes especies de Cu(II). Ademais, un destes ligandos foi derivatizado, incorporando un grupo trifenilfosfonio para aumentar a solubilidade e internalización na célula. A modificación da estructura dos ligandos, levou a síntese dun conxunto de especies máis eficientes, non só para estudos in vitro (auga e medios biolóxicos) senón tamén en células HeLa, onde se observa a aparición dunha sinal de fluorescencia azul que procede, inequívocamnete, do triazol (**2**).

USC
UNIVERSIDADE DE SANTIAGO DE COMPOSTELA

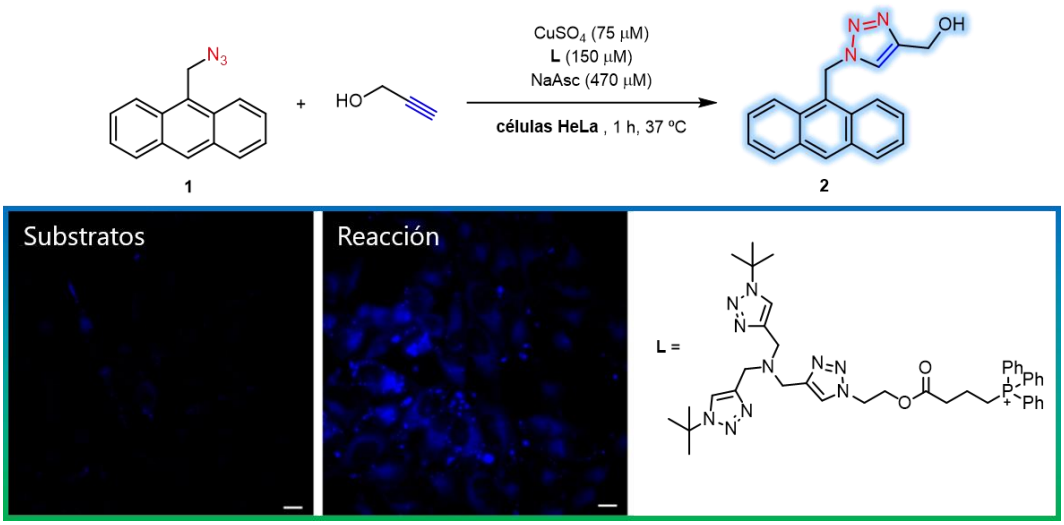

Figura 1. Micrografías de fluorescencia de células HeLa despois da incubación co substratos e o conxunto da reacción. NaAsc = ascorbato de sodio.

Na seguinte sección, sintetízanse e estúdanse diferentes complexos predefinidos de cobre (I), previamente reportados por promover a cicloadición entre alquinos e azidas, destacando entre eles os complexos con ligandos de trispirazol e tristriazol. Nesta parte do proxecto destaca a colaboración co grupo do Prof. Pedro J. Pérez. Os experimentos iniciais en auga en ausencia de ascorbato de sodio revelan unha baixa actividade dos catalizadores, mentres que a presenza de ascorbato de sodio como redutor aumenta considerablemente a actividade, especialmente os complexos mencionados de trispirazol e tristriazol. Sen embargo, demostrouse que estes complexos son moi activos na promoción da cicloadición en ausencia de reductores externos en células vivas. Isto pon de manifesto que a célula ten un ambiente suficientemente redutor como para manter o estado de cobre (I) necesario para o correcto funcionamento da reacción.

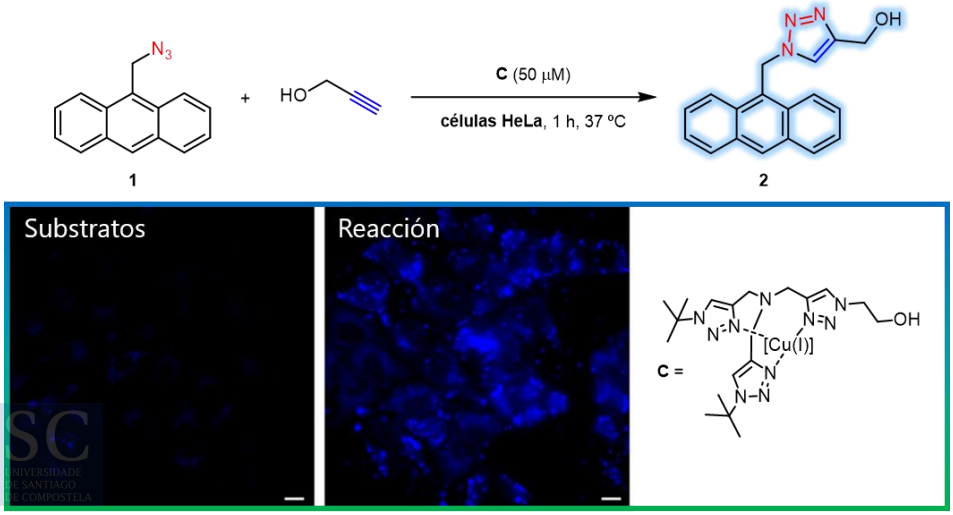

Figura 2. Micrografías de fluorescencia de células HeLa despois da incubación co substratos e o conxunto da reacción có complexo predefinido e na ausencia de ascorbato de sodio.

A continuación, realizarase unha determinación do rendemento da reacción no interior das células vivas mediante fluorescencia. Tendo en conta a cantidade de azida presente na célula, valor medido por HPLC, e a fluorescencia do produto xerado (utilizando a correspondente curva de calibración) calculáronse os rendementos dos diferentes complexos empregados, tanto Cu(I) preparados *in situ* como de Cu(I) predefinido e illados, obtendo un excelente 18% para o complexo de cobre (I) predefinido tristriazol.

Para explicar estes resultados, estúdase en profundidade a diferente internalización dos complexos de cobre, mediante medicións do contido metálico intracelular mediante ICP-MS. Curiosamente, os complexos predefinidos presentan maiores concentracións no interior das células vivas que os preformados *in situ*, o que corresponde cunha maior e mellor interiorización. Finalmente, os ensaios MTT para avaliar a toxicidade dos catalizadores mostraron unha ausencia de toxicidade na concentración na que se estudaron as reaccións descritas.

Como conclusións, neste capítulo foi posible trasladar unha versión discreta da cicloadición CuAAC ao interior de células vivas de mamíferos, de forma eficiente, mediante o emprego de complexos predefinidos de cobre (I). Deste xeito, elimínase o emprego de ascorbato sódico, que xera especies reactivas de osíxeno en combinación con Cu(II), estratexia que adoita ser habitual noutras CuAAC bioortogonais. Tamén foi posible a determinación do rendemento da cicloadición en células.

No **capítulo III** descríbese por primeira vez a realización dunha cicloadición [2+2+2] no interior de células de mamíferos vivas, mediante o uso de diferentes complexos de rutenio. Ademais, o deseño racional dos substratos, como os triinos ou diinos utilizados nesta reacción, permite a síntese de compostos complexos nun só paso dunha maneira intramolecular e intermolecular en presenza de distintas biomoléculas. Isto débese á súa capacidade para atrapar as especies de rutenio estabilizándoas mediante a formación de rutenaciclos. En particular, foi posible preparar dun xeito intracelular metabolitos secundarios como ftalanos ou antraquinonas, compostos que as células de mamíferos non poden preparar ao carecer da vía metabólica correspondente para a súa síntese. Tamén se explorou o uso de compostos "aggregation - induced emission" (AIEgens), compostos que presentan unhas interesantes propiedades espectroscópicas, como alternativa aos fluoróforos orgánicos convencionais.

USC
UNIVERSIDADE DE SANTIAGO DE COMPOSTELA

O capítulo comeza cunha breve introdución ás reaccións de cicloadición máis aló dos procesos 1,3 – dipolares. Usando como modelo a transformación de Diels-Alder coas súas limitacións electrónicas, preséntanse as vantaxes do uso de metais de transición como Pd, Rh, Ru, Ni, Co ou Ir nesta química. Despois diso, o foco centrase en varias cicloadicións catalizadas por rutenio detallandose o mecanismo de reacción para o caso particular das cicloadicións [2+2+2].

Unha vez sentadas as bases, coméntanse os contados casos de cicloadicións en auga, destacando a química do grupo Teplý quenes reportan diferentes reaccións en lisados de bacterias. Por outra banda, o grupo de Young describe a primeira cicloadición [2+2+2] catalizada por rodio en proteínas.

A continuación, procedese a detallar a síntese do triino (**3**), que experimenta unha cicloadición intramolecular promovida polo rutenio xerando un composto poliaromático fluorescente (**4**). A reacción tolera auga, PBS, DMEM e lisados de células HeLa. Como proba de concepto, a transformación realízase en células HeLa utilizando un catalizador de rutenio previamente descrito polo grupo.

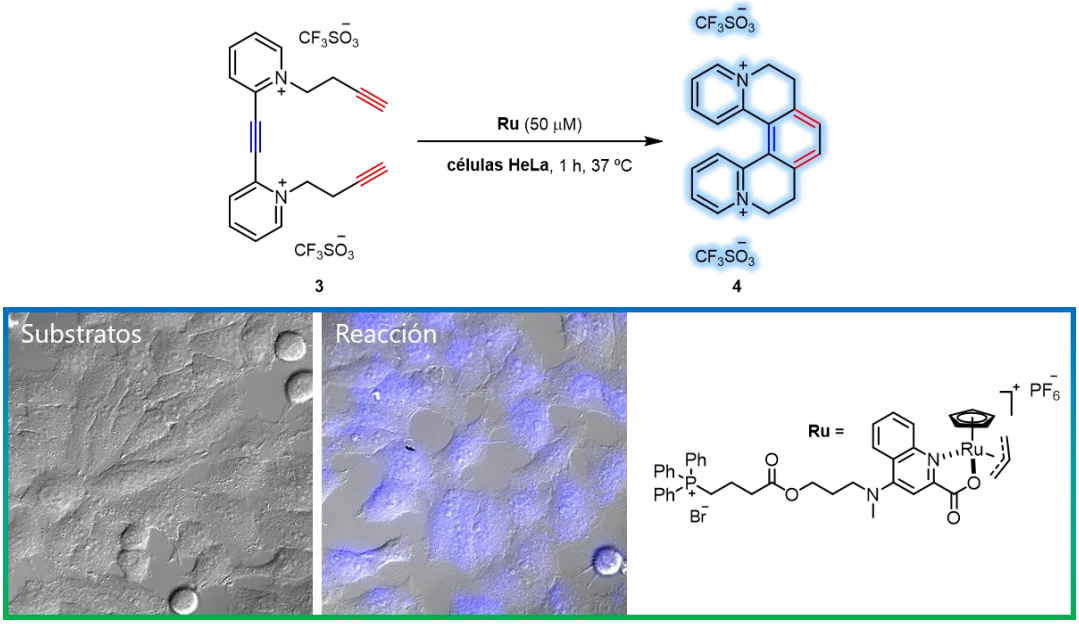

Figura 3. Micrografías de fluorescencia de células HeLa despois da incubación co substratos e o conxunto da reacción.

En vista dos excelentes resultados en células de mamíferos coa versión intramolecular, deseñouse unha cicloadición [2+2+2] intermolecular, que emprega alquino (**5**) e diino (**6**) comerciais para dar o ftalano **7**. Tamén se sintetizan diferentes complexos de rutenio cuxas estruturas están baseadas en precedentes do grupo. Con este sistema obtéñense excelentes resultados en experimentos *in vitro.*

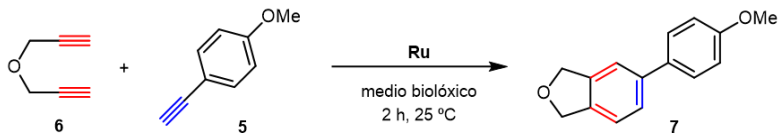

*Figura 4. Síntese do ftalano **7** a partir dos compostos comerciais **5** e **6**.*

Non obstante, debido á carencia de propiedades fluorescentes do produto, selecciónase un novo modelo de reacción (alquino (**5**) e diino (**8**)), que conduce á obtención de antraquinonas, metabolitos secundarios con carácter fluoroxénico e que presentan importantes actividades biolóxicas. Con este sistema, tanto os experimentos en medios biolóxicos como os estudos en células vivas son satisfactorios, observándose a formación do produto (**9**) en tan só 15 minutos, neste último caso.

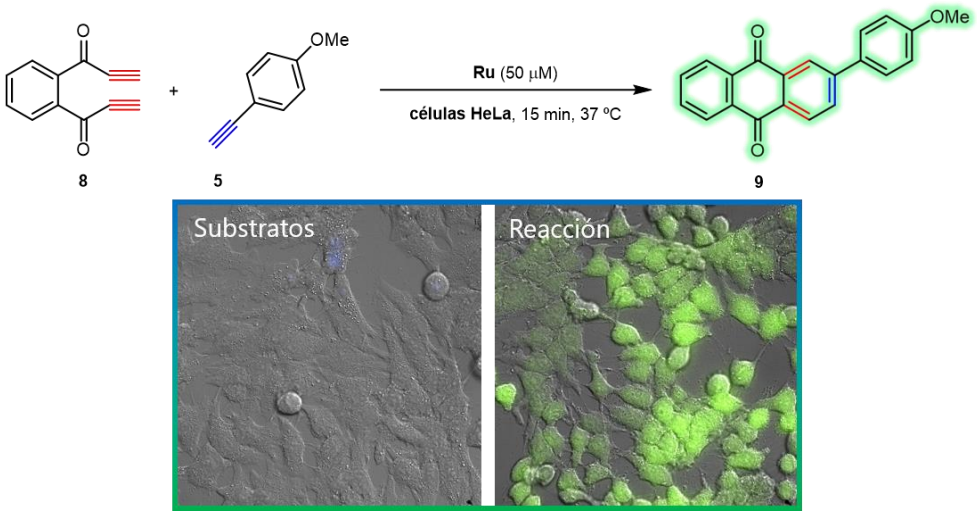

Figura 5. Micrografías de fluorescencia de células HeLa despois da incubación co substratos e o conxunto da reacción.

Na seguinte sección, abórdase a síntese de AIEgens, compostos que presentan fluorescencia ao precipitar e agregar. De acordo con traballos previamente descritos, seleccionáronse diferentes antraquinonas con potencial para exhibir un carácter AIE. Entre elas, a antraquinona, sintetizable a partir do diino (**8**) e o alquino (**10**), presenta un carácter AIE excelente con fluorescencia vermella-laranxa. Ao trasladar este sistema a células, obsérvase a xeración de fluorescencia vermella en forma de agregados ao largo da célula, que se corresponde coa propia sinal de antraquinona (**11**). Por outra banda, as células non son capaces de interiorizar este produto, o que aumenta o valor da transformación desenvolvida xa que proporciona ás células unha "vía de entrada" alternativa para este composto.

USC
UNIVERSIDADE DE SANTIAGO DE COMPOSTELA

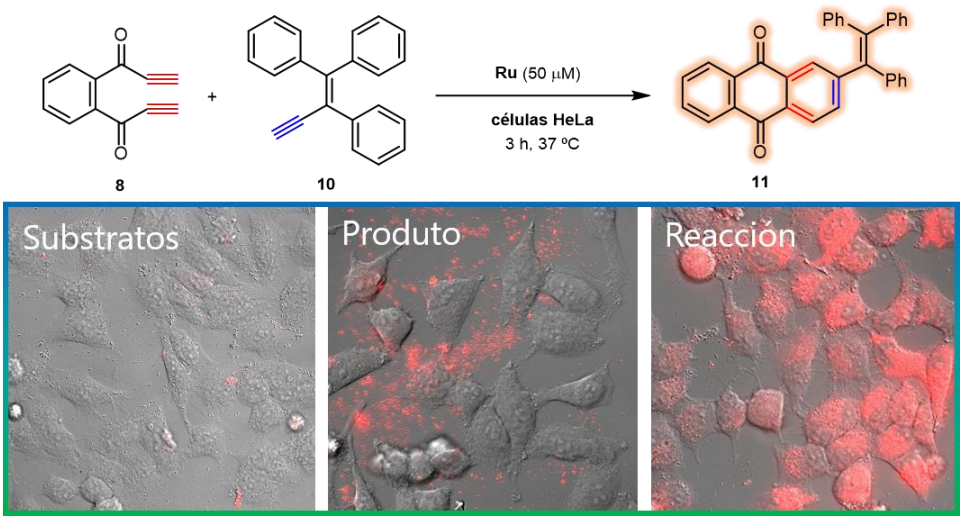

Figura 6. Micrografías de fluorescencia de células HeLa despois da incubación co substratos, o produto e o conxunto da reacción.

De maneira resaltable, a derivatización dun alquino cun grupo trifenilfosfonio, permite a detección por espectroscopia de masas non só da antraquinonas, senón tamén unha máis que notable cantidade do ftalanos xerados intracelularmente. Finalmente, demóstrase que esta estratexia pode ser empregada para levar a cabo de maneira exitosa a reacción no interior das mitocondrias, mediante o uso dun catalizador de rutenio derivatizado cun grupo difenilpireno que actúa como grupo director ao orgánulo celular.

Polo tanto, neste capítulo foron descritas por primeira vez, as cicloadicións [2+2+2] promovidas por rutenio de forma multicompoñente en células de mamíferos. A capacidade do diino para coordinarse e atrapar os diferentes complexos de rutenio parece ser un paso fundamental para levar a cabo a reacción nun medio tan complexo como o interior célula. Cómpre sinalar que esta estratexia permite a síntese de moléculas policíclicas complexas en células vivas, incluso no interior das mitocondrias, nun único paso de reacción.

No **capítulo IV** explorase a combinación da fotocatálise coa química bioortogonal, un campo apenas explorado dende o punto de vista sintético. En concreto, investigáronse as adicións foto-meerwein como unha transformación cun enorme potencial bioortogonal. Demostrase que a adición pode ter lugar en presenza de biomoléculas, medios biolóxicos ou mesmo dentro de células de mamíferos, cunha adecuada selección do fotocatalizador, unha fonte de radical arilo axeitada e un alquino cunha boa capacidade para atrapar radicais.

USC
UNIVERSIDADE DE SANTIAGO DE COMPOSTELA

O capítulo comeza cunha breve introdución á química fotoredox, prestando especial atención ao conxunto dos fotocatalizadores máis empregados neste campo e aos seus mecanismos de acción. A continuación, a sección céntrase na reacción de adición radicalaria foto - meerwein, explicando o seu mecanismo, e destacando a contribución do grupo König ao introducir o uso da luz visible como fonte de enerxía neste tipo de procesos fotoredox.

A continuación, coméntanse dous dos escasos exemplos de reaccións fotoredox en auga para, acto seguido, dar paso a súa contribución á química biolóxica, principalmente centrada na modificación de aminoácidos ou na terapia fotodinámica. Para rematar a introdución do capítulo, destácase o traballo dos grupos de Yinyun Chen e Winssinger, centrado na liberación de sondas, sendo un dos poucos traballos realizados en células de mamíferos. Ademais, preséntase o único traballo con intención sintética dentro do campo da química bioortogonal promovida pola luz, aportado polo Prof. Chen.

Tras a introdución, selecciónanse as sales de diazonio como precursores dos radicais arilo, dada a súa natureza biocompatible e o seu potencial de redución próximo a 0 eV. Decídese enfrontar estas sales, en primeiro lugar, con naftoquinonas, excelentes especies atrapadoras de radicais, en presenza de $Ru(bpy)_3$ ou Eosin Y como fotocatalizadores con un potencial moderado. Ademais, o fotocatalizador metálico ten precedentes de biocompatibilidade nas células. Os resultados obtidos neste estudo inicial, aínda que moderados, serven para confirmar que é posible realizar química radical cun obxectivo sintético, mediante unha selección adecuada dos reactivos de partida.

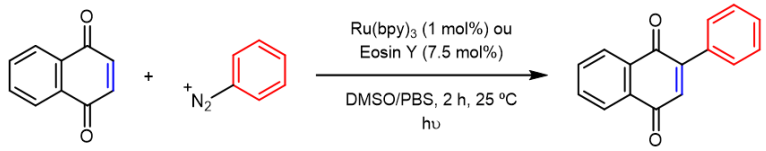

Figura 7. Arilación fotoquímica de naftoquinonas.

O seguinte paso é substituír a naftoquinona por un alquino pobre en electróns como o metil propiolato. Tras reaccionar cunha sal de diazonio de biarilo obtense fenantreno (**12**), mediante unha cicloadición formal [4+2], que tras a primeira adición do radical arilo procede de forma moi eficiente (rendemento cuántico do 0.35%). Para o noso deleite, a transformación mostra moi bos rendementos en auga e PBS, ambos con Eosin Y e $Ru(bpy)_3$ como fotocatalizadores.

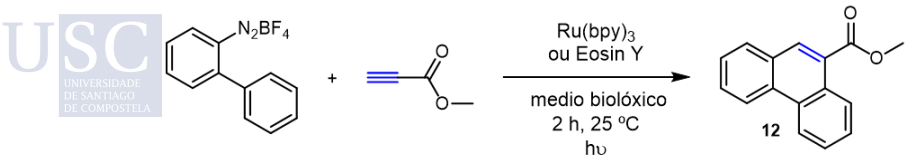

Figura 8. Síntese de fenantrenos en medios biolóxicos.

Despois do proceso de optimización, analízase o efecto da concentración de substratos, podendo reducir a concentración de sal de diazonio a 1 mM, conseguindo excelentes rendementos simplemente cunha adición lenta da sal de diazonio. A continuación, investigase a biocompatibilidade do proceso. Aminoácidos, proteína (BSA), GSH ou incluso células en suspensión conducen a rendementos moi bos. Finalmente, a reacción transfírese a células vivas, confirmando a formación do produto mediante espectroscopia de masas.

Como conclusións do capítulo, confirmouse o comportamento bioortogonal da reacción de adición foto - meerwein en presenza de biomoléculas ou mesmo en células de mamíferos vivas. O uso de fotocatalizadores cun potencial moderado, xunto co uso de sales de diazonio facilmente activables e un bo atrapador de radicais como o alquino, aseguran unha correcta selectividade da reacción. Ademais, demostrase que non é necesario obter produtos fluorescentes para controlar as reaccións que se realizan no interior das células, xa que neste caso, os produtos obtidos (os fenantrenos) pódense detectar mediante espectrometría de masas. Estes primeiros estudos no campo da fotocatálise bioortogonal abren a porta ao uso de novos sistemas, novas fontes de radicais arilo e novas sondas en ambientes celulares vivos.

Conclusión Xeral

Como conclusión xeral, a tese de doutoramento describe o uso de tres tipos diferentes de cicloadición realizados no interior de células de mamíferos HeLa ou A549. A primeira de elas, un proceso tipo CuACC, proporciona unha nova aproximación para a conxugación de moléculas mediante a formación de triazoles. As outras dúas novas transformacións que se presentan nesta tese, desenvolvidas tamén no interior de células vivas, permiten a creación e/ou modificación de moléculas complexas a partir de substratos sinxelos. Un aspecto importante a destacar é que a última transformación é promovida pola luz visible, constituíndo o primeiro exemplo dunha reacción bioortogonal de fotocatálise utilizada con fins sintéticos no interior de células vivas.

USC
UNIVERSIDADE DE SANTIAGO DE COMPOSTELA

EXPERIMENTAL SECTION

USC
UNIVERSIDADE
DE SANTIAGO
DE COMPOSTELA

USC
UNIVERSIDADE
DE SANTIAGO
DE COMPOSTELA

GENERAL INFORMATION FOR SYNTHESIS EXPERIMENTS

Synthetic preparative procedures were performed under an atmosphere of dry nitrogen using vacuum-line and standard Schlenk techniques, unless otherwise indicated. The solvents for organic synthesis were of reagent grade unless otherwise noted. Dry solvents were directly purchased from Aldrich and used without further purification. Water was deionized and purified on a Millipore Milli-Q Integral system. Chemicals were purchased from Sigma Aldrich, Alfa Aesar, Fluka or Acros Organics and used without further purification.

Reactions were carried out without particular precautions to extrude moisture or oxygen, and open to air, unless otherwise stated. Reaction mixtures were stirred using Teflon-coated magnetic stirbars. The abbreviation "r. t." refers to reactions carried out approximately at 20 °C. Temperature was maintained using Thermowatch-controlled heating blocks. Thin layer chromatography (TLC) was performed on Merck 60 (silicagel F254) plates and components were visualized by observation under UV and / or by using staining solutions of $KMnO_4$ or *p*-anisaldehyde and heating. Chromatographic purification of products was accomplished using flash column chromatography on Merck Geduran Si 60 (40 – 63 μm) silica gel (normal phase) or by reversed-phase high-performance liquid chromatography (RP-HPLC). Concentration refers to the removal of volatile solvents via distillation using a rotary evaporator Buchi R-210 equipped with a thermostated bath B-491, a vacuum regulator V-850, and a vacuum pump V700, followed by residual solvent removal under high vacuum.

^{1}H NMR (300 MHz) spectra were recorded at room temperature on a Varian Mercury 300 MHz spectrometer and ^{1}H NMR (500 MHz) spectra were recorded at room temperature on a Bruker DRX500 spectrometer. ^{13}C NMR (125 MHz) spectra were recorded on a Bruker DRX-500 spectrometer. ^{31}P NMR (202 MHz) spectra were recorded on a Bruker DRX-500 spectrometer. The spectra were calibrated to the residual solvent peak, if possible. As an external reference triphenyl phosphate (-18 ppm) was used for ^{31}P NMR spectra. Multiplicities are abbreviated as follows: s = singlet, d = doublet, t = triplet, q = quartet, quint = quintet, m = multiplet, br = broad and combinations of these. NMR spectra were analyzed using MestreNovac NMR data processing software (www.mestrelab.com). The chemical shifts (δ) are given in ppm and the coupling constants (*J*) in Hz. UV measurements were performed using a Jasco V-670 spectrometer. Fluorescence measurements were performed using a Horiba FluoroMaxR-3 Spectrophotometer with the following settings: increment 1.0 nm, averaging time 0.2 s, excitation slit width 2.0 nm, emission slit width 5 nm, using 1 cm quartz cells. PMT voltage 620 V. High resolution mass spectra (HRMS) were acquired using electrospray (ESI) and were recorded at the CACTUS facility of the University of Santiago de Compostela.

USC UNIVERSIDADE DE SANTIAGO

Chapter II:

The copper catalyzed reactions were carried out without particular precautions to extrude moisture or oxygen, and open to air, except when noted otherwise. The evolution of the reactions was studied by fluorescence using a *Tecan infinite F200Pro* microplate reader, with a gain of excitation of 48%.

EPR measurements were performed with a *Bruker EMX* at a temperature of 120 K.

Analytical HPLC was performed on an *Agilent 1260 Infinity II* coupled to an *Agilent Technologies 6120 Quadrupole LC-MS* using a flow rate of 0.35 mL min^{-1} at room temperature. The initial conditions for the HPLC system were: H_2O/MeCN (50/50) followed by a gradual change over 35 min to H_2O/MeCN (0/100). The chromatogram was recoded via UV absorption at $\lambda = 254$ nm.

Chapter III:

Complexes **Ru2** and **Ru8,** have been reported in previous works of the group.[139] If the cationic complexes are purified by HPLC, the counterion is TFA. Otherwise, the counterion of the complexes is PF_6.

Chapter IV:

Experiments with blue light or white light were performed with a KESSIL 32W Lamp.[286]

Experiments with green light were performed with LED's mounted around a laboratory crystallizer.[287] Temperature was kept at room temperature with a fan situated about 10 cm of the reaction.

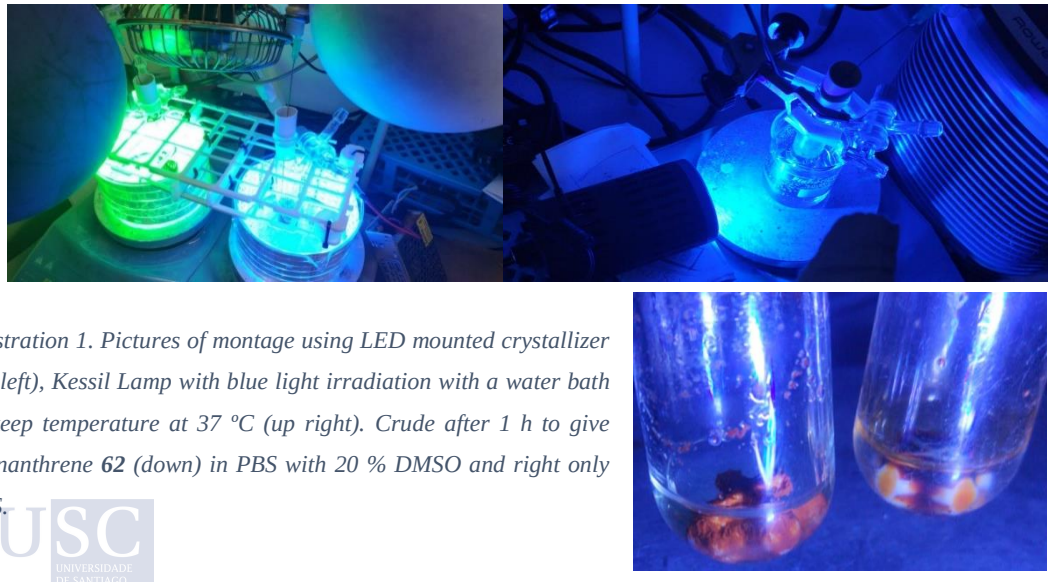

Illustration 1. Pictures of montage using LED mounted crystallizer (up left), Kessil Lamp with blue light irradiation with a water bath to keep temperature at 37 ºC (up right). Crude after 1 h to give phenanthrene ***62*** *(down) in PBS with 20 % DMSO and right only PBS.*

USC UNIVERSIDADE DE SANTIAGO DE COMPOSTELA

[286] https://kessil.com/
[287] https://threelinegroup.com/

GENERAL INFORMATION FOR THE BIOLOGICAL EXPERIMENTS

All steps were performed on a sterile clean bench *Tesltar AV-100* at room temperature. Solutions stored in a fridge were warmed beforehand in a water bath (37 °C). Unless otherwise specified, all incubations were performed in DMEM.

Cell Culture: All cell lines were cultured in DMEM (Dulbecco´s modified Eagle´s medium), 5 mM glutamine, penicillin (100 units/mL) and streptomycin (100 units/mL) (all from *Invitrogen*). Proliferating cultures were maintained in a 5% CO_2 humidified incubator at 37 °C.

For all the experiments, cells were seeded in the corresponding well at the indicated concentration two days before treatment.

Protein quantification: For protein concentration measurements the Bio-Rad *DC* Protein Assay Kit was used (*Bio-Rad* 500-0114).

Fluorescence microscopy: All images were obtained with an *Andor Zyla* mounted on a *Nikon TiE*. Confocal images were acquired in an Andor Dragonfly High Speed Confocal Platform. Images were further processed with *Image J* or NIS software (Nikon).

Microscopy settings: The filter sets for the observation of the fluorescence of the products were as follows:

Widefield: LED λ excitation: 385 nm. Filter cube DAPI-1160B-000 (Semrock): BP 387/11-25 nm, LP 447/60-25 nm and DM 409 nm. Confocal: Laser excitation: 405 nm. LP 450/50 and DM 418 nm.

Widefield: LED λ excitation: 385 nm. Filter cube: BP 375/28x nm, LP 515lp nm and DM 415 nm. Confocal: Laser excitation: 405 nm. LP 525/50 and DM 501 nm.

Widefield: LED λ excitation: 470 nm. Filter cube FITC-3540C-000 (Semrock): BP 482/35 nm, LP 536/40 nm and DM 506 nm. Confocal: Laser excitation: 488 nm. LP 525/50 and DM 501 nm.

TMRE (tetramethylrhodamine, ethyl ester) LED λ excitation: 550 nm. Filter cube TRITC-B-000 (Semrock): BP 543/22-25 nm, LP 593/40-25 nm and DM 562 nm. Confocal: Laser excitation: 561 nm. LP 620/60 and DM 567 nm.

USC UNIVERSIDADE DE SANTIAGO DE COMPOSTELA

USC
UNIVERSIDADE
DE SANTIAGO
DE COMPOSTELA

DISCRETE CU(I) COMPLEXES FOR AZIDE-ALKYNE ANNULATIONS OF SMALL MOLECULES INSIDE MAMMALIAN CELLS

TABLE OF CONTENTS

S1.- Experimental procedures and data

S2.- Spectroscopy studies of substrate 20 and product 21

S3.- Catalytic CuAAC experiments under biological relevant conditions

S4. Quantification by HPLC-MS

S5.- Spectroscopic analysis of the copper complexes

S6.- Selected NMR spectra

S7.- CuAAC experiments in living cells

S8.- Viability assays

S9.- ICP analysis

S10.- Flow cytometry studies

S11.- Quantification of the reaction inside living cells

S12.- References

USC
UNIVERSIDADE DE SANTIAGO DE COMPOSTELA

USC
UNIVERSIDADE
DE SANTIAGO
DE COMPOSTELA

S1.- EXPERIMENTAL PROCEDURES AND DATA

3-Azido-7-hydroxycoumarin (**13**),[1] 2-[(1*E*)-2-(4-azidophenyl)ethenyl]-6-nitro-benzothiazole (**18**),[2] 9-(azidomethyl)-anthracene (**20**),[3] 1-(9-anthracenylmethyl)-1*H*-1,2,3-triazole-4-methanol (**21**),[4] 4-[[bis[[1-(1,1-dimethylethyl)-1*H*-1,2,3-triazol-4-yl]methyl]amino]methyl]-1*H*-1,2,3-triazole-1-ethanol (BTTE **L3**),[5] 4-[[bis[[1-(1,1-dimethylethyl)-1*H*-1,2,3-triazol-4-yl]methyl]amino]methyl]-1*H*-1,2,3-triazole-acetic acid (BTTAA **L1**),[6] 2-carboxiethyl)diphenyl(pyren-1-ylmethyl)phosphonium bromide,[7] [Cu(BrPPh$_2$(OPh-2-OMe))] (**C4**),[8] bis(1,3-di(adamantan-1-yl)-1,3-dihydro-2H-imidazol-2-ylidene)copper ([(IAd)$_2$Cu]PF$_6$) (**C3**)[9] and N-[(tris(3,5-dimethyl-1-*H*-pyrazol-1-yl)methyl))] [(Tpa*)Cu(NCMe)]PF$_6$ (**C1**)[10] were synthesized according to literature procedures and spectroscopic data are in agreement with the bibliographic ones.

1.1 Synthesis of ligands L2-L3

BBTE and BTTE where prepared following the synthetic route shown in scheme S1.[5]

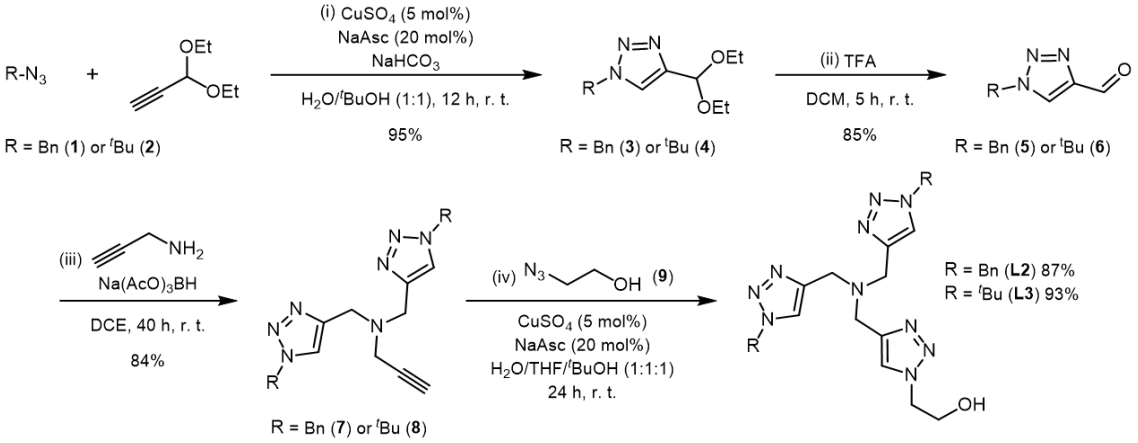

*Figure S1. Synthesis of the ligands **L2** and **L3**. Reagents and conditions: (i) **1** or **2** (1.15 equiv.), 3,3-diethoxyprop-1-yne (1.0 equiv.), H_2O-^{t}BuOH (1:1), $NaHCO_3$ (1.4 equiv.), $CuSO_4 \cdot 5H_2O$ (5 mol%), sodium ascorbate (20 mol%), 12 h, room temperature, 95%; (ii) **3** or **4** (1.0 equiv.), trifluoroacetic acid (2.3 equiv.), dichloromethane, under nitrogen atmosphere, 5 h, room temperature, 85%; (iii) **5** or **6** (2.2 equiv.), prop-2-yn-1-amine (1.0 equiv.), $Na(AcO)_3BH$ (2.5 equiv.), 1,2-dichloroethane, 40 h, room temperature, 84%; (iv) **7** or **8** (1.0 equiv.), **9** (1.5 equiv.), $CuSO_4 \cdot 5H_2O$ (5 mol%), sodium ascorbate (20 mol%), 24 h, room temperature, 93%.*

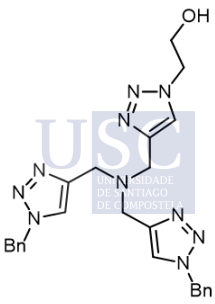

3-(4- ((bis((1-*tert*-Butyl-1H-1,2,3-triazol-4-yl)methyl)amino)methyl)-1H-1,2,3-triazol-1- yl)ethanol (BBTE L2). White solid. **^{1}H-RMN** ($CDCl_3$, 300 MHz): δ = 7.80 (s, 1H), 7.62 (s, 2H), 7.36–7.28 (m, 6H), 7.23 (dd, *J* = 7.5, 1.8, 4H), 5.49 (s, 4H), 4.45 (t, *J* = 5.1, 2H,), 4.01 (t, *J* = 5.1, 2H), 3.72 (s, 6H). **^{13}C NMR** (CDCl3, 126 MHz): δ = 144.3 (2*C*), 143.7, 134.7, 129.1, 128.7, 128.0, 124.8, 123.8 (2C), 60.9, 54.1 (2C), 52.7, 47.5, 46.9 (2C). **HRMS**: Calculated for: $C_{25}H_{29}N_{10}O$: 485.2448; found: 485.2510.

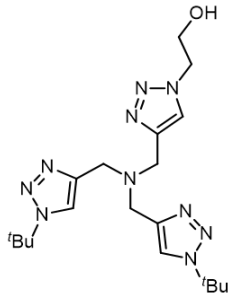

3-(4- ((bis((1-*tert*-Butyl-1H-1,2,3-triazol-4-yl)methyl)amino)methyl)-1H-1,2,3-triazol-1- yl)ethanol (BTTE L3).[5] White solid. **^{1}H-RMN** ($CDCl_3$, 300 MHz): δ = 7.91 (s, 1H), 7.80 (s, 2H), 4.50 (t, *J* = 4.7 Hz, 2H), 4.07 (t, *J* = 4.9 Hz, 2H), 3.79 (s, 2H), 3.77 (s, 4H), 1.67 (s, 18H).

1.3 Synthesis of ligand L4

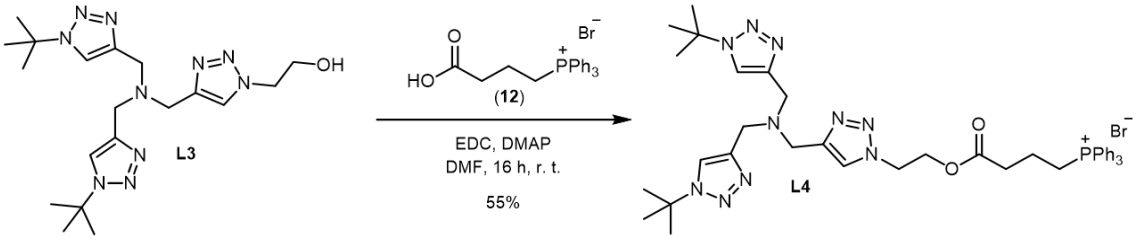

(3-Carboxypropyl)triphenylphosphonium bromide **12** (94.0 mg, 0.22 mmol, 1.0 eq) was dissolved in *N*,*N*-dimethylformamide (2 mL). 1-Ethyl-3-(3-dimethylaminopropyl)carbodiimide (EDC) (104.0 mg, 0.54 mmol, 2.45 equiv.), BTTE (**L3**) (91.6 mg, 0.22 mmol, 1.0 equiv.) and 4-dimethylaminopyridine (DMAP) (52.0 mg, 0.44 mmol, 2.0 equiv.) were subsequently added to the solution. The reaction mixture was left stirring overnight and the solvent was removed under reduced pressure. The crude was purified by flash chromatography on silica gel using DCM / MeOH 9.5:0.5 as eluent. The product **L4** was obtained as a white solid (102 mg, 55%).

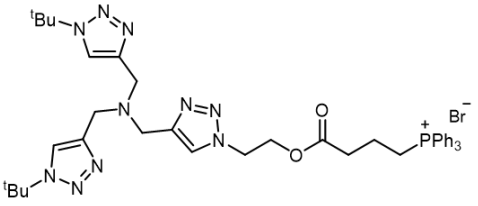

(4-(2-(4-((bis((1-(*tert*-Butyl)-1H-1,2,3-triazol-4-yl)methyl)amino)methyl)-1H-1,2,3-triazol-1-yl)ethoxy)-4-oxobutyl)triphenylphosphonium bromide (BTTE-P L4). White solid. $\mathbf{R_f}$ = 0.3 (DCM / MeOH 9:1) staining $KMnO_4$. **Yield** = 55% (0.14 mmol, 102 mg). **^{1}H RMN** ($CDCl_3$, 500 MHz): δ = 8.11 (s, 1H), 7.89 (s, 2H), 7.81-7.71 (m, 9H), 7.64 (td, *J* = 7.9, 3.5 Hz, 6H), 4.65 (t, *J* = 5.2 Hz, 2H), 4.46 (t, *J* = 5.2 Hz, 2H), 3.81 (ddd, *J* = 16.5, 8.6, 4.9 Hz, 2H), 3.70 (s, 2H), 3.67 (s, 4H), 2.82 (t, *J* = 6.3 Hz, 2H), 1.90–1.77 (m, 2H), 1.60 (s, 18H). **^{13}C NMR** ($CDCl_3$, 126 MHz): δ = 172.2, 144.0, 143.3 (2*C*), 135.1 (d, *J* = 3.1 Hz), 133.6 (d, *J* = 10.6 Hz), 130.5 (d, *J* = 13.1 Hz), 125.1, 121.1 (2C), 118.0 (d, *J* = 86.3 Hz), 62.8, 59.2 (2C), 49.0, 47.6, 47.2 (2C), 33.1 (d, *J* = 18.8 Hz), 30.0 (6x*C*), 21.5 (d, *J* = 52.0 Hz), 17.9 (d, *J* = 2.5 Hz). **^{31}P NMR** ($CDCl_3$, 202 MHz): δ = 22.6. **HRMS**: Calculated for $C_{41}H_{52}N_{10}O_2P^+$: 747.4007; found: 747.4007.

USC DE COMPOSTELA

1.4 Synthesis of complex BTTECuPF$_6$ (C5)

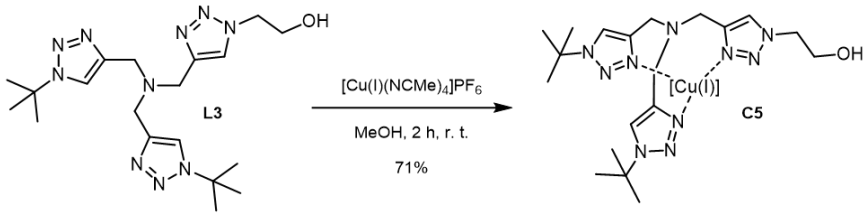

A solution of the ligand **L3** (246 mg, 0.59 mmol, 1.0 equiv.) in 15 mL of methanol was added via cannula over a solution of tetrakis(acetonitrile)copper(I) hexafluorophosphate (220 mg, 0.59, 1.0 equiv.) in 25 mL of methanol. After a few minutes, formation of white precipitate was observed. The mixture was stirred for two hours at room temperature. Methanol was filtered off and the solid was washed with 10 mL of methanol and 10 mL of diethyl ether. The solid was dried under vacuum. BTTECuPF$_6$ (**C5**) was isolated as a white solid (260 mg, 71%).

BTTECuPF$_6$ (C5). White solid. **Yield** = 71% (0.42 mmol, 260 mg). **^{1}H NMR** (DMSO-d$_6$, 500 MHz): δ = 8.34 (s, 2H), 8.16 (s, 1H), 5.07 (t, *J* = 5.3 Hz, 1H), 4.42 (t, *J* = 4.9 Hz, 2H), 3.85 (brs, 6H), 3.78 (brs, 2H), 1.60 (s, 18H). **^{13}C NMR** (DMSO-d6, 125 MHz): δ = 144.0 (2C), 124.7, 121.5 (3C), 60.3, 59.5 (3C), 53.0, 47.0, 29.2 (6C). **Elemental analysis**: Calc. ($C_{19}H_{32}CuF_6N_{10}OP$) 36.51 C, 5.16 H, 22.41 N; found: 36.86 C, 5.15 H, 22.12 N.

1.1 Synthesis of probes 14 and 21

The fluorescent probes **14** and **21** were synthetized through the following CuAAC protocol.

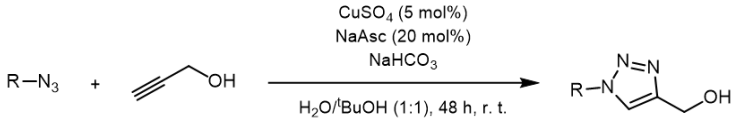

To a round bottom flask containing 1 mL of a mixture H_2O/ ^{t}BuOH (1:1) is added the corresponding azide (**13** or **20**, 1.2 mmol), $NaHCO_3$ (1.68 mmol, 140 mg, 1.4 equiv.), $CuSO_4$ (0.06 mmol, 9.4 mg, 0.05 mol%) and propargyl alcohol (1.2 mmol, 69 μL, 1 equiv.). The reaction was initiated by adding NaAsc (0.24 mmol, 47 mg, 20 mol%) and allowed to react at room temperature for 48 h. The crude was treated with 200 μL of a solution 0.5 M of ethylenediaminetetraacetic acid (EDTA) for 5 min. For **14**, the crude was filtrated and washed with H_2O and DCM, obtaining the product as a brown solid. For **21**, the crude was diluted with H_2O, and extracted with DCM. The combined organic layers were dried over anhydrous $MgSO_4$ and concentrated under reduced pressure. The residue was purified by flash chromatography on silica gel using Hex / EtOAc 1:1 as eluent. The product was isolated as yellow solid.

USC UNIVERSIDADE DE SANTIAGO

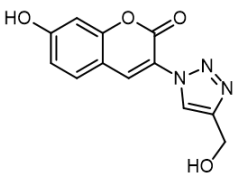

7-Hydroxy-3-(4-(hydroxymethyl)-1H-1,2,3-triazol-1-yl)-2H-chromen-2-one (19). Brown solid. **Yield** = 84% (1 mmol, 257 mg). **^{1}H NMR** (300 MHz, DMSO-d_6) δ 8.55 (s, 1H), 8.38 (s, 1H), 7.72 (d, *J* = 8.4 Hz, 1H), 6.88 (d, *J* = 8.3 Hz, 1H), 6.82 (s, 1H), 5.29 (brs, 1H), 4.59 (d, *J* = 3.9 Hz, 2H).

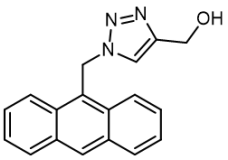

(1-(Anthracen-9-ylmethyl)-1H-1,2,3-triazol-4-yl)methanol (21). Yellow solid. **R_f** = 0.15 (Hex / EtOAc 1:3). **Yield** = 41% (0.49 mmol, 142 mg). **^{1}H NMR** (300 MHz, $CDCl_3$) δ 8.58 (s, 1H), 8.30 (d, *J* = 8.6 Hz, 2H), 8.08 (d, *J* = 8.3 Hz, 1H), 7.64 – 7.48 (m, 5H), 7.10 (s, 1H), 4.61 (s, 2H).

S2. SPECTROSCOPY STUDIES OF SUBSTRATE 20 AND PRODUCT 21

For the UV-Vis spectroscopic studies, solutions of compounds **20** and **21** (5 mM in DMSO) were freshly prepared and diluted with 2 mL of H_2O into a quartz Hellma® fluorescence cuvette with a pathlength 10x10 mm, chamber volume 3.5 mL (final concentration: 100 µM). The samples were analyzed in a *Jasco V-630*UV-Vis spectrophotometer at 25 °C. UV-Vis analyses were performed in the interval of 300-800 nm.

For the fluorescence measurements, solutions of the compounds **20** and **21** (5 mM in DMSO) were freshly prepared and diluted with water into quartz Hellma® fluorescence cuvette with a pathlength 10x10 mm, chamber volume 3.5 mL (final concentration: 20 µM). The samples were analyzed in a *Hoiba FluoroMax-3 f*luorescence Spectrophotometer at 25 °C. The solutions of substrates were excited at 367 nm and the emission spectrum was recorded in the interval 355-700 nm.

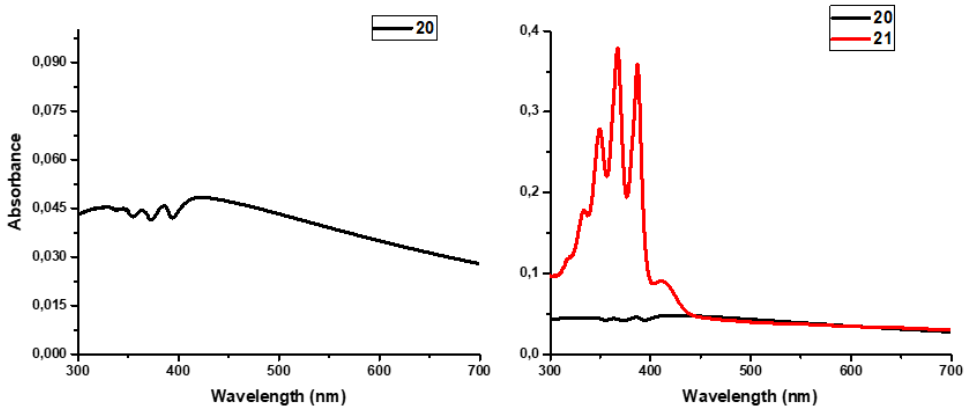

*Figure S2. UV/Vis absorption spectra of **20** in 2 mL of H_2O (100 µM, black line, left figure) and comparison between UV/Vis absorption spectra of **20** and **21** (100 µM, red line, right figure).*

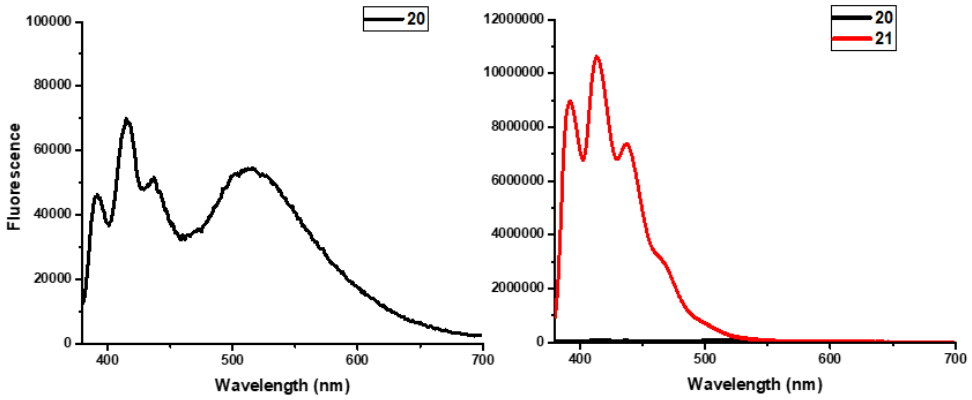

*Figure S3. Fluorescence spectra of **20** in 2 mL of H_2O (20 µM, black line, no emission, left figure) and comparison of fluorescence spectra of **20** and **21** (20 µM, red, line, right figure, λ_{exc} = 385 nm).*

S3. CATALYTIC CuAAC EXPERIMENTS UNDER BIOLOGICAL RELEVANT CONDITIONS

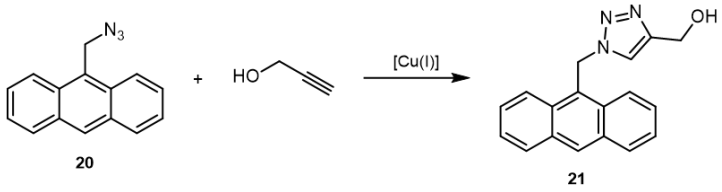

*Figure S4. CuAAC reaction between anthracenyl azide **20** and propargyl alcohol.*

The studies on the catalytic copper azide-alkyne cycloaddition of 9-(azidomethyl)-anthracene **20** and propargyl alcohol under biologically relevant conditions were performed in a microplate of 96 wells.

3.1. Reaction with *in situ* prepared Cu(I) complexes using L1-L4 ligands, and with predefined Cu(I) complexes C1-C5

A fresh solution of $CuSO_4$ (12.5 µL, 10 mM in H_2O) was added to a fresh solution of the ligand (12.5 µL, 20 mM in H_2O and 5% DMSO, 2.0 equiv.) in an eppendorf tube of 500 µL containing 25 µL of milliQ water (with **L2**, solubilization required a little heating). The mixture was stirred for 10 min at room temperature. A stock mixture containing the reactants was prepared in an eppendorf tube by mixing a fresh solution of azide **20** (3.91 µL, 50 mM, DMSO) and a fresh solution of propargyl alcohol (7.82 µL, 50 mM, H_2O), in 1688.27 µL of the corresponding solvent (water or PBS). 87 µL of this mixture was poured into the reaction well of the plate, and mixed with the Cu(II) containing solution (3 µL, 2.5 mM, 0.75 equiv.). Finally, sodium ascorbate was added (10 µL, 25 mM, H_2O) to start the reaction, which was carried out under air at room temperature.

In case of the predefined Cu(I) complexes, a fresh solution of the complexes **C1-C5** (2.5 mM in DMSO) was freshly prepared. Then, 3 µL of this solution was added to the plate well containing the mixture with both substrates (87 µL) and diluted in the chosen solvent (3 µL of water or PBS, or the sodium ascorbate water solution). The experiments were carried out at 25ºC or 37ºC.
Final concentrations in the reaction mixtures: 100 µM azide **20**, 200 µM propargyl alcohol, 75 µM copper, 2.5 mM sodium ascorbate (when present).

The results were analyzed by fluorescence measurements in a microplate reader (Tecan infinite F200Pro). Fluorescence data were obtained by using an excitation wavelength of 360 nm and recorded at 465 nm. Every measured value is the mean value of three aliquots.

Calibration experiments were performed in a 96 wells plate by addition of increasing quantities of a fresh solution of 1-(9-anthracenylmethyl)-1H-1,2,3-triazole-4-methanol **21** (1 mM or 5mM in DMSO) in milliQ water. Higher concentration results in the precipitation of the triazole **21**. The experiments were performed by triplicate, and measured in the fluorescence microplate reader (excitation: 360 nm, emission: 465 nm). The fluorescence results were processed with OriginPro 2016 to obtain the calibration equation needed to quantify the fluorescence of the experiments.

S4. QUANTIFICATION BY HPLC-UV

The CuAAC reaction of **20** and propargyl alcohol with the different complexes was also quantified by using analytical HPLC-UV methods.

General Procedure: The Cu(II) mixtures with the corresponding politriazol ligands were prepared by addition of fresh solutions of $CuSO_4$ (12.5 µL, 10 mM in H_2O) to solutions of the ligand (12.5 µL, 20 mM in H_2O and 5% DMSO) in an eppendorf tube of 500 µL containing 25 µL of milliQ water. The mixture was stirred for 10 min at room temperature under air. The stock mixture containing the reactants was prepared in an eppendorf tube containing 1688.27 µL of water, by mixing a fresh solution of the azide **20** (3.91 µL, 50 mM, DMSO, 1 equiv.) and a fresh solution of propargyl alcohol (7.82 µL, 50 mM, H_2O, 2 equiv.). The mixture was stirred for homogenization. The copper containing mixture (15 µL, 2.5 mM, H_2O) was added to an eppendorf tube containing the above mixture with both reactants (435 µL). Finally, sodium ascorbate was added (50 µL, 25 mM, H_2O, 33 equiv.), and the reaction carried under air at room temperature.

USC UNIVERSIDADE DE SANTIAGO DE COMPOSTELA

In case of the predefined Cu(I) complexes, a fresh solution of the complexes **C1-C5** (2.5 mM in DMSO) was freshly prepared and immediately added (15 µL, 2.5 mM, DMSO) to an eppendorf tube containing the above prepared solution with both substrates (435 µL).

Final concentrations: 100 µM azide **20**, 200 µM propargyl alcohol, 75 µM copper complex and 2.5 mM sodium ascorbate (when present). The reaction was carried out under air and without stirring, unless otherwise is mentioned.

The formation of the products was confirmed by analytical HPLC-UV (254 nm), and quantified using a calibration curve with an internal standard. HPLC method: H_2O/MeCN gradient 95/5 ⟶ 5/95 in 12 min, then 3 min 100% MeCN.

The calibration of azide **20** and triazole **21** was performed in the same HPLC vial, using MeCN as main solvent. The different samples were prepared from a 5 mM fresh stock solution of the analyte in DMSO. Coumarin (870 µM as final concentration) was used as internal standard. The areas obtained from the chromatogram were processed with OriginPro 2016 to obtain the calibration equation needed to quantify the absorbance of the experiments.

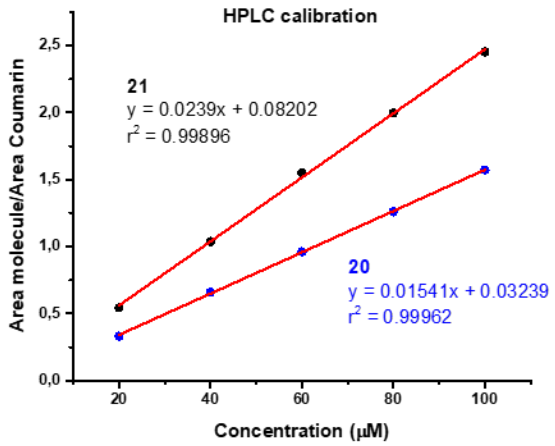

*Figure S5. Standard curve of azide **20** (blue dots) and triazole **21** (black dots). Linear regression curve for 0-100 µM is shown.*

USC UNIVERSIDADE DE SANTIAGO DE COMPOSTELA

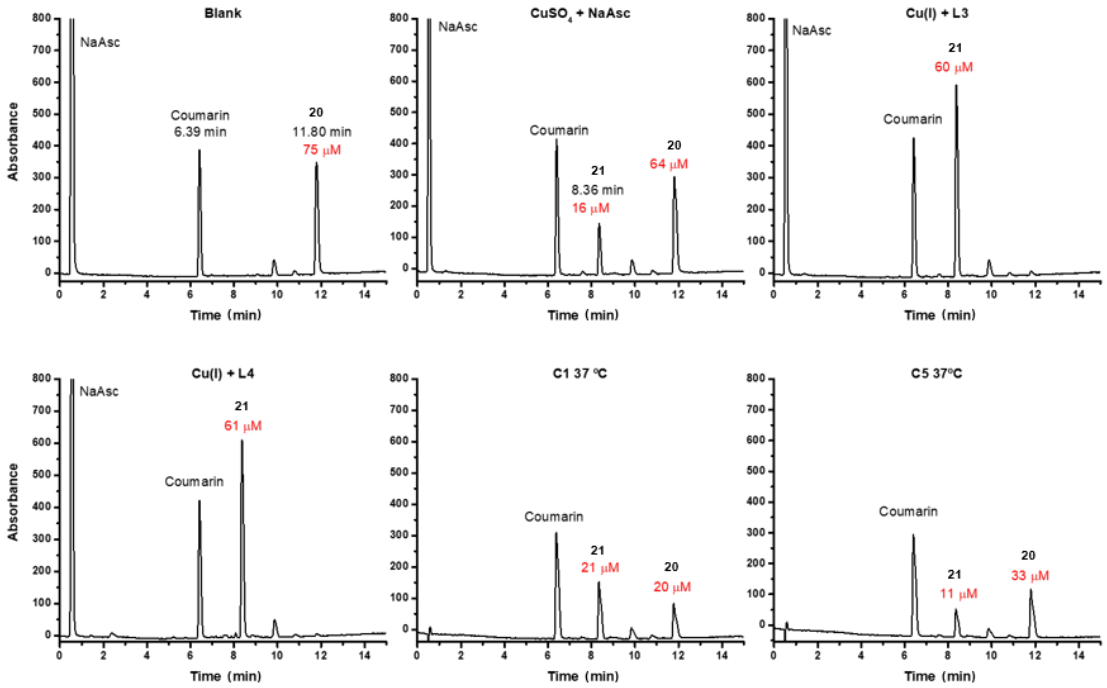

*Figure S6. CuAAC reaction between anthracenyl azide **20** and propargyl alcohol at room temperature or 37 ºC. Yield was determined by analytical HPLC-UV (254 nm).*

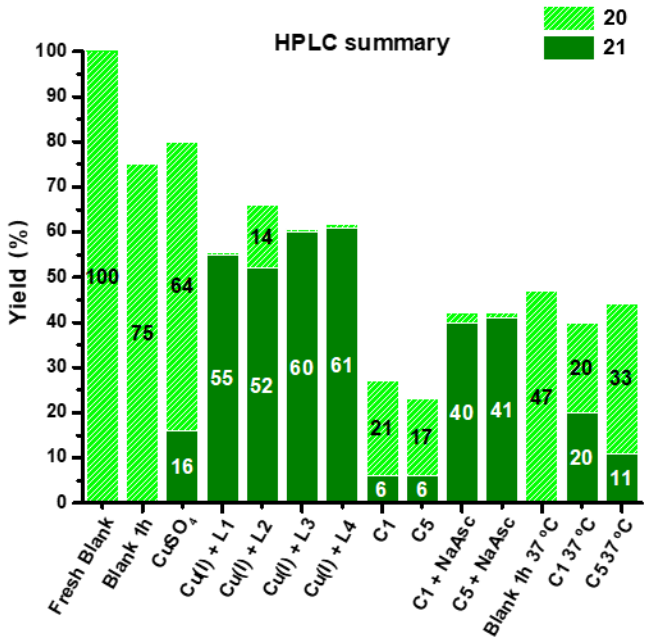

Figure S7. Summary of the CuAAC results obtained using HPLC measurements. Pale green bar corresponds to remaining azide.

S5. SPECTROSCOPIC ANALYSIS OF THE COPPER COMPLEXES

5.1 Monitoring the *in situ* formation of Cu(I) complexes with L3

UV-VIS: The complexes were prepared in situ, under air, by the sequential mixture of a fresh solution of $CuSO_4$ (0.4 mL, 100 mM in H_2O), **L3** (16.7 mg) and a fresh solution of sodium ascorbate (0.32 mL, 500 mM in H_2O) in a 2 mL eppendorf tube containing 1.28 mL of H_2O. The mixture was stirred for 10 min.

Final concentrations: 20 mM $CuSO_4$ (1 equiv.), 20 mM **L3** (2 equiv.) and 80 mM sodium ascorbate (4 equiv.). For the experiments with 2 mM of copper, the mixture was diluted ten times.

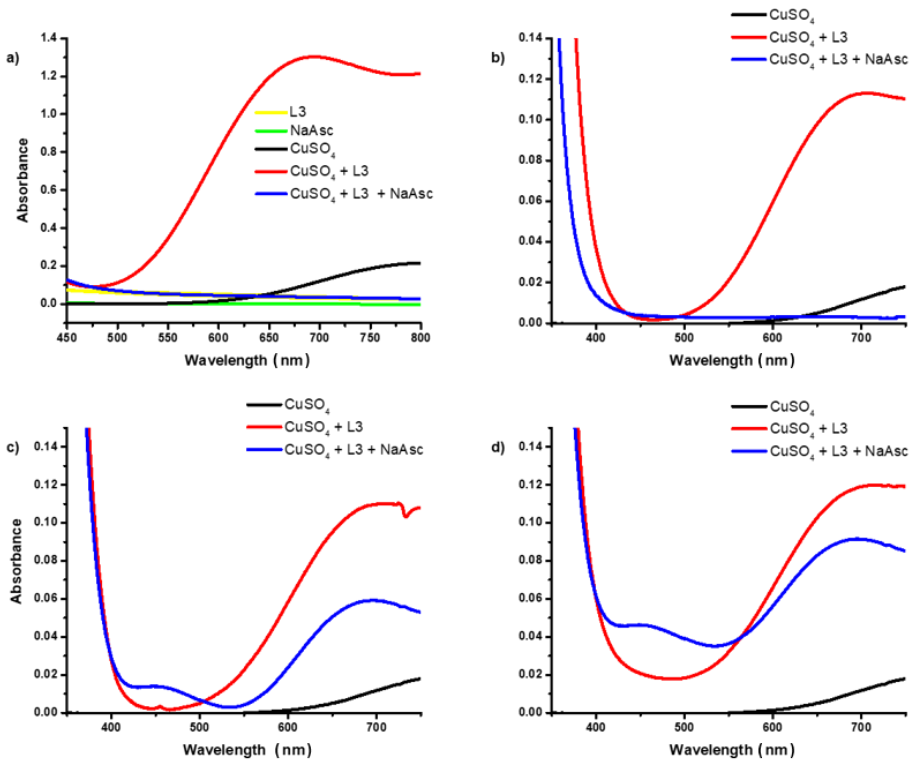

Figure S8. UV spectra at different times. (a) After 10 min of mixing, final concentration of 20 mM of the copper source and L3, and 80 mM of NaAsc; (b) After 10 min of mixing, final concentration of the copper source of 2 mM; (c) The same of (b) after 24 h; (d) The same of (b) after seven days.

NMR: The formation of the copper complexes with **L3** was also monitored by NMR. The experiment was performed in individual NMR tubes using D_2O as deuterated solvent at 25 °C: The complexes were prepared *in situ*, under the air, by the sequential addition in a screw capped vial containing 2 mL of deuterated water, $CuSO_4$ (3.2 mg), **L3** (8.3 mg) and sodium ascorbate (15.8 mg). The final concentration of the mixture is: 10 mM $CuSO_4$ (1 equiv), 10 mM **L3** (1 equiv.) and 40 mM sodium ascorbate (4 equiv.).

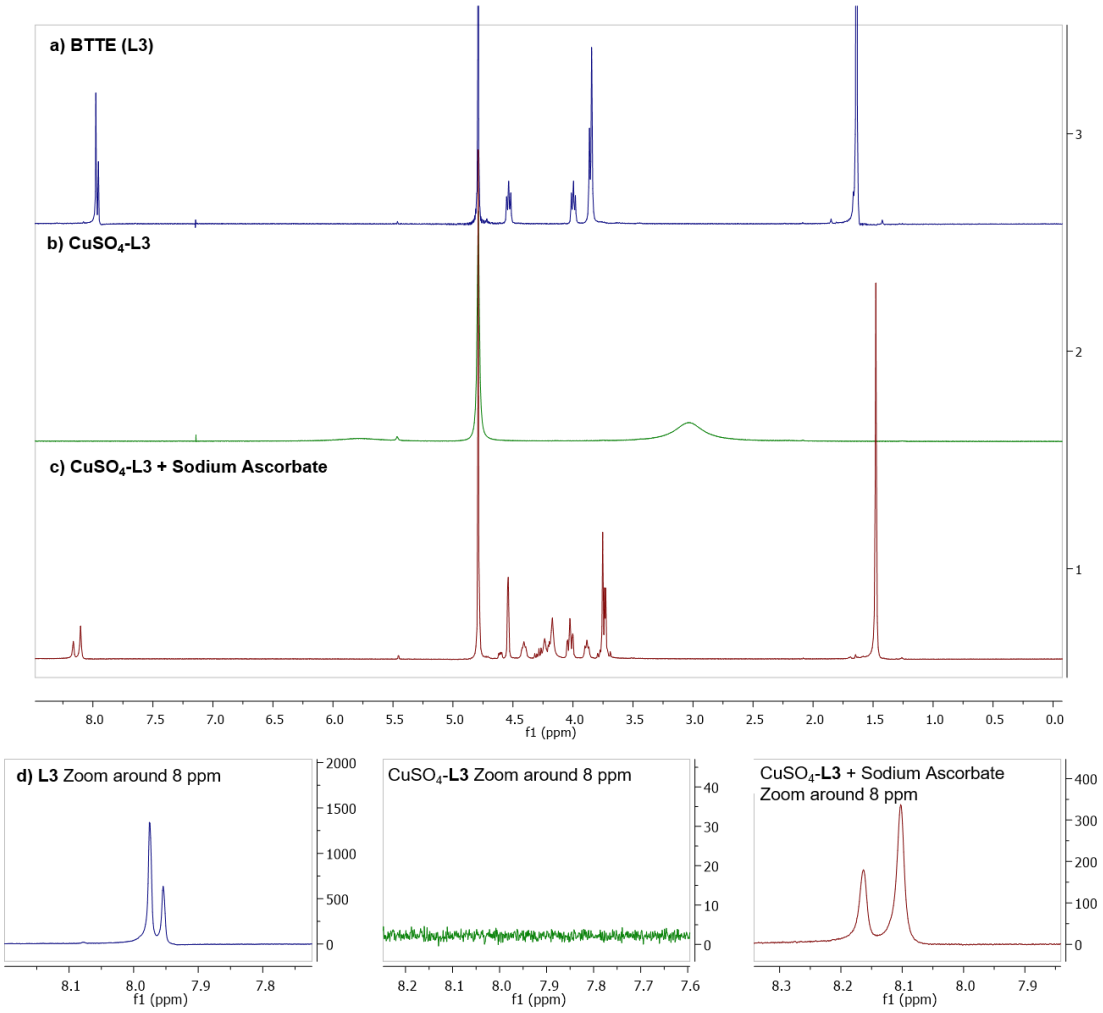

*Figure S9. [1]H NMR spectra (300 MHz) for the in situ made copper complex using **L3** as ligand in D_2O. (a) Spectrum of **L3** ligand (10 mM, blue line); (b) Spectrum of Cu(II) complex with **L3** (10 mM **L3** and 10 mM of $CuSO_4$, green line); (c) Spectrum of the previous mixture after addition of the reductant (10 mM **L3**, 10 mM of $CuSO_4$ and 40mM of sodium ascorbate, red line). NaAsc was directly added to the D_2O solution containing the ligand **L3** and $CuSO_4$, in the NMR tube under N_2; (d) The triazole proton signal of **L3** ligand reappeared at 8.2-8.1 ppm after addition of NaAsc, confirming the presence of diamagnetic Cu(I) species. (d) The triazole proton signal of **L3** ligand reappeared at 8.2-8.1 ppm after addition of NaAsc, confirming the presence of diamagnetic Cu(I) species.*

EPR: The studies were performed at 25 °C. For the initial experiment, a solution of $CuSO_4$ (10 mM, H_2O, 1 equiv.) was mixed with one equivalent of ligand **L3** (10 mM, H_2O, 1 equiv.) and stirred for 10 min. After the EPR measurement at 120 K, 1.1 equiv. of sodium ascorbate (25 mM in H_2O) was added, and the EPR immediately measured. Another measurement was made after addition of other 0.9 equiv. of sodium ascorbate.

USC UNIVERSIDADE DE SANTIAGO DE COMPOSTELA

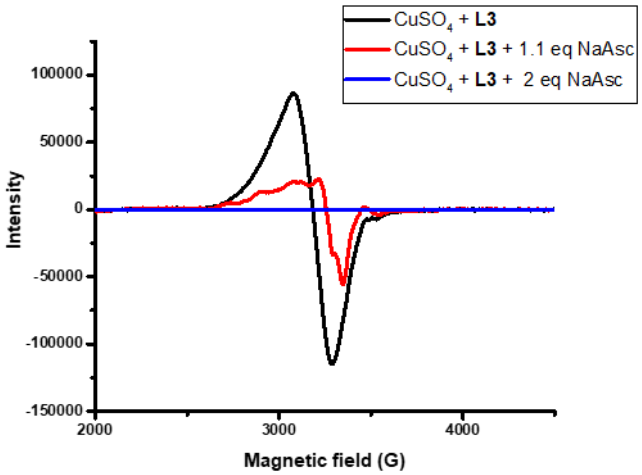

*Figure S10. EPR studies of the formation of copper complexes with **L3**.*

5.2. Predefined Cu(I) complexes C1 and C5. Comparison of their stability by EPR measurements

An initial solution of 10 mM of complexes **C1** or **C5** complexes in DMSO was used for the measurements, without paying any special effort to prevent the presence of air. Samples were taken from this solution at increasing times and frozen in an EPR capillary with liquid nitrogen.

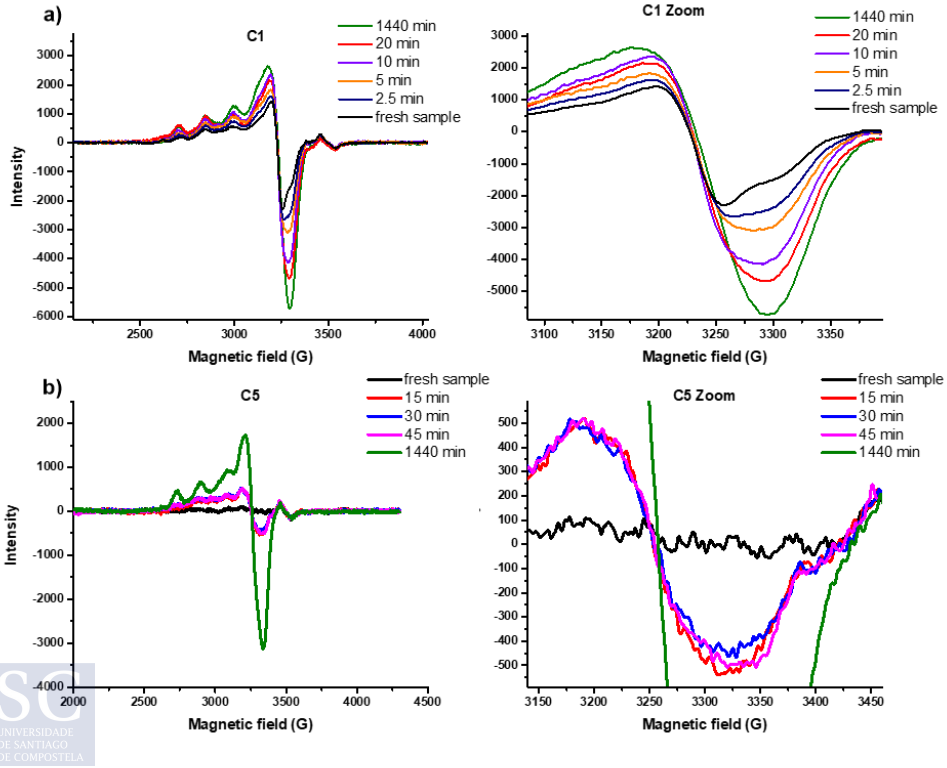

*Figure S11. a) EPR measurements of **C1** and enlarged image and b) EPR measurements of **C5** and enlarged image.*

NMR experiments carried out at time zero, and after 24 h, confirmed the full conversion to the oxidized species after that time, with the disappearance of the signals owing to the paramagnetic behavior of Cu(II). Samples of 24 h were prepared without any taking any special precaution to avoid the oxidation by air.

[Cu(TPA)]PF_6 (C1) in MeCN-d_3

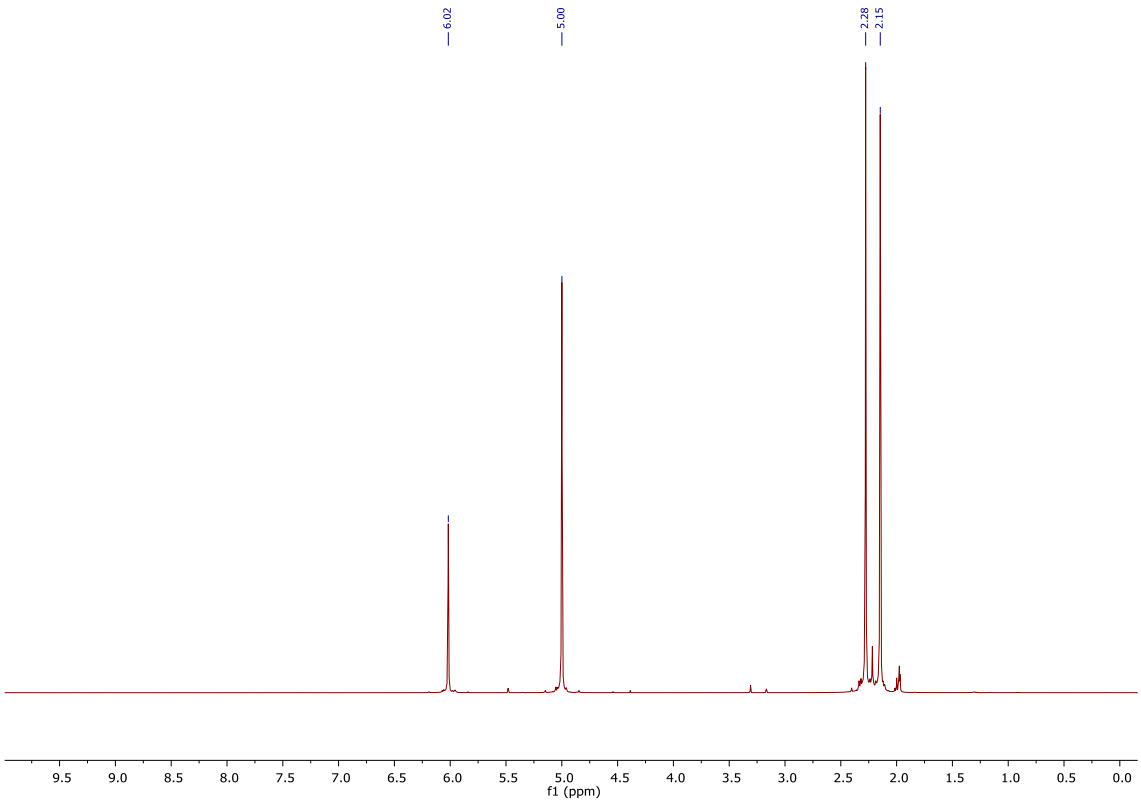

USC
UNIVERSIDADE DE SANTIAGO DE COMPOSTELA

[Cu(TPA)]PF_6 (C1) in MeCN-d_3 24 h

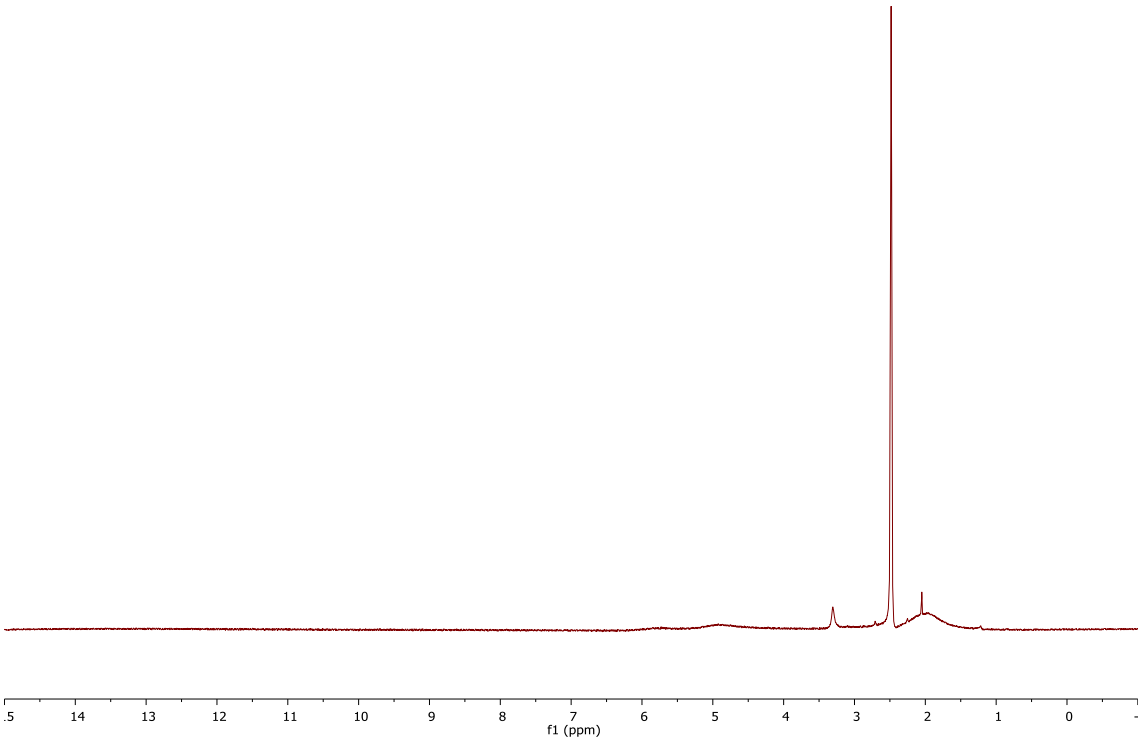

[Cu(BTTE)]PF_6 (C5) in DMSO-d_6

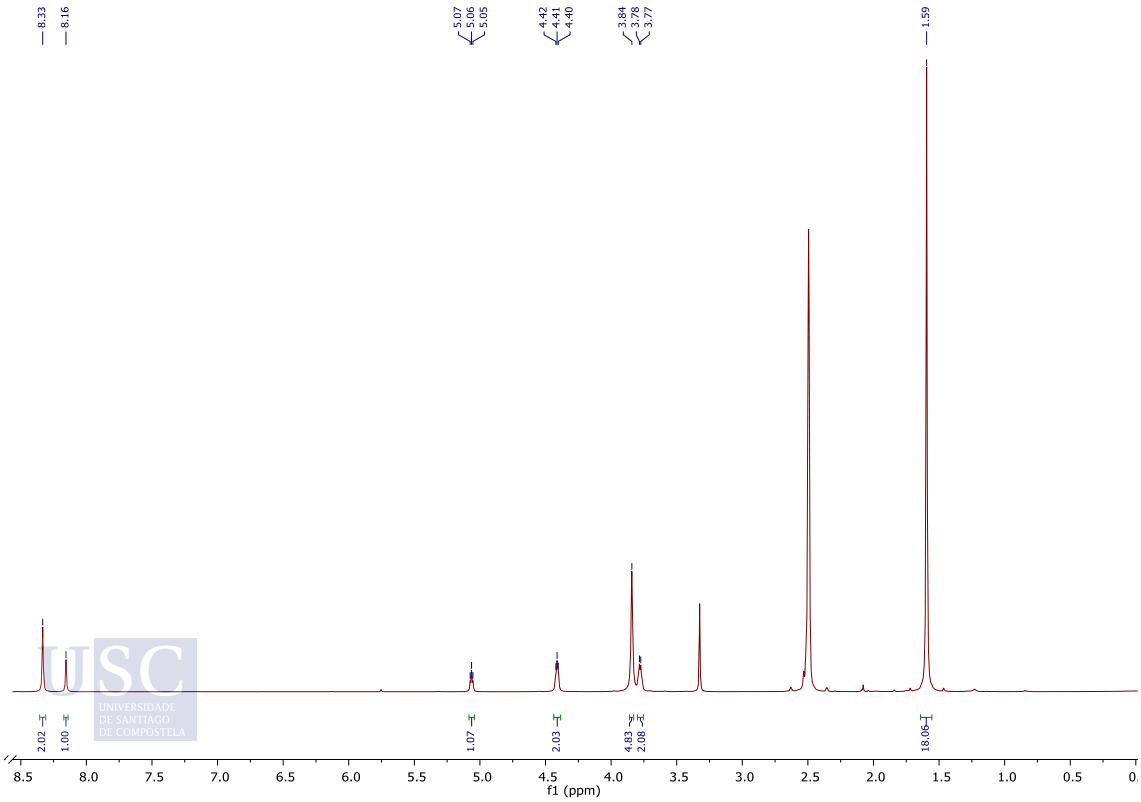

[Cu(BTTE)]PF_6 (C5) in DMSO-d_6 24 h

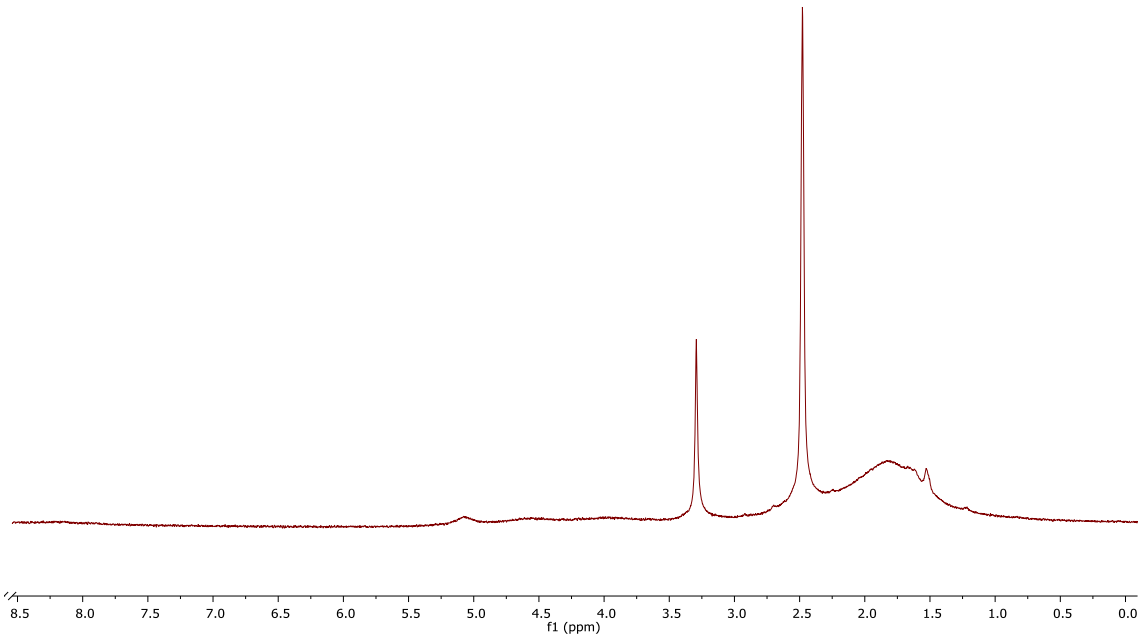

*Figure S12. NMR spectra of solutions of complex **C1** and complex **C5** at the beginning and after 24 h.*

S6. SELECTED NMR SPECTRA

BBTE (L2)

^{1}H NMR (500 MHz, $CDCl_3$)

USC
UNIVERSIDADE DE SANTIAGO DE COMPOSTELA

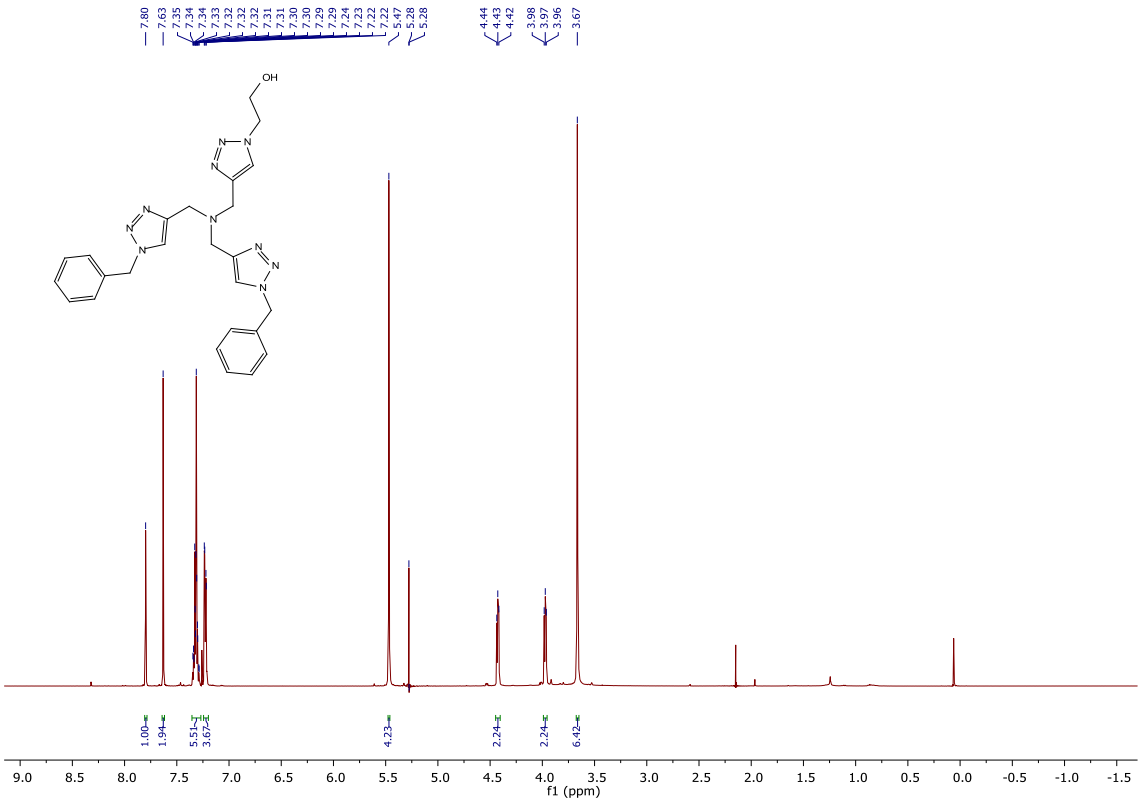

^{13}C NMR (126 MHz, $CDCl_3$)

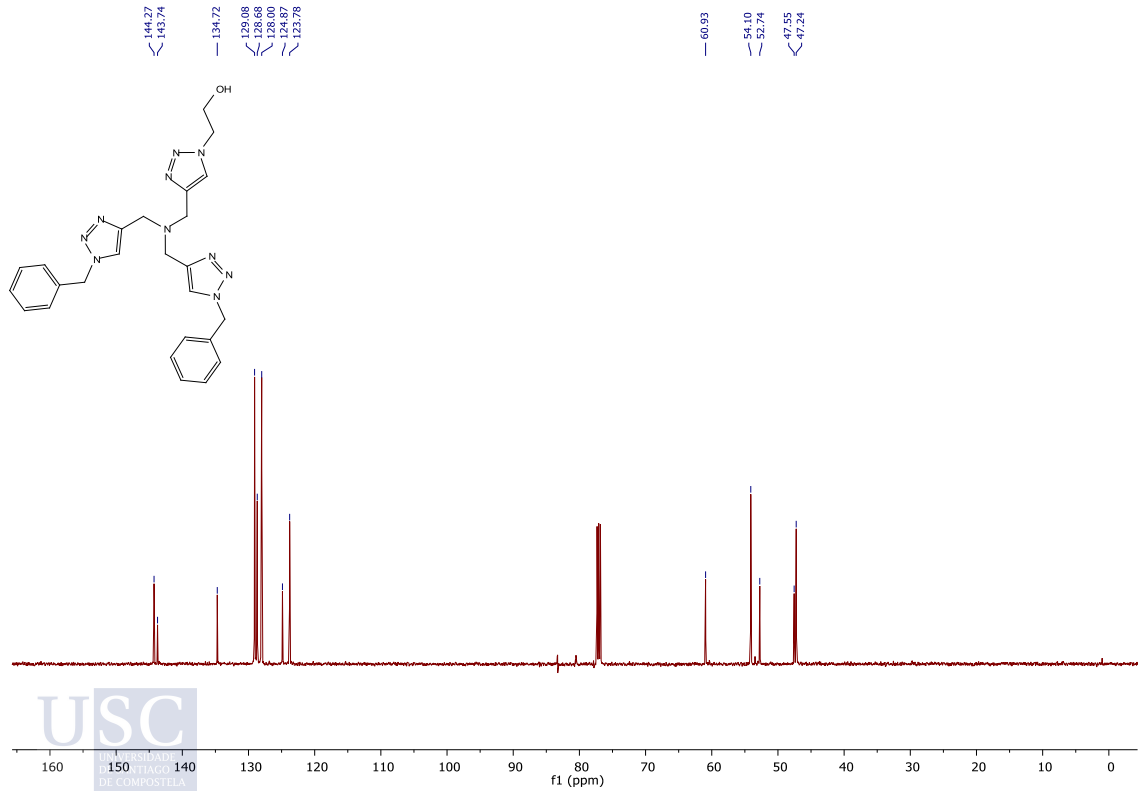

USC UNIVERSIDADE DE SANTIAGO DE COMPOSTELA

DEPT-135 (500 MHz, $CDCl_3$)

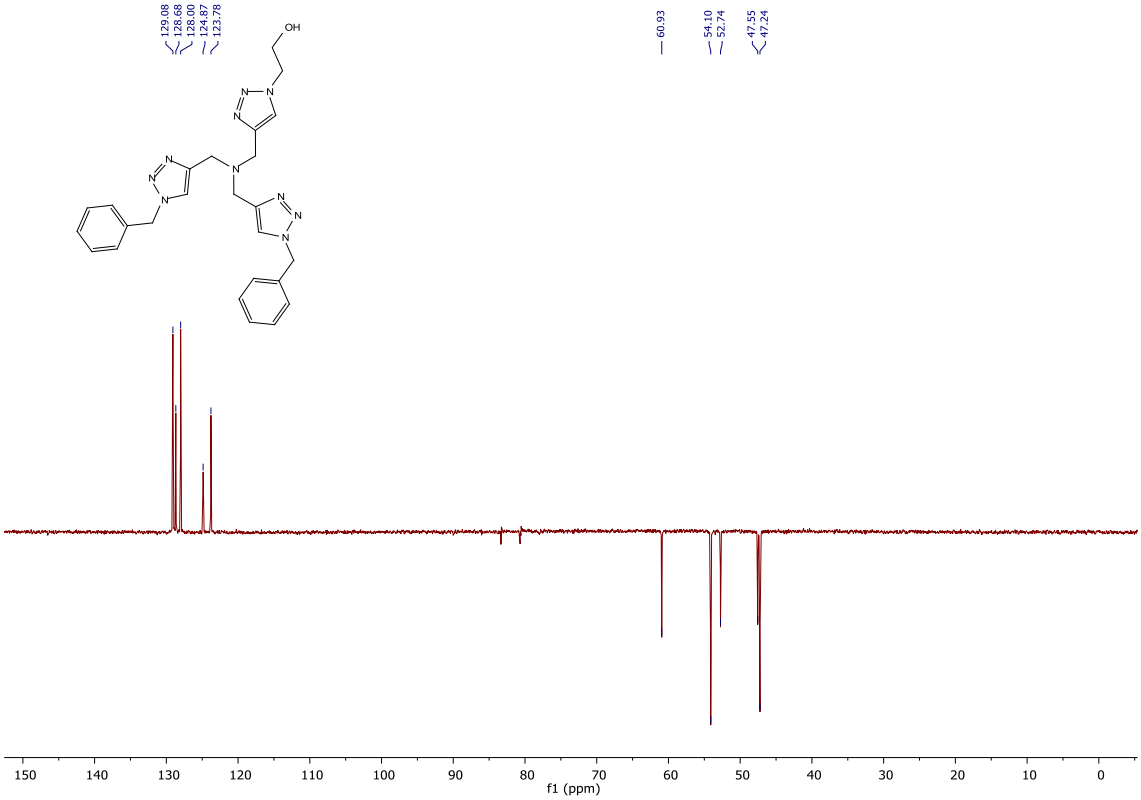

BTTE-P (L4)

^{1}H NMR (500 MHz, $CDCl_3$)

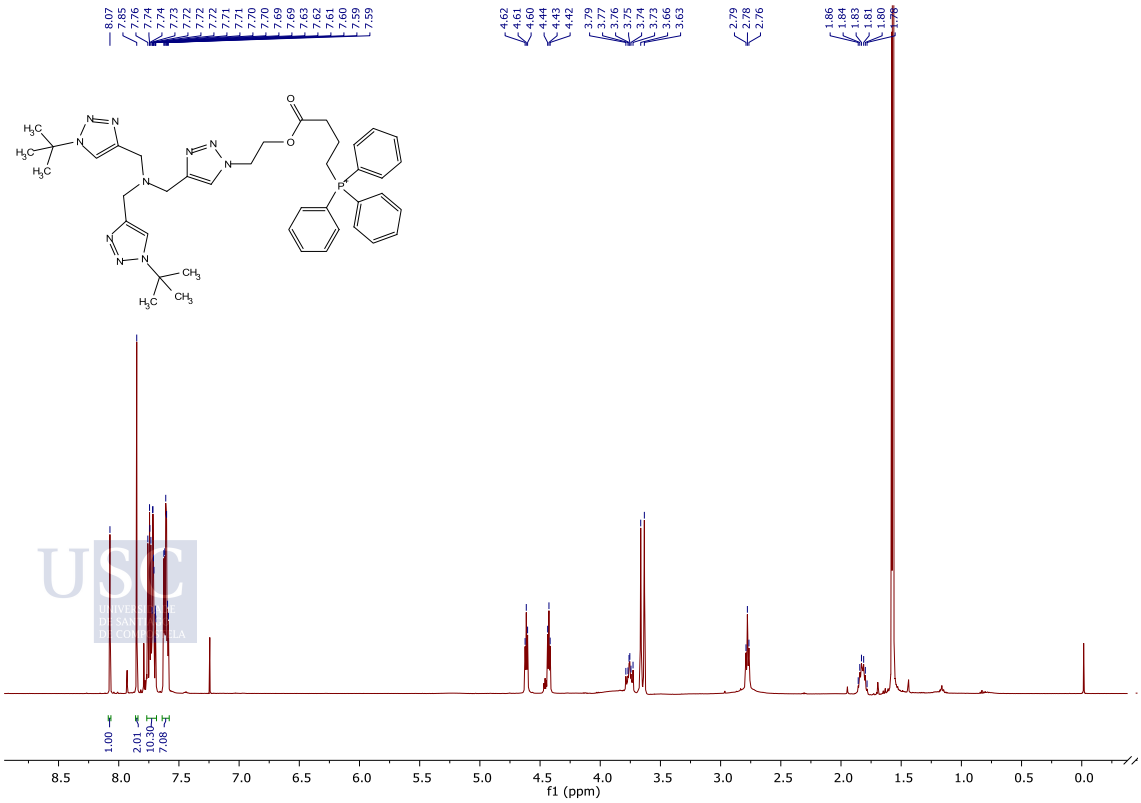

^{13}C NMR (126 MHz, $CDCl_3$)

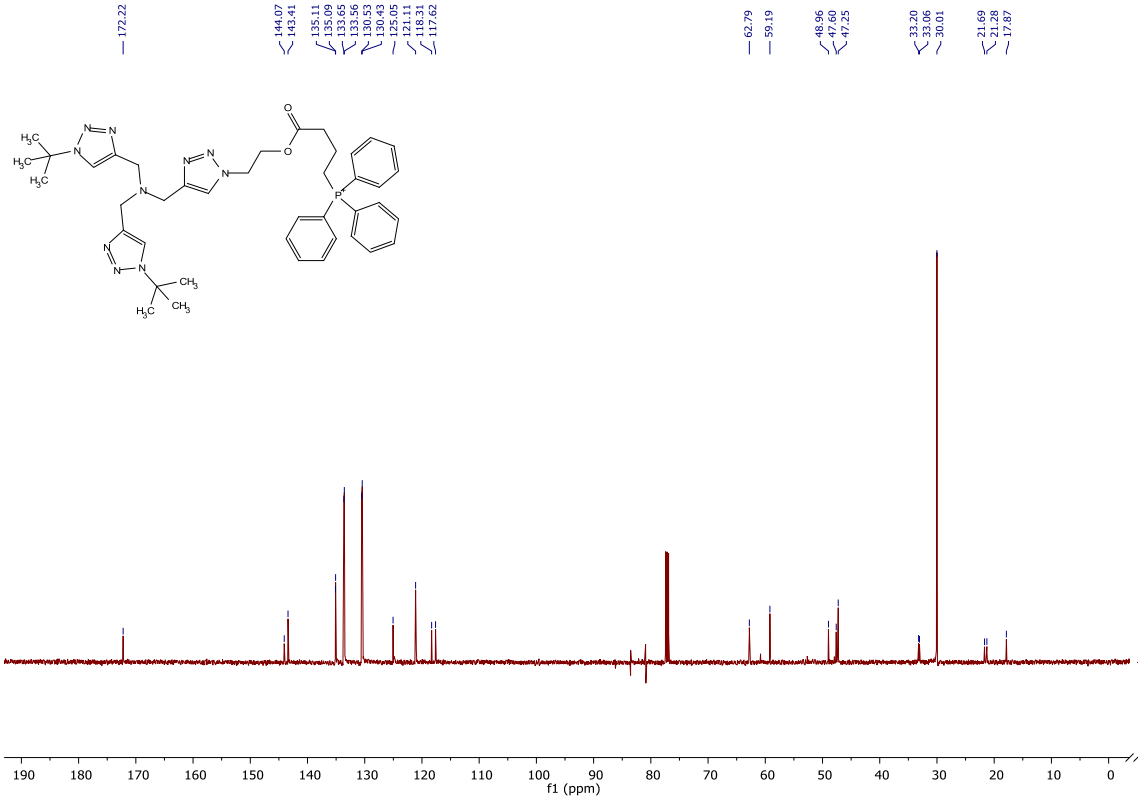

DEPT-135 (500 MHz, $CDCl_3$)

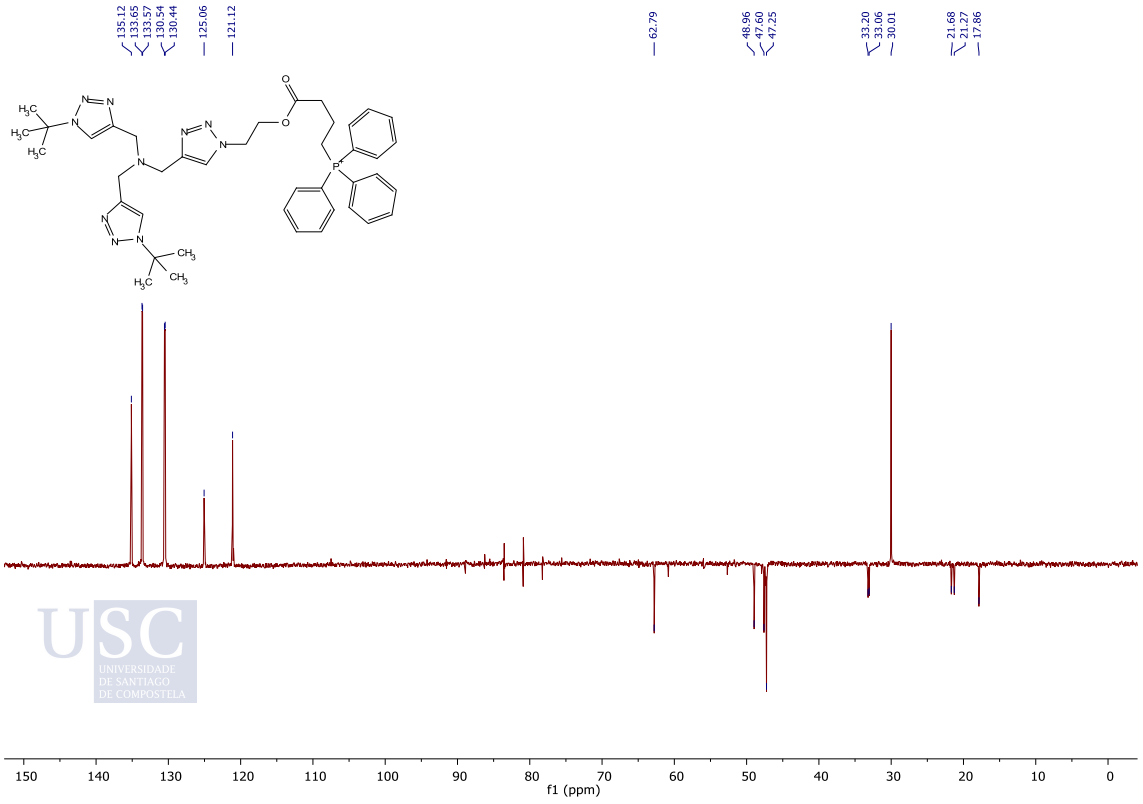

USC UNIVERSIDADE DE SANTIAGO DE COMPOSTELA

[Cu(BTTE)]PF_6 (C5)

^{1}H NMR (500 MHz, $CDCl_3$)

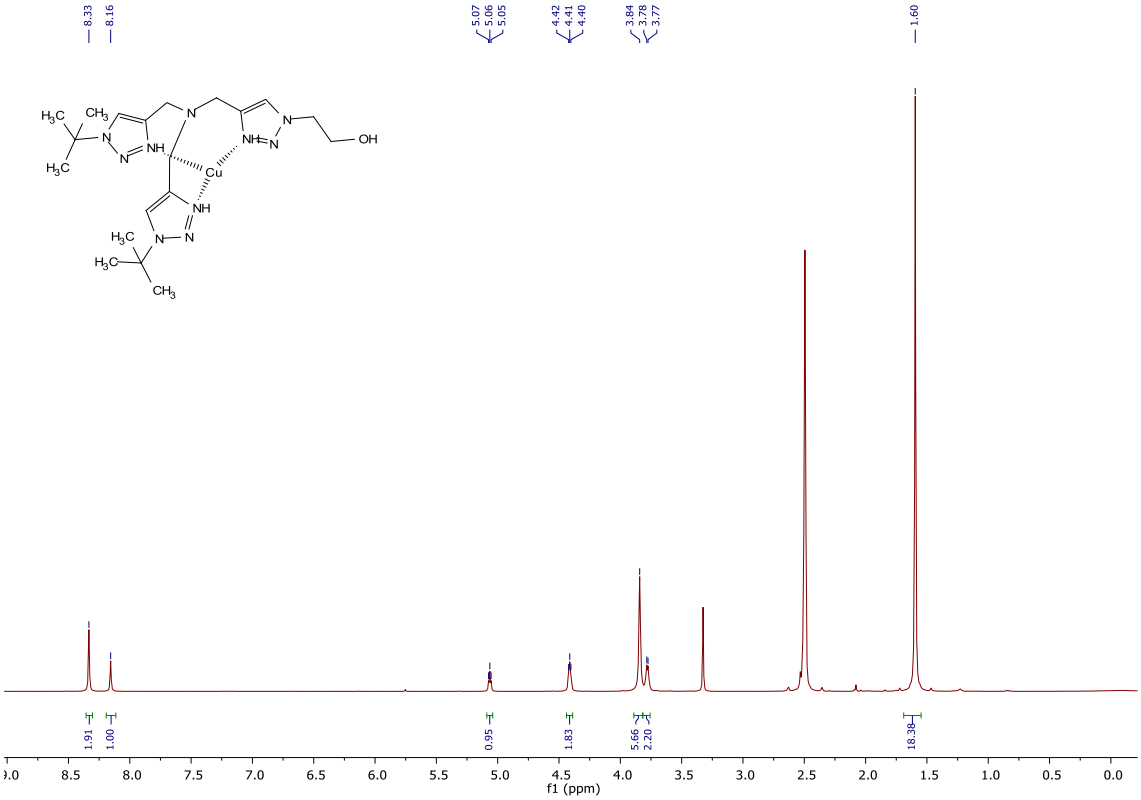

^{13}C NMR (126 MHz, $CDCl_3$)

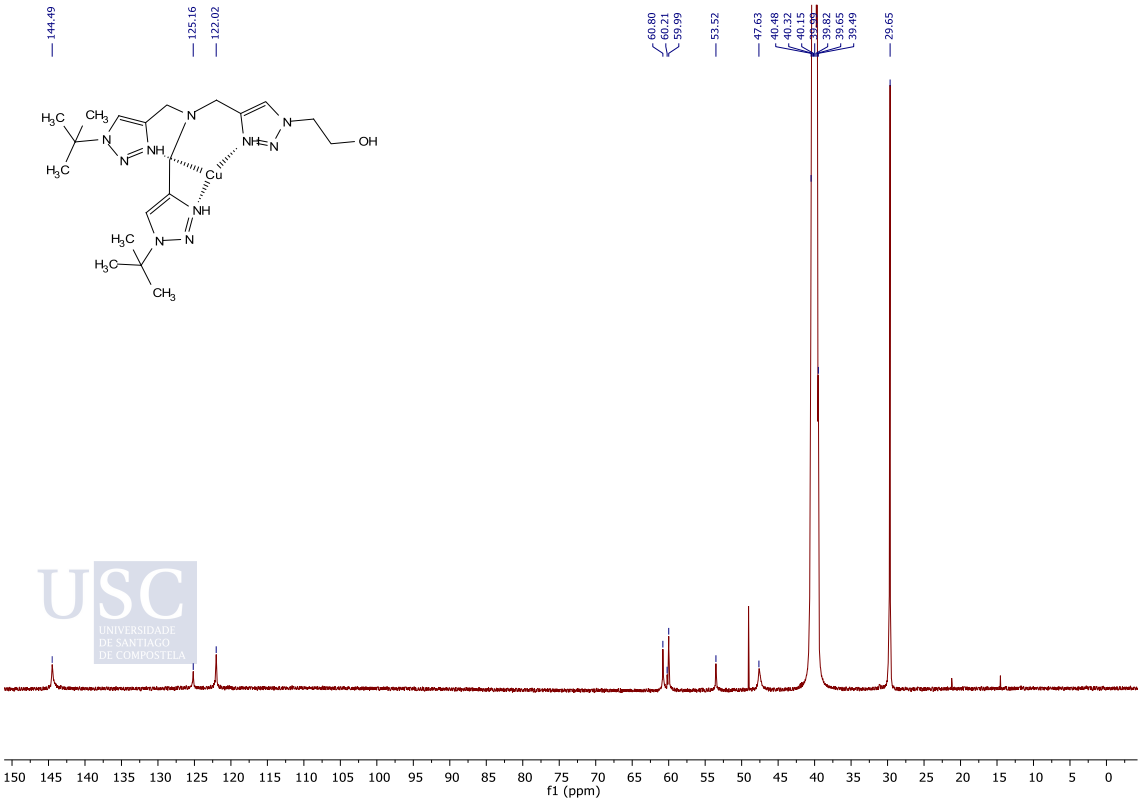

USC UNIVERSIDADE DE SANTIAGO DE COMPOSTELA

S7.- CuAAC EXPERIMENTS IN LIVING CELLS

7.1.- Reactions with *in situ* prepared complexes containing ligands L1-L4

The complexes were prepared as follows: in a 500 µL eppendorf tube were successively added 52 µL of MilliQ-H_2O, 1.875 µL of $CuSO_4$ (100 mM in H_2O) and 18.75 µL of the corresponding ligand (20 mM in H_2O). The solution was kept 1 h at room temperature. Then, 2.34 µL of sodium ascorbate (500 mM in H_2O) were added to the solution, and the mixture incubated for 30 min at room temperature. The final concentration of copper was 2.5 mM. Cells growing on glass coverslips were incubated with the *in situ* made copper complex with ligands **L1-L4** (12 µL of the above solution) in 388 µL of DMEM for 30 minutes, for a final copper concentration of 75 µM. Cells were then washed twice with 400 µL of DMEM and incubated with a solution of propargyl alcohol (200 µM) and anthracenyl azide (**20**) (100 µM) in 400 µL of DMEM for 1 hour. Prior to observation by fluorescence microscopy, the samples were washed twice with 400 µL of DMEM. The coverslips were observed "in vivo" in a fluorescence microscope equipped with adequate filters. Digital pictures of the different samples were taken under identical conditions of gain and exposure.

7.2.- Catalysis with predefined complexes C1-C5

A fresh solution of each catalyst (10 mM in DMSO) in a 2 mL eppendorf tube was prepared before the experiment. Cells growing on glass coverslips were incubated with either catalyst **C1-C5** (50 µM, 2 µL of the fresh solution) in 398 µL of DMEM for 30 minutes. Cells were then washed twice with 400 µL of DMEM and incubated with the mixture of propargyl alcohol (200 µM) and anthracenyl azide (**20**) (100 µM) in 400 µL of DMEM for 1 hour. Prior to observation by fluorescence microscopy, the samples were washed twice with 400 µL of DMEM. The coverslips were observed in a fluorescence microscope equipped with adequate filters. Digital pictures of the different samples were taken under identical conditions of gain and exposure.

S8.- VIABILITY ASSAYS

The toxicity of the *in situ* made copper complexes with ligands **L1-L4**, as well as of the defined complexes **C1-C5** was analyzed by MTT assays in HeLa cell line as follows: 150000 cells per well were seeded in 96 well plates one day before treatment with different concentrations of the catalysts in 100 µL of DMEM. After the adequate time of incubation (2 h or 12 h), Thiazolyl Blue Tetrazolium Bromide (Sigma) was added to the cell culture medium to a final concentration of 0.5 mg mL^{-1}. Cells were then incubated for 4 h to allow the formation of formazan precipitates by metabolically active cells. A detergent solution of 10% SDS (sodium dodecyl sulfate) and 0.01 M HCl was then added and the plate was incubated overnight at room temperature to allow the solubilization of the precipitates.

The quantity of formazan in each well (directly proportional to the number of viable cells) was measured by recording changes in absorbance at 570 nm in a microtiter plate reading spectrophotometer (Tecan Infinite 200 PRO).

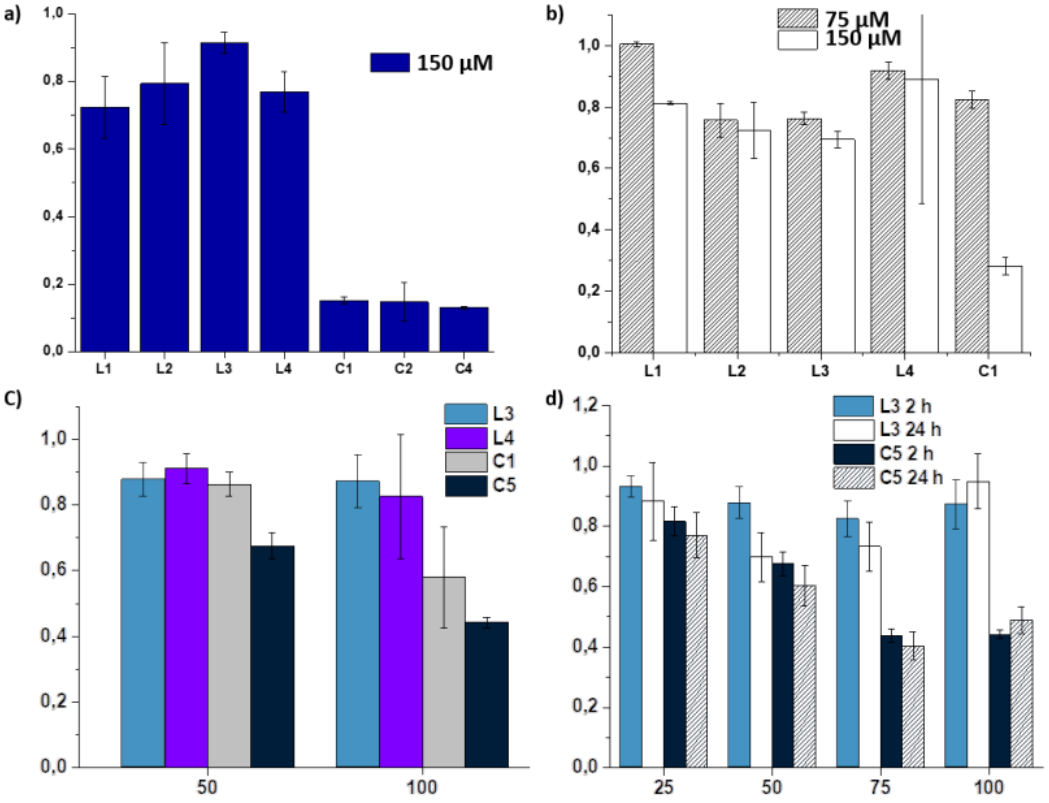

*Figure S13. Viability Assays (MTT). HeLa cells were incubated in cell culture medium containing the indicated amounts of the copper complexes: (a) In situ made Cu(I) complexes with **L1-L4** and predefined complexes **C1**, **C2** and **C4** for 12 h; (b) In situ made Cu(I) complexes with **L1-L4** for 2 h; (c) in situ made Cu(I) complexes with **L3** and **L4** and predefined complexes **C1** and **C5**, after 2 h; (d) in situ made Cu(I) complex with L3 and predefined complex **C5** after 2 h and 24 h. The viability is expressed as the fold change of the absorbance value with respect to untreated cells (value 1.0).*

S9.- ICP ANALYSIS

For the ICP measurements, a total of $3x10^6$ HeLa cells growing in 6 well plates were treated with each copper complex. Each well was incubated with the different *in situ* made copper complexes with **L1- L4** (75 µM, 22.5 µL of the fresh solution) in 728 µL of DMEM, or the different defined Cu(I) complexes **C1-C5** (50 µM, 3.75 µL of the fresh solution) in 747 µL of DMEM for 1 h. Prior to digestion, the samples were washed with 750 µL of DMEM and then twice with 750 µL of PBS. The obtained fractions were digested in duplicate in 500 µL of HNO_3 (70%) by microwave heating and analyzed. For the membrane protein extraction, after incubation with the copper complexes for 1 h, the samples were washed with 750 µL of DMEM and then twice with 750 µL of PBS. Then a commercial kit (MemPER Plus Membrane Protein Extraction Kit -Thermo-Fisher Scientific-) was used to isolate membrane and cytosolic cellular fractions.

9.1 Procedure for Membrane Protein Extraction from HeLa cells with Mem-PER Plus Membrane Protein Extraction Kit

3×10^6 cells were resuspended in 500 µL of DMEM by scraping the cells off the surface of the plate with a cell scraper. Then, the harvested cell suspension was centrifuged at 300 × g for 5 minutes. The cell pellet was washed with 300 µL of Cell Wash Solution and centrifuged at 300 × g for 5 minutes. Carefully the supernatant was removed and discarded. The cells were resuspended in 500 µL of Cell Wash Solution, transferred to a 0.5 mL Eppendorf and centrifuged at 300 × g for 5 minutes. The supernatant was discarded. After addition of 150 µL of Permeabilization Buffer to the cell pellet, the eppendorf was vortexed briefly to obtain a homogeneous cell suspension and then incubated 10 minutes at 4 °C with constant mixing. The permeabilized cells were centrifuged for 15 minutes at 16,000 × g. The supernatant containing cytosolic proteins was carefully removed and transferred to a new eppendorf. Then, 200 µL of Solubilization Buffer were added to the pellet and resuspended by pipetting up and down. The eppendorfs were incubated at 4 °C for 30 minutes with constant mixing. Finally, the eppendorfs were centrifuged at 16,000 × g for 15 minutes at 4 °C and the supernatant containing solubilized membrane and membrane-associated proteins was transferred to a new eppendorf. The obtained fractions were digested in duplicate in HNO_3/H_2O_2 by microwave heating and analyzed.

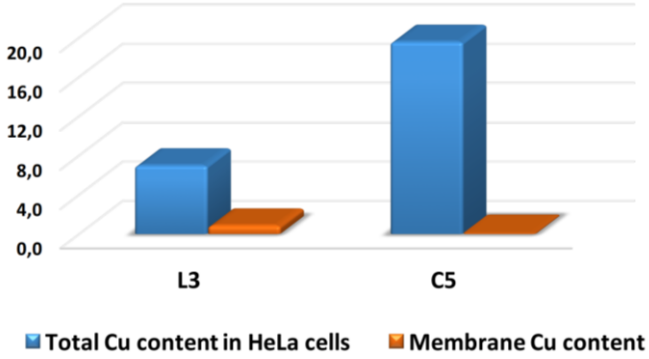

Figure S14. ICP-MS results of the copper accumulated in the membrane of HeLa cells.

S10.- FLOW CYTOMETRY STUDIES

Cytometry studies were performed in HeLa cells: 200000 cells per well were seeded in 96 well plates one day before treatment. Then, it was followed the same protocol described for the experiments in living cells, scaling the experiment to a final volume of 100 µL of DMEM. After the incubation time, cells were washed twice with 100 µL of PBS, harvested with 100 µL of trypsin/EDTA for 15 min and resuspended in 2% FBS in 100 µL of PBS buffer with 5 mM EDTA. The fluorescence was analyzed by flow cytometry. As observed in figure 72 of the main text, quantification by flow cytometry showed clear presence of the product using the violet laser and the emission filter (450/50).

S11.- QUANTIFICATION OF THE REACTION INSIDE LIVING CELLS

General Procedure: The CuAAC reaction of **20** and propargyl alcohol with different copper complexes in living cells was quantified by fluorescence measurements using a microplate reader. The experiments were performed in plates of 12 wells as follows: 100000 cells per well were seeded in 12 well plated two days before treatment with the copper complex and the substrates. For each complex the experiment was done by triplicate. To normalize the results, number of cells was measured after the experiments were performed. For this, after the incubation time with each complex, cells were washed twice with 400 µL of PBS, harvested with 100 µL of trypsin/EDTA for 5 min at 37 °C and resuspended in 300 µL of DMEM buffer. An aliquot of 50 µL was transferred to an 0.500 mL Eppendorf and diluted with 450 µL of PBS. Then cells were measured with *Scepter^{TM} 2.0 Handheld Automated Cell Counter*.

11.1 Reactions with *in situ* prepared complexes containing ligand L3

The complexes were prepared as follows: in a 500 µL eppendorf tube were successively added 52 µL of MilliQ-H_2O, 1.875 µL of $CuSO_4$ (100 mM in H_2O) and 18.75 µL of **L3** (20 mM in H_2O). The solution was kept at room temperature for 1 h. Then, 2.34 µL of sodium ascorbate (500 mM in H_2O) were added to the solution, and the mixture incubated for 30 min at room temperature. The final concentration of copper was 2.5 mM. Cells growing on plates of 12 wells were incubated with the *in situ* made copper complex with ligand **L3** (8 µL of the above solution) in 392 µL of DMEM for 30 minutes, for a final copper concentration of 75 µM. Cells were then washed twice with 400 µL of DMEM and incubated with a solution of propargyl alcohol (200 µM) and anthracenyl azide (**20**) (100 µM) in 400 µL of DMEM for 1 hour. Prior to lysis, the samples were washed with 400 µL of DMEM followed by two washes with PBS (400 µL). Then 100 µL of a solution of 80% of MeOH in water were added to each well. After 5 min and pipetting up they were transferred to a microplate of 96 well. Cells were also incubated only with substrates 20 and propargyl alcohol for 1 h. These cells were treated in the same way and the lysates were used as negative control, to eliminate the fluorescent background signal. The results were analyzed by fluorescence measurements in a microplate reader (Tecan infinite F200Pro). Fluorescence data were obtained by using an excitation wavelength of 360 nm and recorded at 465 nm. Every measured value is the mean value of three aliquots.

USC UNIVERSIDADE DE SANTIAGO DE COMPOSTELA

11.2. Reactions with predefined complexes

A fresh solution of each catalyst (10 mM in DMSO) in a 2 mL eppendorf tube was prepared before the experiment. Cells growing on plate of 12 wells were incubated with catalyst **C** (25-50 µM, 2 µL of the fresh solution) in 398 µL of DMEM for 30 minutes. Cells were then washed twice with 400 µL of DMEM and incubated with the mixture of propargyl alcohol (200 µM) and anthracenyl azide (**20**) (100 µM) in 400 µL of DMEM for 1 hour. Prior to lysis, the samples were washed with 400 µL of DMEM followed by two washes with PBS (400 µL). Then 200 µL of a solution of 80% of MeOH in water were added to each well. After 5 min and pipetting up they were transferred to a microplate of 96 well.

11.3. Calibration

Calibration experiments were performed in a 96 wells plate by addition of increasing quantities of a fresh solution of 1-(9-anthracenylmethyl)-1H-1,2,3-triazole-4-methanol **21** (5mM in DMSO) in a solution of 80% of MeOH in water. Higher concentration results in the precipitation of the triazole **21**. The experiments were performed by triplicate, and measured in the fluorescence microplate reader (excitation: 360 nm, emission: 465 nm). The fluorescence results were processed with OriginPro 2016 to obtain the calibration equation needed to quantify the fluorescence of the experiments in living cells.

11.4. Cellular uptake of substrate 20

To calculate the amount of substrate **20** internalized by the cell the following experiment was performed:

The experiments were performed in plates of 100 mm as follows:

100000 cells per well were seeded in 100 mm plated two days before treatment with substrate **20**. For each measurement, four plates were used.

Cells growing on plate of 100 mm were incubated with the substrate **20** (1.2 µL) in 4 mL of DMEM for 1 hour. Prior to lysis, the samples were washed with 1 mL of DMEM followed by two washes with PBS (1 mL). Then 1 mL of a solution of 80% of MeOH in water was added. After 5min and pipetting up this solution was transferred to a 1.5 mL Eppendorf. Finally, we obtained 4 mL of lysates from the four plates we used. To 982.6 µL of this sample was added 17.4 µL of a stock solution of coumarin 50 mM as internal standard. The sample (10 µL) was injected in the HPLC-UV. Method: H_2O/MeCN gradient 95/5 ⟶ 5/95 in 12 min, then 3 min 100% MeCN.

The calibration of azide **20** was performed in the same HPLC vial, using MeCN as solvent. The different samples were prepared from a 5 mM fresh stock solution of the analyte in DMSO. Coumarin (870 μM as final concentration) was used as internal standard. The areas obtained from the chromatogram were processed with OriginPro 2016 to obtain the calibration equation and applied to quantify the absorbance of the experiments. No differences were appreciated when MeOH or MeCN were used as solvent.

To normalize the results, number of cells was measured after the experiments were performed. For this, after the incubation time, cells were washed twice with 1 mL of PBS, harvested with 1 mL of trypsin/EDTA for 5 min at 37 ºC and resuspended in 3 mL of DMEM buffer. An aliquot of 50 μL was transferred to an 0.500 mL Eppendorf and diluted with 450 μL of PBS. Then cells were measured with *Scepter™ 2.0 Handheld Automated Cell Counter*.

S12.- References

[1] K. Sivakumar, F. Xie, B. M. Cash, S. Long, H. N. Barnhill, Q. Wang, *Org. Lett.* **2004**, *6*, 4603.

[2] A. Herner, I. Nikic, M. Kállay, E. A. Lemke, P. Kele, *Org. Biomol. Chem.* **2013**, *11*, 3297.

[3] V. V. Sreenivasu Mummidivarapu, V. Kumar Hinge, K. Samanta, D. S. Yarramala, C. Pulla Rao, *Chemistry* **2014**, *20*, 14378.

[4] Y. C. Hsieh, J. L. Chir, H. H. Wu, P. S. Chang, A. T. Wu, *Carbohydr. Res.* **2009**, *344*, 2236.

[5] D. S. Del Amo, W. Wang, *J. Am. Chem. Soc.* **2010**, *132*, 16893.

[6] C. Besanceney-Webler, H. Jiang, T. Zheng, L. Feng, D. Soriano Del Amo, W. Wang, L. M. Klivansky, F. L. Marlow, Y. Liu, P. Wu, *Angew. Chem. Int. Ed.* **2011**, *50*, 8051; *Angew. Chem.* **2011**, *123*, 8201.

[7] M. Tomás-Gamasa, M. Martínez-Calvo, J. R. Couceiro, J. L. Mascareñas, *Nat. Commun.* **2016**, *7*, 1.

[8] S. Lal, J. McNally, A. J. P. White, S. Díez-González, *Organometallics* **2011**, *30*, 6225.

[9] S. Díez-González, S. P. Nolan, *Angew. Chem. Int. Ed.* **2008**, *47*, 8881; *Angew. Chem.* **2008**, *120*, 9013.

[10] E. Haldón, M. Delgado-Rebollo, A. Prieto, E. Álvarez, C. Maya, M. C. Nicasio, P. J. Pérez, *Inorg. Chem.* **2014**, *53*, 4192.

USC UNIVERSIDADE DE SANTIAGO DE COMPOSTELA

INTRACELLULAR RUTHENIUM-PROMOTED [2+2+2] CYCLOADDITIONS

TABLE OF CONTENTS

S1.- Experimental procedures and data

S2.- Synthesis of phtalanes and anthraquinone products in organic solvents

S3.- Selected NMR spectra

S4.- Ruthenium promoted cycloaddition in different biological media

S5.- Spectroscopy studies

S6.- Viability assays

S7.- Ruthenium promoted experiments inside living cells

S8.- Identification studies using LC/MS

S9.- Permeabilization experiments

S10.- ICP analysis

S11.- References

USC
UNIVERSIDADE DE SANTIAGO DE COMPOSTELA

USC
UNIVERSIDADE
DE SANTIAGO
DE COMPOSTELA

S1.- EXPERIMENTAL PROCEDURES AND DATA

2,2'-(Ethyne-1,2-diyl)bis(1-(but-3-ynyl)pyridinium)bis(trifluoromethanesulfonate) (**24**),[1] 6,7,12,13-tetrahydro-5,14-diaza[5]helicinium trifluoromethanesulfonate (**25**),[1] (**Ru3**),[2] (**Ru4**),[3] [{Ru(η3 : η3-$C_{10}H_{16}$)Cl(μ-Cl)}$_2$] (**Ru5**),[4] [Ru(η^3 : η^3-$C_{10}H_{16}$)Cl(μ^2-*O*,*O*-O_2CMe)] (**Ru6**)[4] and 4,5-dimethoxyphthalaldehyde (**33**)[5] were synthesized according to literature procedures and spectroscopic data are in agreement with the bibliographic ones.

1.1.- Synthesis of substrates 31, 37 and 38

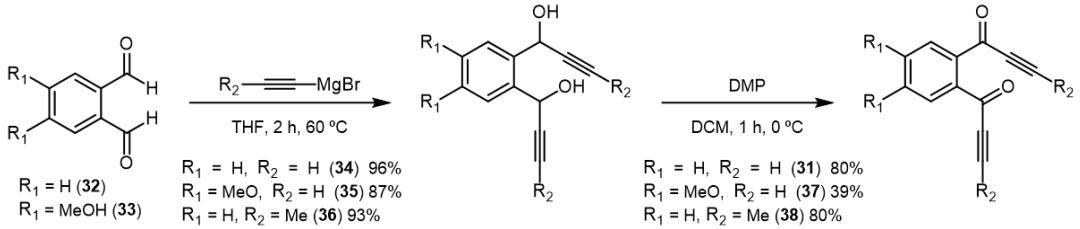

1.1.1.- General procedure for the synthesis of 34, 35 and 36

Procedure adapted from Nishibayashi *et al*.[6]

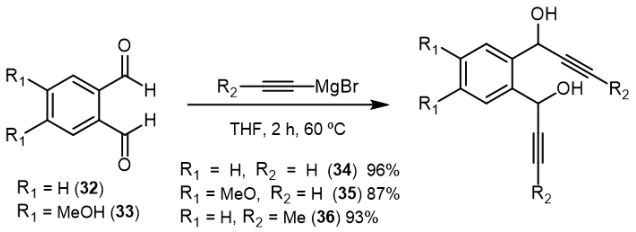

To a flame-dried Schlenk flask containing a 0.5 M solution of the corresponding ethynylmagnesium bromide in THF (20.0 mL, 10.0 mmol, 3.9 equiv.), was added at room temperature *o*-phthalaldehyde (350.0 mg, 2.6 mmol, 1.0 equiv.), and the resulting mixture was stirred at 60 °C for 2 h. The reaction was treated with NH_4Cl sat. (10.0 mL), H_2O (40.0 mL) and extracted with EtOAc (3 x 30.0 mL). The combined organic layers were dried over anhydrous $MgSO_4$ and concentrated under reduced pressure. The residue was purified by flash chromatography on silica gel using Hex / EtOAc 7:3 as eluent. The products were obtained as white solids.

Spectroscopic data are in consonance with those reported in the bibliography.[7]

USC UNIVERSIDADE DE SANTIAGO DE COMPOSTELA

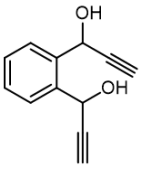

1,1'-(1,2-Phenylene)bis(prop-2-yn-1-ol) (34). White solid. $\mathbf{R_f}$ = 0.2 (Hex / EtOAc 7:3). **Yield** = 96% (2.5 mmol, 466.0 mg). **^{1}H NMR** (300 MHz, $CDCl_3$): δ 7.84 (m, 2H), 7.66 (m, 1H), 7.41 (m, 2H), 7.38 (m, 1H), 5.99 (s, 1H), 5.85 (s, 2H) 3.84 (s, 1H), 3.41 (s, 2H), 2.74 (d, *J* = 2.2 Hz, 2H), 2.72 (d, *J* = 2.3 Hz, 1H). Resonances not specifically assigned to different diastereoisomers.

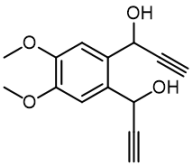

1,1'-(4,5-Dimethoxy-1,2-phenylene)bis(prop-2-yn-1-ol) (35). White solid. $\mathbf{R_f}$ = 0.2 (Hex / EtOAc 7:3). **Yield** = 87% (2.26 mmol, 556.5 mg). **^{1}H NMR** (500 MHz, $CDCl_3$): δ 7.32 (s, 1H), 6.90 (s, 2H), 5.22 (s, 3H), 4.71 (s, 1.5) 3.98 (s, 4.5H), 3.95 (s, 4.5H), 3.90 (s, 3H). Resonances not specifically assigned to different diastereoisomers.

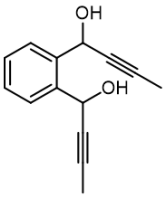

1,1'-(1,2-Phenylene)bis(but-2-yn-1-ol) (36). White solid. $\mathbf{R_f}$ = 0.2 (Hex / EtOAc 7:3). **Yield** = 93% (2.4 mmol, 520.0 mg). **^{1}H NMR** (500 MHz, $CDCl_3$): δ 7.81 (m, 2H), 7.62 (m, 2H), 7.37 (m, 2H), 7.34 (m, 2H), 5.96 (s, 2H), 5.82 (s, 2H), 3.66 (m, 2H), 3.24 (m, 2H), 1.94 (d, *J* = 2.2 Hz, 6H), 1.91 (d, *J* = 2.3 Hz, 6H). **^{13}C NMR** (126 MHz, $CDCl_3$): δ 138.7 (2xC), 138.3, 129.0, 129.0, 128.0, 84.3, 83.9, 78.5, 78.1, 63.6, 62.2, 3.9, 3.9. Resonances not specifically assigned to different diastereoisomers. **HRMS-ESI**: Calculated for $C_{14}H_{14}O_2Na^+$: 237.0886; found: 237.0885.

1.1.2.- General procedure for the synthesis of 31, 37 and 38

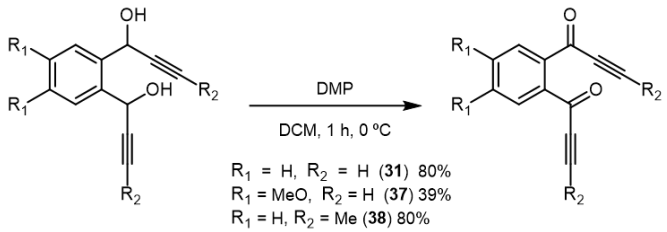

In a round bottom flask was dissolved the corresponding 1, 1'-(1,2-phenylene)-bis(prop-2-yn-1-ol) (2.2 mmol, 1.0 equiv.) in 25.0 mL of CH_2Cl_2. Dess-Martin reagent (DMP, 5.3 mmol, 2.2 g, 2.4 equiv.) was added in one portion at 0 °C and left stirring for 1 h. The reaction was treated with $NaHCO_3$ sat. (40.0 mL) and extracted with Et_2O (3 x 50.0 mL). The combined organic layers were dried over anhydrous $MgSO_4$ and concentrated under reduced pressure. The residue was purified by flash chromatography on silica gel using Hex / EtOAc 7:3 as eluent.

For *in-vitro* experiments, products required further purification by semipreparative-HPLC, using a column Luna C18 250 x 10 mm 5 µm and a flow rate of 3 mL / min at room temperature. For the solvent system, initial conditions H_2O / CH_3CN 95:5 were used, increasing the apolar character to H_2O / CH_3CN 5:95 in 20 min.

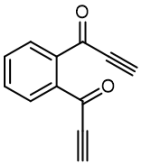

1,1'-(1,2-Phenylene)bis(prop-2-yn-1-one) (31). White solid $\mathbf{R_f}$ = 0.4 (Hex / EtOAc 7:3). **Yield** = 80% (1.7 mmol, 315.0 mg). **^{1}H NMR** (500 MHz, $CDCl_3$): δ 7.86 (dd, *J* = 5.6, 3.3 Hz, 2H), 7.67 (dd, *J* = 5.7, 3.3 Hz, 2H), 3.45 (s, 2H). **^{13}C NMR** (126 MHz, $CDCl_3$): δ 178.5, 138.3, 132.6, 130.2, 81.7, 80.7. **HRMS-ESI**: Calculated for $C_{12}H_7O_2^+$: 183.0441; found: 183.0442.

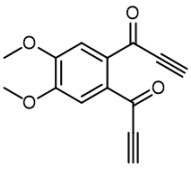

1,1'-(4,5-dimethoxy-1,2-phenylene)bis(prop-2-yn-1-one) (37). White solid. $\mathbf{R_f}$ = 0.5 (Hex / EtOAc 1:1). **Yield** = 39% (0.86 mmol, 207.8 mg). **^{1}H NMR** (500 MHz, $CDCl_3$): δ 7.31 (s, 2H), 4.00 (s, 6H), 3.40 (s, 2H). **^{13}C NMR** (126 MHz, $CDCl_3$): δ 177.45, 151.81, 132.17, 112.52, 80.92 (2xC), 56.44. **HRMS-ESI**: Calculated for $C_{14}H_{11}O_4^+$ = 243.0652; found: 243.0651.

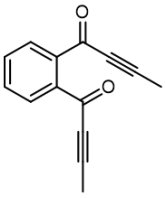

1,1'-(1,2-Phenylene)bis(but-2-yn-1-one) (38). White solid. $\mathbf{R_f}$ = 0.35 (Hex / EtOAc 7:3). **Yield** = 80% (1.7 mmol, 361.0 mg). **^{1}H NMR** (500 MHz, $CDCl_3$): δ 7.77 (dd, *J* = 5.7, 3.3 Hz, 2H), 7.56 (dd, *J* = 5.7, 3.2 Hz, 2H), 2.06 (s, 6H). **^{13}C NMR** (126 MHz, $CDCl_3$): δ 179.4, 139.0, 131.7, 129.5, 93.7, 79.9, 4.44. **HRMS-ESI:** Calculated for $C_{14}H_{11}O_2^+$: 211.0754; found: 211.0754.

1.2.- Synthesis of substrate 53

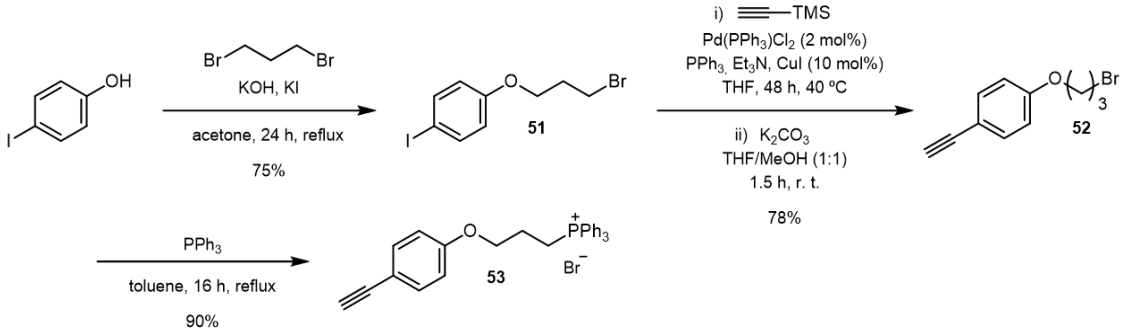

1.2.1.- Synthesis of 1-(3-bromopropoxy)-4-iodobenzene 51

Procedure adapted from Zhen *et al*.[8]

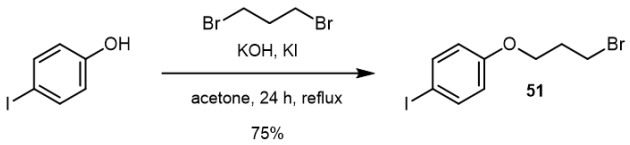

In a round bottom flask was dissolved 4-iodofenol (4.5 mmol, 1.0 g, 1.0 equiv.), 1,3-dibromopropane (22.7 mmol, 2.3 mL, 5.0 equiv.), KOH (22.3 mmol, 1.3 g, 4.9 equiv.) and KI (0.4 mmol, 68.2 mg, 0.1 equiv.) in 45.0 mL of acetone. The mixture was refluxed for 24 h. The solid was removed by filtration, and the solvent evaporated under reduced pressure.

The crude was purified by flash chromatography on silica gel using hexane as eluent. The product was obtained as a white solid.

Spectroscopic data are in consonance with those reported in the bibliography.[8]

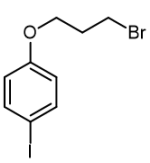

1-(3-Bromopropoxy)-4-iodobenzene. (51) White solid. $\mathbf{R_f}$ = 0.5 (Hex). **Yield** = 75% (3.4 mmol, 1150.8 mg). **^{1}H NMR** (300 MHz, $CDCl_3$): δ 7.56 (d, *J* = 9.0 Hz, 2H), 6.69 (d, *J* = 9.0 Hz, 2H), 4.07 (t, *J* = 5.8 Hz, 2H), 3.59 (t, *J* = 6.4 Hz, 2H), 2.31 (quint, *J* = 6.1 Hz, 2H).

1.2.2.- Synthesis of 1-(3-bromopropoxy)-4-ethynylbenzene 52

Procedure adapted from Hoover *et al*.[9]

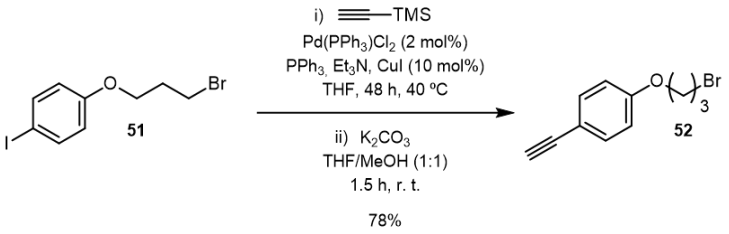

In a flame dried Schlenk was dissolved $Pd(Ph_3)_2Cl_2$ (0.03 mmol, 93.6 mg, 0.02 equiv.), triphenylphosphine (0.2 mmol, 44.4 mg, 0.1 equiv.), CuI (0.16 mmol, 30.0 mg, 0.1 equiv.) in 0.75 mL of distilled trimethylamine and 8.5 mL of distilled THF. The mixture was heated to 40 °C under inert atmosphere for 20 min. Afterwards, 1-(3-bromopropoxy)-4-iodobenzene (1.6 mmol, 528.0 mg, 1.0 equiv.) and ethynyltrimethylsilane (4.7 mmol, 0.7 mL, 3.0 equiv.) were added and allowed to react for 24 h. The crude was filtered through celite, concentrated under reduced pressure and purified by flash chromatography on silica gel using hexane as eluent. The product was obtained as an oil (81%, 1.3 mmol, 390.6 mg).

TMS removal protocol: In a round bottom flask was dissolved {[4-(3-bromopropoxy)phenyl]ethynyl}trimethylsilane (1.1 mmol, 347.0 mg, 1.0 equiv.) and K_2CO_3 (5.6 mmol, 790.0 mg, 5.0 equiv.) in 4.0 mL MeOH and 4.0 mL THF. The resulting mixture was stirred at room temperature for 2 h. The reaction was diluted with CH_2Cl_2 (30.0 mL) and the combined organic layers were washed with water (3 x 20.0 mL), brine (20.0 mL), dried over anhydrous $MgSO_4$ and concentrated under reduced pressure. The product was obtained as an oil.

USC UNIVERSIDADE DE SANTIAGO DE COMPOSTELA

Spectroscopic data are in consonance with those reported in the bibliography.[9]

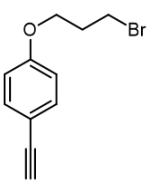

1-(3-Bromopropoxy)-4-ethynylbenzene 1-(3-bromopropoxy)-4-ethynylbenzene. (52). Oil. $\mathbf{R_f}$ = 0.2 (Hex). **Yield** = 78% (1.3 mmol, 298.4 mg). **^{1}H NMR** (300 MHz, $CDCl_3$): δ 7.43 (d, *J* = 8.9 Hz, 2H), 6.84 (d, *J* = 8.9 Hz, 2H), 4.04 (t, *J* = 5.8 Hz, 2H), 3.36 (t, *J* = 6.7 Hz, 2H), 3.00 (s, 1H), 2.28 (quint, 6.3 Hz, 2H).

1.2.3.- Synthesis of [3-(4-ethynylphenoxy)propyl]triphenylphosphonium 53

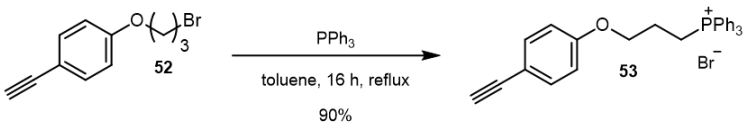

In a round bottom flask, 1-(3-bromopropoxy)-4-ethynylbenzene (0.7 mmol, 175.0 mg, 1.0 equiv.) and triphenylphosphine (0.7 mmol, 191.5 mg, 1.0 equiv.) were dissolved in 1.5 mL toluene. The mixture was refluxed for 16 h and the resulting precipitate was filtrated, washed with toluene and dried under reduced pressure. The product **53** was obtained as an off-white solid.

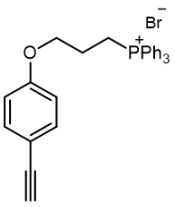

[3-(4-Ethynylphenoxy)propyl]triphenylphosphonium (53). Off-white solid. $\mathbf{R_f}$ = 0.15 (CH_2Cl_2 / MeOH 95:5). **Yield** = 90% (0.7 mmol, 330.4 mg). **^{1}H NMR** (500 MHz, $CDCl_3$): δ 7.78 (m, 9H), 7.66 (m, 6H), 7.28 (d, *J* = 8.6 Hz, 2H), 6.75 (d, *J* = 8.6 Hz, 2H), 4.28 (t, *J* = 5.3 Hz, 2H), 3.87 (m, 2H), 2.94 (s, 1H), 2.14 (m, 2H). **^{13}C NMR** (126 MHz, $CDCl_3$): δ 158.5, 135.3 (d, *J* = 2.9 Hz, 3xC), 133.7 (d, *J* = 10.1 Hz, 6xC), 133.6 (2xC), 130.6 (d, *J* = 12.6 Hz, 6xC), 117.8 (d, *J* = 86.5 Hz, 3xC), 114.7 (2xC), 114.5, 83.6, 76.1, 66.6 (d, *J* = 16.8 Hz), 22.7 (d, *J* = 3.3 Hz), 19.9 (d, *J* = 53.2 Hz). **^{31}P NMR** (202 MHz, $CDCl_3$): δ 25.61. **HRMS-ESI**: Calculated for $C_{29}H_{26}OP^+$: 421.1716; found: 421.1714.

1.3.- Synthesis of 45, 47 and 49

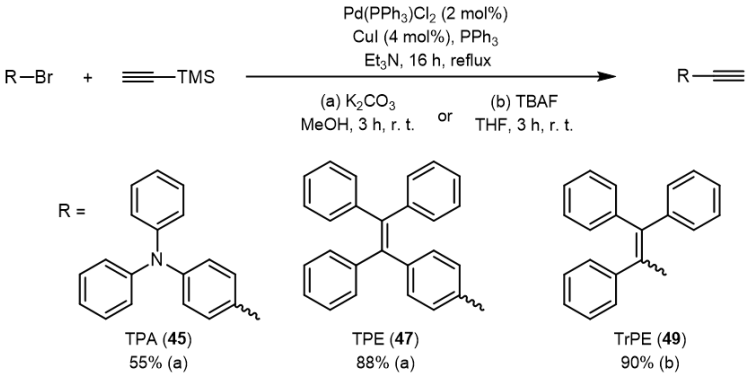

1.3.1.- Synthesis of [2-(4-bromophenyl)ethene-1,1,2-triyl]tribenzene

Procedure adapted from Liu *et al.*[10]

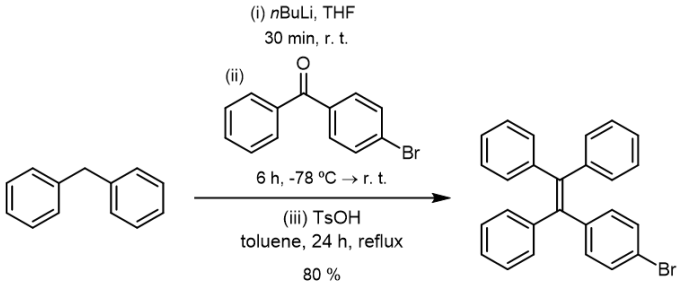

In a flame dried Schlenk containing 10.0 mL of distilled THF and diphenylmethane (5.3 mmol, 0.9 mL, 1.1 equiv.) was added stepwise a solution of 2.5 M *n*BuLi in hexane (5.0 mmol, 2.0 mL, 1.0 equiv.) and allowed to react for 30 min under inert atmosphere and room temperature, to produce an orange-red diphenyl lithium solution. Then, the solution was cooled to -78 ºC and 4-bromo benzophenone (5.0 mmol, 1.3 g, 1.0 equiv.) was added. The reaction mixture was stirred at room temperature for 6 h. After that, the mixture was quenched with the addition of NH_4Cl sat. (10.0 mL), extracted with CH_2Cl_2 (20.0 mL), dried over anhydrous $MgSO_4$ and concentrated under reduced pressure.

The resulting solid was dissolved in 12.5 mL of toluene and a catalytic amount of *p*-toluensulfonic acid was added. The mixture was allowed to reflux for 24 h and then washed with K_2CO_3 (10% in water, 3 x 10.0 mL), water (3 x 10.0 mL) and brine (10.0 mL). Then the organic combined layers were dried over anhydrous $MgSO_4$ and concentrated under reduced pressure. The crude product was purified by flash chromatography on silica gel using Hex / EtOAc 9:1 as eluent. The product was obtained as a white solid.

Spectroscopic data are in consonance with those reported in the bibliography.[10]

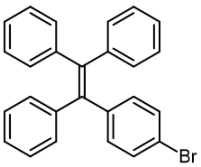

[2-(4-Bromophenyl)ethene-1,1,2-triyl]tribenzene. White solid. $\mathbf{R_f}$ = 0.6 (Hex / EtOAc 9:1). **Yield** = 80% (4.0 mmol, 1.7 g). **^{1}H NMR** (300 MHz, $CDCl_3$): δ 7.22 (d, *J* = 8.2 Hz, 2H), 7.11 (m, 9H), 7.02 (m, 6H), 6.90 (d, *J* = 8.2 Hz, 2H).

1.3.2.- Synthesis of 45 and 47

Procedure adapted from Kobayashi *et al*.[11]

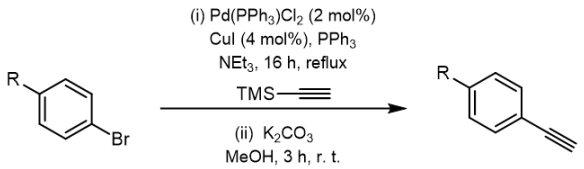

In a flame dried round bottom flask, CuI (0.14 mmol, 27.4 mg, 0.04 equiv.), $PdCl_2(PPh_3)_2$ (0.072 mmol, 50.4 mg, 0.02 equiv.) and triphenylphosphine (0.14 mmol, 37.7 mg, 0.04 equiv.) were dissolved in 7.5 mL of fresh distilled trimethylamine. The mixture was heated at 40 ºC under inert atmosphere for 20 min. Then the corresponding arylbromide (3.6 mmol, 1.47 g, 1.0 equiv.) and ethynyltrimethylsilane (5.4 mmol, 0.8 mL, 1.5 equiv.) were added and the reaction mixture was heated to reflux and allowed to react overnight.

The solvent was removed under reduced pressure, and 30.0 mL of EtOAc were added. The crude was filtered with celite, and the filtrate was washed with water (3 x 20.0 mL), brine (20.0 mL), dried over anhydrous $MgSO_4$ and concentrated under reduced pressure. The crude product was purified by flash chromatography on silica gel using hexane as eluent. The products were obtained over 95% yield as solids.

TMS removal protocol: In a round bottom flask, the TMS protected alkyne (3.5 mmol, 1.5 g, 1.0 equiv.) and K_2CO_3 (7.1 mmol, 980.0 mg, 2.0 equiv.) were dissolved in 15.0 mL of MeOH. The resulting mixture was stirred at room temperature for 3 h and then diluted with 50.0 mL of CH_2Cl_2, washed with water (3 x 30 mL) and brine (30.0 mL), dried over anhydrous $MgSO_4$ and concentrated under reduced pressure.

Spectroscopic data are in consonance with those reported in the bibliography.

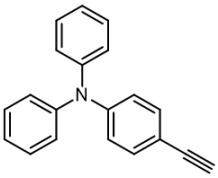

4-Ethynyl-N,N-diphenylaniline (45).[12] White solid. $\mathbf{R_f}$ = 0.5 (Hex / EtOAc 9:1). Yield = 55% (1.98 mmol, 533.3 mg). **^{1}H NMR** (300 MHz, $CDCl_3$): δ 7.36-7.24 (m, 6H), 7.11-7.02 (m. 6H), 6.96 (d, *J* = 8.7 Hz, 2H), 3.02 (s, 1H).

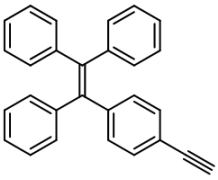

[2-(4-Ethynylphenyl)ethene-1,1,2-triyl]tribenzene (47).[13] White solid. $\mathbf{R_f}$ = 0.65 (Hex / EtOAc 9:1). **Yield** = 88% (4.6 mmol, 1.13 g). **^{1}H NMR** (300 MHz, $CDCl_3$): δ 7.23 (d, *J* = 8.1 Hz, 2H), 7.10 (m, 9H), 6.99 (m, 8H), 3.03 (s, 1H).

1.3.3.- Synthesis of substrate 49

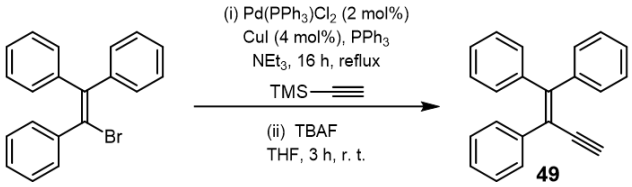

In a flame dried round bottom flask, CuI (0.14 mmol, 27.4 mg, 0.04 equiv.), $PdCl_2(PPh_3)_2$ (0.07 mmol, 50.4 mg, 0.02 equiv.) and triphenylphosphine (0.14 mmol, 37.7 mg, 0.04 equiv.) were dissolved in 7.5 mL of fresh distilled trimethylamine. The mixture was heated to 40 ºC under inert atmosphere for 20 min. Then (2-bromoethene-1,1,2-triyl)tribenzene (3.6 mmol, 1.5 g, 1.0 equiv.) and ethynyltrimethylsilane (5.4 mmol, 0.8 mL, 1.5 equiv.) were added and the reaction mixture was heated to reflux and allowed to react overnight.

The solvent was removed under reduced pressure, and 30.0 mL of EtOAc were added. The crude was filtered with celite, and the filtrate was washed with water (3 x 20. 0 mL) and brine (20.0 mL), dried over anhydrous $MgSO_4$ and concentrated under reduced pressure.

The crude product was purified by flash chromatography on silica gel using hexane as eluent. The product was obtained as a pale-yellow solid (97%, 3.5 mmol, 1.2 g).

TMS removal protocol: In a round bottom flask trimethyl(3,4,4-triphenylbut-3-en-1-yn-1-yl)silane (3.2 mmol, 1.2 g, 1.0 equiv.) was dissolved in 18.0 mL of THF. Then the mixture was cooled to 0 ºC and 4.0 mL of TBAF (1M, 4.0 mmol, 1.3 equiv.) were added stepwise and allowed to react at room temperature for 1 h. The reaction was cooled again and quenched with $NaHCO_3$ sat. The mixture was extracted with Et_2O (30.0 mL) and the combined organic fractions were washed with water (3 x 20.0 mL), brine (20.0 mL), dried over anhydrous $MgSO_4$ and concentrated under reduced pressure. The crude product was purified by flash chromatography on silica gel using Hex / Et_2O 99:1 as eluent. The product **49** was obtained as a pale-yellow solid.

Spectroscopic data are in consonance with those reported in the bibliography.[14]

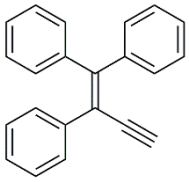

(**8b**)

But-1-en-3-yne-1,1,2-triyltribenzene (49). Pale yellow solid $\mathbf{R_f}$ = 0.25 (Hex / Et_2O 99:1). **Yield** = 90% (2.9 mmol, 807.5 mg). **^{1}H NMR** (300 MHz, $CDCl_3$): δ 7.49 (m, 2H), 7.34 (m, 5H), 7.14 (m, 6H), 6.96 (m, 2H), 3.06 (s, 1H).

USC UNIVERSIDADE DE SANTIAGO DE COMPOSTELA

S2.- SYNTHESIS OF PHTALANES AND ANTHRAQUINONE PRODUCTS IN ORGANIC SOLVENTS

2.1.- General procedure of the synthesis of 5-phenyl-phthalanes in organic solvents

Procedure adapted from Itoh *et al*.[15]

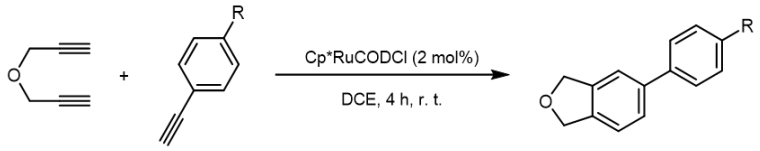

In a flame-dried Schlenk, Cp*Ru(COD)Cl (0.01 mmol, 3.6 mg, 2% mol) was dissolved in 2.0 mL of dichloroethane and the corresponding phenylacetylene (1.0 mmol, 4.0 equiv.) was added stepwise. Then, a degassed solution of propargyl ether (0.5 mmol, 52.0 µl, 1.0 equiv.) in 3.0 mL of DCE was added. The solution was stirred for 4 h, and then concentrated under reduced pressure. The residue was purified by flash chromatography on silica gel using Hex / EtOAc as eluent.

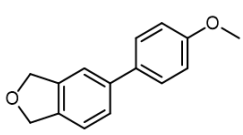

5-(4-Methoxyphenyl)-1,3-dihydroisobenzofuran (29). White solid. $\mathbf{R_f}$ = 0.25 (Hex / EtOAc 9:1). **Yield** = 75% (0.4 mmol, 84.9 mg). **^{1}H NMR** (500 MHz, $CDCl_3$): δ 7.55 (dt, *J* = 8.7, 2 Hz, 2H), 7.49 (d, *J* = 8.3 Hz, 1H), 7.44 (s, 1H), 7.31 (d, *J* = 7.8 Hz, 1H), 7.02 (dt, *J* = 8.7, 1.9 Hz, 2H), 5.19 (s, 2H), 5.19 (s, 2H), 3.89 (s, 3H). **^{13}C NMR** (126 MHz, $CDCl_3$): δ 159.6, 140.8, 140.4, 138.02, 134.0, 128.6 (2xC), 126.5, 121.6, 119.7, 114.7 (2xC), 74.0, 73.8, 55.8. **HRMS-ESI**: Calculated for $C_{15}H_{15}O_2^+$: 227.1067; found: 227.1067.

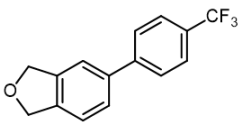

5-(4-(Trifluoromethyl)phenyl)-1,3-dihydroisobenzofuran (30). White solid. Rf = 0.3 (Hex / EtOAc 9:1). **Yield** = 90% (0.45 mmol, 118.9 mg). **^{1}H NMR** (300 MHz, CDCl3): δ 7.67 (m, 3H), 7.50 (d, J = 2H), 7.34 (d, *J* = 8.0, 1H), 7.30 (d, *J* = 7.7, 1H), 5.18 (s, 2H), 5.11 (s, 2H). **^{19}F NMR** (282 MHz, $CDCl_3$): δ -62.90.

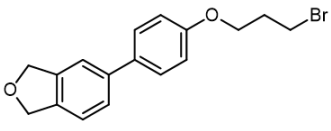

5-[4-(3-Bromopropoxy)phenyl]-1,3-dihydroisobenzofuran. White solid. $\mathbf{R_f}$ = 0.3 (Hex / EtOAc 9:1). **Yield** = 82% (0.4 mmol, 136.6 mg). **^{1}H NMR** (500 MHz, $CDCl_3$): δ 7.51 (d, *J* = 8.8 Hz, 2H), 7.46 (dd, *J* = 7.8, 1.2 Hz, 1H) 7.41 (s, 1H), 7.28 (d, *J* = 7.8 Hz, 1H), 6.98 (d, *J* = 8.8 Hz, 2H), 5.16 (s, 4H), 4.09 (t, *J* = 5.8 Hz, 2H), 3.40 (t, *J* = 6.7 Hz, 2H), 2.30 (quint, *J* = 6.3 Hz, 2H). **^{13}C NMR** (126 MHz, $CDCl_3$): δ 158.3, 140.3, 140.0, 137.7, 133.9, 128.2 (2xC), 126.2, 121.2, 119.3, 114.90 (2xC), 73.6, 73.5, 67.4, 33.0, 2.6. **HRMS-ESI**: Calculated for $C_{17}H_{18}BrO_2^+$: 333.0485; found: 333.0477.

2.1.1 Synthesis of 5-[4-(3-triphenylphosphoniumpropoxy]phenyl)phthtalane (56)

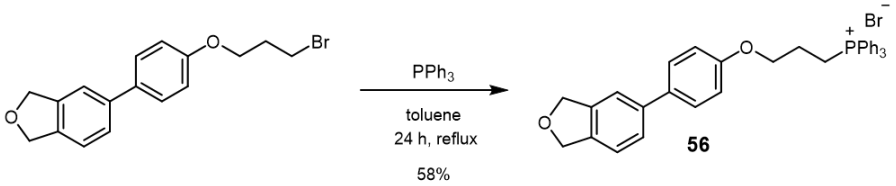

In a round bottom flask, 5-[4-(3-bromopropoxy)phenyl]phthtalane (135.0 mg, 0.4 mmol, 1.0 equiv.) and triphenylphosphine (105.0 mg, 0.4 mmol, 1.0 equiv.) were dissolved in 1.0 mL of toluene. The mixture was refluxed for 24 h and the resulting precipitate was filtered, washed with toluene and dried under reduced pressure. The obtained solid was further purified by flash chromatography on silica gel using CH_2Cl_2 / MeOH 9:1 as eluent. The product (**56**) was obtained as a white solid.

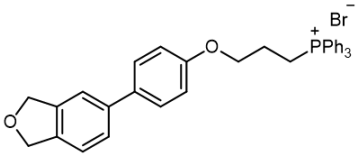

5-[4-(3-Triphenylphosphoniumpropoxy)phenyl]phthtalane (56). White solid. $\mathbf{R_f}$ = 0.4 (CH_2Cl_2 / MeOH 9:1). **Yield** = 58% (0.3 mmol, 137.9 mg). **^{1}H NMR** (500 MHz, $CDCl_3$): δ 7.79 (m, 9H), 7.69 (m, 6H), 7.42 (dt, *J* = 8.8, 2 Hz, 2H), 7.38 (dd, *J* = 7.8, 1.3 Hz, 1H), 7.34 (s, 1H), 7.24 (d, *J* = 7.9 Hz, 1H), 6.92 (dt, *J* = 8.8, 2 Hz, 2H), 5.10 (s, 4H), 4.33 (t, *J* = 5.5 Hz, 2H), 3.88 (m, 2H), 2.20 (m, 2H). **^{13}C NMR** (126 MHz, $CDCl_3$): δ 157.6, 140.1, 139.8, 137.5, 135.2 (d, *J* = 2.7 Hz, 3xC), 133.8, 133.6 (d, 10.1 Hz, 6xC), 130.6 (d, *J* = 12.6 Hz, 6xC), 128.1 (2xC), 126.0, 121.2, 119.1, 117.8 (d, *J* = 86.4 Hz, 3C), 115.0 (2xC), 73.4, 73.3, 66.6 (d, *J* = 16.4 Hz), 22.8 (d, *J* = 3.2 Hz) 20.0 (d, *J* = 53.2). **^{31}P NMR** (202 MHz, $CDCl_3$): δ 25.78. **HRMS-ESI:** Calculated for $C_{35}H_{32}O_2P^+$: 515.2134, found: 515.2138.

2.2.- General procedure for the synthesis of 2-phenyl-9, 10-anthraquinones in organic solvents

Procedure adapted from Itoh et al.[16]

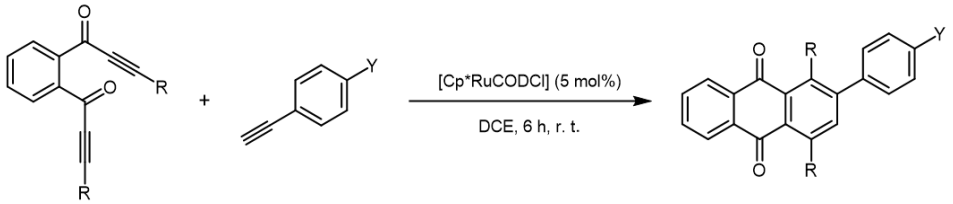

To a flame-dried Schlenk, Cp*Ru(COD)Cl (0.02 mmol, 6.0 mg, 5 mol%) was dissolved in 1.0 mL of dichloroethane. Then, the corresponding phenylacetylene (1.2 mmol, 4.0 equiv.) was added stepwise, followed by the addition of a degassed solution of 1,2-bis(propiolyl) benzene (0.3 mmol, 1.0 equiv.) in 4.0 mL of DCE via syringe for 20 min at room temperature.

The solution was stirred for 6 h and concentrated under reduced pressure. The residue was purified by flash chromatography on silica gel using Hex / EtOAc as eluent.

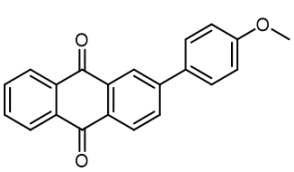

2-(4-Methoxyphenyl)-9-10-anthraquinone (41). Bright yellow solid. $\mathbf{R_f}$ = 0.4 (Hex / EtOAc 9:1). **Yield** = 55% (0.2 mmol, 51.9 mg). **^{1}H NMR** (500 MHz, $CDCl_3$): δ 8.49 (d, *J* = 1.9 Hz, 1H), 8.33 (m, 3H), 7.97 (dd, *J* = 8.1, 2.0 Hz, 1H) 7.80 (m, 2H), 7.68 (d, *J* = 8.8 Hz, 2H), 7.03 (d, *J* = 8.8, 2H), 3.88 (s, 3H). **^{13}C NMR** (126 MHz, $CDCl_3$): δ 183.7, 183.3, 160.9, 146.8, 134.5, 134.4, 134.3, 134.1, 134.1, 132.1, 132.0, 131.7, 128.9 (2xC), 128.5, 127.7, 127.6, 125.2, 115.0 (2xC), 55.8. **HRMS-ESI**: Calculated for $C_{21}H_{15}O_3^+$: 315.1016; found: 315.1013.

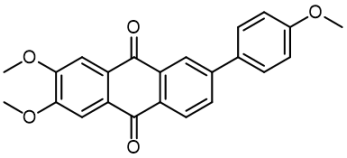

2,3-Dimethoxy-6-(4-methoxyphenyl)-9,10-anthraquinone (42). Yellow solid. Rf = 0.6 (Hex / EtOAc 1:1). **Yield** = 69% (0.1 mmol, 26.4 mg). **^{1}H NMR** (500 MHz, $CDCl_3$): δ 8.43 (d, *J* = 1.9 Hz, 1H), 8.28 (d, *J* = 8.1 Hz, 1H), 7.92 (dd, *J* = 8.1, 2.0 Hz, 1H), 7.72 (s, 2H), 7.68 (d, *J* = 8.8 Hz, 2H), 7.03 (d, *J* = 8.8 Hz, 2H), 4.07 (d, *J* = 1.1 Hz, 6H), 3.88 (s, 3H). **^{13}C NMR** (126 MHz, $CDCl_3$): δ 181.64, 181.23, 159.34, 152.85, 152.71, 145.04, 132.95, 130.63, 130.42, 130.26, 127.66, 127.53, 127.47 (2xC), 126.80, 123.68, 113.54 (2xC), 107.40, 107.34, 55.53 (2xC), 54.41. **HRMS-ESI**: Calculated for $C_{23}H_{19}O_5^+$: 375.1224; found: 375.1227.

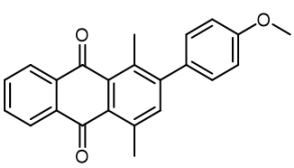

1,4-Dimethyl-2-(4-methoxyphenyl)-9,10-anthraquinone (43). Bright yellow solid. $\mathbf{R_f}$ = 0.4 (Hex / EtOAc 9:1). **Yield** = 43% (0.1 mmol, 44.2 mg). **^{1}H NMR** (500 MHz, $CDCl_3$): δ 8.18 (ddd, *J* = 7.2, 5.3, 3.3 Hz, 2H), 7.74 (dd, *J* = 5.8, 3.3 Hz, 2H), 7.42 (s, 1H), 7.26 (m, 2H), 6.99 (m, 2H), 3.88 (s, 3H), 2.82 (s, 3H), 2.64 (s, 3H). **^{13}C NMR** (126 MHz, $CDCl_3$): δ 186.9, 186.0, 159.4, 149.0, 139.4, 139.3, 138.0, 134.9, 134.4, 134.2, 133.5, 133.5, 133.2, 131.9, 130.5 (2xC), 126.6, 126.5, 113.9 (2xC), 55.5, 23.8, 20.6. **HRMS-ESI**: Calculated for $C_{23}H_{19}O3^+$: 343.1329; found: 343.1327.

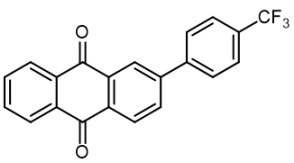

2-(4-(trifluoromethyl)phenyl)-9,10-anthraquinone (44). White solid. Rf = 0.4 (Hex / EtOAc 9:1). Yield = 52% (0.2 mmol, 36.7 mg). **^{1}H NMR** (500 MHz, $CDCl_3$): 8.43 (s, 1H), 8.30 (d, *J* = 7.9 Hz, 1H), 8.24 (s, 2H), 7.92 (d, *J* = 7.6 Hz, 1H), 7.80 – 7.64 (m, 6H). **^{13}C NMR** (126 MHz, $CDCl_3$): δ 181.89, 181.63, 144.16, 141.40, 133.29, 133.19, 132.96, 132.51, 132.47, 131.76, 131.43, 129.82 (q, *J* = 32.7 Hz), 127.19, 126.67 (2xC), 126.32, 126.26, 125.07 (q, *J* = 3.5 Hz, 2xC), 124.78, 123.00 (q, *J* = 272.2 Hz). **^{19}F NMR** (282 MHz, $CDCl_3$): δ -62.62. **HRMS-ESI**: Calculated for $C_{21}H_{12}F_3O_2^+$: 353.0784; found: 353.0783.

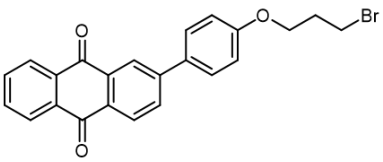

2-[4-(3-Bromopropoxy)phenyl]-9,10-anthraquinone (54). Bright yellow solid. $\mathbf{R_f}$ = 0.4 (Hex / EtOAc 9:1). **Yield** = 52% (0.2 mmol, 65.7 mg). **^{1}H NMR** (500 MHz, $CDCl_3$): δ 8.48 (d, *J* = 1.6 Hz, 1H), 8.33 (m, 3H), 7.96 (dd, *J* = 8.1, 1.7 Hz, 1H), 7.80 (m, 2H), 7.68 (d, *J* = 8.7 Hz, 2H), 7.03 (d, *J* = 8.6 Hz, 2H), 4.11 (t, *J* = 5.8 Hz, 2H), 3.40 (t, *J* = 6.7 Hz, 2H), 2.32 (quint, *J* = 6.2 Hz, 2H). **^{13}C NMR** (126 MHz, $CDCl_3$): δ 183.5, 183.0, 159.6, 146.5, 134.3, 134.1, 134.0, 133.8, 133.8, 131.8, 131.7, 131.6, 128.7 (2xC), 128.2, 127.4, 127.3, 125.0, 115.3 (2xC), 67.6, 33.0, 2.5. **HRMS-ESI**: Calculated for $C_{23}H_{18}BrO_3^+$: 421.0434; found 421.0423.

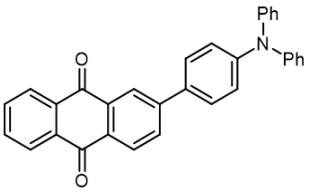

2-(4-(Diphenylamino)phenyl)anthracene-9,10-dione (46).[17] Red solid. $\mathbf{R_f}$ = 0.6 (Hex / EtOAc 7:3). Yield = 15% (0.045 mmol, 20.3 mg). **^{1}H NMR** (300 MHz, $CDCl_3$): δ 8.54 (s, 2H), 8.37–8.30 (m, 3H), 8.03–7.97 (m, 2H), 7.88–7.78 (m, 2H), 7.68–7.59 (m, 2H), 7.33 (t, *J* = 6.0 Hz, 2H), 7.22–7.15 (m, 6H), 7.14–7.07 (t, *J* = 6.0 Hz, 2H).

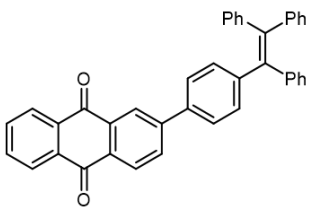

2-[4-(1,2,2-Triphenylvinyl)phenyl]anthracene-9,10-dione (48). Pale yellow solid. $\mathbf{R_f}$ = 0.35 (Hex / EtOAc 9:1). **Yield** = 40% (0.1 mmol, 64.6 mg). **^{1}H NMR** (500 MHz, $CDCl_3$): δ 8.49 (d, *J* = 1.8 Hz, 1H), 8.35 (s, 1H), 8.33 (t, *J* = 4.2 Hz, 2H), 7.97 (dd, *J* = 8.1, 1.9 Hz, 1H), 7.81 (m, 2H), 7.50 (d, *J* = 8.3 Hz, 2H), 7.12 (m, 17H). **^{13}C NMR** (126 MHz, $CDCl_3$): δ 182.3, 181.9, 145.4, 143.6, 142.5, 142.5, 142.4, 140.8, 139.1, 135.6, 133.2, 133.0, 132.8, 132.7, 132.6, 131.1 (2xC), 131.1, 131.0, 130.4 (2xC), 130.3 (2xC), 130.3 (2xC), 127.0, 126.8 (2xC), 126.8 (2xC), 126.7 (2xC), 126.3, 126.2, 125.7, 125.6, 125.6, 125.5 (2xC), 124.3. **HRMS-ESI**: Calculated for $C_{40}H_{27}O_2^+$: 539.1979; found: 539.2000.

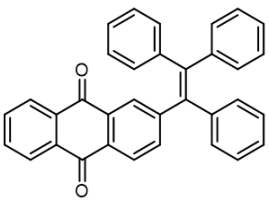

2-(1,2,2-Triphenylvinyl)-9,10-anthraquinone (50). Bright orange solid. $\mathbf{R_f}$ = 0.25 (Hex / EtOAc 7:3). **Yield** = 73% (0.2 mmol, 108.0 mg). **^{1}H NMR** (500 MHz, $CDCl_3$): δ 8.27 (m, 1H), 8.23 (m, 1H), 8.04 (d, *J* = 8.0 Hz, 1H), 7.98 (d, *J* = 1.6, 1H), 7.76 (m, 2H), 7.46 (dd, *J* = 8.0, 1.8 Hz, 1H), 7.13 (m, 9H), 7.06 (m, 6H). **^{13}C NMR** (126 MHz, $CDCl_3$): δ 183.5, 183.2, 150.9, 144.2, 143.2, 143.1, 142.8, 139.7, 137.2, 134.4, 134.3, 134.1, 134.0, 133.5, 131.7 (2xC), 131.7 (2xC), 131.6 (2xC), 130.6, 128.5 (2xC), 128.5 (2xC), 128.2 (2xC), 127.7, 127.6, 127.5 (2xC), 127.4, 127.2. **HRMS-ESI**: Calculated for $C_{34}H_{23}O_2^+$: 463.1693; found: 463.1693.

USC UNIVERSIDADE DE SANTIAGO DE COMPOSTELA

2.2.1. Synthesis of {3-[4-(9,10-anthraquinone)phenoxy]propyl}triphenylphosphonium bromide (55)

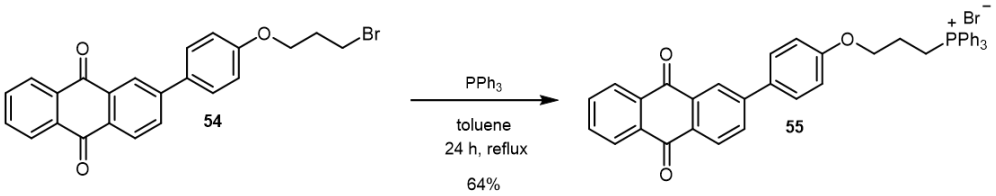

In a round bottom flask, 2-[4-(3-bromopropoxy)phenyl]-9,10-anthraquinone (0.07 mmol, 28.0 mg, 1.0 equiv.) and triphenylphosphine (0.07 mmol, 17.5 mg, 1.0 equiv.) were dissolved in 1.0 mL of toluene. The mixture was refluxed for 24 h and the resulting precipitate was filtered, washed with toluene and dried under reduced pressure. The obtained solid was further purified by flash chromatography on silica gel using CH_2Cl_2 / MeOH 95:5 as eluent. The product (**55**) was obtained as a white solid.

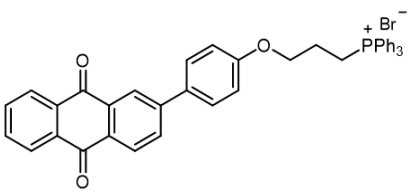

{3-[4-(9,10-Dioxo-9,10-dihydroanthracen-2-yl)phenoxy]propyl}triphenylphosphonium bromide (55). White solid. $\mathbf{R_f}$ = 0.3 (CH_2Cl_2 / MeOH 95:5). **Yield** = 64% (0.03 mmol, 22.1 mg). **^{1}H NMR** (500 MHz, $CDCl_3$): δ 8.44 (s, 1H), 8.31 (m, 3H), 7.94 (d, J = 8.1 Hz, 1H), 7.86 (m, 6H), 7.81 (m, 5H), 7.71 (m, 6H), 7.62 (d, *J* = 8.5 Hz, 2H), 7.00 (d, *J* = 8.5 Hz, 2H), 4.42 (t, *J* = 5.0 Hz, 2H), 4.03 (m, 2H), 2.24 (m, 2H). **^{13}C NMR:** (126 MHz, $CDCl_3$): δ 183.4, 182.9, 159.1, 146.4, 135.3 (d, *J* = 2.9 Hz, 3xC), 134.2, 134.1, 134.0, 133.9 (d, *J* = 10.0 Hz, 6xC), 133.8, 133.7, 131.9, 131.7, 131.7, 130.7 (d, *J* = 12.6 Hz, 6xC), 128.7 (2xC), 128.2, 127.4, 127.3, 124.9, 118.2 (d, *J* = 86.4, 3xC), 115.4 (2xC), 66.9 (d, *J* = 16.8 Hz), 23.0 (d, *J* = 3.4 Hz), 20.1 (d, *J* = 53.0 Hz). **^{31}P NMR** (202 MHz, $CDCl_3$): δ 24.80. **HRMS-ESI**: Calculated for $C_{41}H_{32}O_3P^+$: 603.2084; found 603.2083.

S3.- SELECTED NMR SPECTRA

1,1'-(1,2-Phenylene)bis(but-2-yn-1-ol) (36)

^{1}H NMR (500 MHz, $CDCl_3$)

USC UNIVERSIDADE DE SANTIAGO DE COMPOSTELA

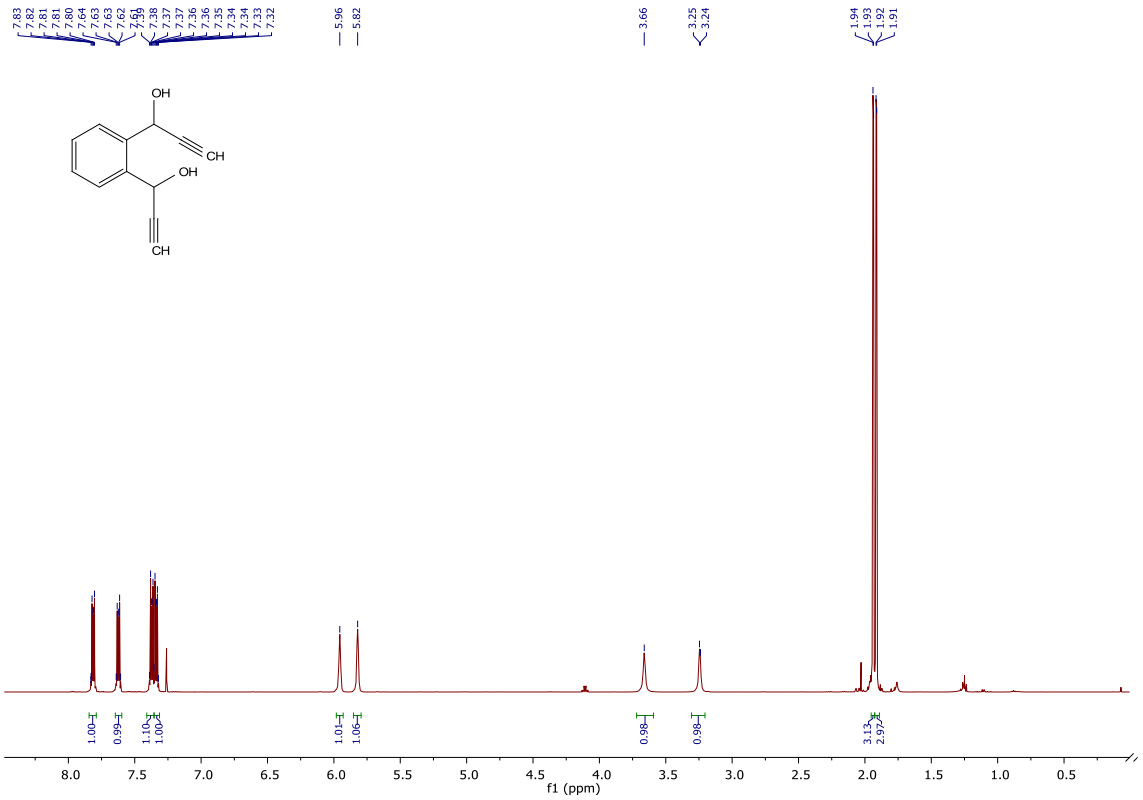

^{13}C NMR (126 MHz, $CDCl_3$)

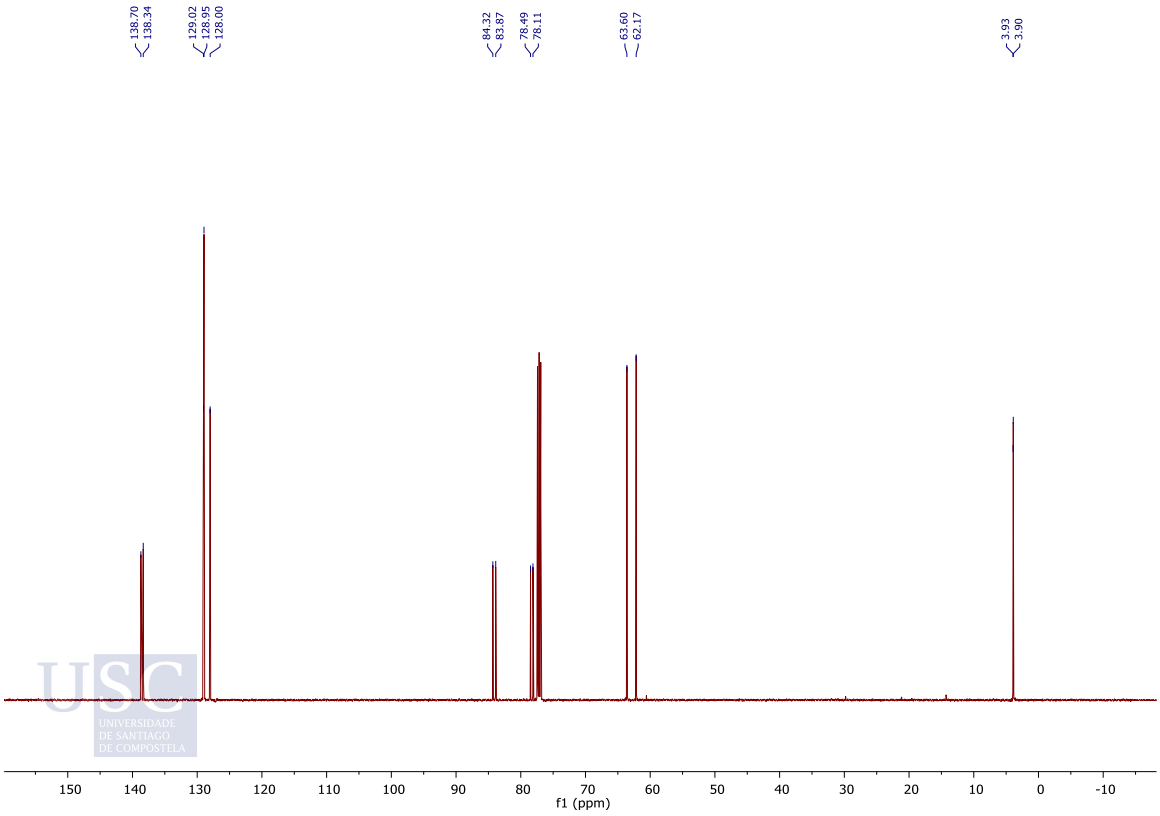

USC
UNIVERSIDADE
DE SANTIAGO
DE COMPOSTELA

DEPT-135 (500 MHz, $CDCl_3$)

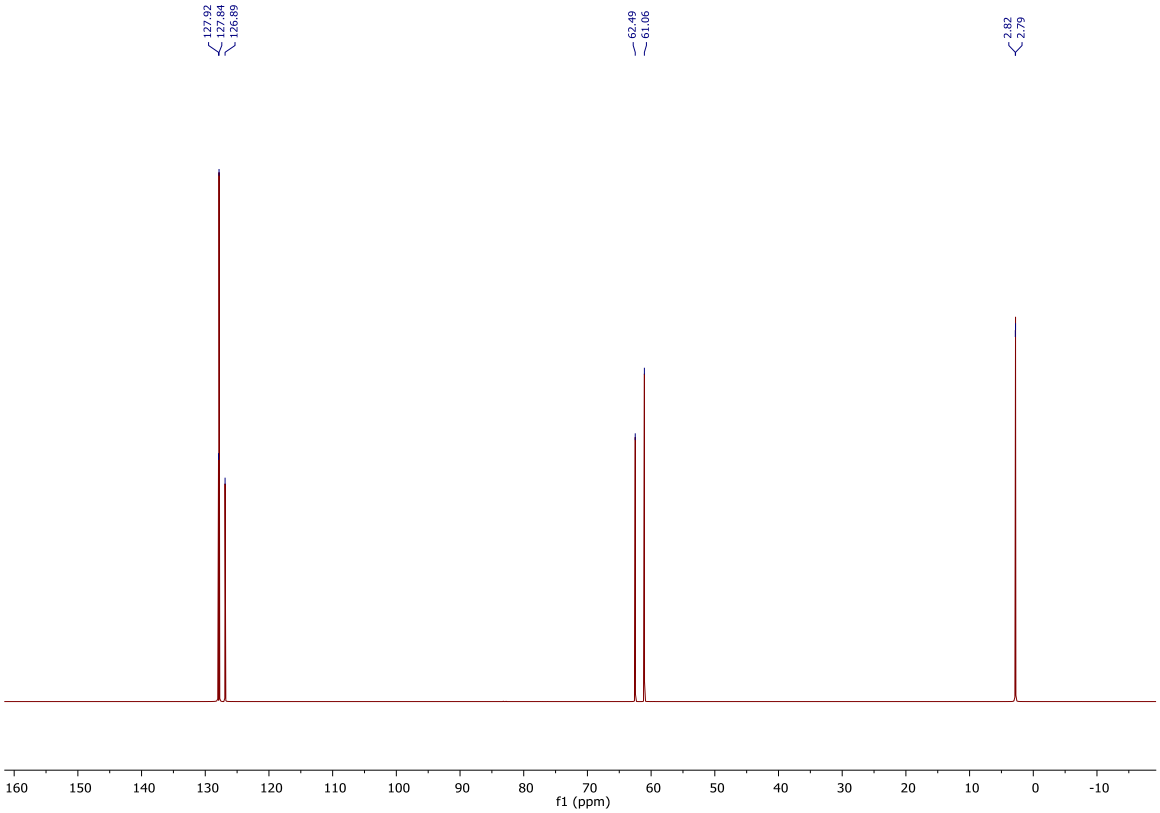

1,1'-(1,2-Phenylene)bis(prop-2-yn-1-one) (31)

^{1}H NMR (500 MHz, $CDCl_3$)

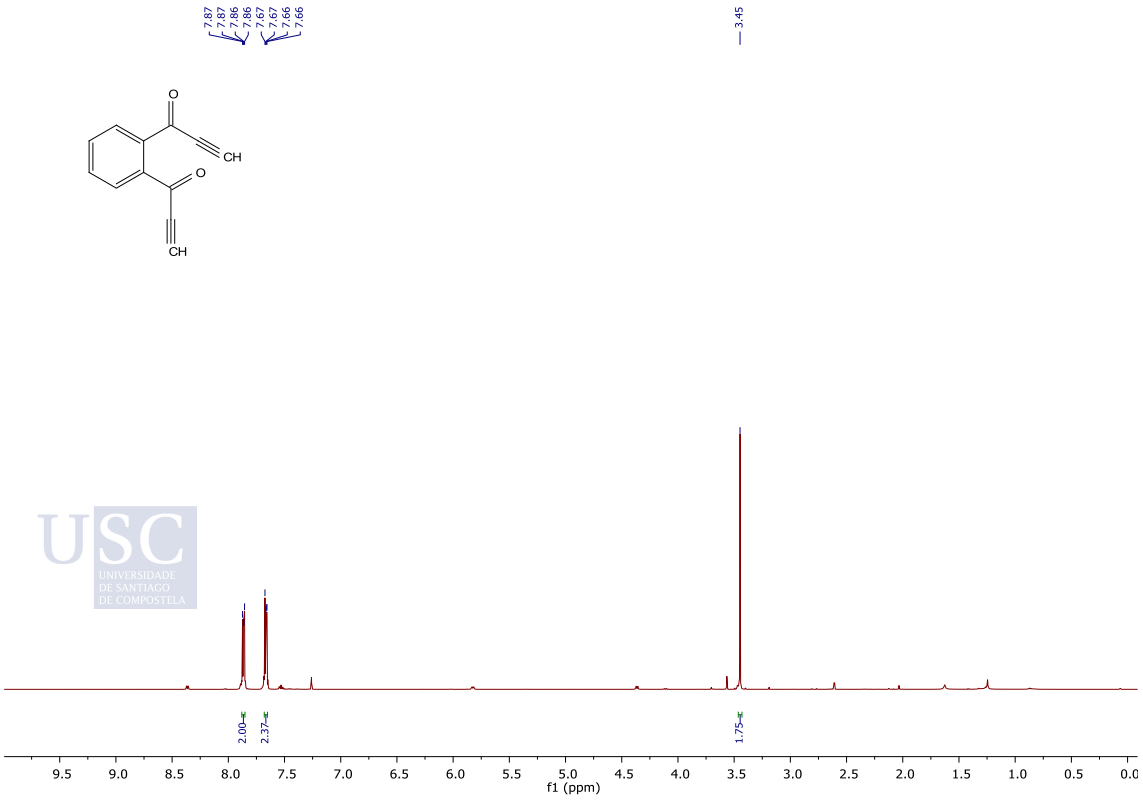

USC UNIVERSIDADE DE SANTIAGO DE COMPOSTELA

^{13}C NMR (126 MHz, $CDCl_3$)

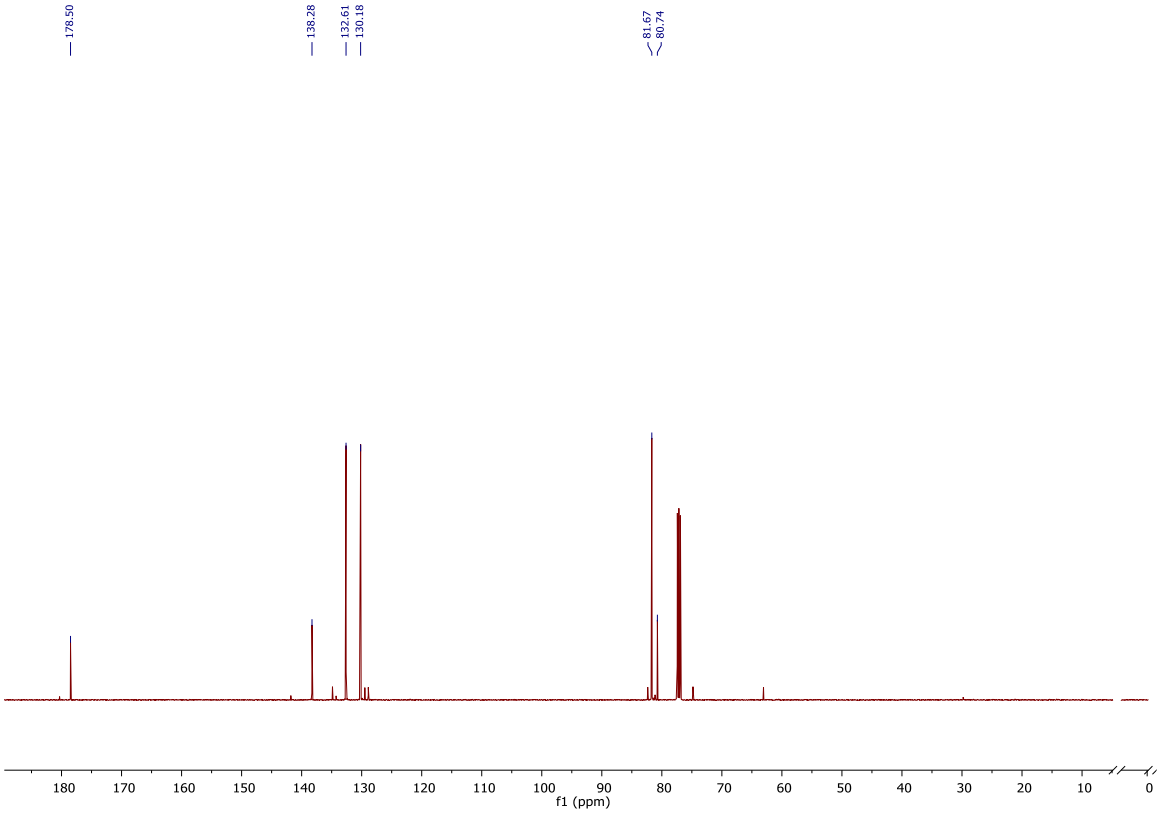

DEPT-135 (500 MHz, $CDCl_3$)

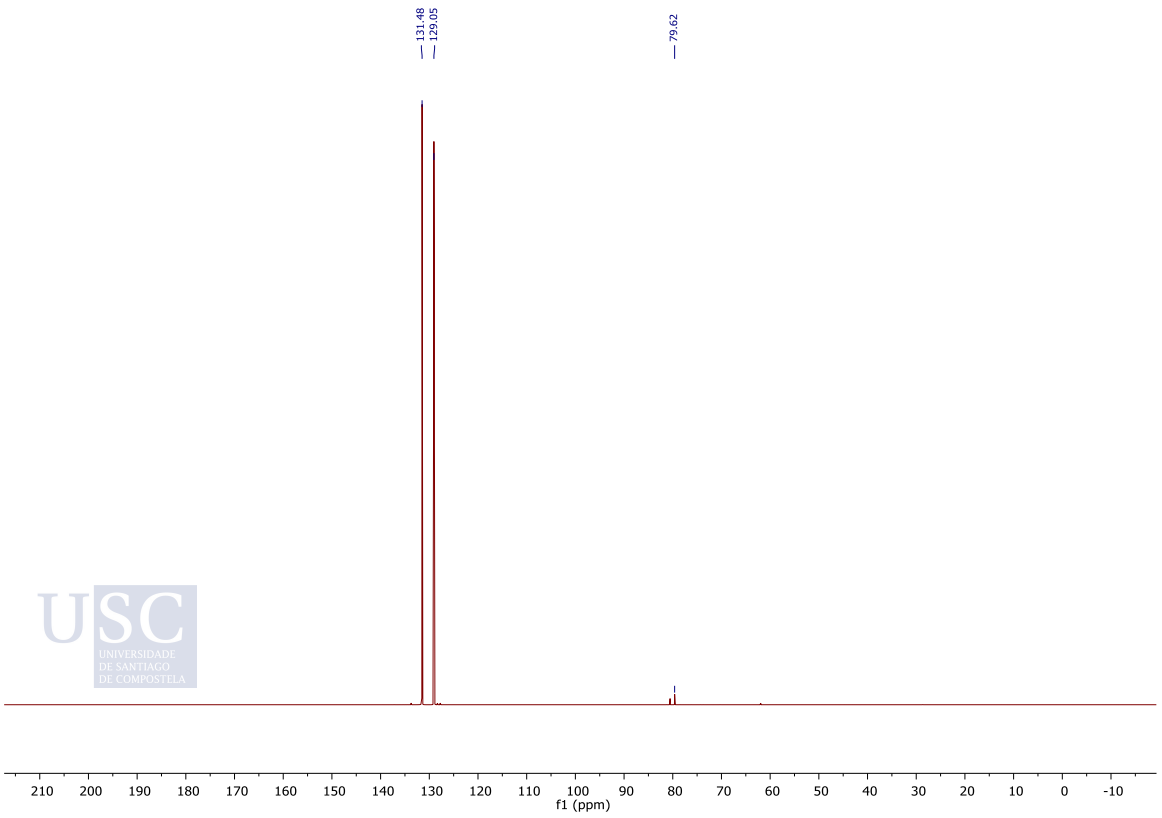

USC UNIVERSIDADE DE SANTIAGO DE COMPOSTELA

1,1'-(4,5-Dimethoxy-1,2-phenylene)bis(prop-2-yn-1-one) (37)

^{1}H NMR (500 MHz, $CDCl_3$)

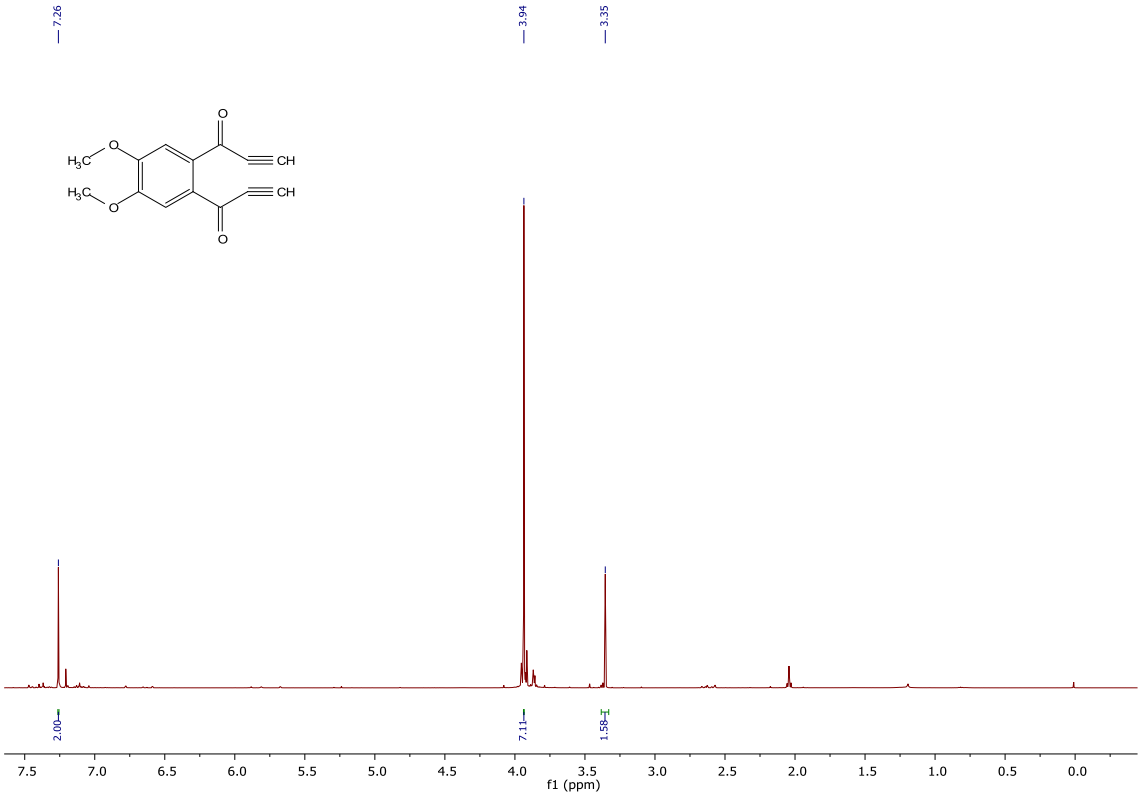

^{13}C NMR (126 MHz, $CDCl_3$)

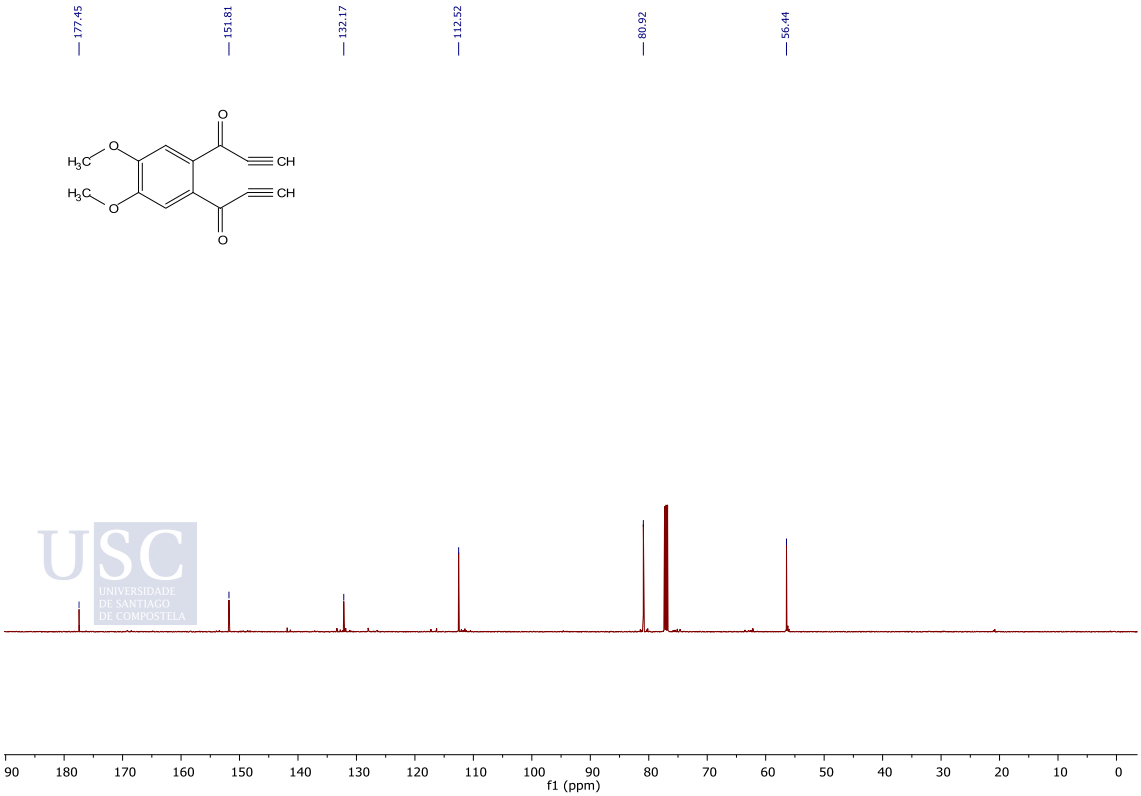

USC UNIVERSIDADE DE SANTIAGO DE COMPOSTELA

DEPT-135 (500 MHz, $CDCl_3$)

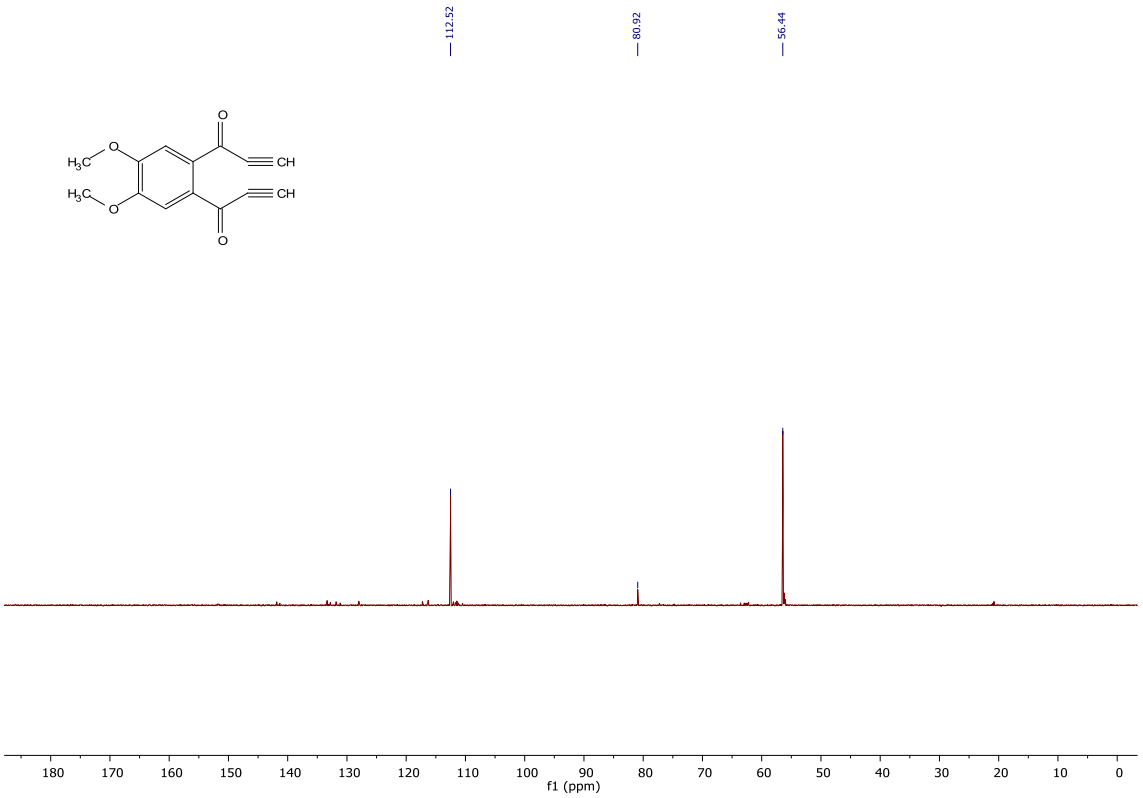

1,1'-(1,2-Phenylene)bis(but-2-yn-1-one) (38)

^{1}H NMR (500 MHz, $CDCl_3$)

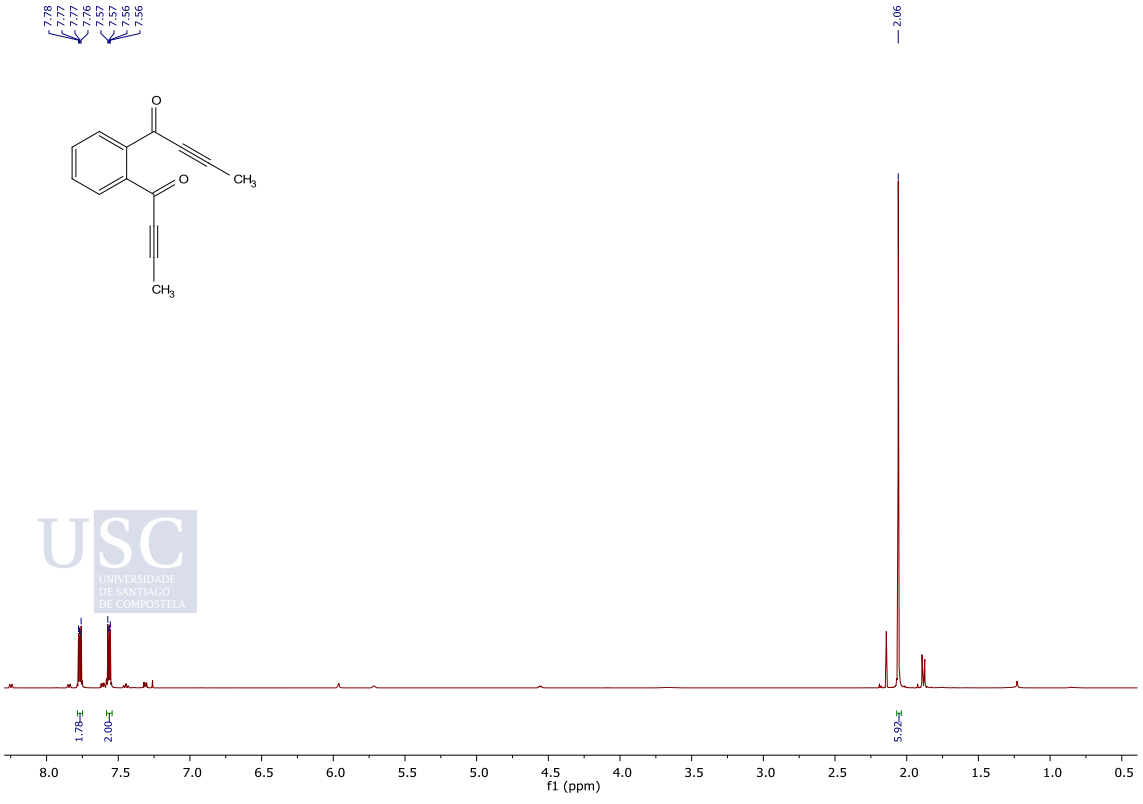

USC UNIVERSIDADE DE SANTIAGO DE COMPOSTELA

^{13}C NMR (126 MHz, $CDCl_3$)

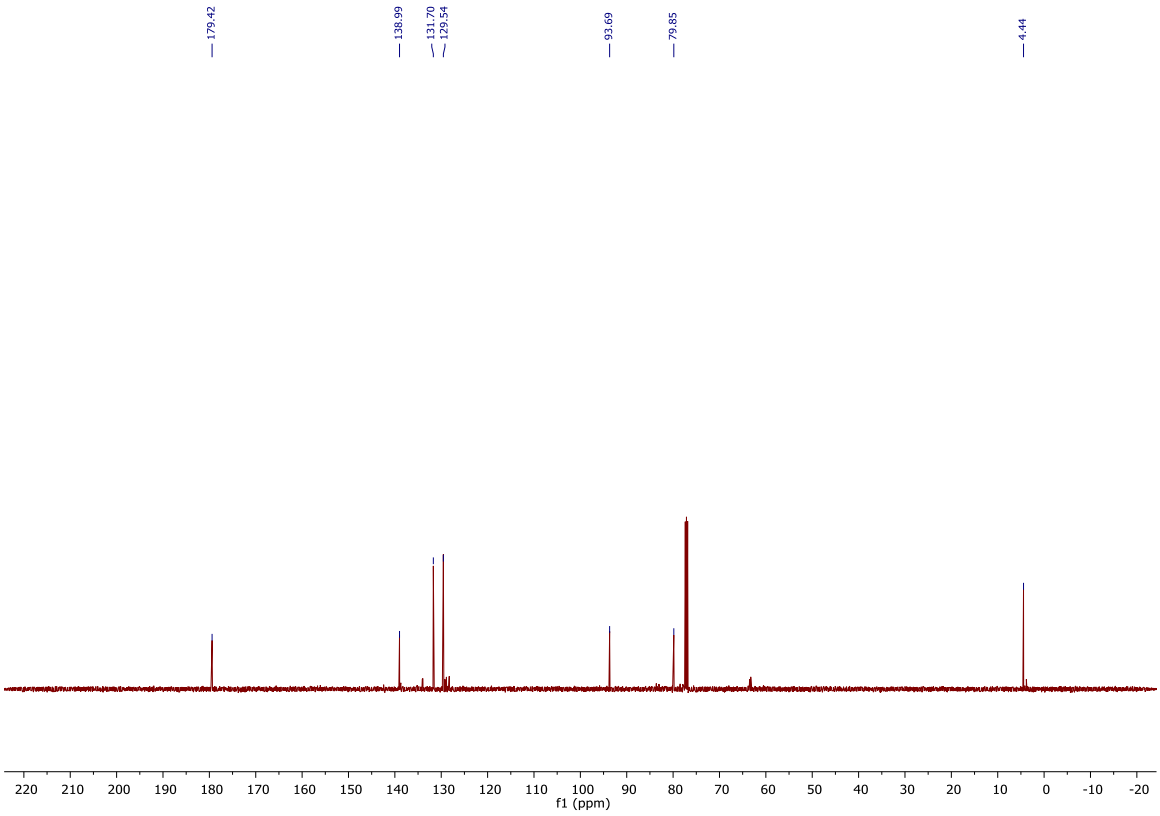

DEPT-135 (500 MHz, $CDCl_3$)

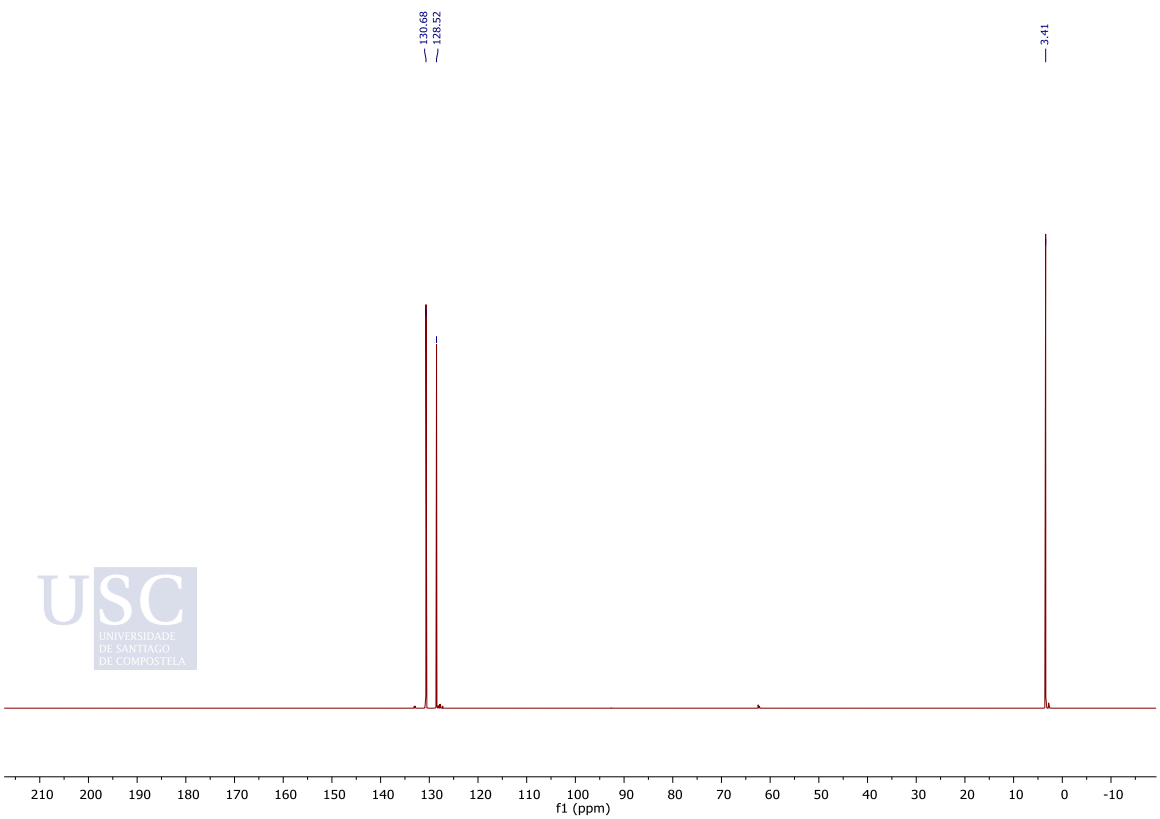

USC UNIVERSIDADE DE SANTIAGO DE COMPOSTELA

[3-(4-Ethynylphenoxy)propyl]triphenylphosphonium (53)

^{1}H NMR (500 MHz, $CDCl_3$)

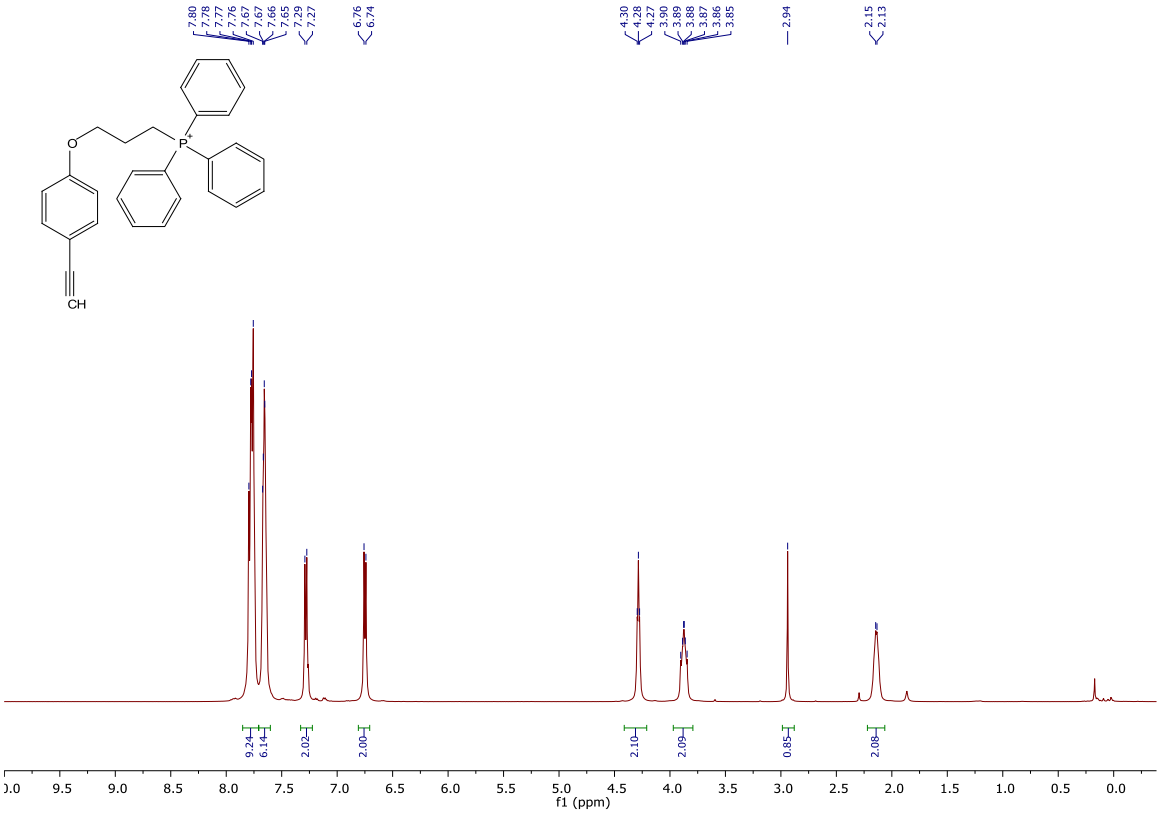

^{13}C NMR (126 MHz, $CDCl_3$)

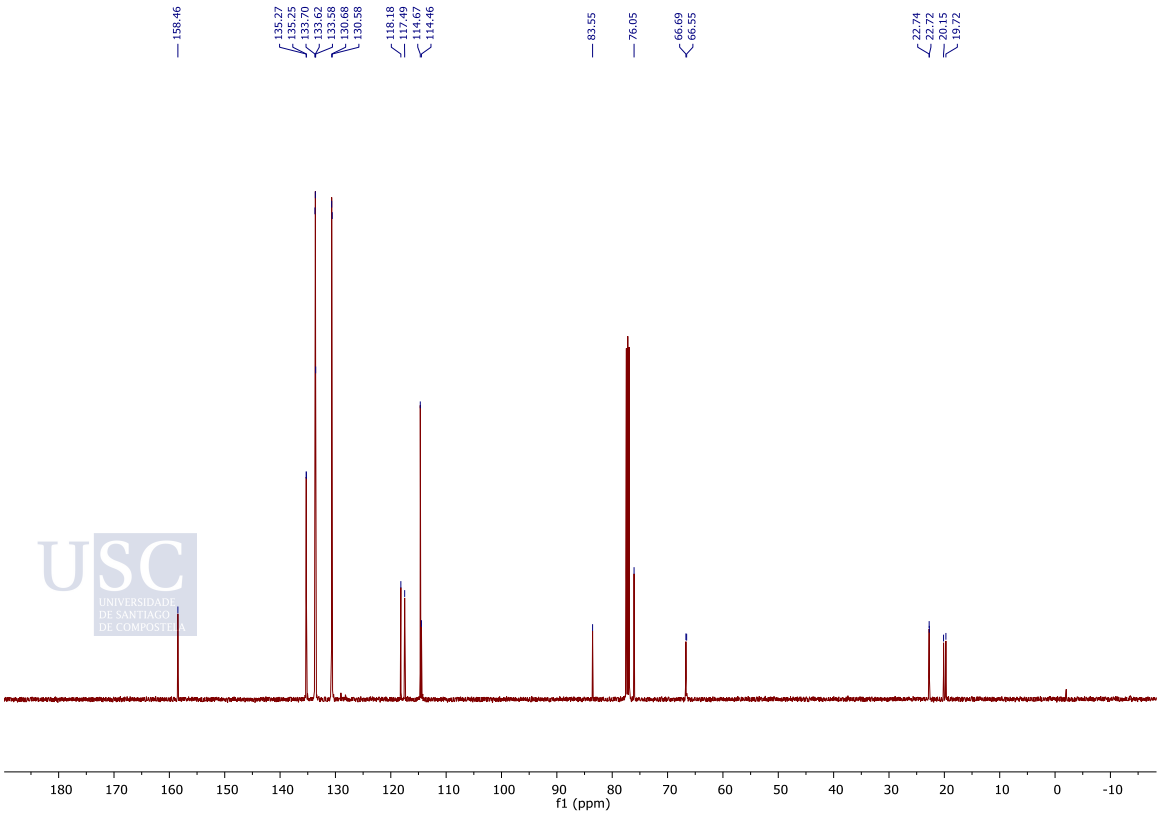

USC UNIVERSIDADE DE SANTIAGO DE COMPOSTELA

DEPT-135 (500 MHz, $CDCl_3$)

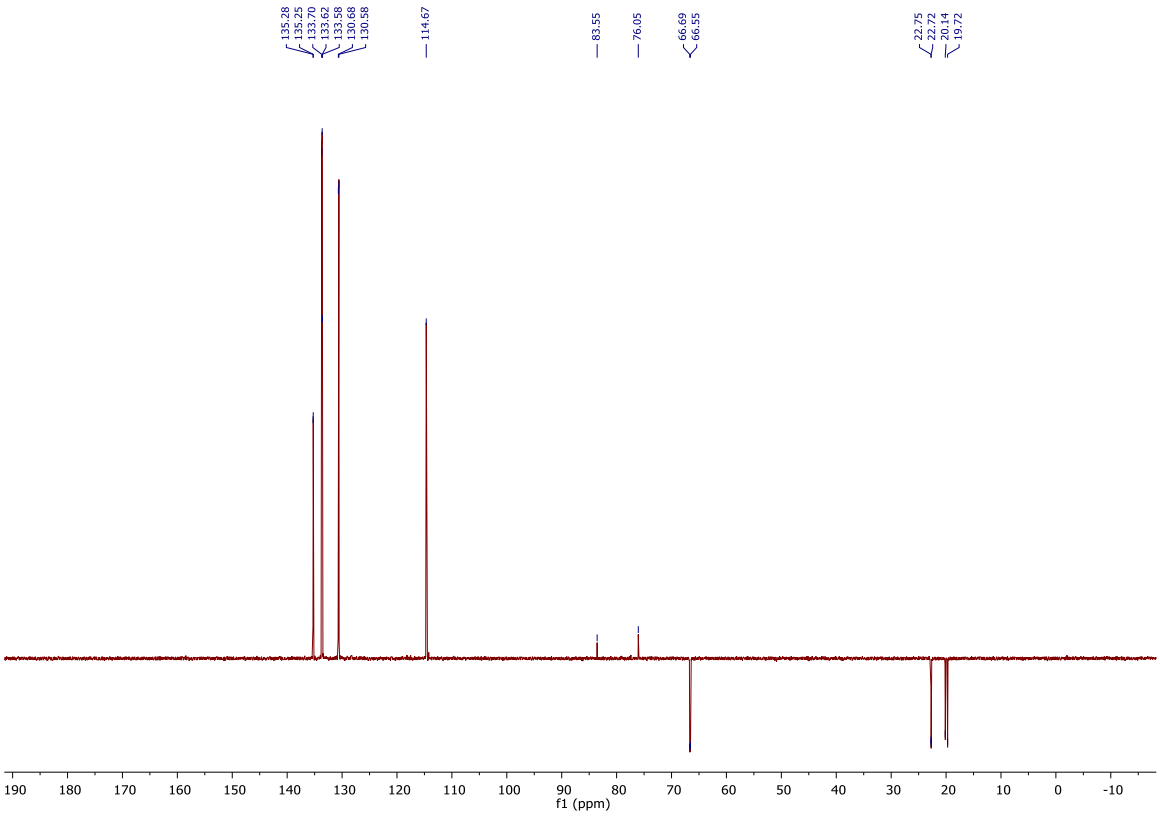

^{31}P NMR (202 MHz, $CDCl_3$)

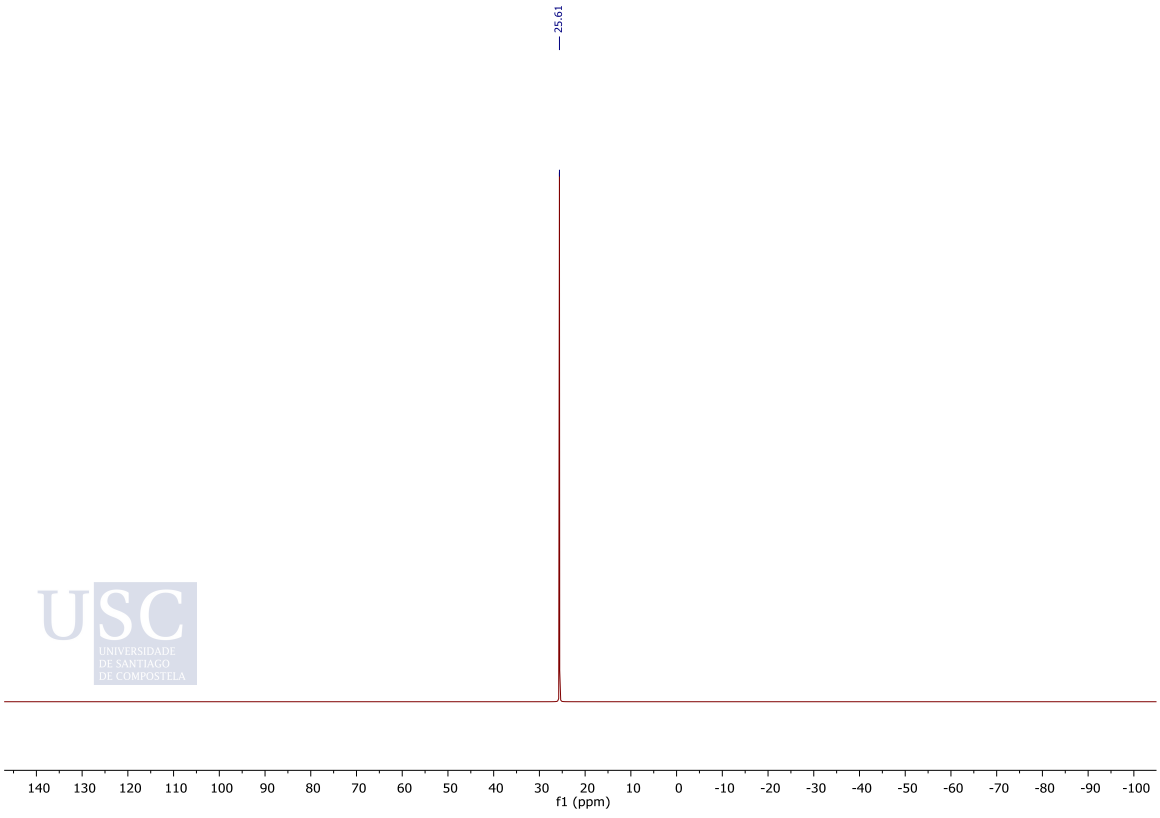

USC UNIVERSIDADE DE SANTIAGO DE COMPOSTELA

5-(4-Methoxyphenyl)-1,3-dihydroisobenzofuran (29)

^{1}H NMR (500 MHz, $CDCl_3$)

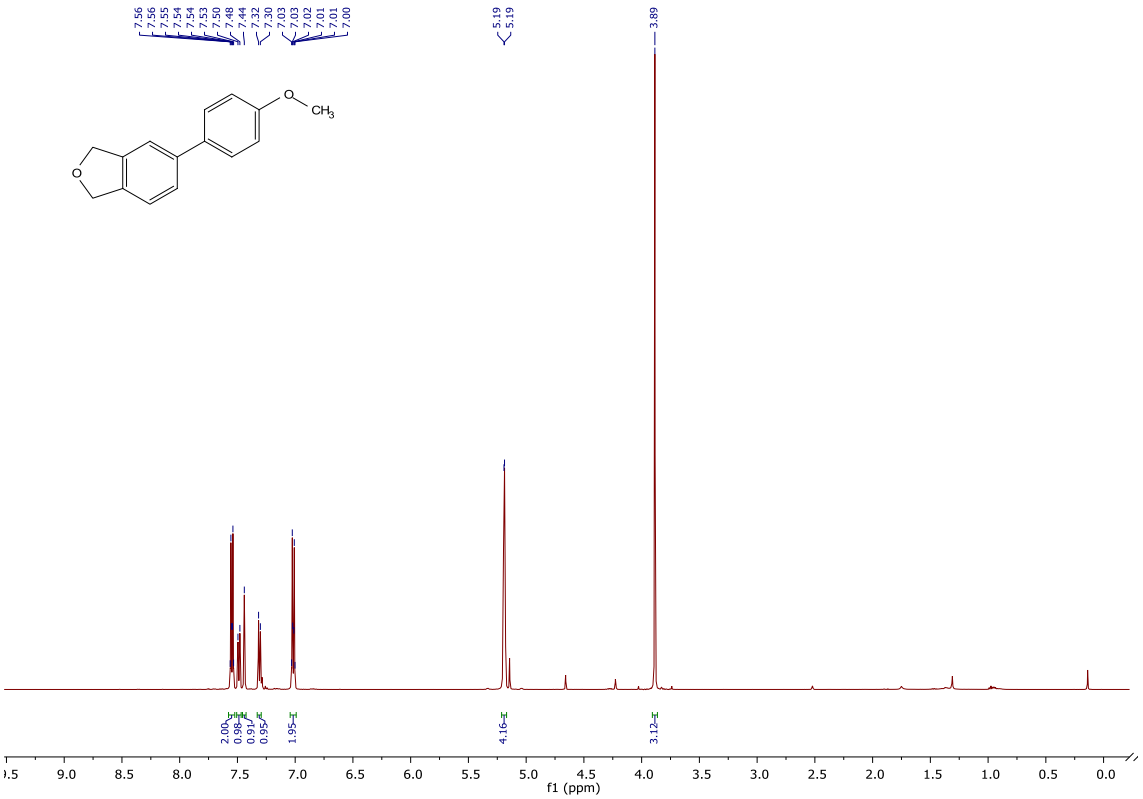

^{13}C NMR (126 MHz, $CDCl_3$)

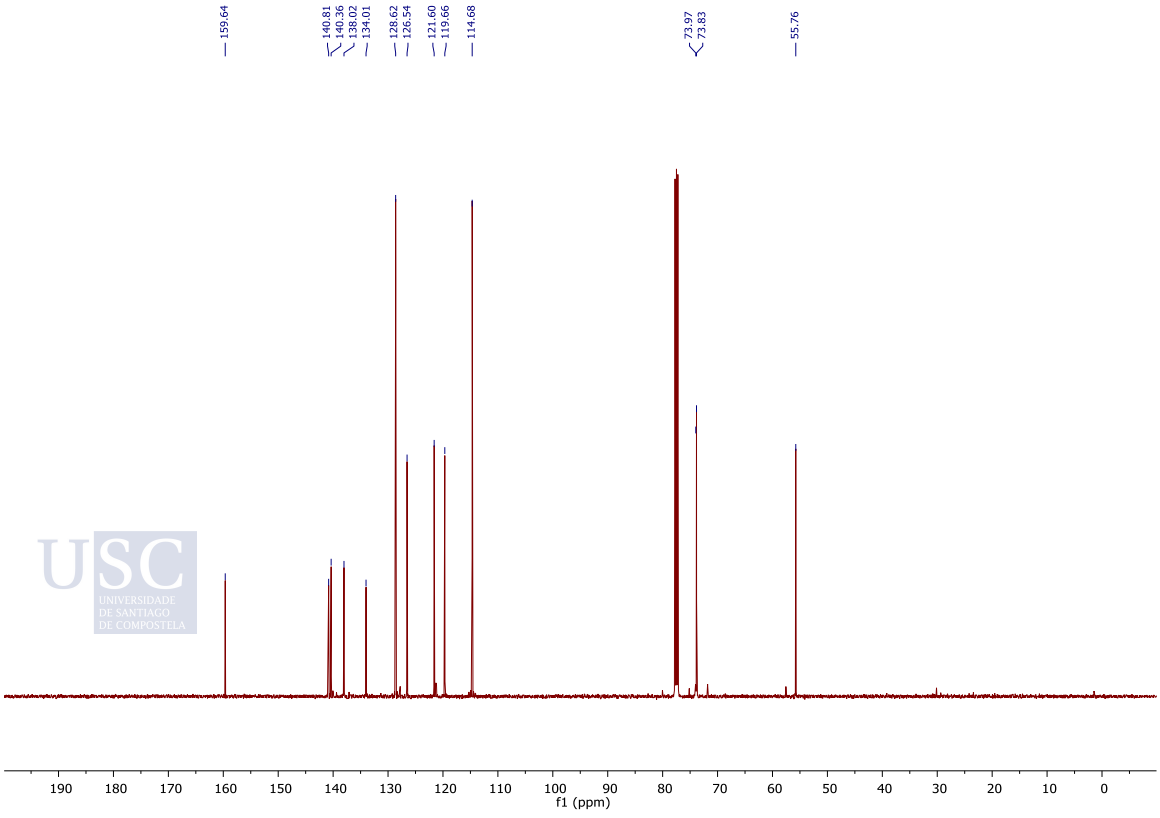

USC UNIVERSIDADE DE SANTIAGO DE COMPOSTELA

DEPT-135 (500 MHz, $CDCl_3$)

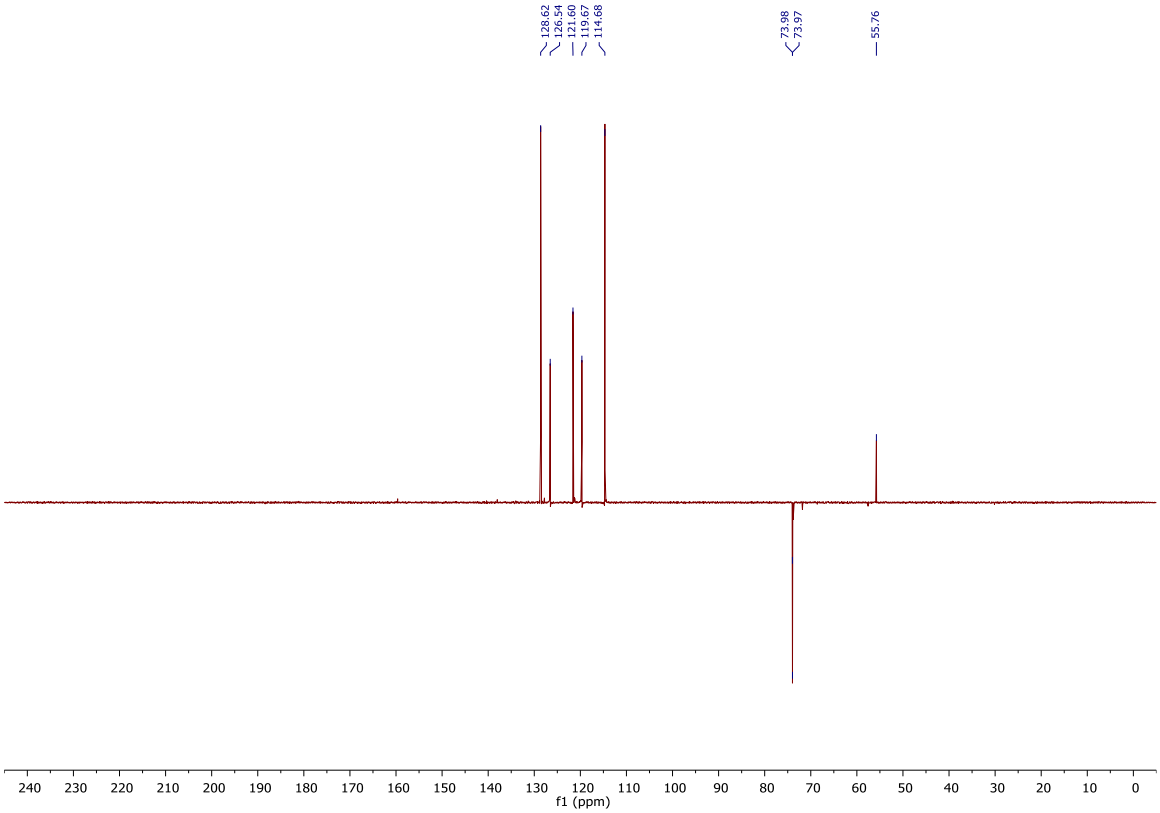

5-[4-(3-Bromopropoxy)phenyl]-1,3-dihydroisobenzofuran

^{1}H NMR (500 MHz, $CDCl_3$)

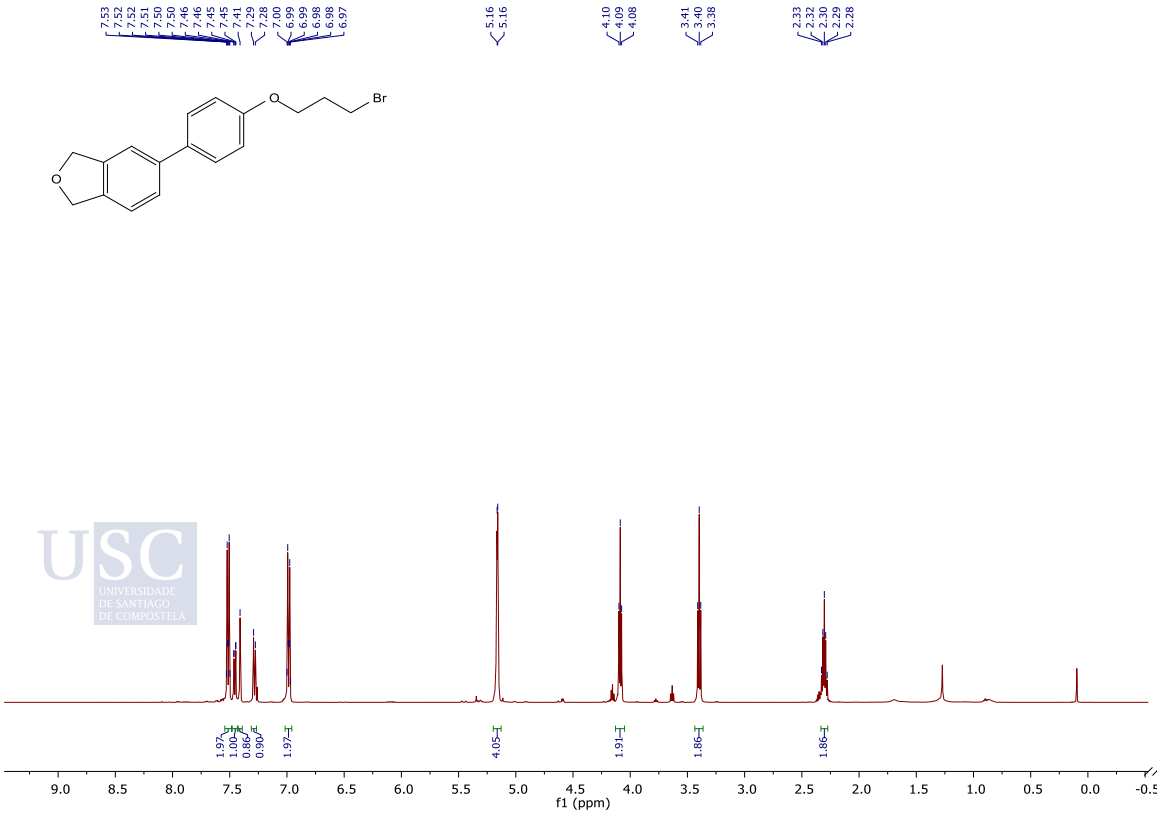

USC UNIVERSIDADE DE SANTIAGO DE COMPOSTELA

^{13}C NMR (126 MHz, $CDCl_3$)

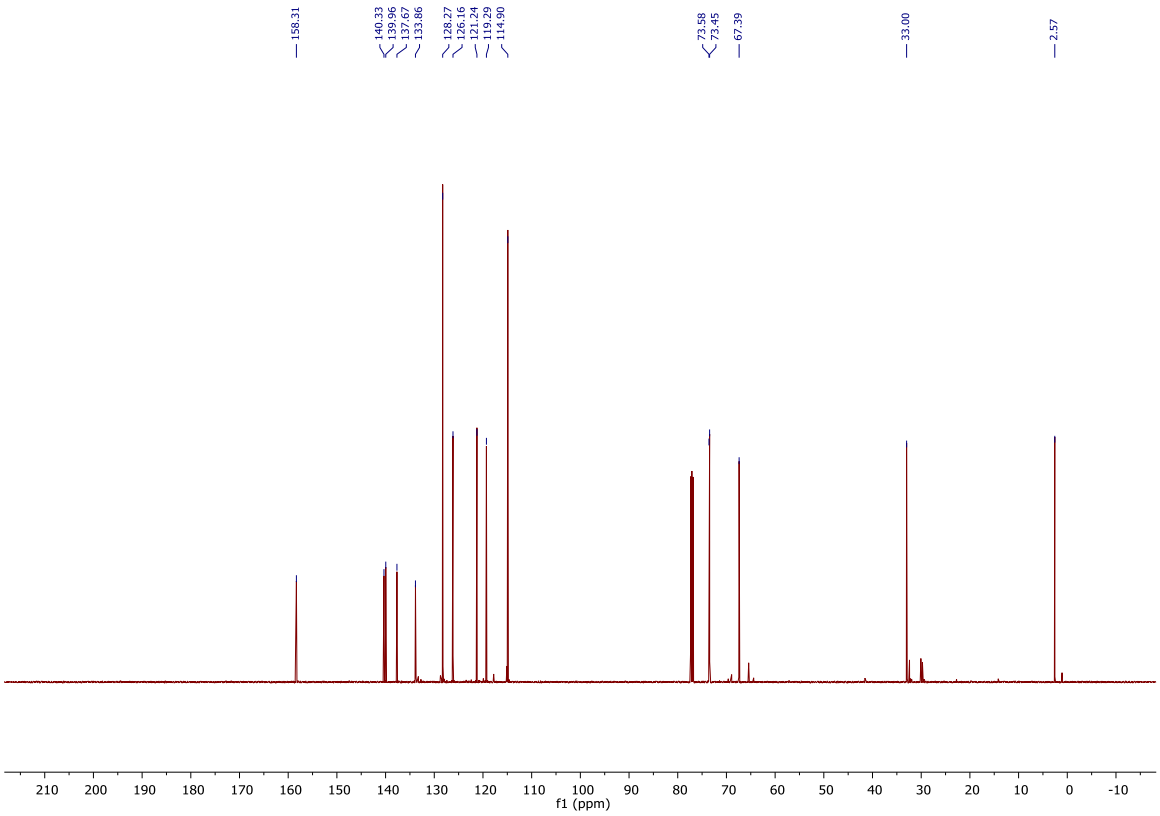

DEPT-135 (500 MHz, $CDCl_3$)

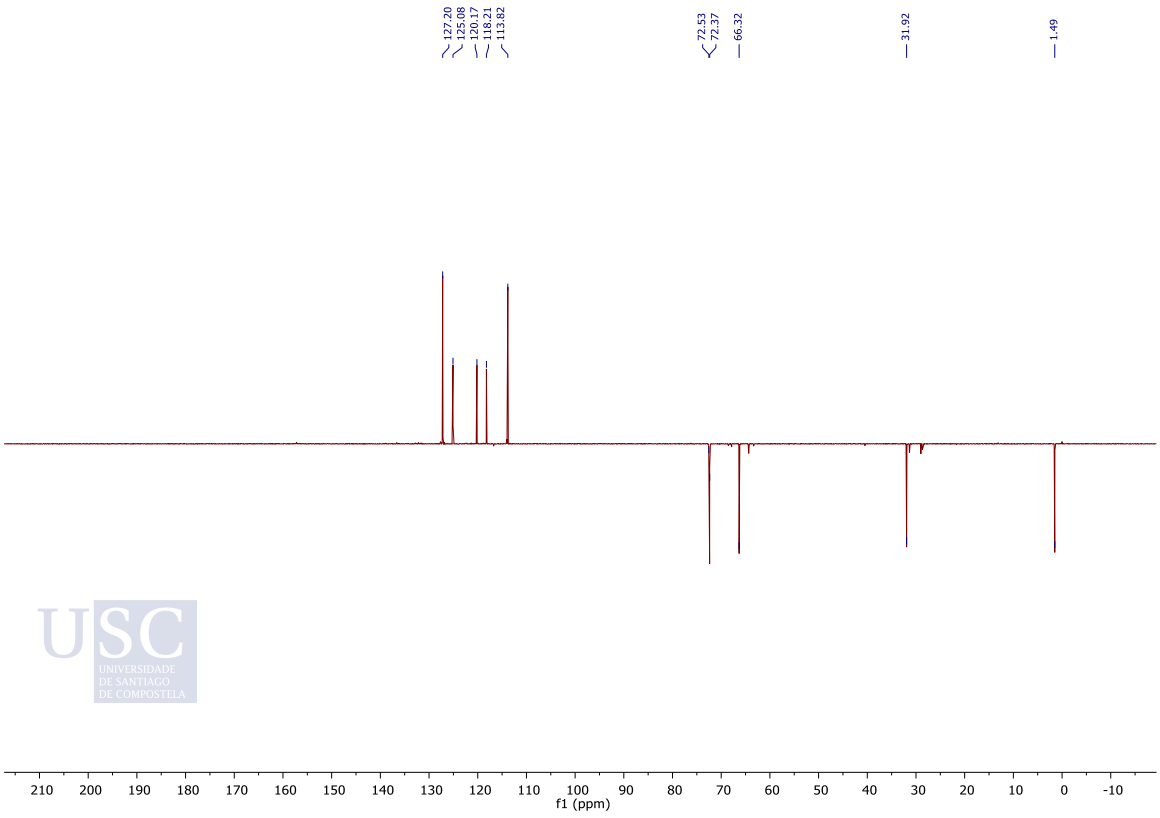

USC UNIVERSIDADE DE SANTIAGO DE COMPOSTELA

5-[4-(3-Triphenylphosphoniumpropoxy)phenyl]phthtalane (56)

^{1}H NMR (500 MHz, $CDCl_3$)

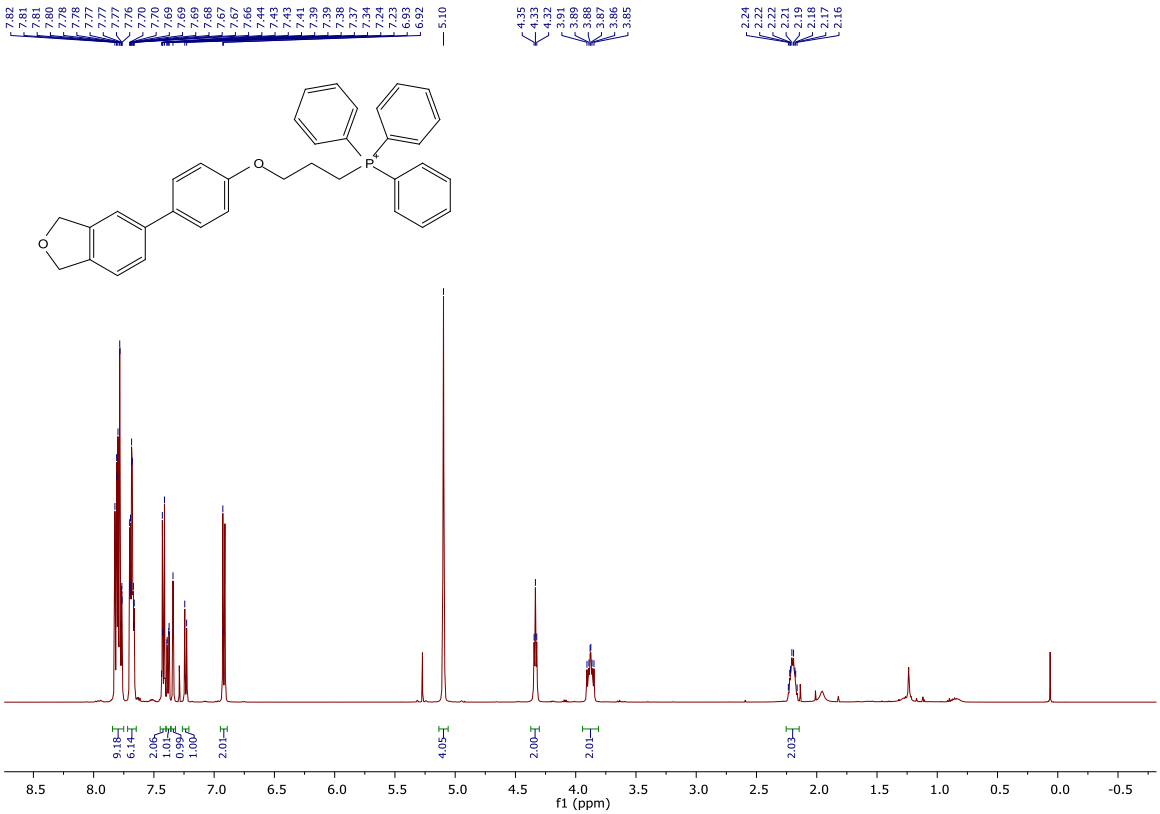

^{13}C NMR (126 MHz, $CDCl_3$)

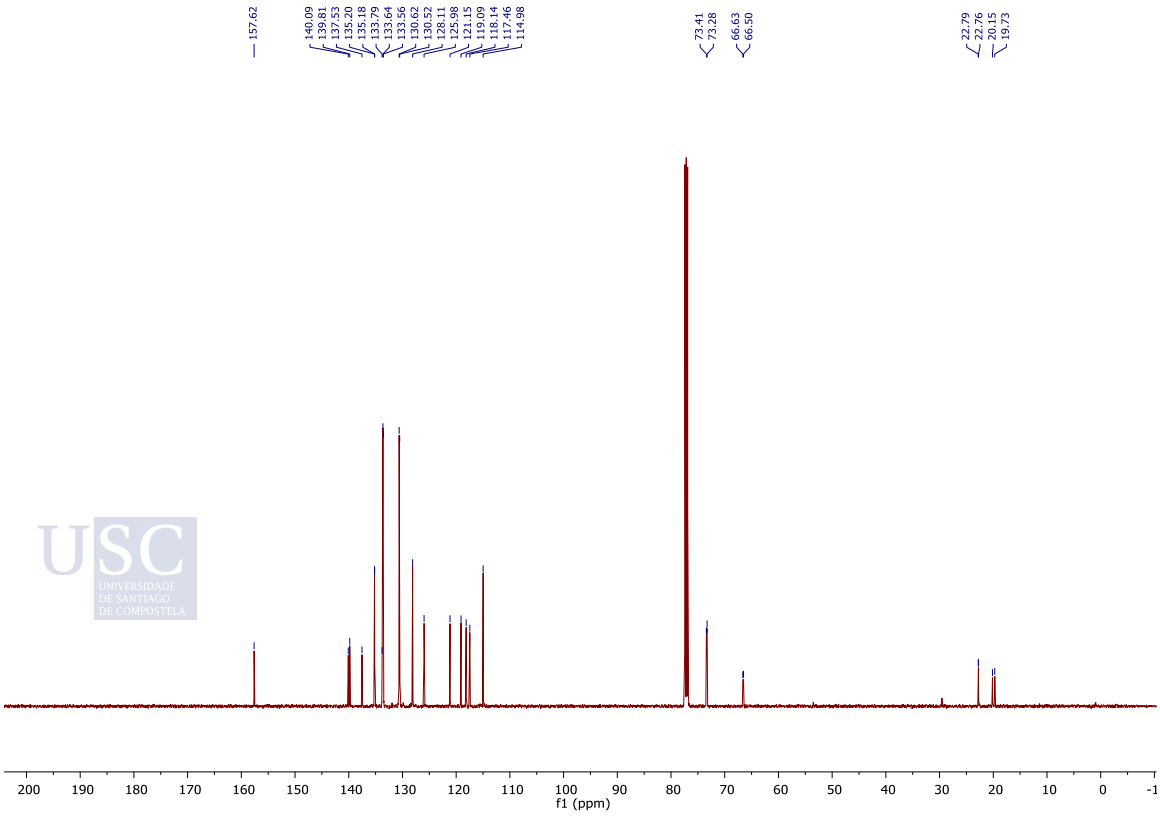

USC UNIVERSIDADE DE SANTIAGO DE COMPOSTELA

DEPT-135 (500 MHz, $CDCl_3$)

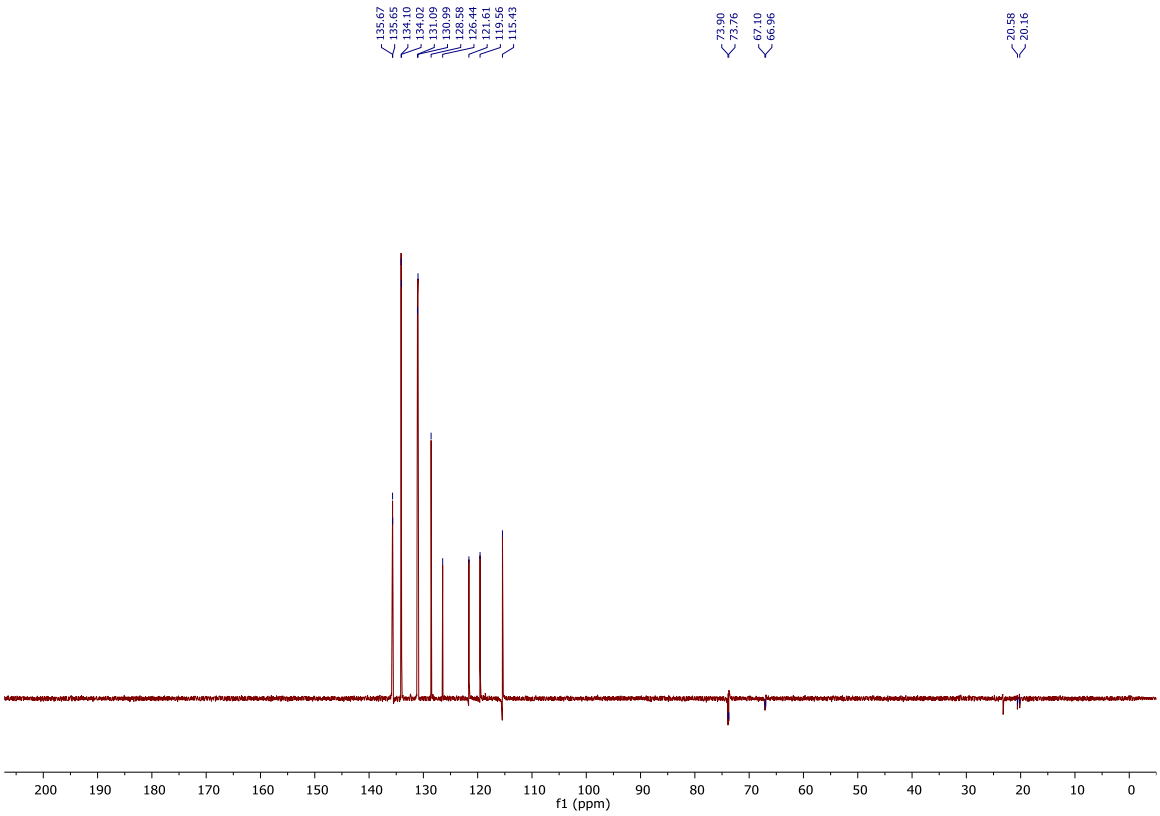

^{31}P NMR (202 MHz, $CDCl_3$)

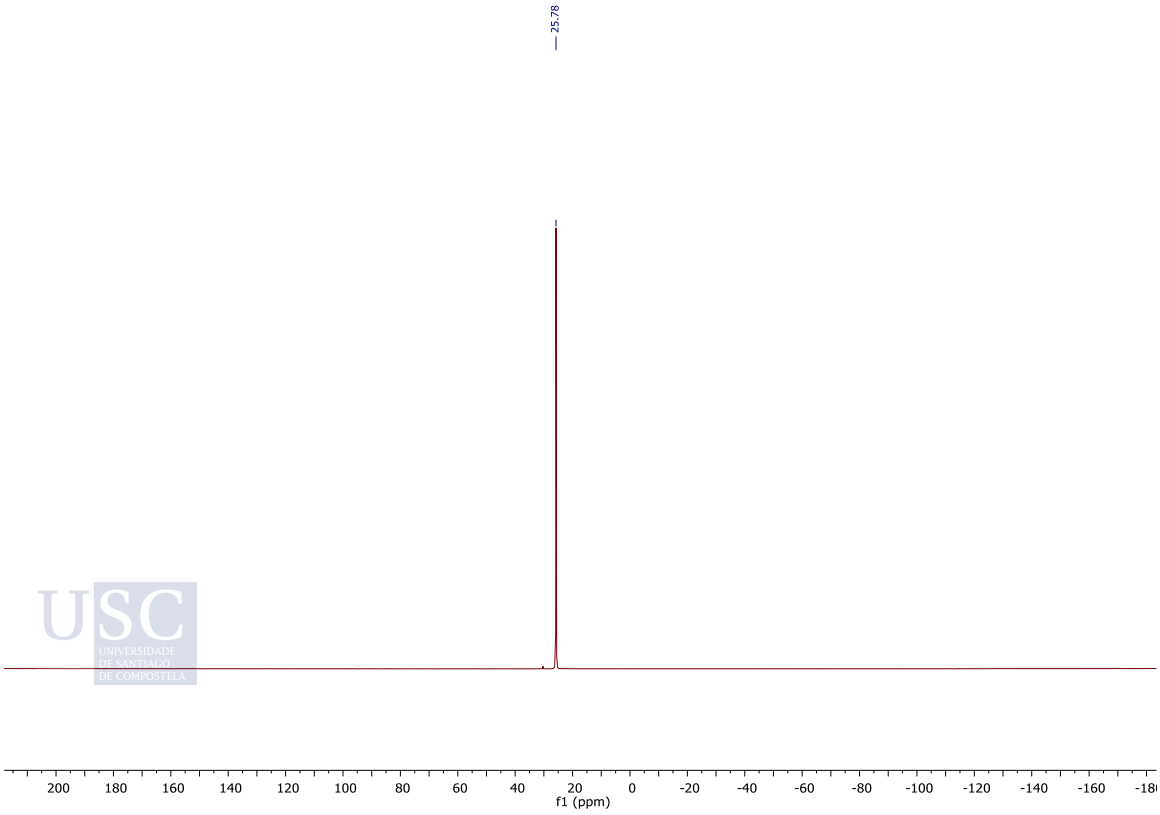

USC UNIVERSIDADE DE SANTIAGO DE COMPOSTELA

2-(4-Methoxyphenyl)-9-10-anthraquinone (41)

^{1}H NMR (500 MHz, $CDCl_3$)

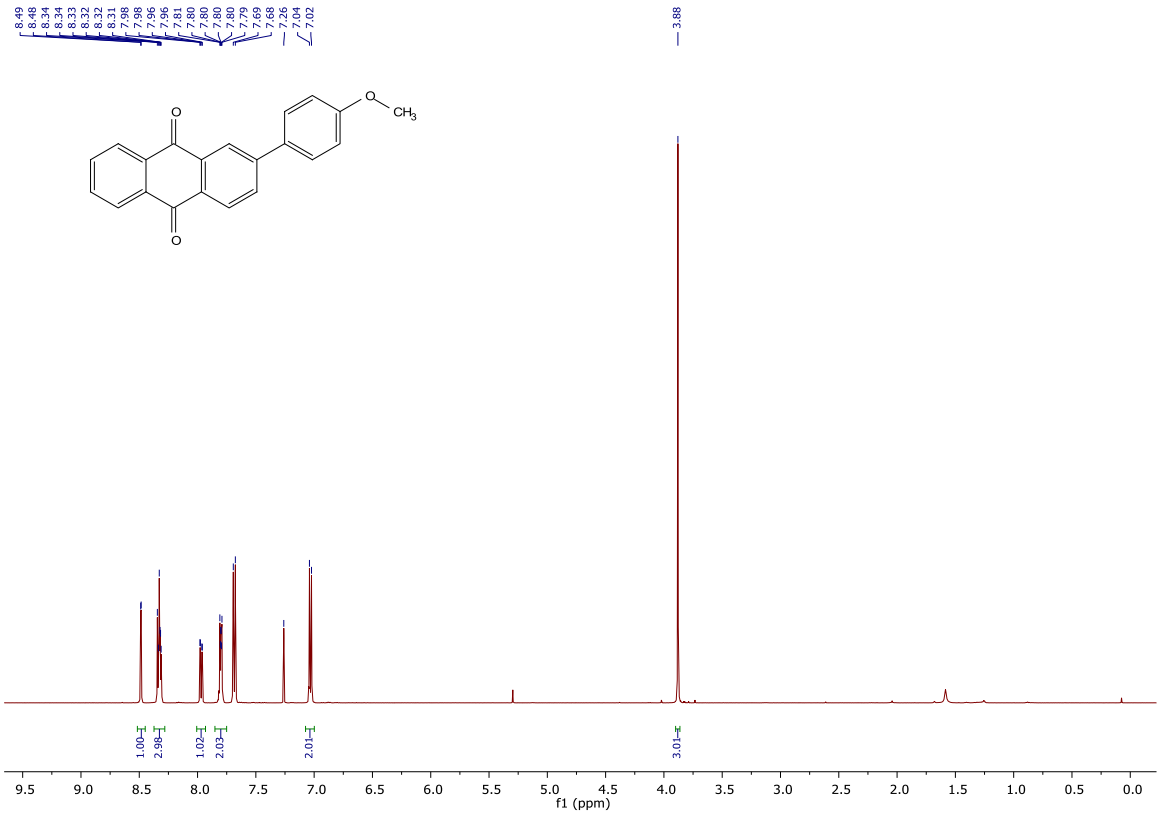

^{13}C NMR (126 MHz, $CDCl_3$)

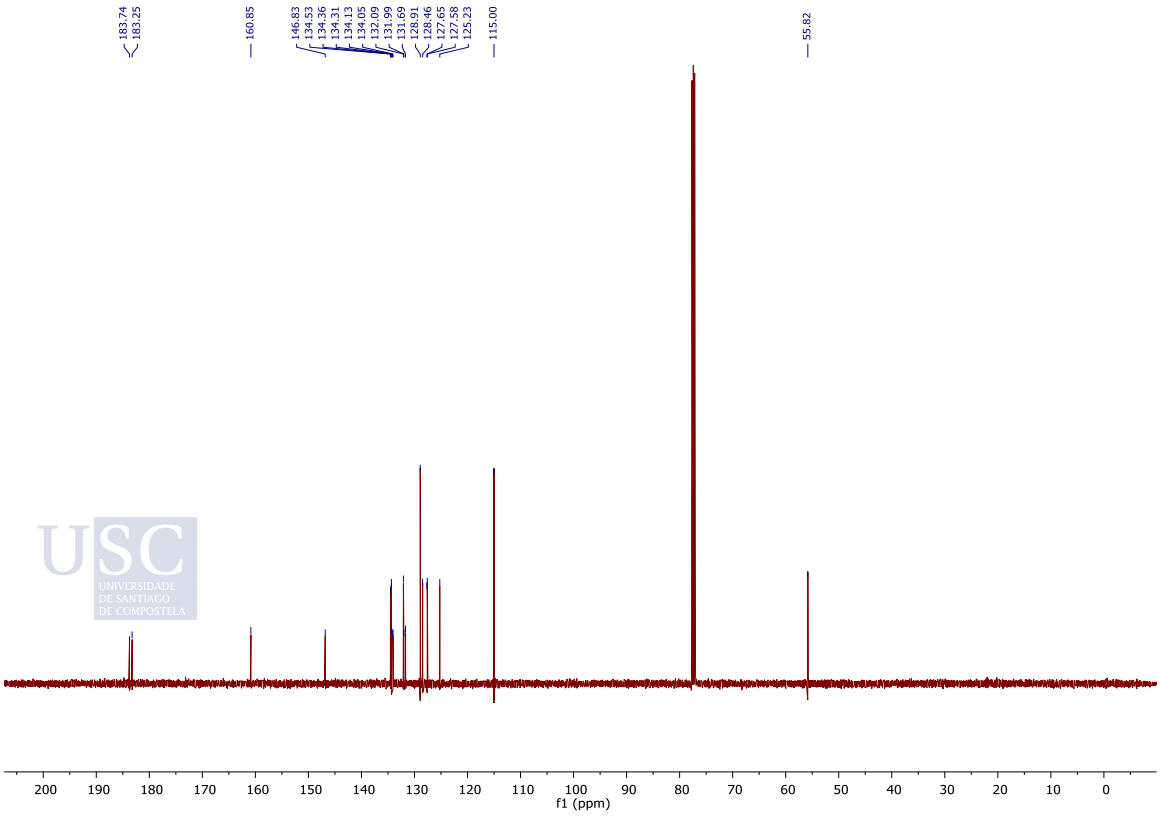

USC UNIVERSIDADE DE SANTIAGO DE COMPOSTELA

DEPT-135 (500 MHz, $CDCl_3$)

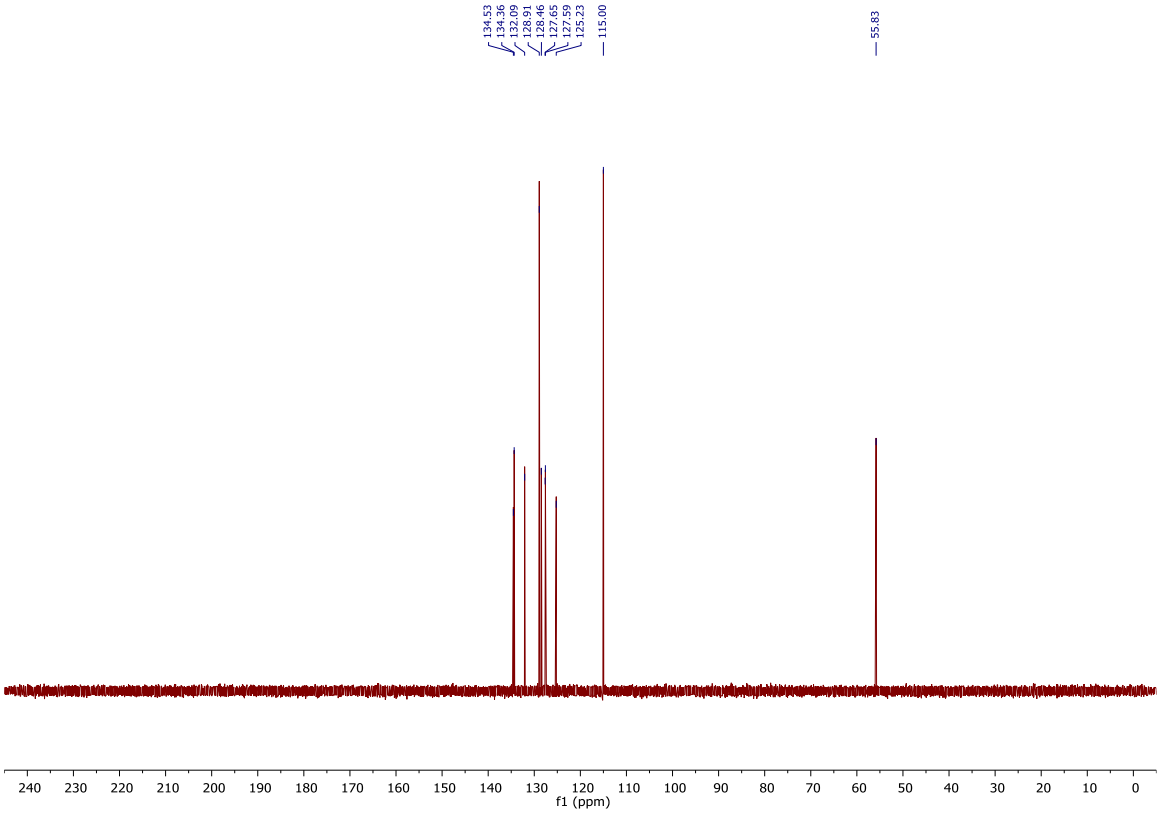

2,3-Dimethoxy-6-(4-methoxyphenyl)-9,10-anthraquinone (42)

^{1}H NMR (500 MHz, $CDCl_3$)

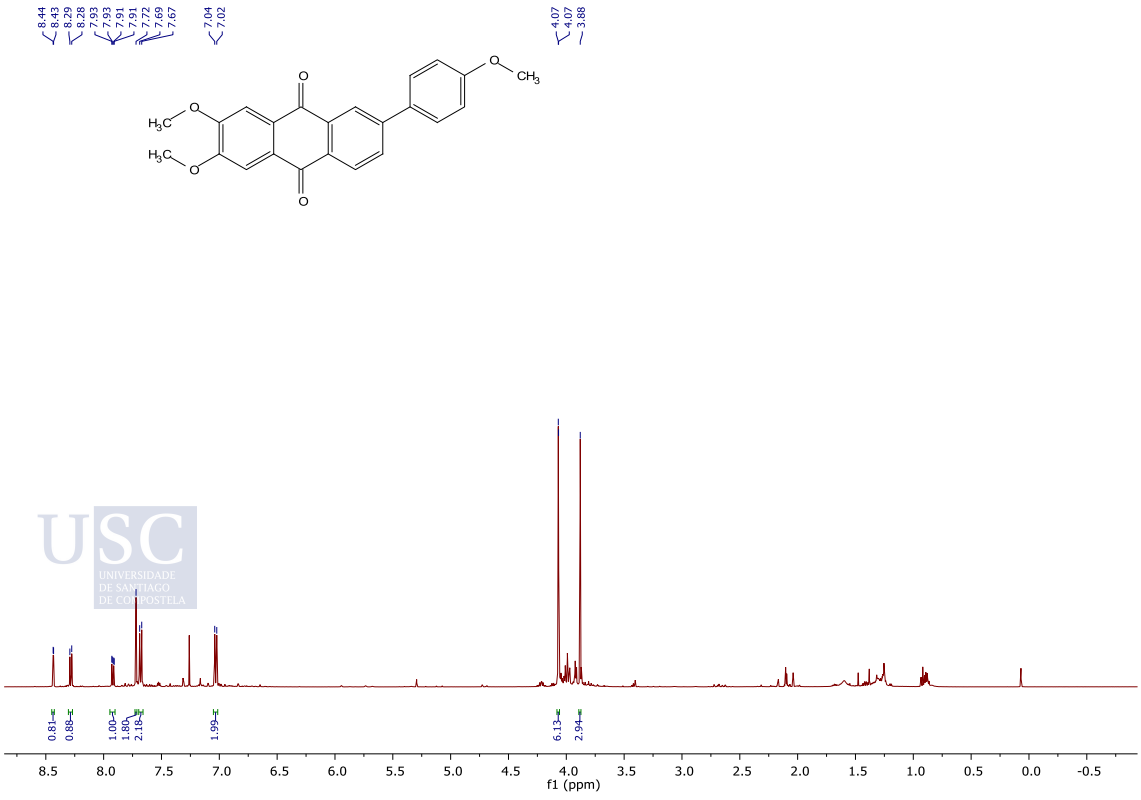

^{13}C NMR (126 MHz, $CDCl_3$)

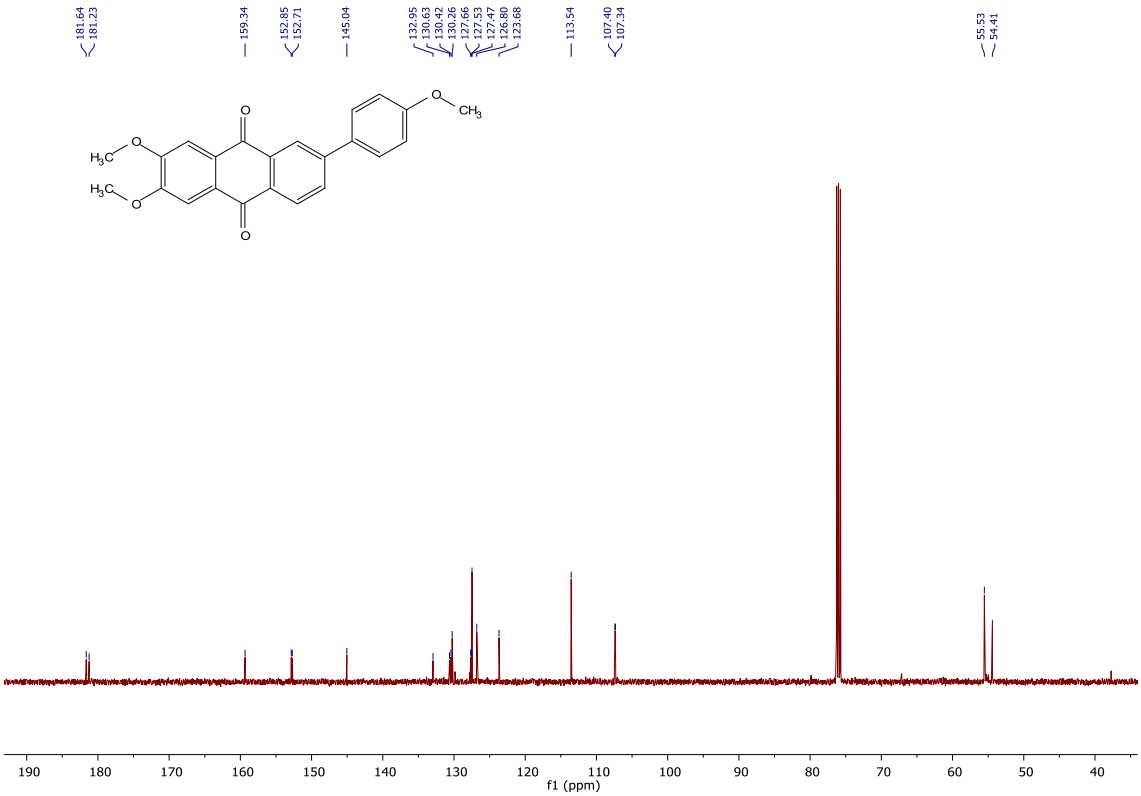

DEPT-135 (500 MHz, $CDCl_3$)

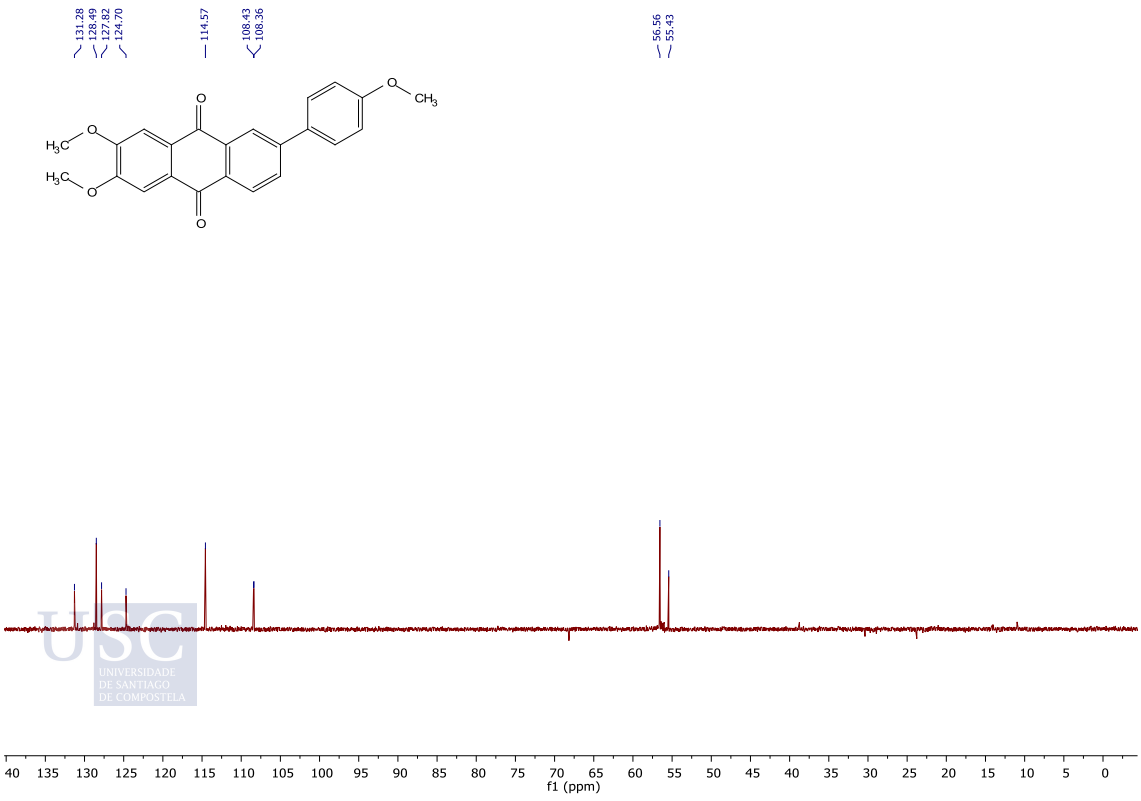

USC
UNIVERSIDADE
DE SANTIAGO
DE COMPOSTELA

1,4-Dimethyl-2-(4-methoxyphenyl)-9,10-anthraquinone (43)

^{1}H NMR (500 MHz, $CDCl_3$)

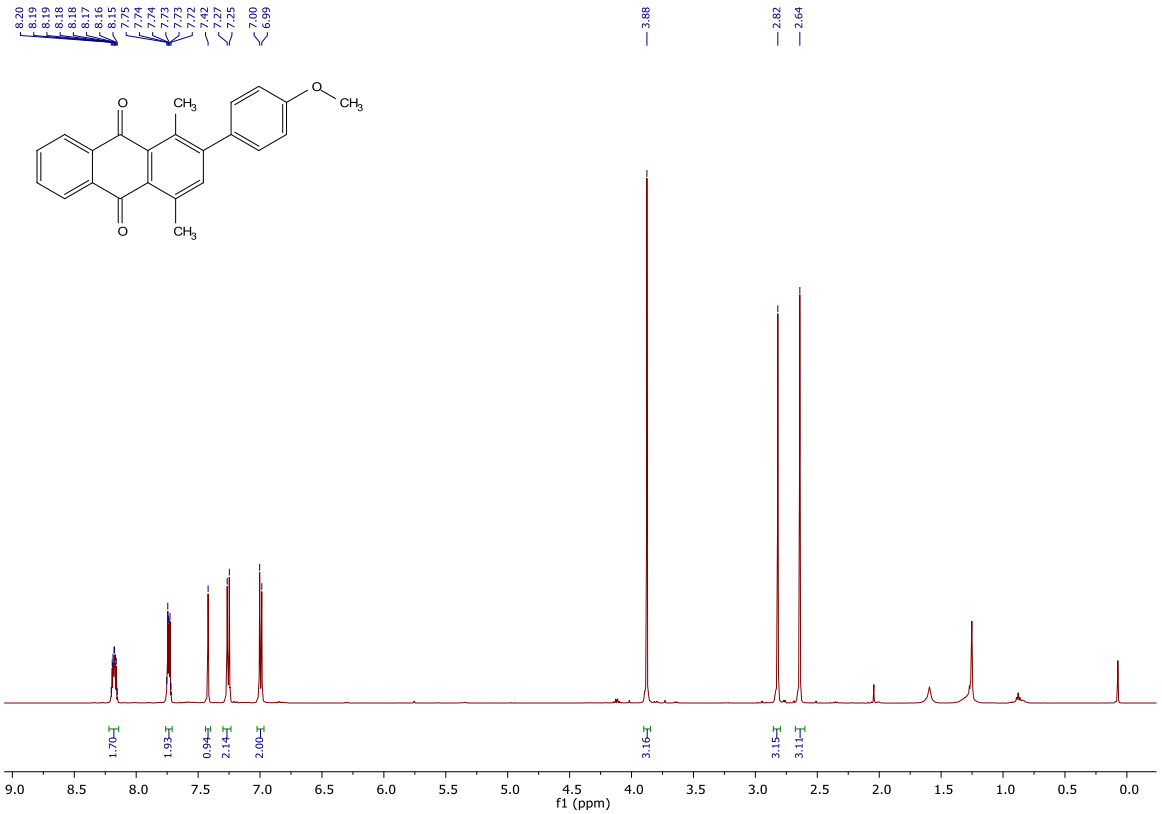

^{13}C NMR (126 MHz, $CDCl_3$)

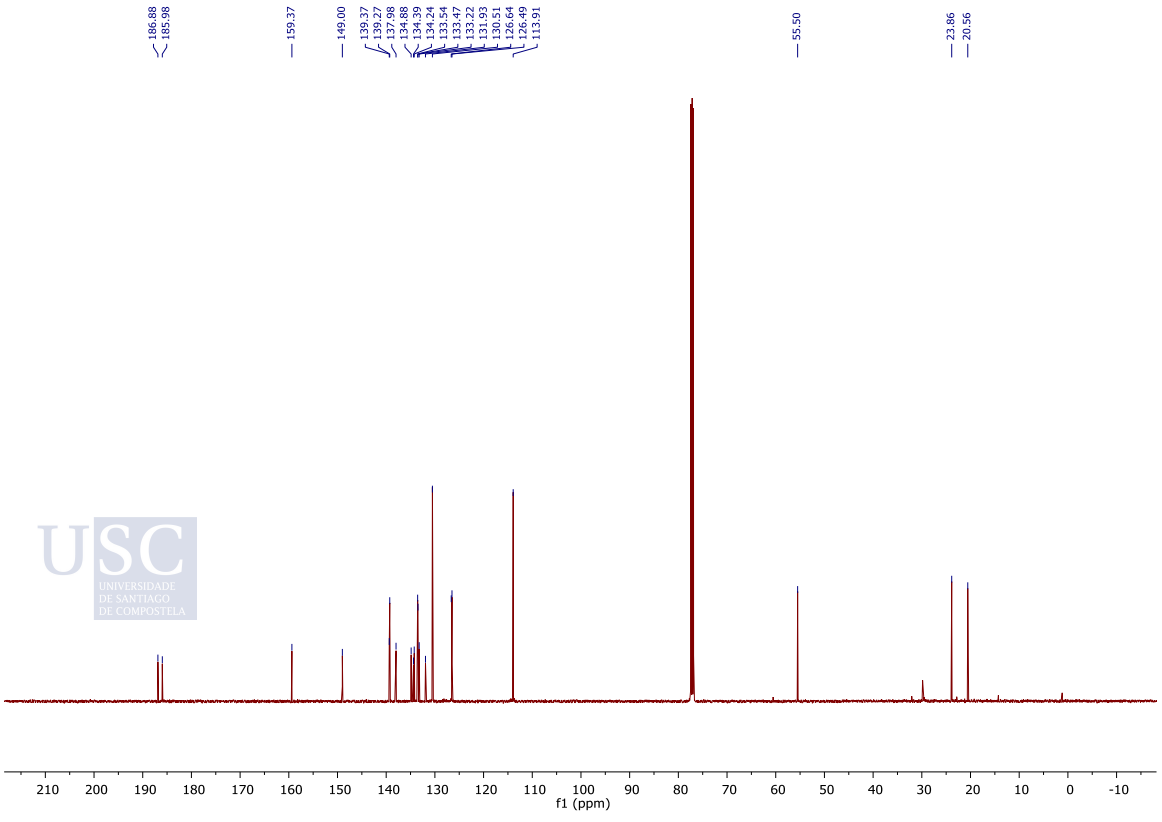

USC
UNIVERSIDADE DE SANTIAGO DE COMPOSTELA

DEPT-135 (500 MHz, $CDCl_3$)

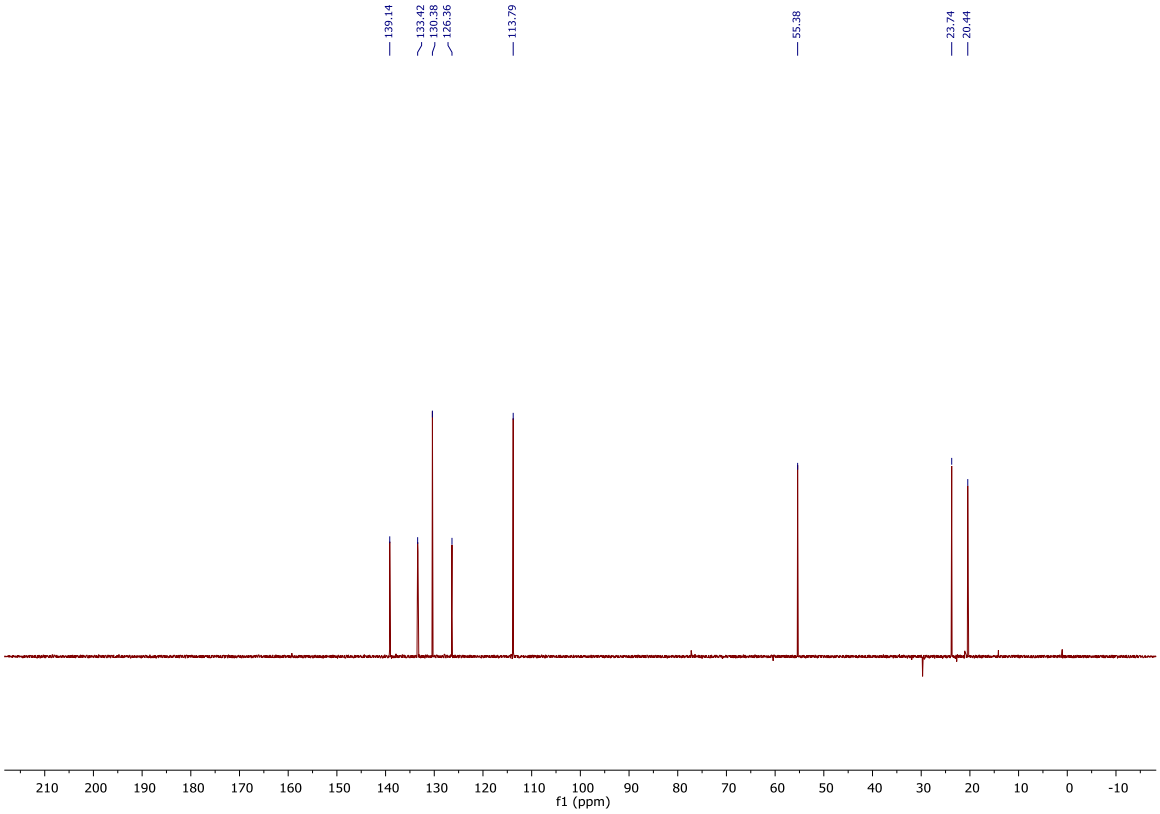

2-(4-(trifluoromethyl)phenyl)-9,10-anthraquinone (44)

^{1}H NMR (500 MHz, $CDCl_3$)

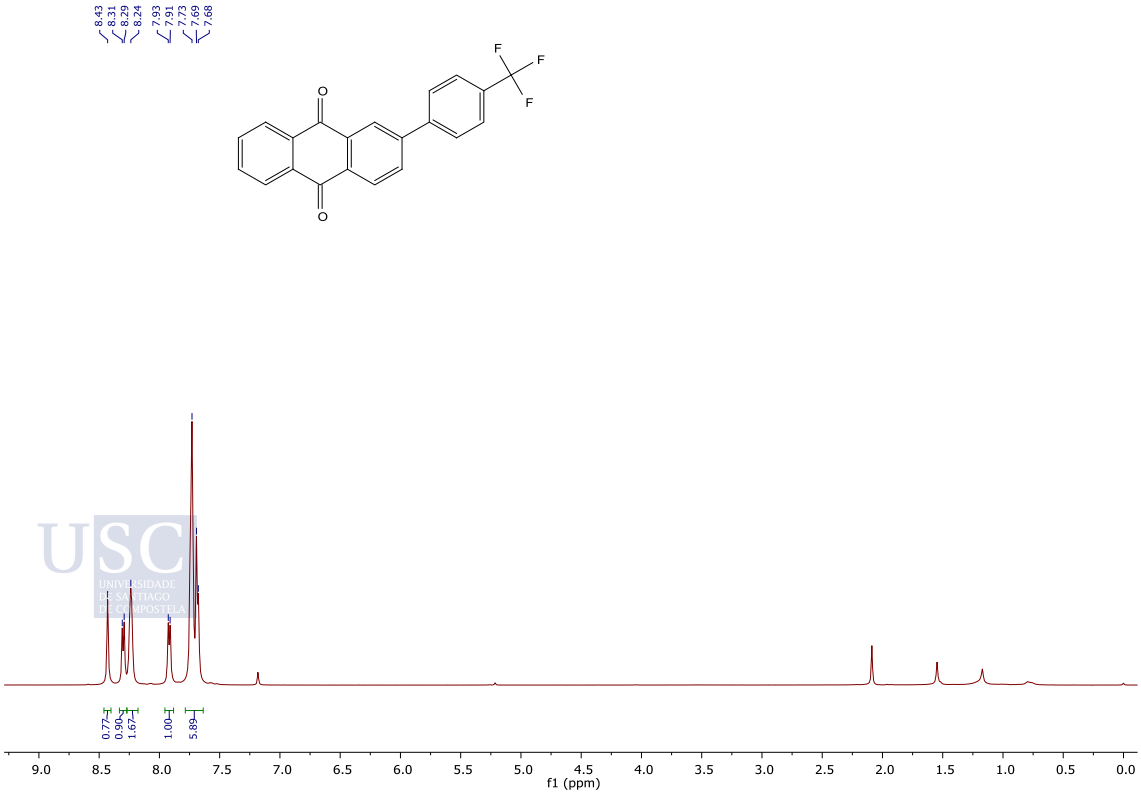

^{13}C NMR (126 MHz, $CDCl_3$)

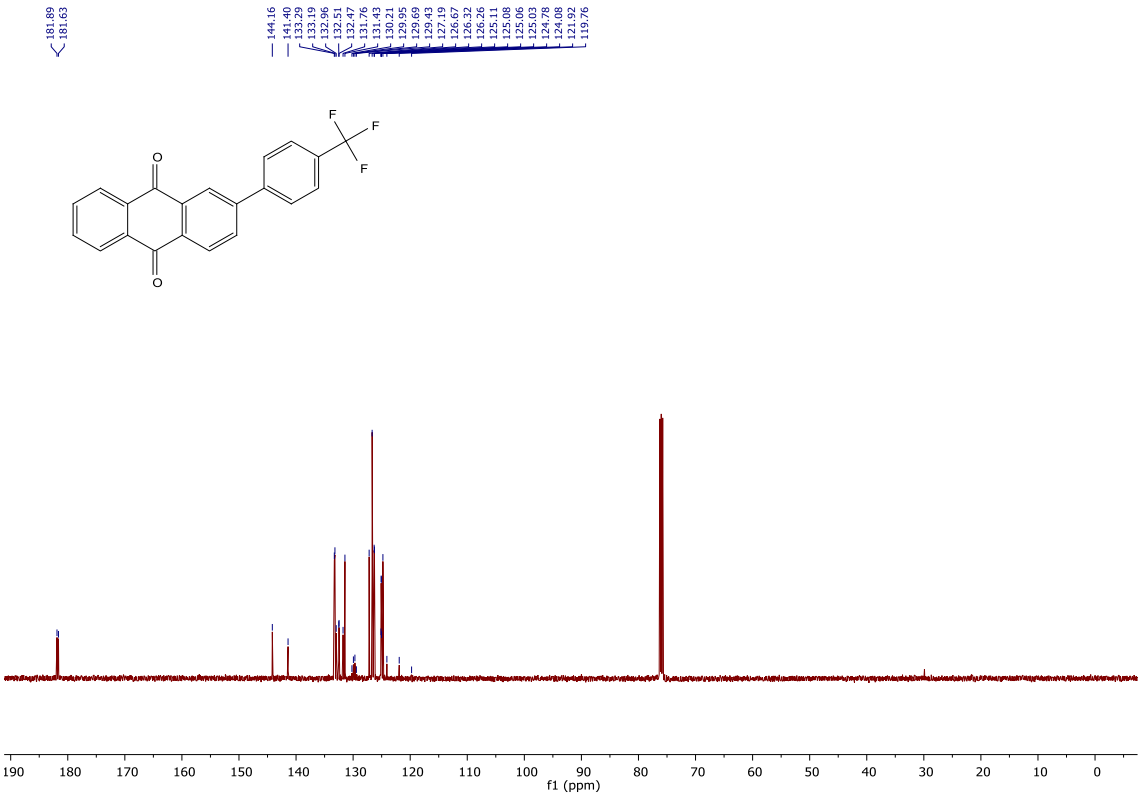

DEPT-135 (500 MHz, $CDCl_3$)

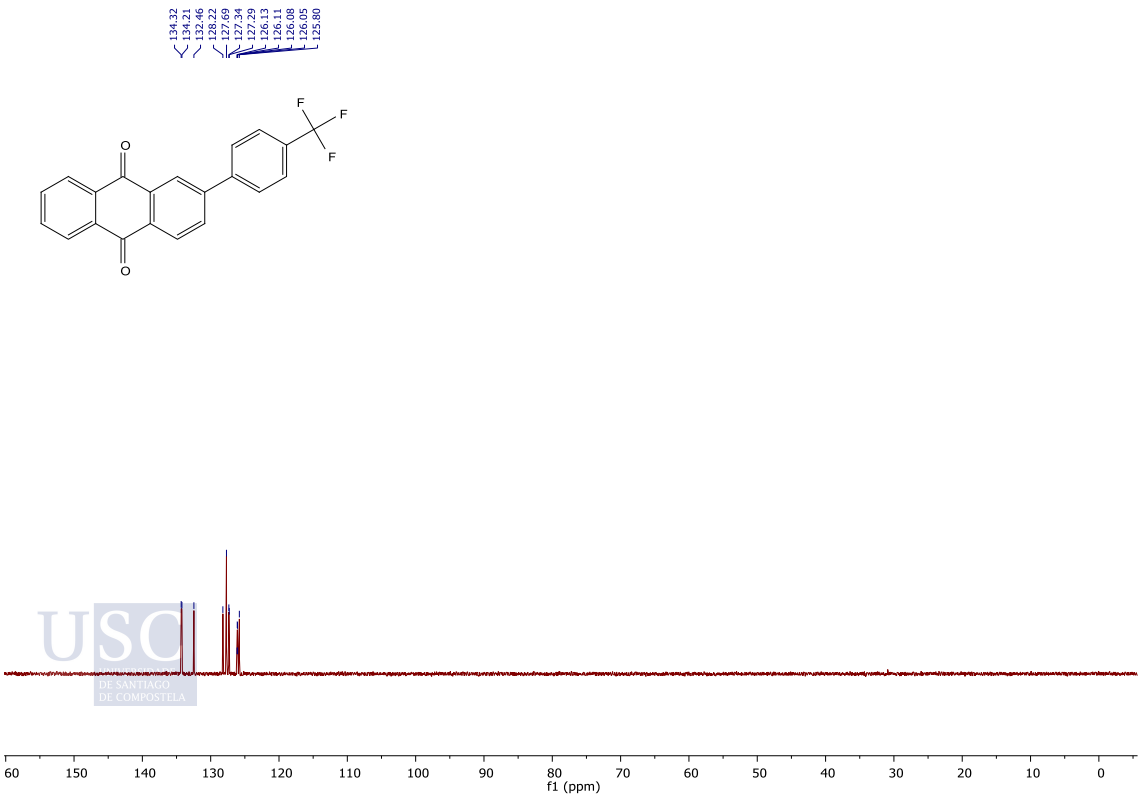

USC UNIVERSIDADE DE SANTIAGO DE COMPOSTELA

^{19}F NMR (282 MHz, $CDCl_3$)

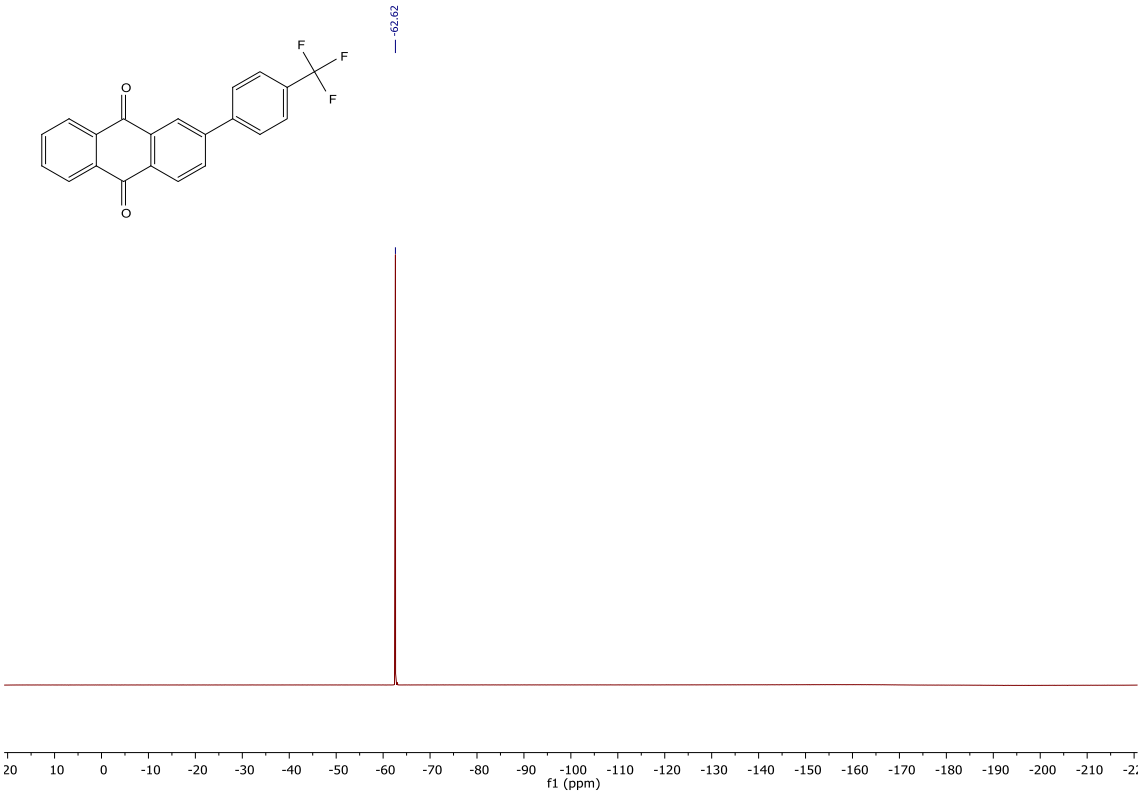

2-[4-(3-Bromopropoxy)phenyl]-9,10-anthraquinone (54)

^{1}H NMR (500 MHz, $CDCl_3$)

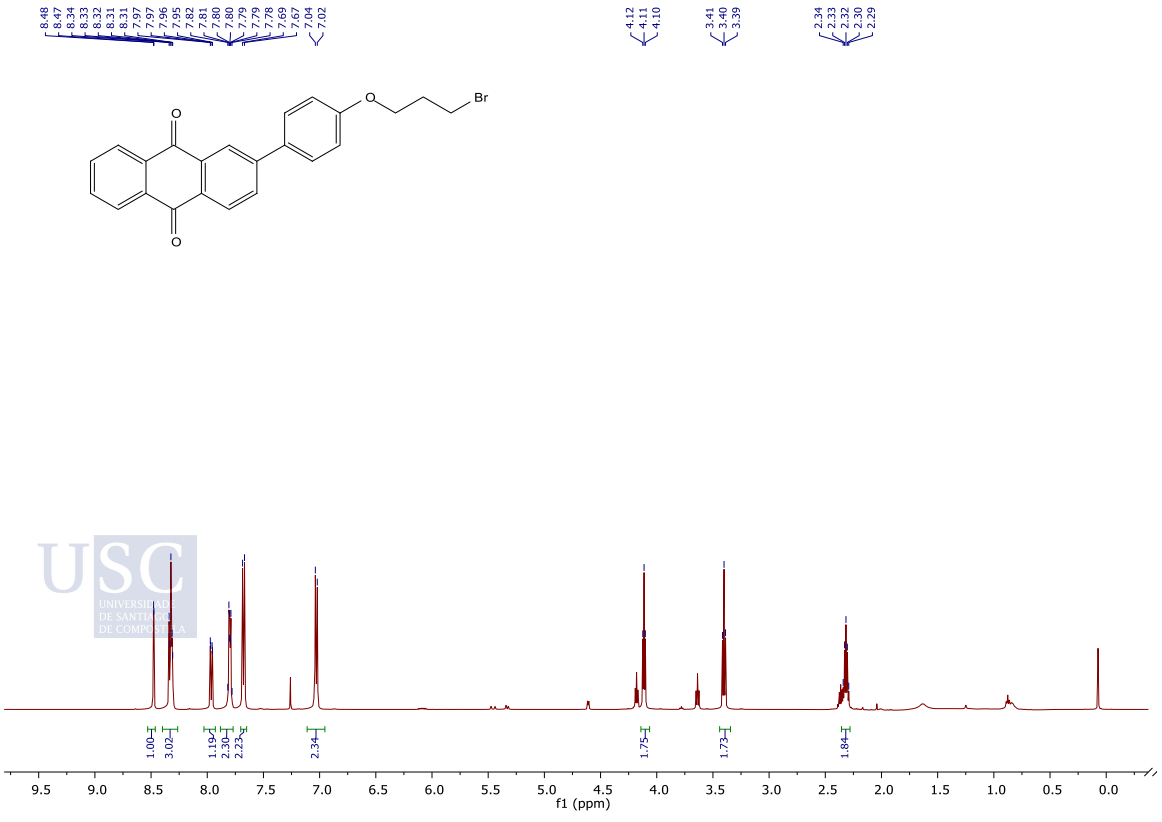

USC UNIVERSIDADE DE SANTIAGO DE COMPOSTELA

^{13}C NMR (126 MHz, $CDCl_3$)

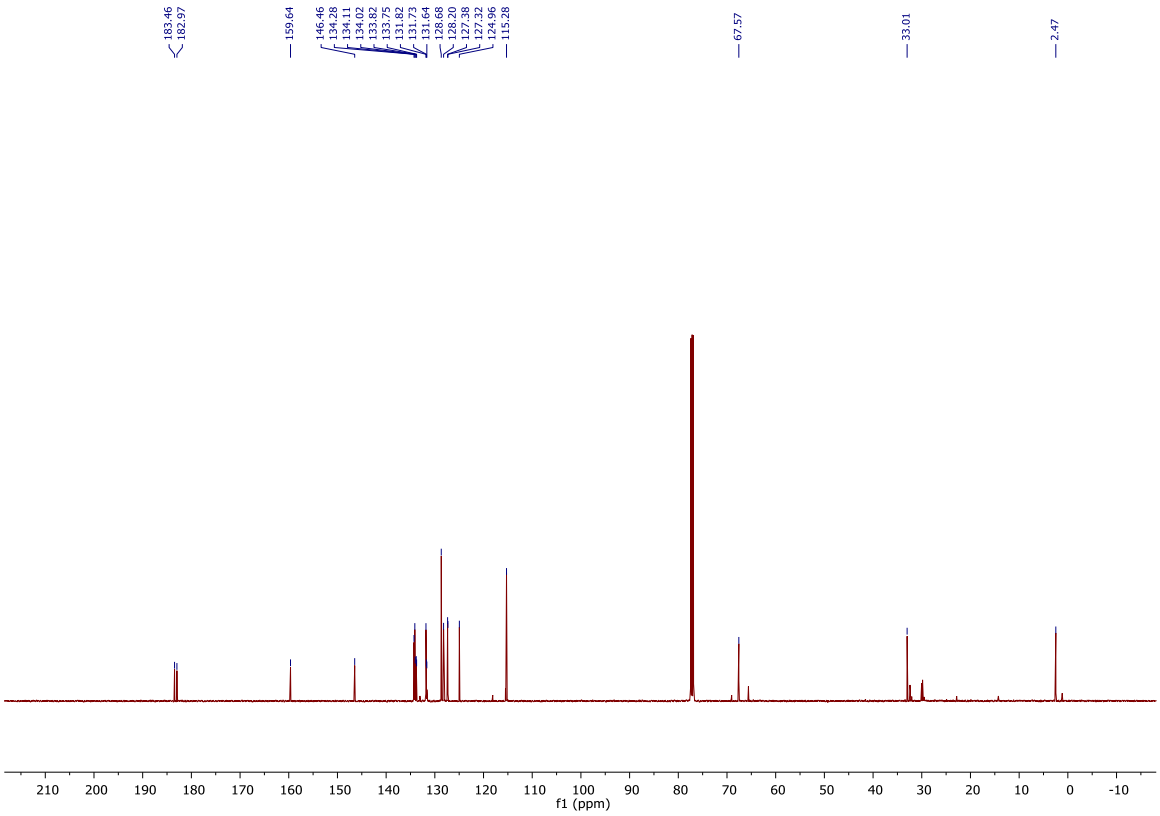

DEPT-135 (500 MHz, $CDCl_3$)

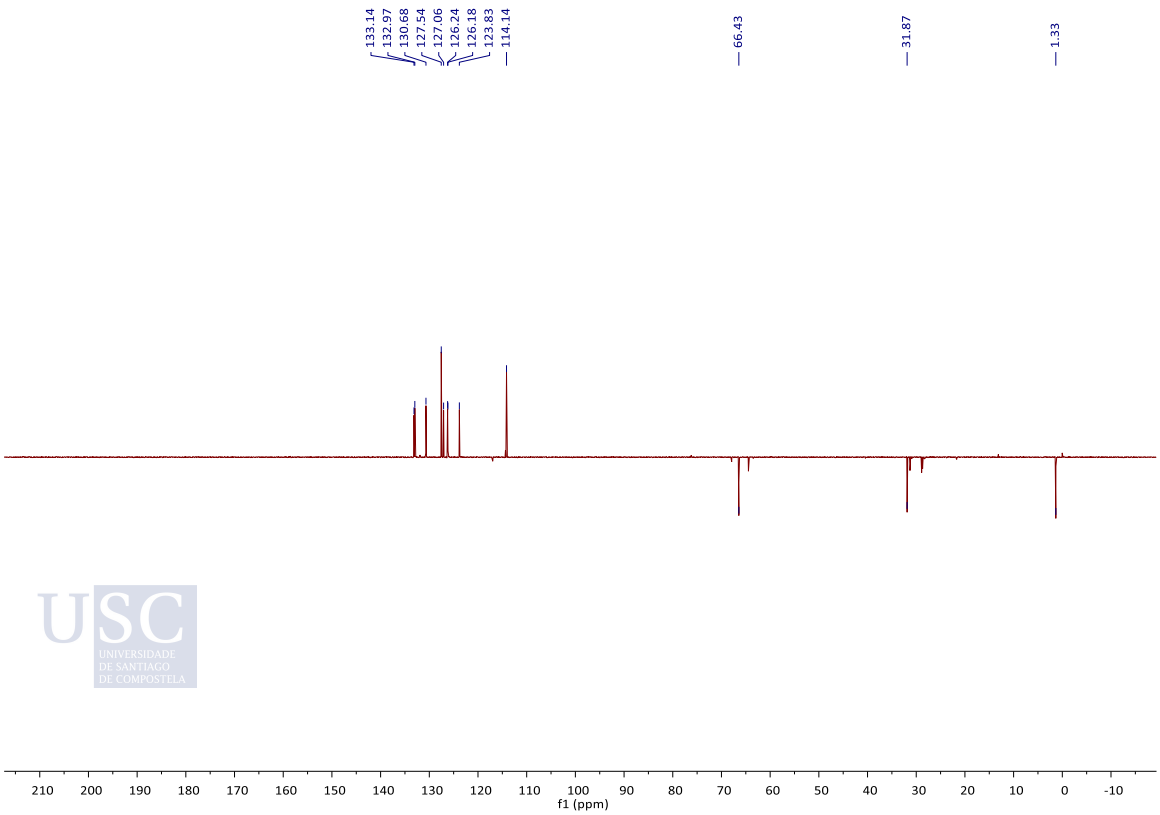

USC
UNIVERSIDADE DE SANTIAGO DE COMPOSTELA

{3-[4-(9,10-dioxo-9,10-dihydroanthracen-2-yl)phenoxy]propyl}triphenylphosphonium bromide (55)

^{1}H NMR (500 MHz, $CDCl_3$)

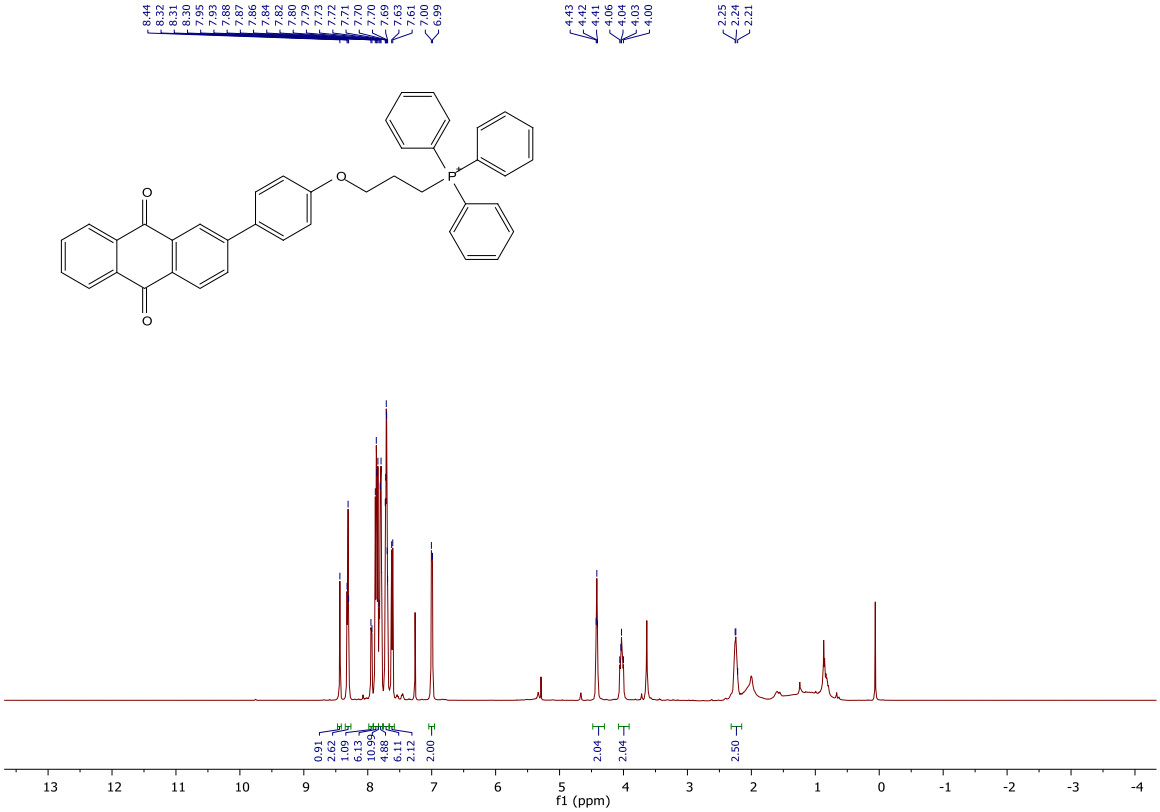

^{13}C NMR (126 MHz, $CDCl_3$)

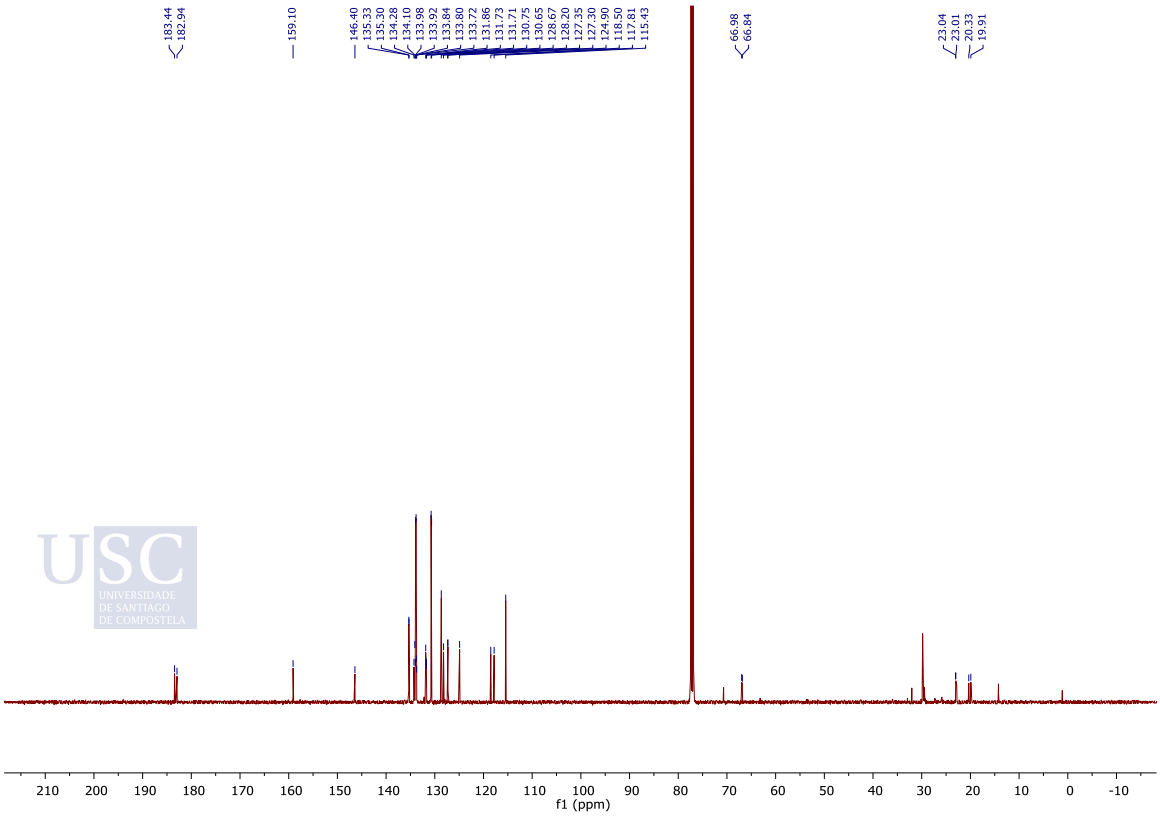

USC UNIVERSIDADE DE SANTIAGO DE COMPOSTELA

DEPT-135 (500 MHz, $CDCl_3$)

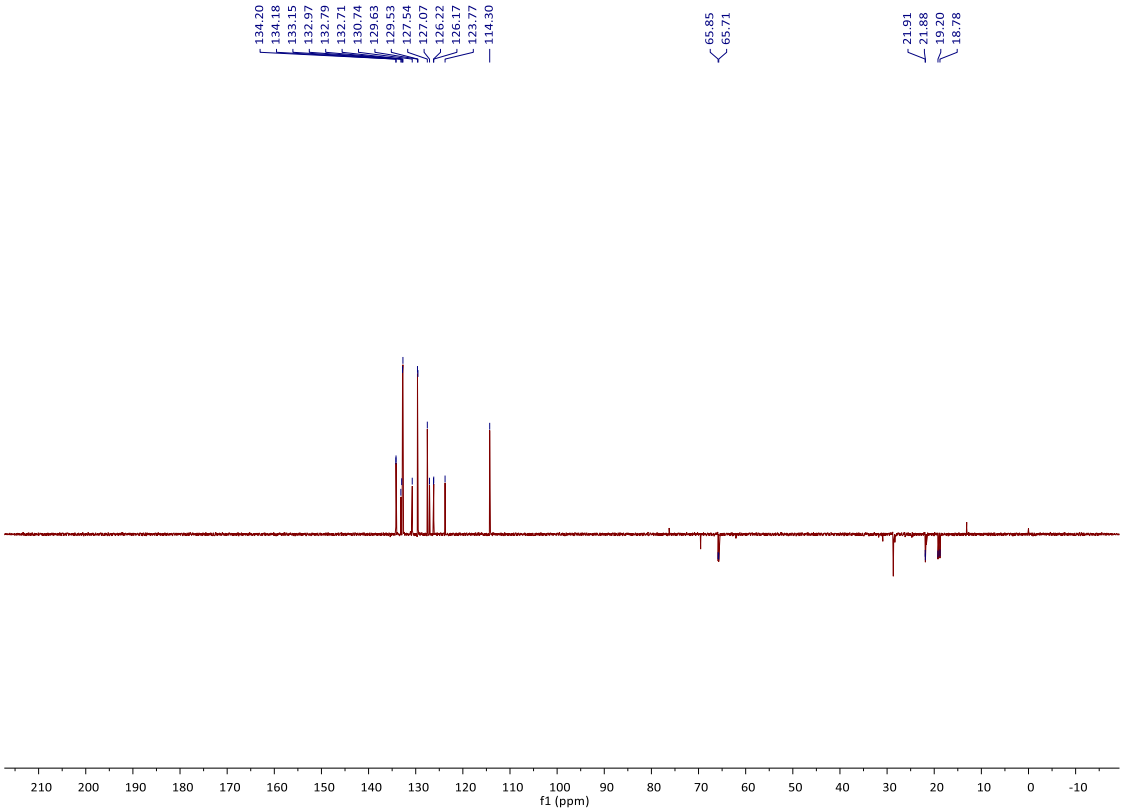

^{31}P NMR (202 MHz, $CDCl_3$)

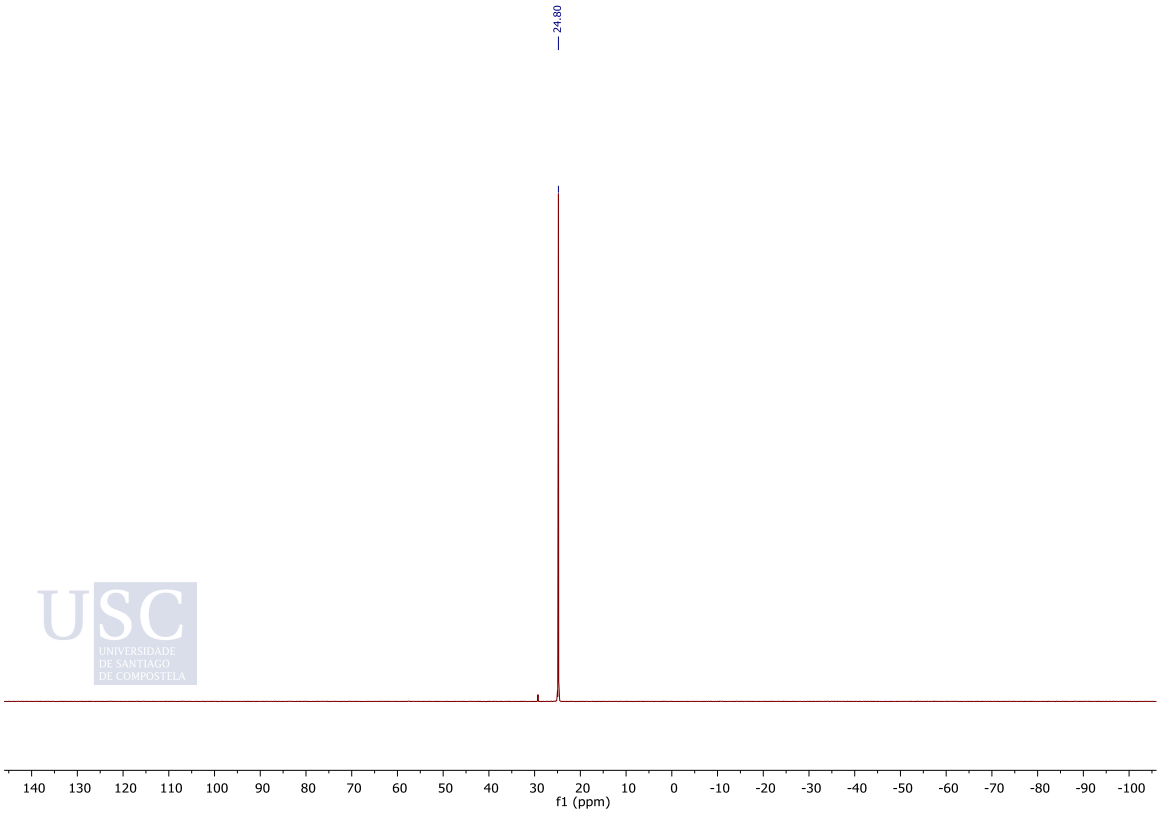

USC UNIVERSIDADE DE SANTIAGO DE COMPOSTELA

2-[4-(1,2,2-Triphenylvinyl)phenyl]anthracene-9,10-dione (48)

^{1}H NMR (500 MHz, $CDCl_3$)

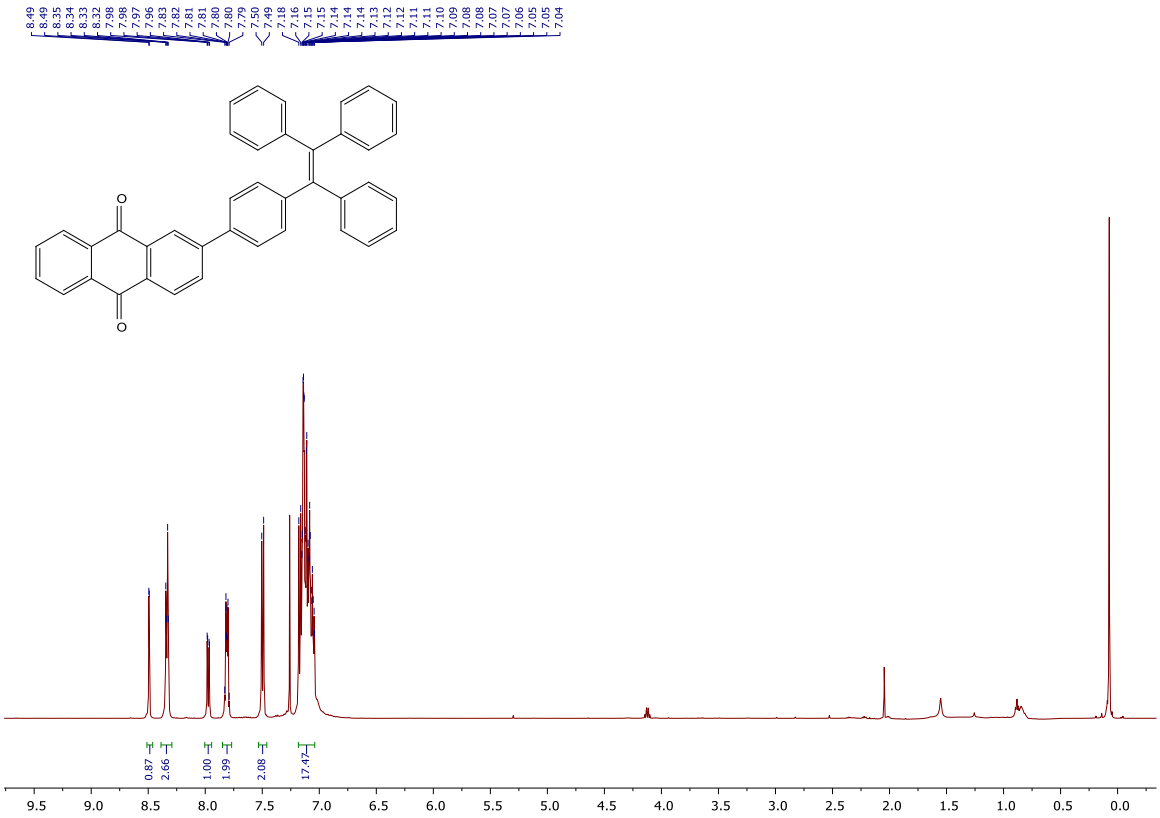

^{13}C NMR (126 MHz, $CDCl_3$)

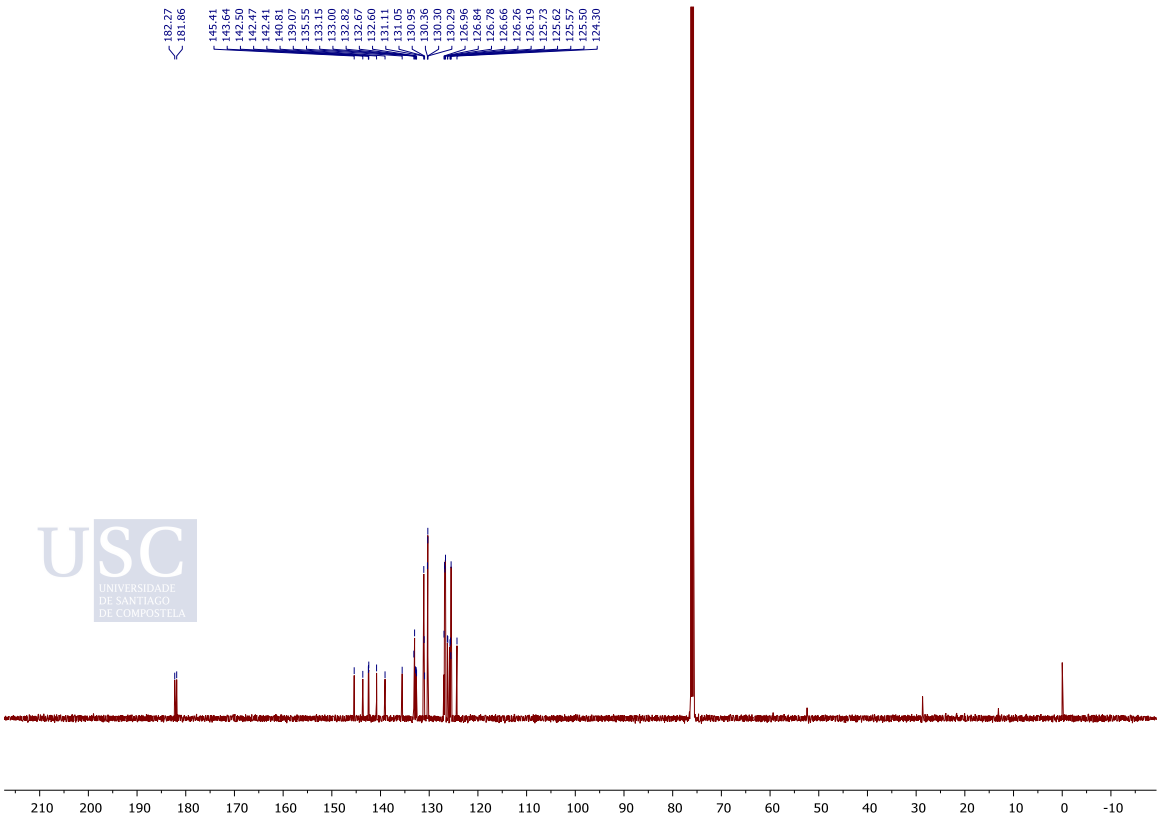

USC
UNIVERSIDADE DE SANTIAGO DE COMPOSTELA

DEPT-135 (500 MHz, $CDCl_3$)

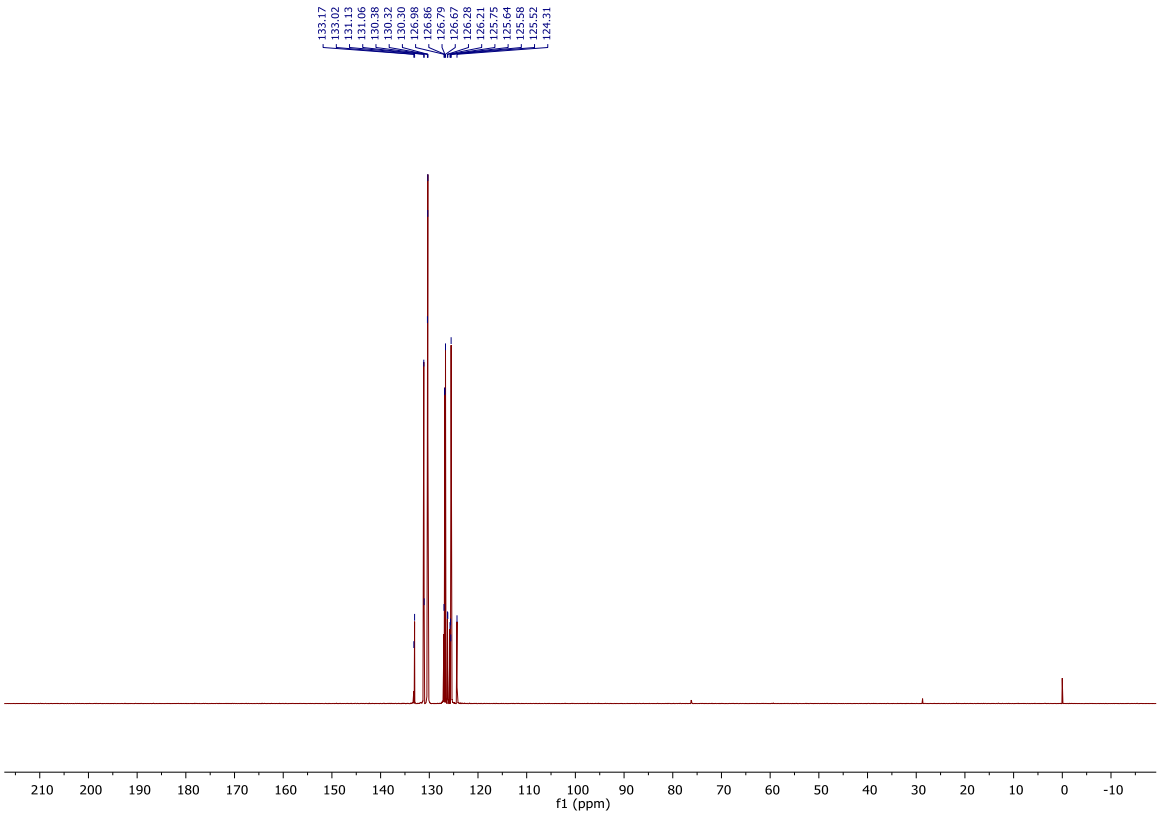

2-(1,2,2-Triphenylvinyl)-9,10-anthraquinone (50)

^{1}H NMR (500 MHz, $CDCl_3$)

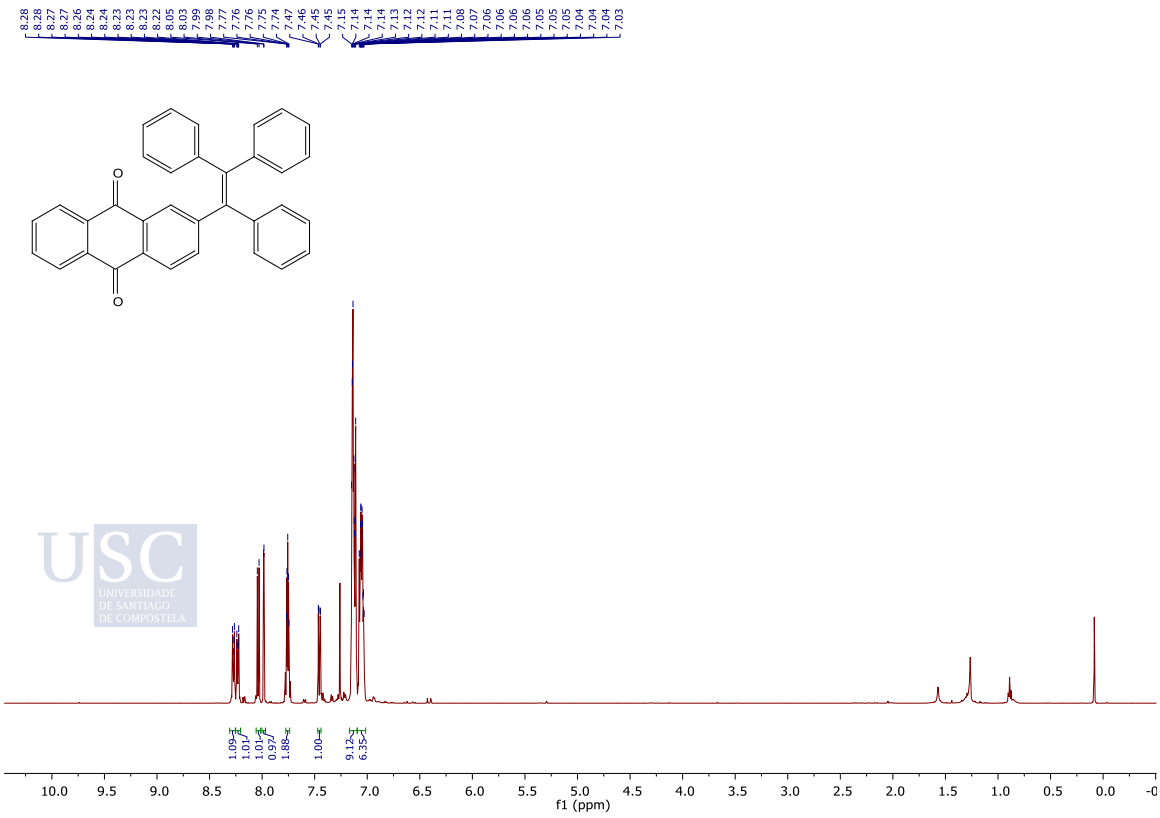

USC UNIVERSIDADE DE SANTIAGO DE COMPOSTELA

^{13}C NMR (126 MHz, $CDCl_3$)

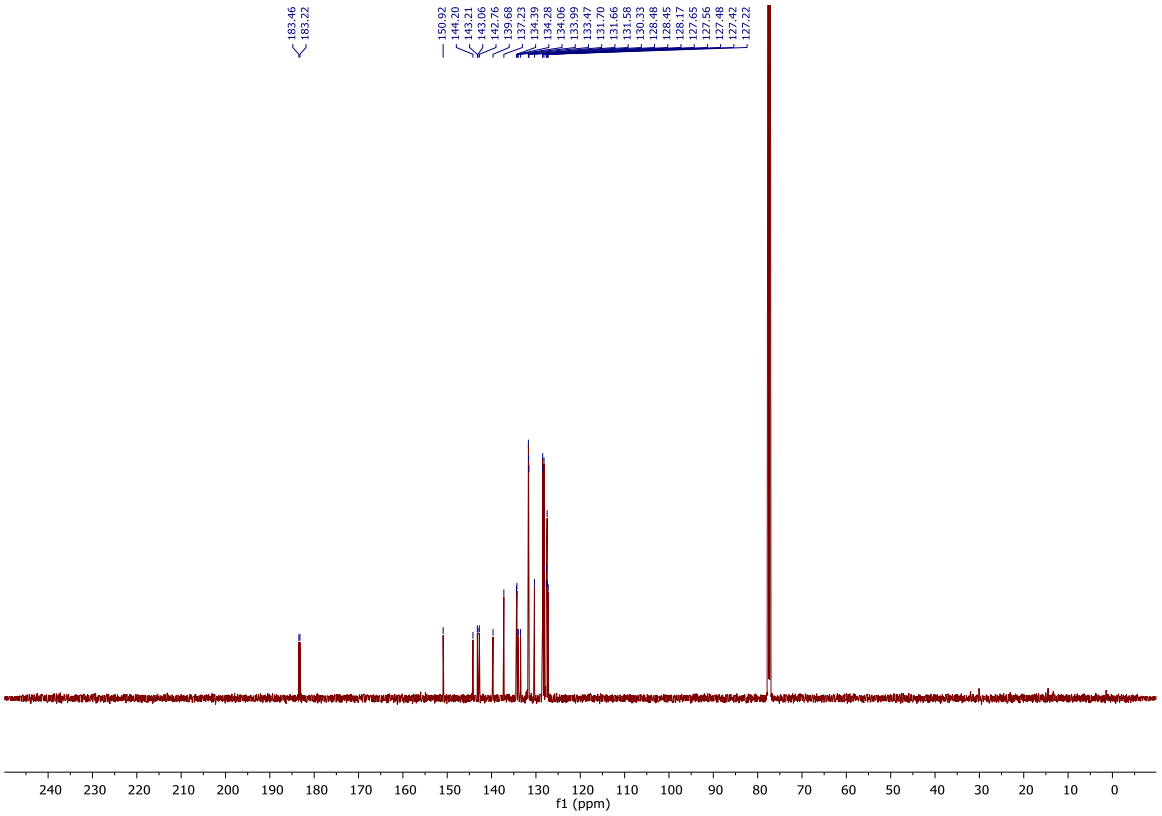

DEPT-135 (500 MHz, $CDCl_3$)

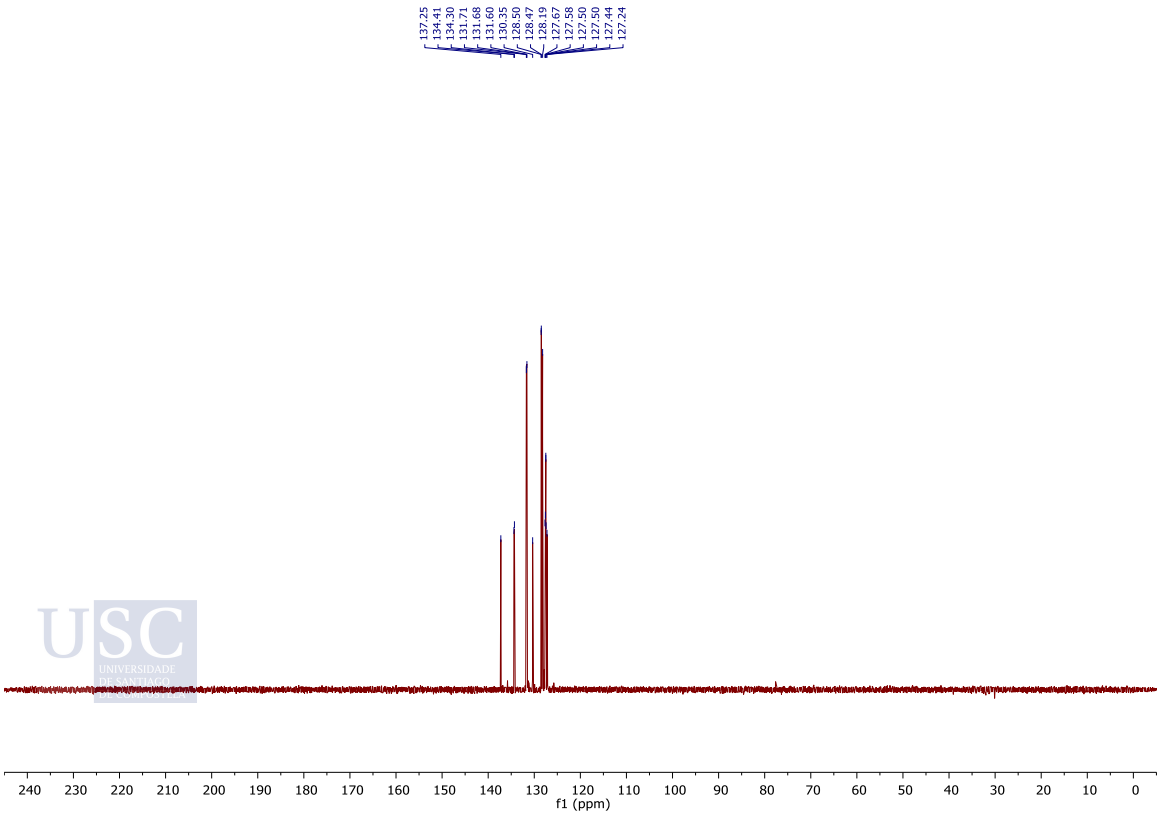

USC UNIVERSIDADE DE SANTIAGO DE COMPOSTELA

S4.- RUTHENIUM PROMOTED CYCLOADDITIONS IN DIFFERENT BIOLOGICAL MEDIA

4.1.- Representative general procedure for the ruthenium promoted cycloadditions in different biological media (exemplified for the diyne 26, using Ru1 as catalyst and PBS as solvent)

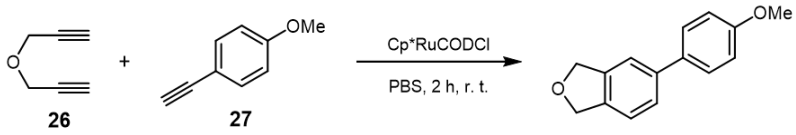

26 27

Ru1 was added to a screw caped vial containing a stir bar and PBS (phosphate-buffered saline solution, pH 7, 5.0 mL), followed by the addition of diyne **26** and alkyne **27**. The reaction mixture was stirred at room temperature. After 2 h, the reaction mixture was frozen and lyophilized. Samples were analyzed by ^{1}H-NMR employing trimethoxybenzene as internal standard and $CDCl_3$ as solvent (δ = 6.080, 3H and 3.753, 9H). (Exception: in those reactions where triphenylphosphonium-containing alkyne was used, d_6-DMSO was employed as solvent). The obtained yields for the different substrates using different biological media are reported in the main manuscript, as well as the catalyst loading.

4.2.- Representative NMR spectra for the ruthenium promoted cycloadditions in different biological media

24 25

USC UNIVERSIDADE DE SANTIAGO DE COMPOSTELA

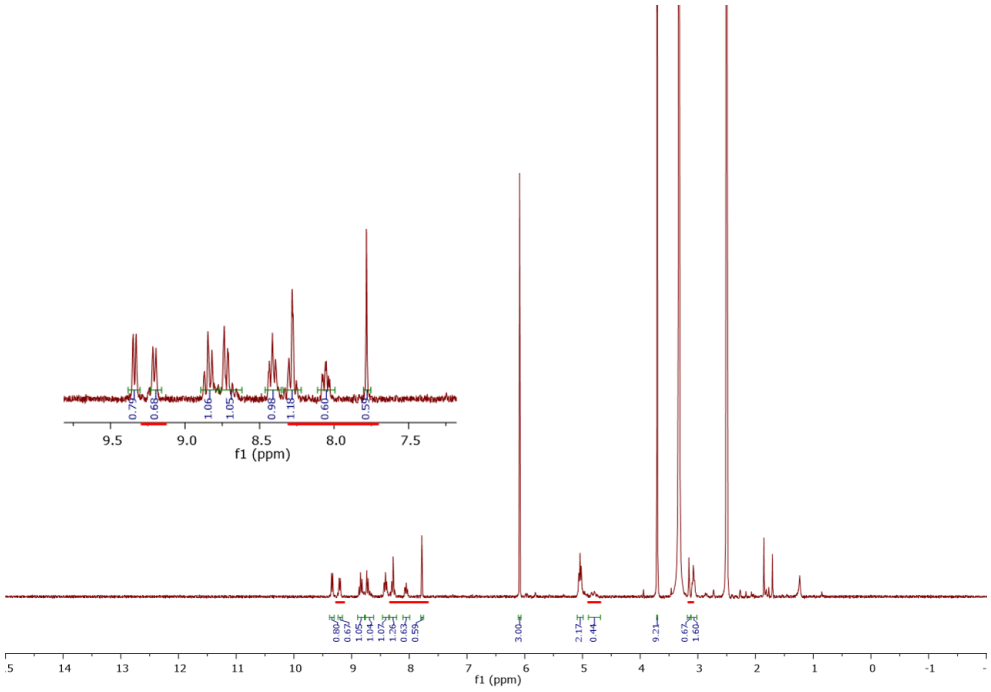

Figure S1. *Crude NMR spectra of the [2+2+2] cycloaddition reaction of substrate* ***24*** *in PBS. Red underlined signalscorrespond to the remaining substrate.*

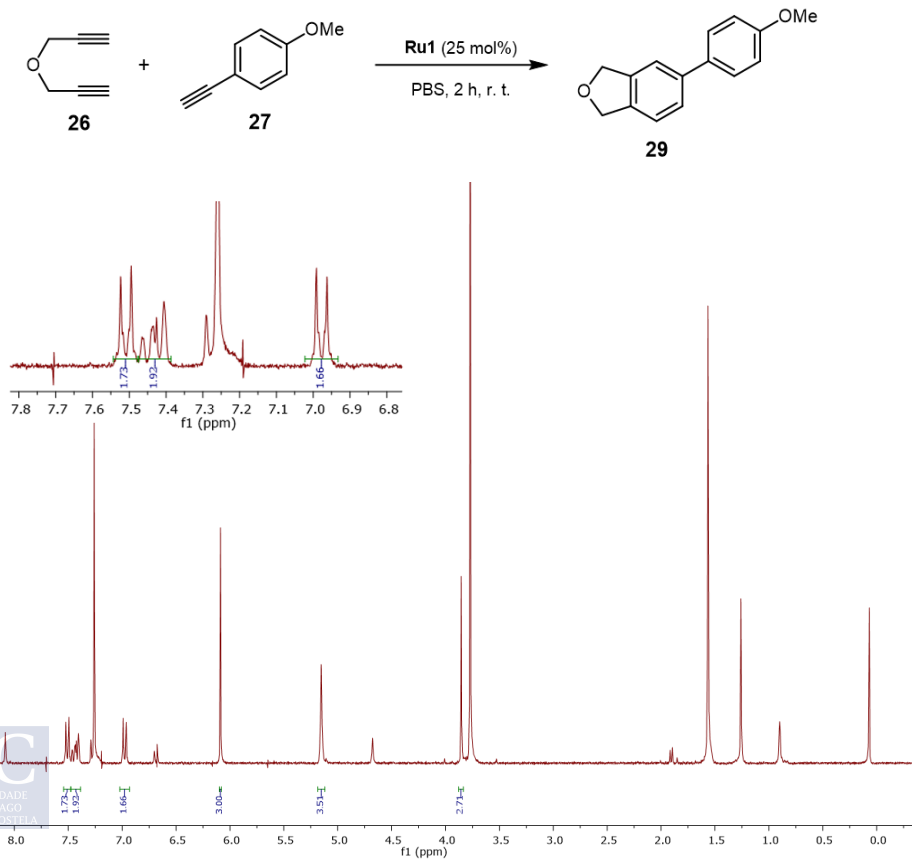

Figure S2. *Crude NMR spectra of the [2+2+2] cycloaddition reaction between substrates* ***26*** *and* ***27*** *in PBS.*

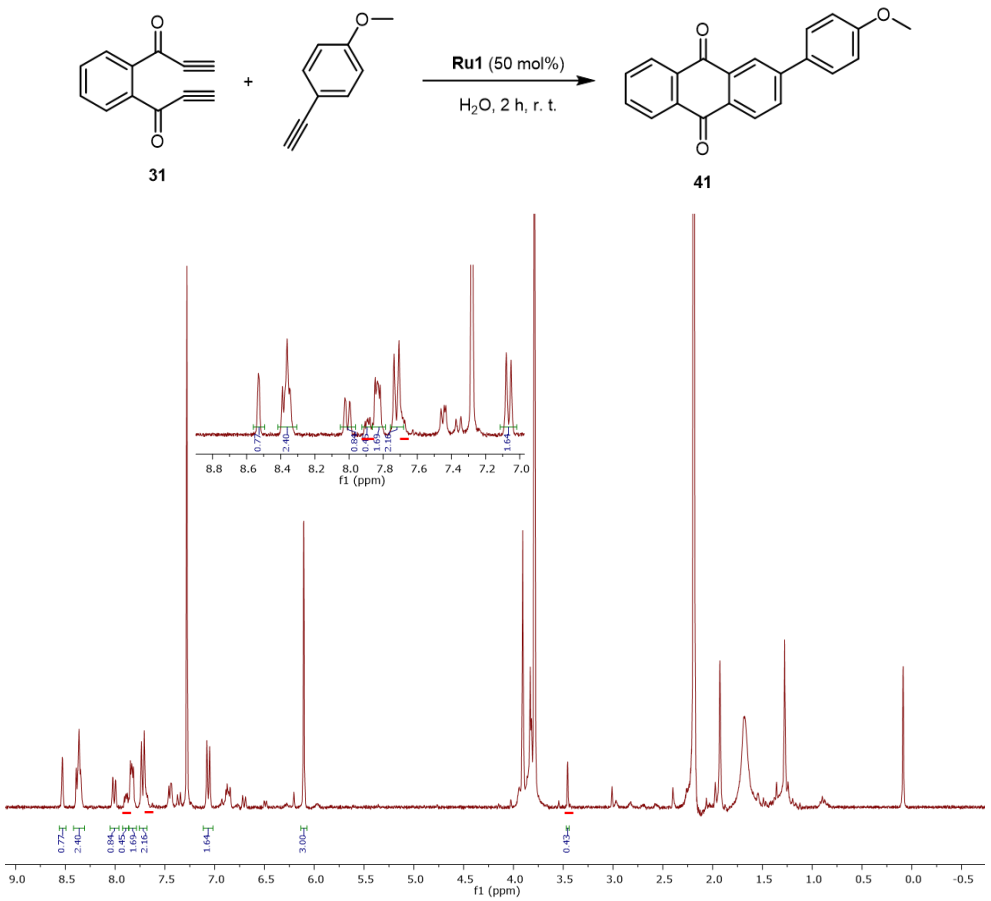

Figure S3. *Crude NMR spectra of the [2+2+2] cycloaddition reaction of substrates* ***6*** *and* ***4a*** *in H_2O. Red underlined signals correspond to the remaining substrate.*

S5.- SPECTROSCOPY STUDIES

For the UV-Vis spectroscopic studies, solutions of the compounds under research (5 mM in DMSO) were freshly prepared and diluted with 1 mL H_2O into a quartz Hellma® fluorescence cuvette with a pathlength 10x4 mm, chamber volume 1.5 mL (final concentration: 100 µM). The samples were analyzed in a Jasco V-630UV-Vis spectrophotometer at 25 °C. UV-Vis, and analyses were performed in the interval of 300-800 nm. For the fluorescence measurements, the solutions compounds (5 mM in DMSO) were freshly prepared and diluted with water into quartz Hellma® fluorescence cuvette with a path length 10x10 mm, chamber volume 3.5 mL (final concentration: 20 µM). The samples were analyzed in a Hoiba FluoroMax-3 fluorescence Spectrophotometer at 25 °C. The solutions of substrates were excited at 385 nm and the emission spectrum was recorded in the interval 400-700 nm.

The AIE character of **50** was also studied by fluorescence in different proportions of THF / H_2O.

S6.- VIABILITY ASSAYS

The toxicity was analyzed by using MTT[18] assays in HeLa cell line. A comparison study of the different compounds was carried out.

MTT assay: 15000 cells per well were seeded in 96-well plates two days before treatment with different concentrations of **Ru1** (10-100 µM), or of substrates (10-100 µM). After 6, 12 or 24 h of incubation, HEPES containing 3-(4,5-dimethylthiazol-2-yl)-2,5-diphenyl tetrazolium bromide (MTT) was added to a final concentration of 0.5 mg/mL. Cells were then incubated for 4 h to allow the formation of formazan precipitates by metabolically active cells. A detergent solution of 10% SDS and 0.01 M HCl was then added and the plate was incubated overnight at 37 °C to allow the solubilization of the precipitates. The quantity of formazan in each well (directly proportional to the number of viable cells) was measured by recording changes in absorbance at 570 nm in a microtiter plate reading spectrophotometer (*Tecan Infinite 200 PRO*).

Cytotoxicity studies of **Ru2** and **Ru8** were reported in previous work of the group.[2]

S7.- RUTHENIUM PROMOTED EXPERIMENTS IN LIVING CELLS

7.1.- Intramolecular [2+2+2] Ru-mediated cycloaddition: Generation of Heliquat 24

HeLa cells were seeded on glass coverslips two days before treatment. Then, they were incubated with catalyst [**Ru**] (20 to 50 µM) for 30 min. Cells were then washed twice with DMEM and incubated with substrate **24** (100 µM) for 1 h. Prior to observation by fluorescence microscopy, the samples were washed twice with fresh DMEM.

The coverslips were observed *in vivo* in a fluorescence microscope equipped with adequate filters. Digital pictures of the different samples were taken under identical conditions of gain and exposure.

7.2.- Intermolecular [2+2+2] Ru-mediated cycloaddition: Synthesis of anthraquinones

A549 or HeLa cells were seeded on glass coverslips two days before treatment. Then, they were incubated with catalyst [**Ru**] (20 to 50 µM) for 30 min – 1 h. Cells were then washed twice with DMEM and incubated with substrates **31** and **27** (50 and 150 µM, respectively) for 2 h. Prior to observation by fluorescence microscopy, the samples were washed twice with fresh DMEM. The coverslips were observed *in vivo* in a fluorescence microscope equipped with adequate filters. Digital pictures of the different samples were taken under identical conditions of gain and exposure.

USC UNIVERSIDADE DE SANTIAGO

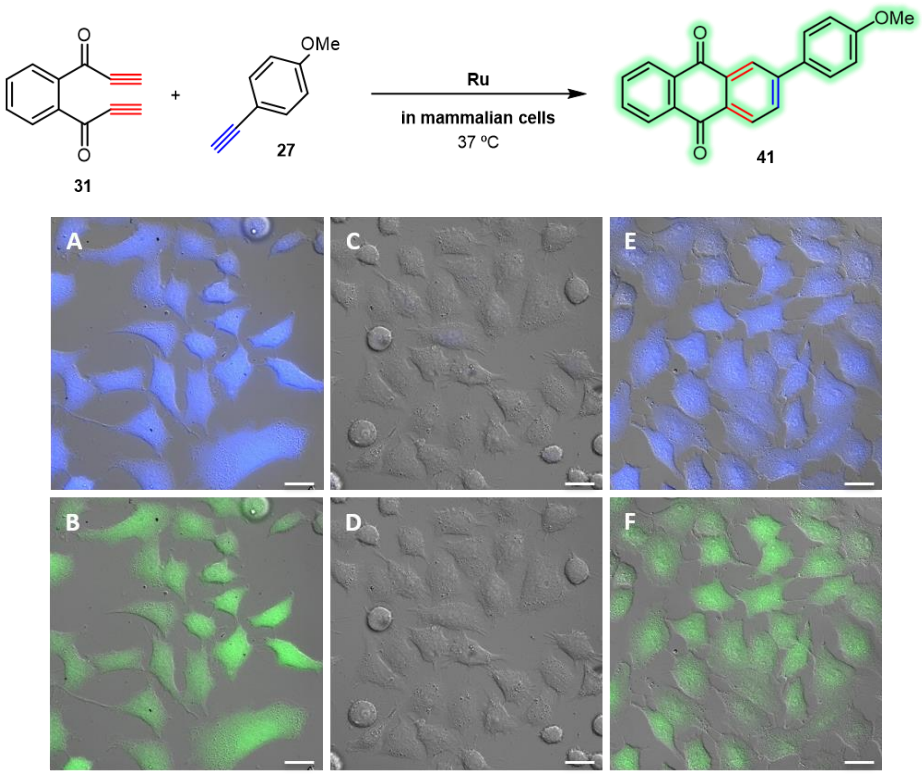

Figure S4. *Reactivity of ruthenium complexes in living cells. Ruthenium mediated [2+2+2] cycloaddition of 1,6-diyne* ***31*** *and alkyne* ***27****. Fluorescence micrographies corresponding to intracellular transformations in A549 cells: (A) cells incubated with product* ***41*** *(Merge of brightfield and blue channel); (B) cells incubated with product* ***41*** *(Merge of brightfield and green channel); (C) cells incubated with substrates* ***31*** *and* ***27*** *(Merge of brightfield and blue channel); (D) cells incubated with substrates* ***31*** *and* ***27*** *(Merge of brightfield and green channel); € cells incubated with* ***Ru2****, washed and treated with substrates* ***31*** *and* ***27*** *(Merge of brightfield and blue channel); (F) cells incubated with* ***Ru2****, washed and treated with substrates* ***31*** *and* ***27*** *(Merge of brightfield and green channel). Reaction conditions: cells were incubated with* ***Ru2*** *(50 µM) for 30 min, followed by two washings with DMEM and treatment with substrates* ***31*** *and* ***27*** *(50 and 150 µM, respectively) for 2 h. Scale bar: 12.5 µm.*

USC
UNIVERSIDADE DE SANTIAGO DE COMPOSTELA

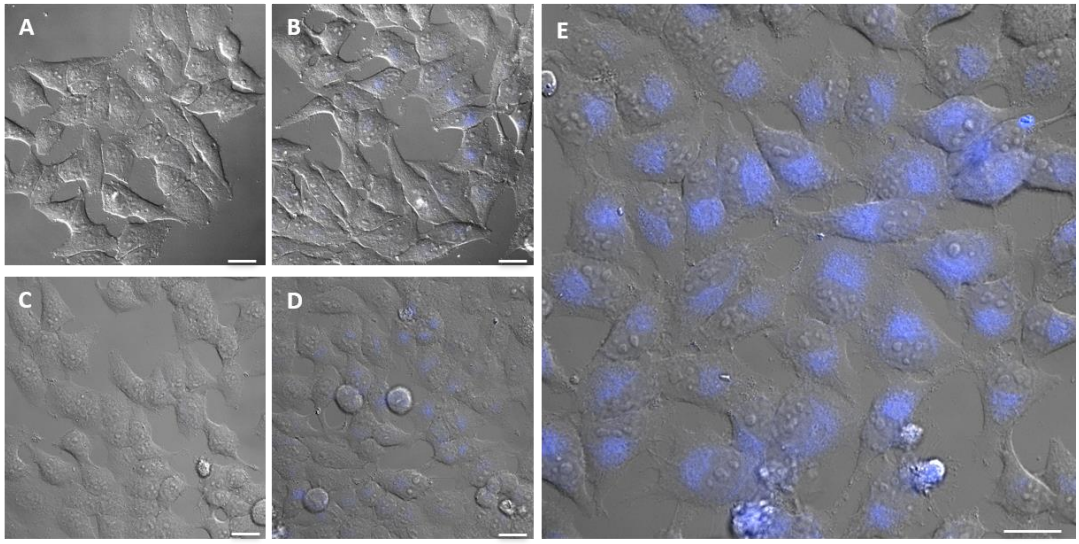

Figure S5. *Reactivity of ruthenium complexes in living cells; Control experiments. Fluorescence micrographies of HeLa cells (brightfield and blue channel): (A) cells incubated with alkyne **27**; (B) cells incubated with diyne **31**; (C) cells incubated with **Ru1**, washed and treated with substrate **27**; (D) cells incubated with **Ru1**, washed and treated with substrate **31**; (E) cells incubated with **Ru1**, washed and treated with substrates **31** and **27**. Reaction conditions: Cells were incubated with **Ru1** (50 µM) for 30 min, followed by two washings with DMEM and treatment with substrates **31** and **27** (50 and 150 µM, respectively) for 30 min. Scale bar: 12.5 µm.*

7.3.- Intermolecular [2+2+2] Ru-mediated cycloaddition: Synthesis of AIEgens

HeLa cells were seeded on glass coverslips two days before treatment. Then, they were incubated with catalyst [**Ru**] (20 to 50 µM) for 30 min. Cells were then washed twice with DMEM and incubated with substrates **31** and **49** (50 and 150 µM, respectively) for 3 h. The addition of substrate **49** was performed in small portions. Prior to observation by fluorescence microscopy, the samples were washed twice with fresh DMEM. The coverslips were observed *in vivo* in a fluorescence microscope equipped with adequate filters. Digital pictures of the different samples were taken under identical conditions of gain and exposure.

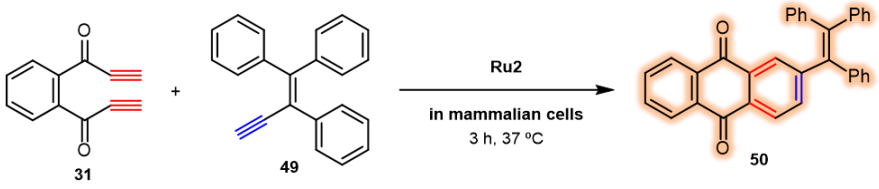

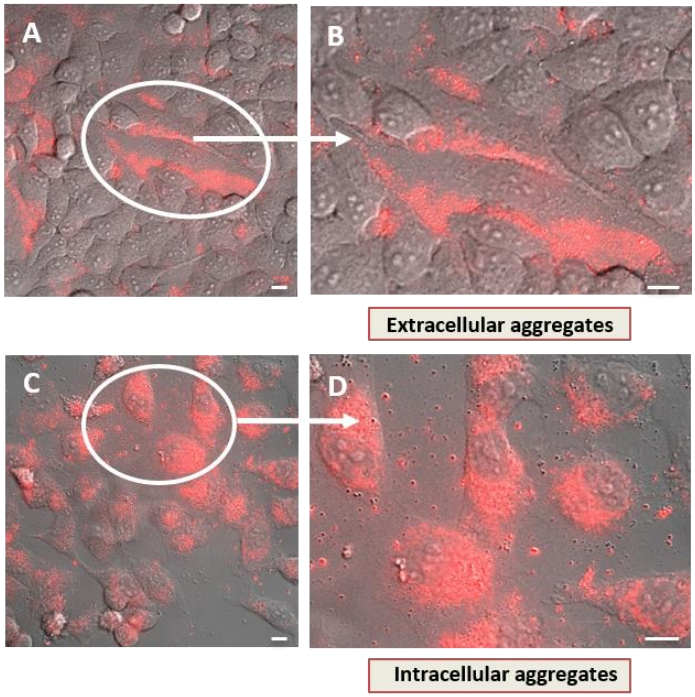

Figure S6. *Behavior of AIEs in living cells. (a) Ruthenium mediated [2+2+2] cycloaddition of 1,6-diyne* ***31*** *and alkyne* ***49:*** *(A) cells incubated with anthraquinone* ***50*** *(brightfield and red channel); (D) Zoom of panel C. (A) cells incubated with* ***Ru2****, washed and treated with substrates* ***31*** *and* ***49*** *(brightfield and red channel); (B) Zoom of panel A. Reaction conditions: cells were incubated with* ***Ru2*** *(50 μM) for 1 h, followed by two washings with DMEM and treatment with substrates* ***31*** *and* ***49*** *(50 and 150 μM, respectively) for 3 h. Scale bar: 12.5 μm.*

7.4.- Intracellular assembly of AIEgen 50 using different ruthenium complexes

This information complements that included in the main manuscript.

After following the above standard protocol for intracellular reactions, cells were finally incubated with mitochondrial marker (100 nM) for 10 min. Prior to observation by fluorescence microscopy, the samples were washed twice with fresh DMEM. The coverslips were observed *in vivo* in a fluorescence microscope equipped with adequate filters. Digital pictures of the different samples were taken under identical conditions of gain and exposure.

USC
UNIVERSIDADE DE SANTIAGO DE COMPOSTELA

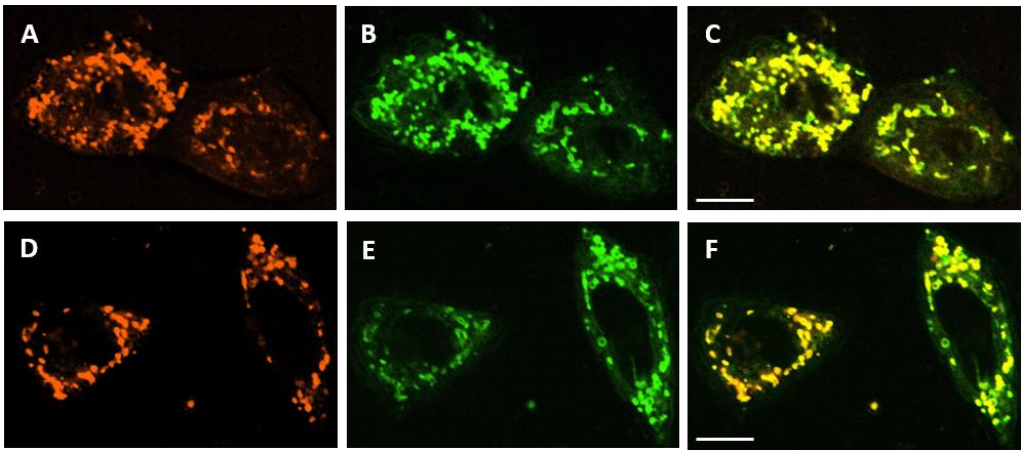

Figure S7. *Localized synthesis of AIEgen **50** in the mitochondria using **Ru3**, 1,6-diyne **31** and alkyne **49**. Fluorescence micrographies corresponding to intracellular transformations in HeLa cells: (A,D) cells incubated with **Ru3**, washed and treated with substrates **31** and **49** (red channel); (B,E) mitochondrial labeling with mitochondrial marker (green channel); (C,F) merging of A and B, and D and E. Reaction conditions: Cells were incubated with **Ru3** (50 µM) for 1 h, followed by two washings with DMEM and treatment with substrates **31** and **49** (50 and 150 µM, respectively) for 3 h. Cells were finally incubated with mitochondrial marker (100 nM) for 10 min. Scale bar: 12.5 µm.*

S8.- IDENTIFICATION STUDIES USING LC/MS

For the identification of the products **55** and **56** generated in the ruthenium promoted cycloaddition reaction inside HeLa cells, a total of 12 x 10^6 HeLa cells growing in 6 plates of 100 mm were used.

The experiments were performed in plates of 100 mm as follows: 2000000 cells per well were seeded in 100 mm plated two days before treatment. For each measurement, six plates were used. Cells were incubated with catalyst [**Ru**] (50 µM) for 50 minutes followed by two washing steps with DMEM. Then, cells were incubated with substrates **53** and either **26** or **31**, (150 and 50 µM, respectively) for 4 h. Afterwards, the reaction media was collected for analysis in a 50 mL Falcon. Prior to extraction, cells were washed with 3 mL of DMEM, followed by 3 mL of PBS and the washings were also collected separately in two 50 mL Falcons. Then the cell monolayer was treated with 500 µL of MeOH. After 5 min and pipetting up this solution was transferred to a 15 mL Falcon. Finally, we obtained 4 mL of methanolic extracts from the eight plates employed. All the samples were lyophilized for 3 days and dissolved in CH_3CN until reaching a theoretical concentration of 250 µM.

For the quantification of the product, the obtained samples (250 µM in CH_3CN) were centrifuged at 13500 rpm for 15 minutes and the supernatant was collected. In the case of the methanolic extract, it was diluted 1:4 using CH_3CN / H_2O 6:4. However, in the case of the samples of the reaction media and washing steps, no dilution was required.

Each sample was injected in a Bruker Elute coupled with times TOF using a column Zorba eclipse BXDC18 2.1 x 10 mm 1.8 µm and a flow rate of 0.4 mL/min at room temperature. For the solvent system, initial conditions H_2O / CH_3CN (40:60) were used for 0.5 min and followed by a gradual change over 4 min to H_2O / CH_3CN (20:80). Afterwards, CH_3CN percentage was increased to 98% CH_3CN in 0.2 min and maintained for 2 min. Then, initial conditions were recovered in a gradual change over 0.2 min, and maintained for 1.8 min.

S9.- PERMEABILIZATION EXPERIMENTS

HeLa cells were seeded on glass coverslips two days before treatment. Then, they were washed twice with cold transfer buffer (25 mM HEPES pH 7.3, 125 mM potassium acetate, 2 mM magnesium acetate, 5 mM sodium acetate and 1 mM EDTA). Then cells were treated with 25 µg/mL Digitonin in transfer buffer for 3 min on ice, followed by two washing steps with 10 µg/mL of BSA in transfer buffer. Finally, cells were incubated with product **50** (25-50 µM) for 15 min. Prior to observation by fluorescence microscopy, the samples were washed twice with fresh DMEM. The coverslips were observed *in vivo* in a fluorescence microscope equipped with adequate filters. Digital pictures of the different samples were taken under identical conditions of gain and exposure.

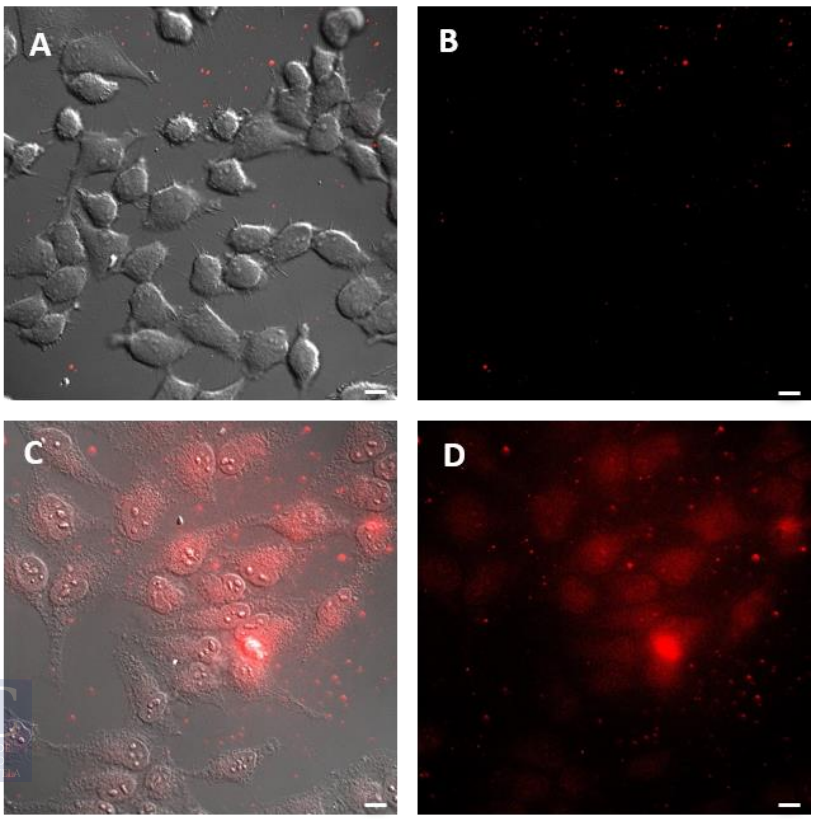

Figure S8. *Fluorescence micrographies corresponding to the uptake of* ***50*** *by HeLa cells. (A,B) Fluorescent signal of product* ***50*** *before Digitonin treatment (brightfield and red channel, respectively); (C,D) Fluorescent signal of product* ***50*** *after Digitonin treatment (brightfield and red channel, respectively). Scale bar: 12.5 µm.*

S10.- ICP ANALYSIS

The experiments were performed in 6 well plates as follows: 100000 cells per well were seeded in 6 well plates two days before treatment.

For the ICP measurements, a total of 3 x 10^6 HeLa cells growing in 6 well plates were treated with different concentrations of **[Ru]** in DMEM for 1 h. Prior to digestion, the samples were washed with fresh DMEM and then twice with PBS. The obtained fractions were digested in duplicate in HNO_3 / H_2O_2 by microwave heating and analyzed.

ICP analysis of **Ru2-Ru3** are reported in previous work of the group.[2]

10.1. Representative figure of ICP analysis

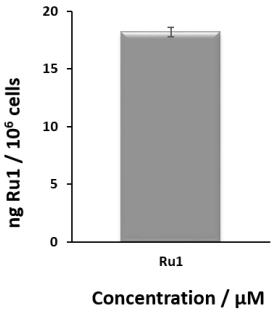

Figure S17. ICP-MS measurements of ruthenium content in HeLa cells incubated with 50 µM of **Ru1** complex, after washing and nitric treatment. The analysis reflects all ruthenium accumulated in the cell. Error bars represent the standard error of three independent experiments. ICP values: **Ru1** (50 µM, 1 h) = 18.2 ng/10^6 cells. In comparison **Ru2** is uptaken 10 times better than **Ru1**, and **Ru8** more than 50 times better than **Ru1**.

S11.- REFERENCES

[1] L. Adriaenssens, L. Severa, J. Vávra, T. Šálová, J. Hývl, M. Čížková, R. Pohl, D. Šaman, F. Teplý, *Collect. Czech. Chem. Commun*. **2009**, *74*, 1023.

[2] M. Tomás-Gamasa, M. Martínez-Calvo, J. R. Couceiro, J. L. Mascareñas, *Nat. Commun.* **2016**, *7*, 12538.

[3] T. Völker, F. Dempwolff, P. L. Graumann, E. Meggers, *Angew. Chem. Int. Ed.* **2014**, *53*, 10536.

[4] C. Vidal, M. Tomás-Gamasa, P. Destito, F. López, J. L. Mascareñas, *Nat. Commun.* **2018**, *9*, 1913.

[5] L. Kleist, S. Michaelis, K. Bartho, O. Graebner, M. Schlief, M. Dreger, A. K. Schrey, M. Sefkow, F. Kroll, H. Koester, Y. Luo, *J. Med. Chem.* **2016**, *59*, 4664.

[6] M. Shibata, K. Nakajima, Y. Nishibayashi, *Chem. Commun.* **2014**, *50*, 7874.

[7] Y. Liu, S. Zhou, G. Li, B. Yan, S. Guo, Y. Zhou, H. Zhang, P. G. Wang, *Adv. Synth. Cat.* **2008**, *350*, 797.

[8] L. Zhang, X. Lou, Y. Yu, J. Qin, Z. Li, *Macromolecules* **2011**, *44*, 5186**.**

[9] G. C. Hoover, J. Ham, C. Tang, E. I. Carrera, D. S. Seferos, *Canadian Journal of Chemistry* **2018**, *96*, 929.

[10] Q. Yu, X. Su, T. Zhang, Y.-M. Zhang, M. Li, Y. Liu, S. X.-A. Zhang, *J. Mater. Chem. C.* **2018**, *6*, 2113.

USC UNIVERSIDADE DE SANTIAGO

[11] T. Furuyama, J. Shinozaki, T. T. Tasso, H. Maeda, M. Segi, N. Kobayashi, *Tetrahedron Lett.* 2017, *58*, 4243.

[12] Y. Yamaguchi, T. Ochi, Y. Matsubara, Z. Yoshida, *J. Phys. Chem. A.* **2015**, *11*, 8630.

[13] R. Hu, J. W. Y. Lam, J. Liu, H. H. Sung, I. D. Williams, Z. Yue, K. S. Wong, M. M. F. Yuen, B. Z. Tang, *Polymer Chem.* **2012**, *3*, 1481.

[14] K. S. Feldman, D. K. Hester, C. S. López, O. N. Faza, *Org. Lett.* **2008**, *10*, 1665.

[15] Y. Yamamoto, R. Ogawa, K. Itoh, *Chem. Commun.* 2000, 549.

[16] Y. Yamamoto, K. Hata, T. Arakawa, K. Itoh, *Chem. Commun.* 2003, 1290.

[17] B. Huang, Y. Ji, Z. Li, N. Zhou, W. Jiang, Y. Feng, B. Lin, Y. Sun, *J. Lumin.* **2017**, *187*, 414.

[18] M. V. Berridge, P. M. Herst, A. S Tan, *Biotechnol. Annu. Rev.* 2005, *11*, 127.

USC
UNIVERSIDADE DE SANTIAGO DE COMPOSTELA

USC
UNIVERSIDADE
DE SANTIAGO
DE COMPOSTELA

PHOTOREDOX CATALYSIS IN LIVE MAMMALIAN CELLS

TABLE OF CONTENTS

S1 Experimental procedures and data

S2. Selected NMR spectra

S3. Photo-Meerwein arylation in different biological media

S4 Diazonium salt stability assays

S5. Viability assays

S6. Photo-Meerwein arylation inside living cells

S7. References

USC
UNIVERSIDADE
DE SANTIAGO
DE COMPOSTELA

USC
UNIVERSIDADE
DE SANTIAGO
DE COMPOSTELA

S1.- EXPERIMENTAL PROCEDURES AND DATA

S1.1. Synthesis of diazonium salts 58 and 59

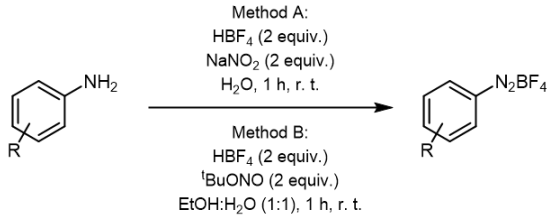

Method A:

To a round bottom flask containing 10 mmol of the corresponding amine, 4 mL of EtOH and 3.75 mL of an aqueous HBF_4 solution (48%, 2 equiv.) were added. After the dissolution of the amine, the reaction vessel was cooled to 0 °C and 2 mL of an aqueous solution containing $NaNO_2$ (0.7 g of, 20 mmol, 2 equiv.) was added dropwise. The mixture was allowed to react at room temperature for 1 h. Afterwards, 20 mL of Et_2O were added and the resulting precipitate was filtered and washed with Et_2O. Further purification was achieved by precipitating the product with Et_2O from a solution of the solid in acetone.

Method B:

To a round bottom flask containing 10 mmol of the corresponding amine, 3 mL of EtOH and 2.6 ml of an aqueous HBF_4 solution (48%, 2 equiv.) were added. After the dissolution of the amine, the reaction vessel was cooled to 0 °C and 2.64 mL of ^tBuONO (90%, 20 mmol, 2 equiv.) were added dropwise. The mixture was allowed to react at room temperature for 1 h. Afterwards, 20 mL of Et_2O were added and the resulting precipitate was filtered and washed with Et_2O. Further purification was achieved by precipitating the product with Et_2O from a solution of the solid in acetone.

Spectroscopic data are in consonance with those reported in the bibliography.[1]

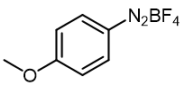

4-Methoxybenzenediazonium tetrafluoroborate (58). Pallid grey solid. **Yield** = 92% (9.2 mmol, 2.04 g). ^{1}H-NMR (300 MHz, d_6-DMSO): δ (ppm) 8.62 (dd, *J* = 9.5 Hz, 1.6 Hz, 2H), 7.49 (dd, *J* = 9.5, 2.0 Hz, 2H), 4.04 (s, 3H).

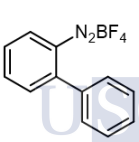

[1,1'-Biphenyl]-2-diazonium tetrafluoroborate (61). Yellow solid. **Yield** = 81% (8.1 mmol, 2.17 g) ^{1}H-NMR (300 MHz, d_6-DMSO): δ (ppm) 8.90 (d, *J* = 8.0 Hz, 1H), 8.32 (t, *J* = 7.8 Hz, 1H), 8.02 (m, 2H), 7.85 (m, 2H), 7.68 (m, 3H).

USC UNIVERSIDADE DE SANTIAGO DE COMPOSTELA

1.2. Synthesis of naphthoquinone products

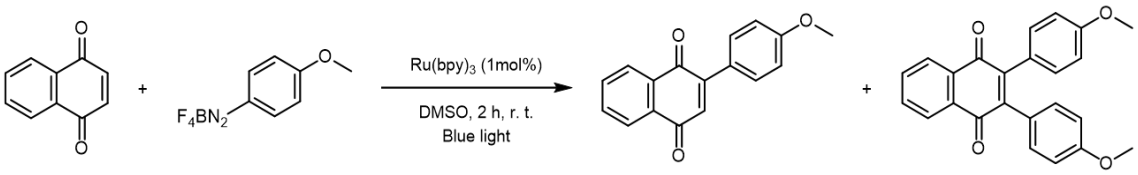

To an Ar purged Schlenk flask 4-methoxybenzenediazonium tetrafluoroborate **58** (44.4 mg, 0.2 mmol, 1 equiv.), naphthoquinone **57** (158.2 mg, 1 mmol, 5 equiv.) and $[Ru(bpy)_3][PF_6]_2$ (1.7 mg, 0.002 mmol, 1 mol%) 1 mL of deoxygenated DMSO was added. After gentle stirring, the reaction was initiated with the irradiation of a Kessil 32 W blue lamp and allowed to react for 2 h under fan refrigeration. The crude was diluted with brine, extracted with Et_2O, and further purified by flash chromatography on silica gel using Hex / acetone (9:1) as eluent.

Spectroscopic data are in consonance with those reported in the bibliography.[2]

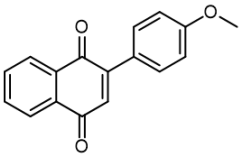

2-(4-Methoxyphenyl)-1,4-naphthoquinone (59a). Yellow solid. $\mathbf{R_f}$ = 0.12. **Yield** = 68% (0.14 mmol, 37 mg). **^{1}H NMR** (300 MHz, $CDCl_3$): δ (ppm) 8.14 (m, 2H), 7.76 (m, 2H), 7.58 (d, *J* = 8.8 Hz, 1H), 7.04 (s, 1H), 6.99 (d, *J* = 8.8 Hz, 2H), 3.87 (s, 3H).

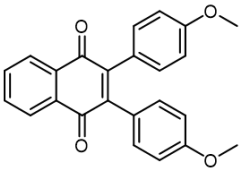

2,3-Bis(4-methoxyphenyl)-1,4-naphthoquinone (59b). Yellow solid. $\mathbf{R_f}$ = 0.06. **Yield** = 16% (0.04 mmol, 11.8 mg). **^{1}H NMR** (300 MHz, $CDCl_3$): δ (ppm) 8.18 (m, 2H), 7.77 (m, 2H), 7.03 (d, *J* = 8.7 Hz, 4H), 6.78 (d, *J* = 8.8 Hz, 4H), 3.78 (s, 6H).

1.3. Synthesis of tetraphenylethene (60)

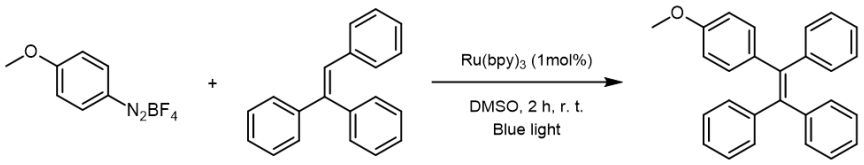

To an Ar purged Schlenk flask containing 4-methoxybenzenediazonium tetrafluoroborate (44.4 mg, 0.2 mmol, 1 equiv.), triphenylethylene (256.3 mg, 1 mmol, 5 equiv.) $Ru(bpy)_3(PF_6)_2$ (1.7 mg, 0.002 mmol, 1 mol%), 1 mL of deoxygenated DMSO was added. After gentle stirring, the reaction was initiated with the irradiation of a Kessil 32 W blue lamp and allowed to react for 2 h under fan refrigeration. The crude was diluted with brine, extracted with Et_2O and further purified by flash chromatography on silica gel using Hex – Hex / AcOEt (9.5:0.5) as eluent.

Spectroscopic data are in consonance with those reported in the bibliography.[3]

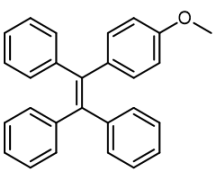

1-(4-Methoxyphenyl)1-1,2,2-triphenylethylene (60). White solid. Yield = 54% (0.11 mmol, 31.2 mg) **^{1}H NMR** (300 MHz, $CDCl_3$): δ 7.15 – 7.01 (m, 15H), 6.95 (d, *J* = 8.7 Hz, 2H), 6.65 (d, *J* = 8.8 Hz, 2H), 3.75 (s, 3H).

1.4 Synthesis of phenanthrene products

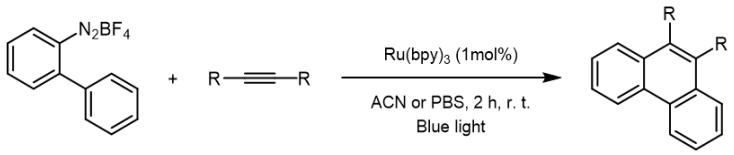

To an Ar purged Schlenk flask containing [1,1'-biphenyl]-2-diazonium tetrafluoroborate (**61**) (53.6 mg, 0.2 mmol, 1 equiv.) and $Ru(bpy)_3(PF_6)_2$ (1.7 mg, 0.002 mmol, 1 mol%) 0.6 mL of deoxygenated solvent (ACN or PBS) were added. After gentle stirring, 1 mmol (5 equiv.) of the corresponding alkyne was added, and the reaction was initiated with the irradiation of a Kessil 32 W blue lamp and allowed to react for 2 h under fan refrigeration. The crude was extracted with AcOEt, washed with brine (ammonium chloride for **65**) and further purified by flash chromatography on silica gel using Hex / EtOAc as eluent.

Spectroscopic data are in consonance with those reported in the bibliography.

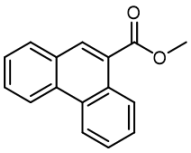

Methyl phenanthrene-9-carboxylate (62).[4] White solid. $\mathbf{R_f}$ = 0.4 (Hex / EtOAc 8:2). Reaction in PBS. **Yield** = 84% (0.17 mmol, 39.7 mg). **^{1}H NMR** (300 MHz, $CDCl_3$): δ 8.94 – 8.90 (m, 1H), 8.77 – 8.67 (m, 2H), 8.48 (s, 1H), 7.97 (d, *J* = 7.1 Hz, 1H), 7.80 – 7.60 (m, 4H), 4.05 (s, 3H).

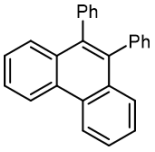

9,10-Diphenylphenanthrene (63).[5] White solid. $\mathbf{R_f}$ = 0.25 (Hex). Reaction in ACN. **Yield** = 27% (0.054 mmol, 17.8 mg). **^{1}H NMR** (300 MHz, $CDCl_3$): δ 8.82 (d, *J* = 8.3 Hz, 2H), 7.67 (ddd, *J* = 8.3, 6.7, 1.6 Hz, 2H), 7.57 (dd, *J* = 8.4, 1.6 Hz, 2H), 7.50 (dd, *J* = 6.8, 1.2 Hz, 2H), 7.29 – 7.13 (m, 10H).

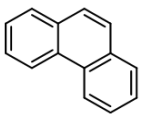

Phenanthrene (64).[6] White solid. $\mathbf{R_f}$ = 0.5 (Hex). Reaction in ACN and using TMS-protected ethyne as alkyne partner. **Yield** = 50% (0.1 mmol, 17.8 mg). **^{1}H NMR** (300 MHz, $CDCl_3$): δ 8.72 (d, *J* = 8.7 Hz, 2H), 7.98 – 7.84 (m, 2H), 7.76 (s, 2H), 7.66 – 7.59 (m, 4H).

USC UNIVERSIDADE DE SANTIAGO DE COMPOSTELA

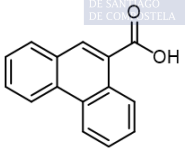

Phenanthrene-9-carboxylic acid (65).[7] White solid. $\mathbf{R_f}$ = 0.15 (Hex / EtOAc 7:3). Reaction in PBS. **Yield** = 82% (0.16 mmol, 36.5 mg). **^{1}H NMR** (300 MHz, d_6-DMSO): δ 13.23 (s, 1H), 9.00 – 8.79 (m, 3H), 8.51 (s, 1H), 8.14 (d, *J* = 7.6 Hz, 1H), 7.81 (t, *J* = 7.4 Hz, 1H) 7.76 – 7.53 (m, 3H).

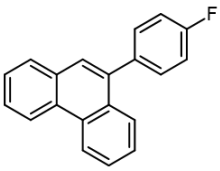

9-(4-Fluorophenyl)phenanthrene (66).[8] White solid. **Rf** = 0.25 (Hex). Reaction in PBS. **Yield** = 60% (0.12 mmol, 32.7 mg). **^{1}H NMR** (300 MHz, $CDCl_3$): δ 8.80 (d, *J* = 8.3 Hz, 1H), 8.74 (d, *J* = 8.0 Hz, 1H), 7.90 (m, 2H), 7.67 (m, 4H), 7.62 – 7.44 (m, 3H), 7.24 (tt, *J* = 8.8, 2.4 Hz, 2H). **^{19}F NMR** (282 MHz, $CDCl_3$): δ (ppm) -63.40.

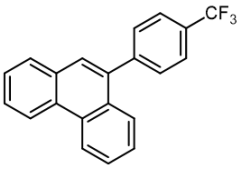

9-(4-Trifluoromethyl)phenyl)phenanthrene (67).[8] White solid. **R_f** = 0.25 (Hex). Reaction in PBS. Yield = 8i2% (0.164, 52.9 mg). **^{1}H NMR** (300 MHz, $CDCl_3$): δ 8.80 (d, *J* = 8.3 Hz, 1H), 8.74 (d, *J* = 8.1 Hz, 1H), 7.91 (dd, *J* = 7.7, 1.3 Hz, 1H), 7.81 (m, 3H), 7.75 – 7.61 (m, 6H), 7.56 (ddd, *J* = 8.2, 7.0, 1.2 Hz, 1H). **^{19}F NMR** (282 MHz, $CDCl_3$): δ -62.83.

S2. SELECTED ^{1}H NMR SPECTRA

Methyl phenanthrene-9-carboxylate (62)

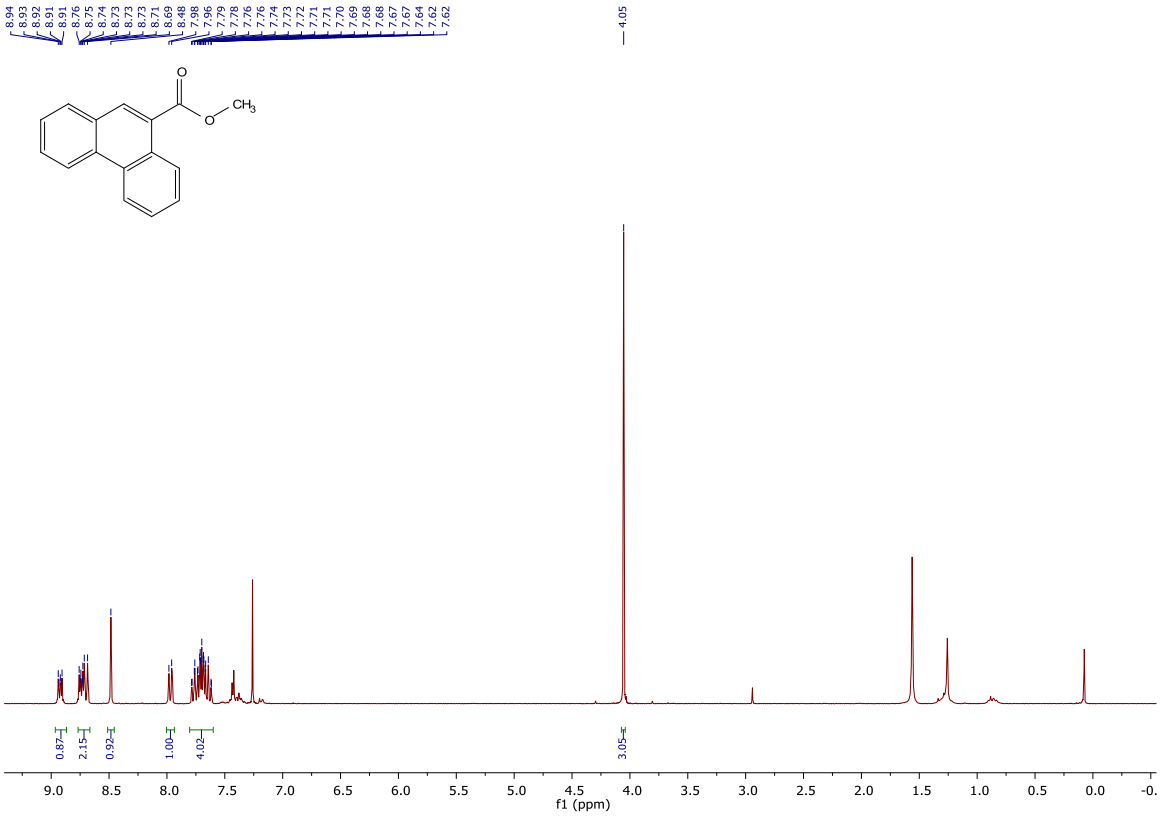

USC
UNIVERSIDADE DE SANTIAGO DE COMPOSTELA

Phenanthrene-9-carboxylic acid (65)

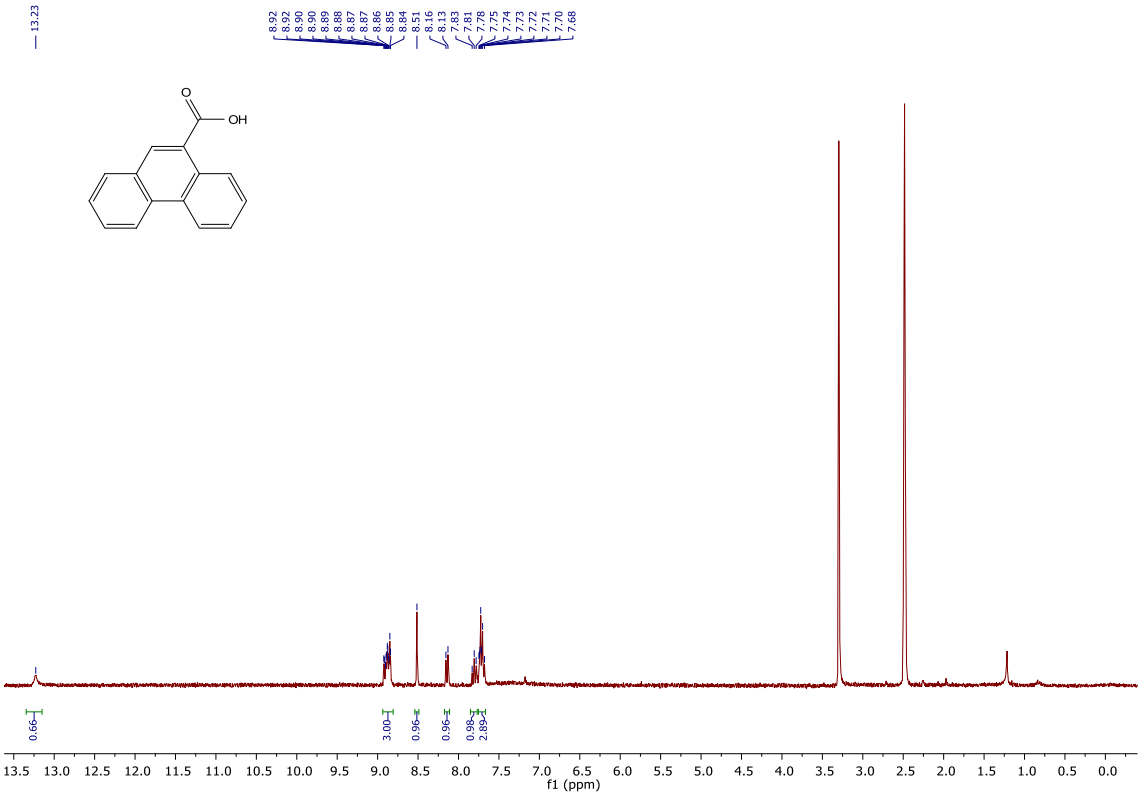

9-(4-Trifluoromethyl)phenyl)phenanthrene (67)

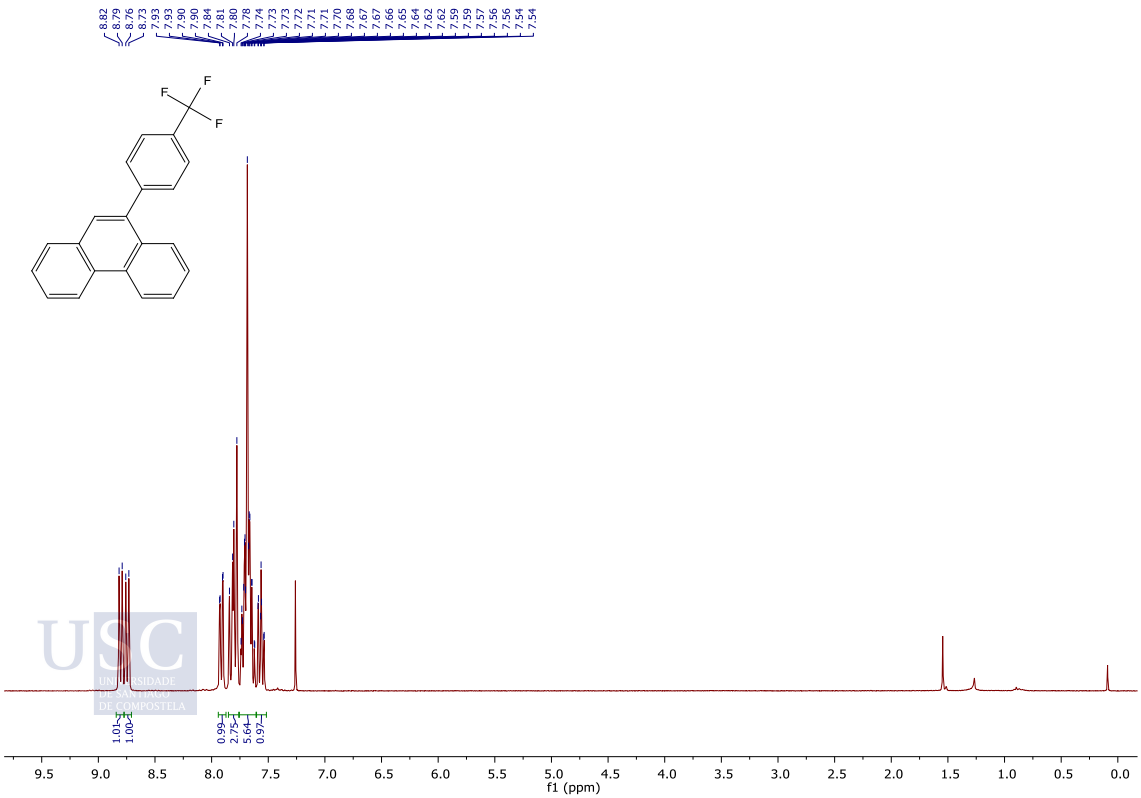

USC UNIVERSIDADE DE SANTIAGO DE COMPOSTELA

S3. PHOTO-MEERWEIN ARYLATION IN DIFFERENT BIOLOGICAL MEDIA

3.1.- Representative general procedure for the photo-Meerwein arylation in different biological media

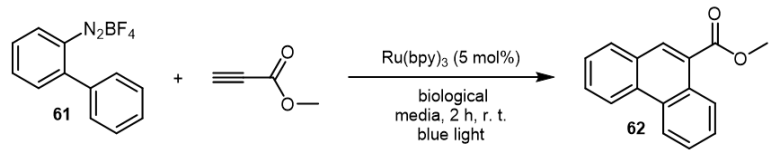

To an Ar purged Schlenk flask containing 13.5 mg of [1,1'-biphenyl]-2-diazonium tetrafluoroborate (0.05 mmol) and 2.2 mg of $Ru(bpy)_3(PF_6)_2$ (0.0025 mmol, 5 mol%) is added 5 mL of deoxygenated solvent (PBS, DMEM or Lys). After a gentle stirring, 0.25 mmol (5 equiv.) of the corresponding alkyne is added, and the reaction initiated with the irradiation of a Kessil 32 W blue lamp, and allowed to react for 2 h under fan refrigeration. The crude is extracted with AcOEt, the organic phase evaporated and samples analyzed by ^1H NMR using nitromethane as internal standard. The obtained yields for the different substrates using different biological media are reported in the main manuscript, as well as the catalyst loading.

3.2.- Representative NMR spectra for the photo-Meerwein arylation in different biological media

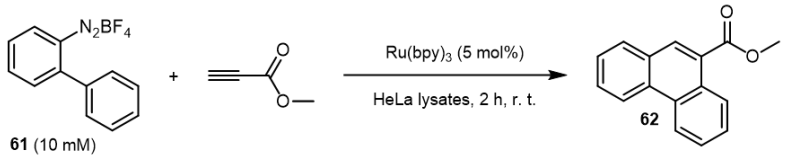

USC
UNIVERSIDADE
DE SANTIAGO
DE COMPOSTELA

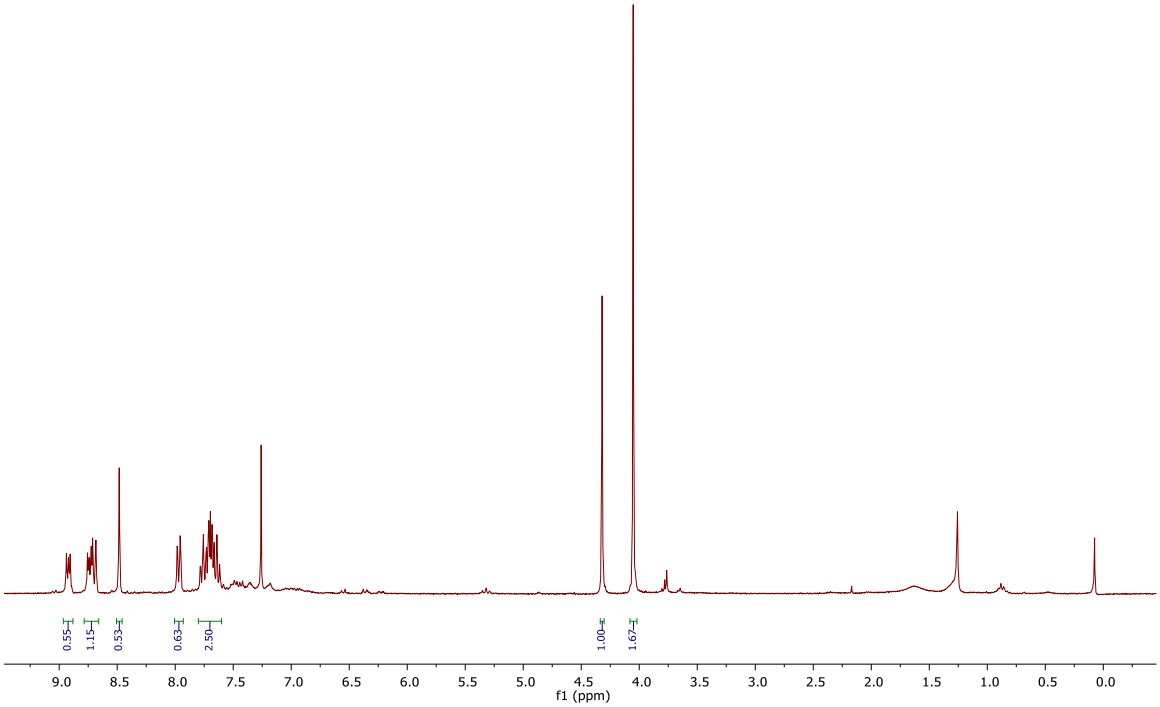

*Figure S1. Crude NMR with **61** and methyl propiolate in HeLa lysates (2mg/mL)*

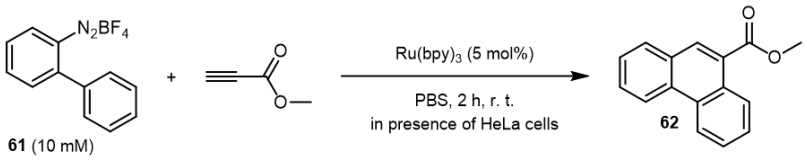

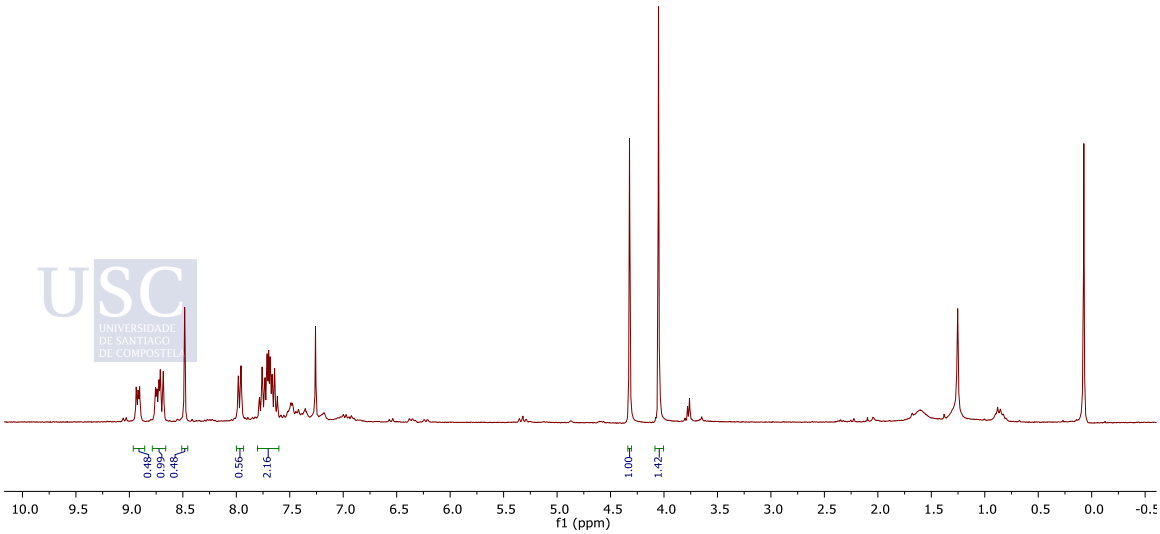

USC UNIVERSIDADE DE SANTIAGO DE COMPOSTELA

*Figure S2. Crude NMR with **61** and methyl propiolate in presence of cells ($1 \cdot 10^6$ cells/mL)*

S4 DIAZONIUM SALT STABILITY ASSAYS

Stability of diazonium salt **61** was tested in different solvents (DMSO, H_2O and PBS) at room temperature, following its decomposition by ^1H NMR. For studies in DMSO or H_2O, NMR tubes were prepared by dissolving 10 mg of the diazonium salt **61** (0.037 mmol) and 2.1 mg of trimethoxybenzene (DMSO, 0.012 mmol ,0.33 equiv.) or 2.4 μL of dimethyl sulfone (H_2O and PBS, 0.037 mmol, 1 equiv.) as internal standard, in 1mL of the corresponding deuterated solvent. For PBS experiments, a sample of 1 mL of non-deuterated PBS was lyophilized and diluted with 1 mL of D_2O to obtain deuterated PBS.

In figure S3 are summarized the stability results after 30 min or 60 min. Diazonium salt did not suffer degradation in DMSO or H_2O under 30 min. Nevertheless, a 15% or 20% of degradation was observed in phosphate buffer, after 30 or 60 min, respectively. This behavior could be attributed to the exchange of the counterion BF_4.

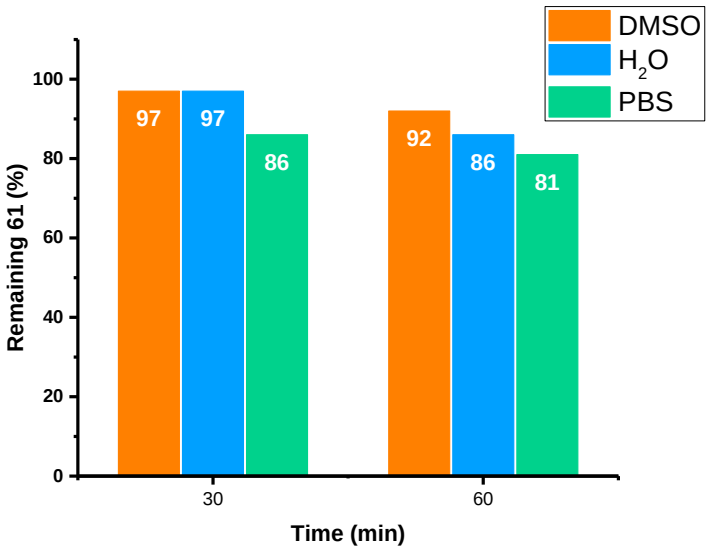

*Figure S3. Evolution of diazonium salt **61** in different solvents.*

USC UNIVERSIDADE DE SANTIAGO DE COMPOSTELA

4.1 Representative NMR spectra of the evolution of diazonium salt 61 in solution

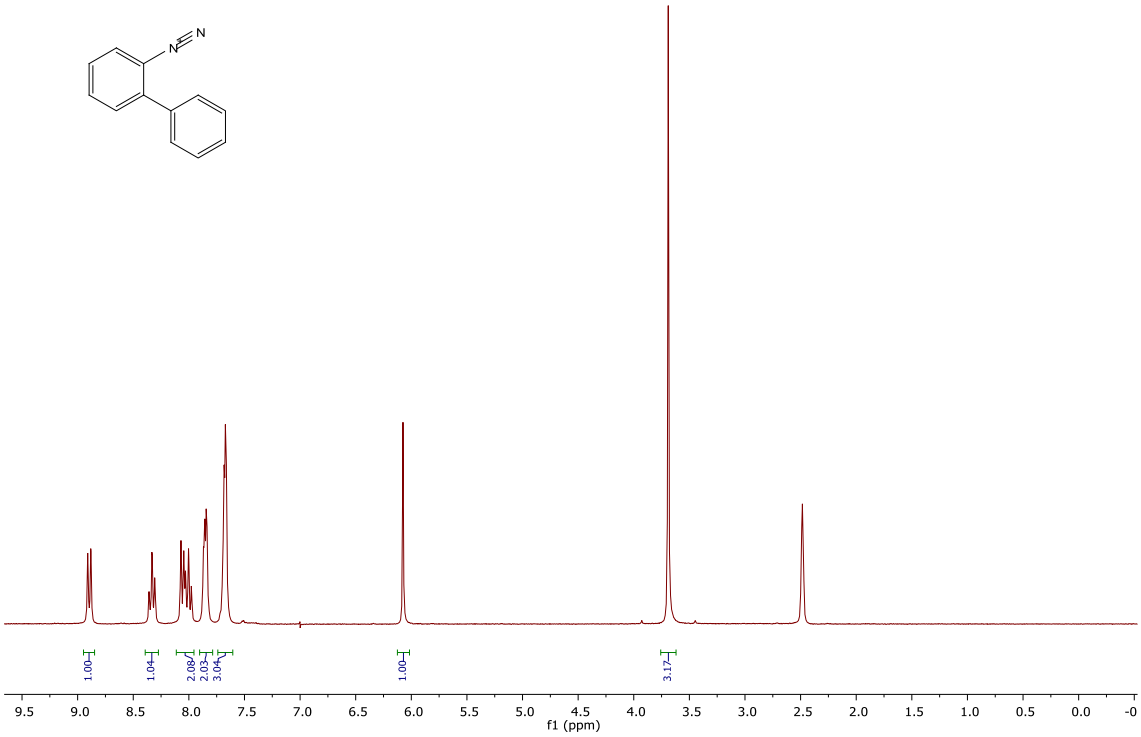

*Figure S4. NMR spectra of **61** in DMSO at time "0" using TMB as internal standard (1H:1H).*

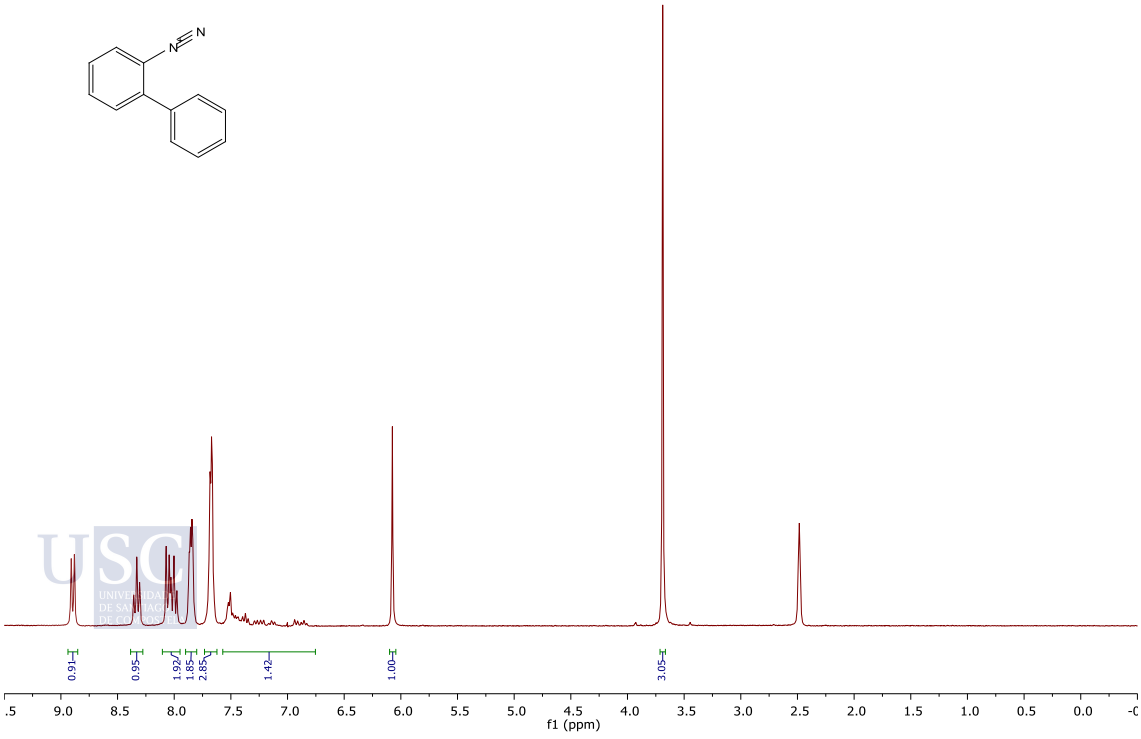

*Figure S5. NMR spectra of **61** in DMSO after 1h using TMB as internal standard (1H:1H).*

S5.- VIABILITY ASSAYS

The toxicity was analyzed by MTT assays in HeLa cell line. A comparison study of the different compounds was carried out.

MTT assay: 15000 cells per well were seeded in 96-well plates two days before treatment with different concentrations of $Ru(bpy)_3$ (10-100 µM), substrates or product (10-100 µM). The effect of the intracellular generation of product was also evaluated. Moreover, the viability of the cells after the irradiation was also tested. After 6, 12 or 24 h of incubation, HEPES containing 3-(4,5-dimethylthiazol-2-yl)-2,5-diphenyl tetrazolium bromide (MTT) was added to a final concentration of 0.5 mg/mL. Cells were then incubated for 4 h to allow the formation of formazan precipitates by metabolically active cells. A detergent solution of 10% SDS and 0.01 M HCl was then added and the plate was incubated overnight at 37 °C to allow the solubilization of the precipitates. The quantity of formazan in each well (directly proportional to the number of viable cells) was measured by recording changes in absorbance at 570 nm in a microtiter plate reading spectrophotometer (*Tecan Infinite 200 PRO*).

6.- PHOTO-MEERWEIN ARYLATION INSIDE LIVING CELLS

For the identification of **62** generated in the photo-promoted reaction inside HeLa, A549 or Vero cells, a total of 12 x 10^6 cells growing in 8 plates of 100 mm were used.

The experiments were performed in plates of 100 mm as follows: 2000000 cells per well were seeded in 100 mm plated two days before treatment. For each measurement, eight plates were used. Cells were incubated with catalyst $Ru(bpy)_3$ (50 µM) and diazonium salt **61** (100 µM) and propargyl alcohol (100 µM) for 30 min. Prior to irradiation, the cells were washed twice with fresh DMEM and then treated with HEPES. Well plates containing cells were disposed as shown in illustration 2. Irradiated at 15 cm of distance under fan refrigeration for 30 min.

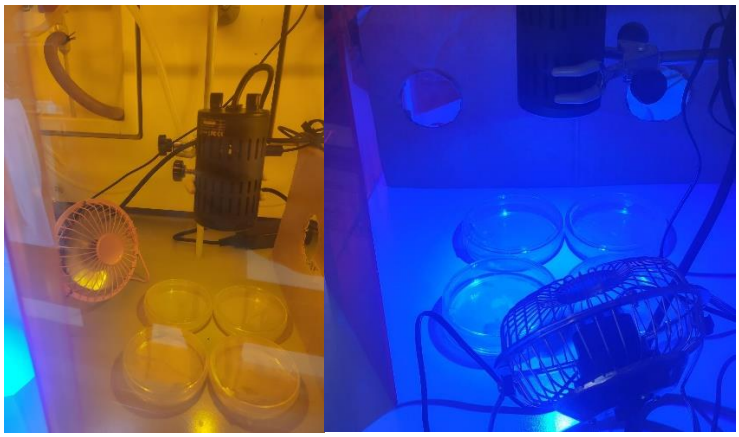

Illustration 2. Montage for cell irradiation.

Afterwards, the reaction media was collected for analysis in a 50 mL Falcon. Prior to extraction, cells were washed with 3 mL of DMEM, followed by 3 mL of PBS and the washings were also collected separately in two 50 mL Falcons. Then the cell monolayer was treated with 1 mL of MeOH. After 5 min and pipetting up this solution was transferred to a 15 mL Falcon. Finally, we obtained 8 mL of methanolic extracts from the eight plates employed. All the samples were lyophilized for 3 days and dissolved in CH_3CN until reaching a theoretical concentration of 250 µM.

For the quantification of the product, the obtained samples (250 µM in CH_3CN) were centrifuged at 13500 rpm for 15 minutes and the supernatant was collected. In the case of the methanolic extract, it was diluted 1:4 using CH_3CN / H_2O (6:4). However, in the case of the samples of the reaction media and washing steps, no dilution was required.

Each sample was injected in a Bruker Elute coupled with time TOF using a column Zorba eclipse BXDC18 2.1 x 10 mm 1.8 µm and a flow rate of 0.5 mL/min at room temperature. For the solvent system, initial conditions H_2O / CH_3CN (40:60) were used for 1 min and followed by a gradual change over 7 min to CH_3CN. Then, initial conditions were recovered in a gradual change over 0.2 min, and maintained for 1.8 min.

S7. REFERENCES

[1] B. Xing, C. Ni, J. Hu, *Angew. Chem. Int. Ed.* **2018**, *57*, 9896.
[2] M. T. Molina, C. Navarro, A. Moreno, A. G. Csáky, *Org. Lett.* **2009**, *11*, 4938.
[3] H. Jiang, Q. Xu, Z. Wang, *J. Of Supercritical Fluids*, **2009**, *49*, 377.
[4] T. Xiao, X. Dong, Y. Tang, L. Zhou, *Adv. Synth. Catal.* **2012**, *354*, 3195.
[5] C. Wang, S. Rakshit, F. Glorius, *J. Am. Chem. Soc.* **2010**, *132*, 14006.
[6] M. Tobisu, K. Yamakawa, T. Shimasaki, N. Chatani, *Chem. Commun.* **2011**, *47*, 2946.
[7] K. Nemoto, H. Yoshida, N. Egusa, N. Morohashi, T. Hattori, *J. Org. Chem.* **2010**, *75*, 7855.
[8] D. García-Cuadrado, P. de Mendoza, A. A. C. Braga, F Maseras, A. M. Echavarren, *J. Am. Chem. Soc.* **2007**, *129*, 6880.
[9] I. J. S. Fairlamb, J. D. Firth, *Org. Lett.* **2020**, *22*, 7057.

USC
UNIVERSIDADE DE SANTIAGO DE COMPOSTELA

USC
UNIVERSIDADE
DE SANTIAGO
DE COMPOSTELA

LIST OF PUBLICATIONS

USC
UNIVERSIDADE
DE SANTIAGO
DE COMPOSTELA

USC
UNIVERSIDADE
DE SANTIAGO
DE COMPOSTELA

Title	Discrete Cu(I) complexes for azide-alkyne annulations of small molecules inside mammalian cells
Authors	Joan Miguel Ávila, María Tomás Gamasa, Andrea Olmos Verge, Pedro J. Pérez, José Luis Mascareñas Cid.
Year	2018
Journal	Chemical Science
Volume, pages	9, 1947-1952
Impact Factor	9.825
PhD student contribution	Synthesis of probes, the majority of catalysts and its characterization. Experiments in plate reader and HPLC, UV-Fluorescence, EPR. Cells data treatment (no cell handling or HPLC cell analysis)

Title	Intracellular Ruthenium-Promoted (2+2+2) Cycloadditions
Authors	Joan Miguel Ávila, María Tomás Gamasa, José Luis Mascareñas Cid.
Year	**2020**
Journal	Angewandte Chemie International Edition
Volume, pages	59, 17628-17633
Impact Factor	15.34
PhD student contribution	Synthesis of probes, the majority of catalysts and its characterization. Reaction studies, UV-Fluorescence. Cells data treatment (no cell handling or HPLC cell analysis).

USC UNIVERSIDADE DE SANTIAGO DE COMPOSTELA

USC
UNIVERSIDADE
DE SANTIAGO
DE COMPOSTELA

USC
UNIVERSIDADE
DE SANTIAGO
DE COMPOSTELA

Since the recent incorporation of bioorthogonal reactions as new tools for cell research, chemical biology has been boosted, revolutionizing closely related fields like imaging, drug development or biotechnology due to its ability to manipulate small exogenous compounds in living systems without disturbing the host metabolism. During this thesis, we have explored the potential of organometallic chemistry in the bioorthogonal field. We have discovered that predefined Cu(I) complexes promote intracellular CuAAC with high efficiency. Moreover, Ru [2+2+2] cycloaddition has been successfully employed for the intracellular synthesis of biomolecules in specific organelles. Finally, the use of light has been investigated in the Meerwein arylation, that proceeds with excellent chemoselectively and yields in biological settings.